A Complex, Linked Watershed-Reservoir Hydrology and Water Quality Model Application for the Occoquan Watershed, Virginia

Zhongyan Xu

Dissertation submitted to the faculty of
Virginia Polytechnic Institute and State University
in partial fulfillment of the requirements for the degree of

Doctor of Philosophy
in
Civil and Environmental Engineering

Adil N. Godrej, Chair

Theo Dillaha III

Thomas J. Grizzard, Jr.

John C. Little

David L. Trauger

December 2005
Falls Church, Virginia

Keywords: Water quality models, Hydrological models, Linked models, HSPF, CE-QUAL-W2

A Complex, Linked Watershed-Reservoir Hydrology and Water Quality Model Application for the Occoquan Watershed, Virginia

Zhongyan Xu

(ABSTRACT)

The Occoquan Watershed is a 1515 km^2 basin located in northern Virginia and contains two principal waterbodies: the Occoquan Reservoir and Lake Manassas. Both waterbodies are principal drinking water supplies for local residents and experience eutrophication and summer algae growth. They are continuously threatened by new development from the rapid expansion of the greater Washington D.C. region. The Occoquan model, consisting of six HSPF and two CE-QUAL-W2 submodels linked in a complex way, has been developed and applied to simulate hydrology and water quality activities in the two major reservoirs and the associated drainage areas. The studied water quality constituents include temperature, dissolved oxygen, ammonium nitrogen, oxidized nitrogen, orthophosphate phosphorus, and algae. The calibration of the linked model is for the years 1993-95, with a validation period of 1996-97. The results show that a successful calibration can be achieved using the linked approach, with moderate additional effort. The spatial and temporal distribution of hydrology processes, nutrient detachment and transport, stream temperature and dissolved oxygen were well-reproduced by HSPF submodels. By using the outputs generated by HSPF submodels, the CE-QUAL-W2 submodels adequately captured the water budgets, hydrodynamics, temperature, temporal and spatial distribution of dissolved oxygen, ammonium nitrogen, oxidized nitrogen, orthophosphate phosphorus, and algae in Lake Manassas and Occoquan Reservoir. This demonstrates the validity of linking two types of state-of-the-art water quality models: the watershed model HSPF and the reservoir model CE-QUAL-W2.

One of the advantages of the linked model approach is to develop a direct cause-and-effect relationship between upstream activities and downstream water quality. Therefore, scenarios of various land use proposals, BMP implementation, and point source management can be incorporated into HSPF applications, so that the

CE-QUAL-W2 submodels can use the boundary conditions corresponding with these scenarios to predict the water quality variations in the receiving waterbodies. In this research, two land use scenarios were developed. One represented the background condition assuming all the land covered by forest and the other represented the environmental stress posed by future commercial and residential expansion. The results confirm the increases of external nutrient loads due to urbanization and other human activities, which eventually lead to nutrient enrichment and enhanced algae growth in the receiving waterbodies. The increases of external nutrient loads depend on land use patterns and are not evenly spread across the watershed. The future development in the non-urban areas will greatly increase the external nutrient production and BMPs should be implemented to reduce the potential environmental degradation. For the existing urban areas, the model results suggest a potential threshold of nutrient production despite future land development. The model results also demonstrate the catchment function of Lake Manassas in reducing nutrient transport downstream.

Acknowledgements

This work would not have been possible without the constant help and support from my advisor Adil N. Godrej, who gave me an opportunity to explore the other side of the world and encouraged me to achieve my dreams. I would also like to thank Theo Dillaha III, Thomas J. Grizzard Jr., John C. Little, and David L. Trauger, not only for serving as my committee members, but also for encouraging my education during my years at Virginia Tech.

For all the people who helped me out at the Occoquan Watershed Monitoring Laboratory, I would love to thank you one more time. Thanks, Mary Lou Daniel and Harry Post for answering numerous questions regarding the water quality data. Thanks, Barb Angelotti and Alicia Tingen for always being encouraging and supportive. And thanks for all the field staff and laboratory staff for collecting and analyzing the water quality samples, which provided a solid data support for the research.

I also acknowledge the financial support from institutional members of the Occoquan Watershed program who continue to provide the funding for the Occoquan Model project, which made my Ph.D studies possible. Special credit goes to Mr. Normand Goulet, Ms. Traci Kammer Goldberg, Ms. Evelyn Mahieu, Mr. Steve Bennett and other people who oversaw the project.

Above all, I want to thank my parents for their constant love and support throughout my education and my life. I am grateful to my father, Jian Xu, for his encouraging words and for always being proud of my achievements. Thanks so much to my mother, Jinling Zhong, for staying by my side and being supportive. I could not have made it without both of you in my life. I would like to thank my husband, Hongwei Gu, for his undying love, support and friendship for the past years.

Table of Contents

List of Figures

List of Tables

List of Abbreviations

AGNPS	Agricultural Non-Point-Source Pollution Model
ANSWERS	Areal Nonpoint Source Watershed Environment Response Simulation
AWT	Advanced Wastewater Treatment
BASINS	Better Assessment Science Integrating Point and Nonpoint Sources
BMP	Best Management Practices
BOD	Biochemical Oxygen Demand
CBOD	Carbonaceous Biochemical Oxygen Demand
COD	Chemical Oxygen Demand
CREAMS	Chemicals, Runoff and Erosion from Agricultural Management Systems
DECS	Delaware Estuary Comprehensive Study
DEM	Digital Elevation Model
DO	Dissolved Oxygen
DoD	Department of Defense
EDRD	Electronic Daily Rainfall Database
EFDC	Environmental Fluid Dynamics Code
ET	Evapotranspiration
FW	Fairfax Water
GIS	Geographic Information System
GLEAMS	Groundwater Loading Effects of Agricultural Management Systems
GRASS	Geographic Resources Analysis Support System
HEC	Hydrological Engineering Center
HMS	Hydrological Modeling System
HSP	Hydrocomp Simulation Programming
HSPF	Hydrological Simulation Program–Fortran
HUC	Hydrological Unit Code
ISIS	Integrated Surface Irradiance Study
MMS	Modules Modeling System
MUSLE	Modified Universal Soil Loss Equation

N	Nitrogen
NCDC	National Climatic Data Center
NH4-N	Ammonium Nitrogen
NHD	National Hydrography Database
NOAA	National Oceanic and Atmospheric Administration
NPS	Nonpoint Source Model
NVRC	Northern Virginia Regional Commission (previously NVPDC)
NVPDC	Northern Virginia Planning District Commission (currently NVRC)
NWS	National Weather Service
OP	Orthophosphate Phosphorus
OWML	Occoquan Watershed Monitoring Laboratory
Ox-N	Oxidized Nitrogen
P	Phosphorus
PD	Percentage Difference
PEST	Parameter ESTimation
POTW	Publicly-Owned Treatment Works
PRMS	Precipitation Runoff Modeling System
RTJ	Robert Trent Jones Golf Course
SCS	Soil Conservation Service
SIN	Soluble Inorganic Nitrogen
SMS	Surface Water Modeling System
SPARROW	Spatially Referenced Regression Model
STATSGO	State Soil Geographic Database
SWAT	Soil and Water Assessment Tool
SWM	Stanford Watershed Model
SWMM	Storm Water Management Model
SWRRB	Simulator for Water Resources in Rural Basins
TMDL	Total Maximum Daily Loads
TVA	Tennessee Valley Authority
UOSA	Upper Occoquan Sewage Authority
USDA	United States Department of Agriculture

USEPA	United States Environmental Protection Agency
USGS	United States Geological Survey
USLE	Universal Soil Loss Equation
VSCO	Virginia State Climatology Office
VSWCB	Virginia State Water Control Board
W2	CE-QUAL-W2
WASP	Water Quality Analysis Simulation Program
WDMUtil	Watershed Data Management Utility
WEPP	Water Erosion Prediction Project
WES	Waterways Experiment Station
WMS	Watershed Modeling System
WSE	Water Surface Elevation

Chapter 1. Introduction

Among the various technical tools in water resources management strategies, modeling is a specific tool that allows quick analysis of water quantity and quality under diverse scenarios. It is an analytical tool that applies mathematical equations to represent and predict the natural processes within watersheds and waterbodies. When direct measurements are not available or cannot be completed, modeling provides best available data that characterize temporal and spatial variation of water quality. It helps users to understand the physical, chemical and biological processes within the watersheds, and helps to identify the critical processes and areas that control the water quality in watersheds and receiving waterbodies. It also predicts the impact of planned actions on water quality and ecosystems. Another application of modeling is to run models under diverse management scenarios. The results can provide a quick assessment of alternative management programs and thus allow decision makers to estimate and evaluate the pros and cons among different management strategies.

Mathematical models can be categorized based on different criteria. One fundamental category is based on the physical subject that a model attempts to describe. Rainfall-runoff models intend to depict the hydrological processes within a watershed. They depict how the precipitation is transferred into surface flow, interflow and groundwater flow. In many cases, they are able to estimate the sediment erosion and overland transport during storm events, and describe the transport and fate of associated water quality constituents. Unlike point source pollution, the runoff, sediment and associated water quality components enter the watercourses in an indiscrete and diffuse fashion. The models describing these processes are sometimes called nonpoint source models or watershed models.

On the other hand, receiving water quality models describe the transport and fate of water quality constituents in the receiving waterbodies, such as rivers, streams and reservoirs. They simulate the phenomena such as lake stratification, dissolved oxygen (DO) sag and eutrophication. The traditional applications of the receiving water quality models use upstream observations as boundary conditions to reflect the impact of upstream activities

on downstream water quality. However, real-world data for these boundary conditions are normally not collected at a frequency to fully describe the temporal variations of these driving forces. In addition, the impacts of upstream activities are not dynamically reflected in the model applications.

Recently, the contribution from nonpoint source pollution has been emphasized more and more. The concepts as well as the related legislation practices affect model development and applications. In the model development area, hybrid models are more and more popular. They integrate the rainfall-runoff and the receiving water quality models into one package and reflect the integral nature by describing a watershed and downstream receiving waterbodies as a complete unit. Both point source and nonpoint source pollution are considered. In the model application area, there are more and more linked model practices. Based on characteristics of the local watersheds and waterbodies, the nature of pollution sources and other specific considerations, the project managers, shareholders and scientists choose the best available models that describe the processes in each compartment. Then the modelers integrate these different models into one package in order to describe the big picture. These practices make it easier for decision makers to account for local specifications when evaluating water resources management plans, and for the public to understand the decision-making procedures.

1.1 *Model History*

The Occoquan Model effort can be traced back to the late 1970s when the digital revolution made mathematical simulation possible for a complex natural system. In 1977-1978, the mainframe model, named Occoquan Basin Computer Model (Hydrocomp Inc. 1978), was developed from Hydrocomp Simulation Programming (HSP) and Nonpoint Source Model (NPS). The modified HSP simulated hydrological processes while NPS estimated sediment erosion and other nonpoint source loads. Later, receiving water sub-models were added to represent Lake Manassas and Occoquan Reservoir as two-layer lakes. After the Upper Occoquan Sewage Authority (UOSA) Advanced Wastewater Treatment (AWT) plant went into operation, the model was modified in 1982 to account for the impact of UOSA. The discharge from UOSA was represented as a

point source in the model. The model had several successful applications including in a Fairfax County court case "Occoquan Basin Downzoning" in 1985 (NVPDC 1987).

The process to convert the mainframe model to a PC model was started in 1994, and several model upgrade procedures were taken to provide an "up-to-date defensible tool to review future conditions and the consequent requirements that may be indicated" (NVPDC 1994). After a watershed model review, HSPF replaced NPS/HSP as a pollutant loading and transport model. More importantly, a better reservoir model was decided upon to replace the simplified two-layer model for the Occoquan Reservoir to fully represent the reservoir water quality associated with stratification and dam operations. After careful evaluation, CE-QUAL-W2 was added to the model application. The resultant model proposed a simple linked model framework to enhance the accuracy of reservoir responses to alternative control strategies and to provide technical information on other management decisions such as BMP development. The simple linked model was not completed until 2003.

However, Lake Manassas, another principal waterbody in the Occoquan Watershed and a principal drinking water supply for the City of Manasssas, was not fully represented in the model application. In the mainframe version of the Occoquan Model, Lake Manassas was simulated as a two-layer lake. However, the details of the layers were not known due to poor documentation. During the major model update in 1994, no additional effort was taken to update the representation of Lake Manassas. As a result, the two-layer water quality model for Lake Manassas was not converted into a better hydrodynamic water quality model as was done for the Occoquan Reservoir. Instead, it was further simplified in the linked model applications and was represented as a completely-mixed lake in HSPF. Such simplification cannot fully represent the physical, chemical and biological processes in Lake Manassas. Furthermore, it cannot accurately estimate its impact on the downstream water quality. In the linked model application, Lake Manassas was a weak link.

1.2 *Research Goal and Objectives*

The principal goals of this research were to develop, calibrate and validate a complex linked model to simulate hydrology and water quality in the Occoquan Watershed and its principal waterbodies (Lake Manassas and Occoquan Reservoir), and to explore its application to land use scenarios.

To achieve this, the following objectives were proposed:

1. To develop a complex linked hydrology and water quality model for the Occoquan Watershed, which allows better representation of the physical, chemical and biological processes in the watershed and two principal waterbodies: Occoquan Reservoir and Lake Manassas;
2. To calibrate and validate the linked model, including hydrology, nutrients (nitrogen and phosphorus), temperature, dissolved oxygen, and algae; and,
3. To investigate the potential impact of urbanization on nutrient enrichment in the Occoquan Reservoir and to identify the critical land areas in the watershed.

1.3 *Dissertation Outline*

This dissertation includes an introductory chapter, a literature review chapter, independent chapters in a technical paper format, a chapter on algae simulation, a summary chapter, and a complete list of literature cited, followed by an appendix section.

Chapter 1: Introduction — This chapter provides an introduction to the current study, including the background, and discusses research objectives.

Chapter 2: Literature Review — This chapter reviews literature related to hydrology and water quality modeling, receiving water quality modeling, and linked model applications.

Chapter 3: The Hydrological Calibration and Validation of a Linked Watershed-Reservoir Model for the Occoquan Watershed, Virginia — This paper investigates the water budgets in the watershed and two waterbodies. Resulting data were

compared with observed flow data and water surface elevation data to evaluate the performance of the complex linked model.

Chapter 4: Temperature and Dissolved Oxygen Calibration and Validation of a Linked Model for the Occoquan Watershed, Virginia — This paper investigates the capability of the complex linked model to capture the spatial and temporal distribution of temperatures and DO in streams and two principal waterbodies.

Chapter 5: Modeling Soluble Inorganic Nitrogen Transport and Fate, and the Impact of Land Use Changes in the Occoquan Watershed Using a Linked Model Application — This paper investigates the transport and fate of two nitrogen species: ammonium nitrogen and oxidized nitrogen in the watershed and two principal waterbodies. Two land use development scenarios were developed and their impacts on nitrogen enrichment in the Occoquan Reservoir were investigated.

Chapter 6: Modeling Phosphorus Transport and the Impact of Land Use Changes on Receiving Water Quality in the Occoquan Watershed by Using a Linked Model Application — This paper investigates the transport and fate of orthophosphate phosphorus in the Occoquan Watershed and two principal waterbodies. Two land use development scenarios were developed and their impacts on phosphorus enrichment in the Occoquan Reservoir were investigated.

Chapter 7: Modeling Algae Dynamics and the Impact of Land Use Changes on Receiving Water Quality in the Occoquan Watershed by Using a Linked Model Application — This chapter investigates the algae dynamics in two principal waterbodies. The impact of increased upstream nutrient loads due to land development on the algae growth in the Occoquan Reservoir was investigated.

Chapter 8: Conclusions and Recommendations — This chapter provides a summary of research results and reviews whether the objectives have been achieved. Recommendations for future research and modeling improvement have also been included.

Literature Cited: This section provides a complete list of literature references cited.

Appendices: These provide research results that were not included in previous chapters. They include discussion on meteorological data collection and infilling; watershed delineation and segmentation; bathymetry and segmentation of Lake Manassas and Occoquan Reservoir; land use data; initial HSPF hydrology calibration using PEST; and the impacts of land use development on nutrient load production in individual segments, and hydrology activities in the Watershed.

Chapter 2. Literature Review

This section provides a review of the science behind two types of water quality models: rainfall-runoff models and receiving water models. Some widely-used public domain water quality models and their applications are also discussed.

2.1 *Rainfall-Runoff Models*

Rainfall-runoff models describe hydrology and pollutant generation during rainfall events, as well as transportation from source areas to the receiving waterbodies. In most cases, rainfall-runoff models provide hydrographs and loading histograms to describe the flow and load distribution over continuous hydrological events.

Rainfall-runoff models have a long history. The development of concepts and theories on the hydrological system can be tracked back to the early period of human history when the Greek philosopher Theophrastus described the hydrological cycle in the atmosphere and the Roman engineer Marcus Vitruvius described the one in the soil profile (Chow, et al. 1988). Since then, the study of hydrological systems has focused on concept development, such as infiltration, evaporation and transpiration, surface runoff, subsurface flow, and base flow.

2.1.1 Surface Water Hydrology

Hydrological modeling was originated in the 1850s when Mulvaney (1850) described the peak flow discharge as the product of the rainfall intensity, the area of the catchment and a coefficient dependent on the catchment characteristics. The method, also called the rational method, introduced a mathematical approach to describe the rainfall-runoff relationship. Although the rational method has been questioned due to its simplification, it is still widely used in storm sewer design. In 1932, Sherman introduced the unit hydrograph concept that results from one-inch excess rainfall in a specific drainage area (Sherman 1932). The method describes a linear relationship between direct runoff and excess rainfall, and is used to develop the direct runoff and streamflow hydrographs. In

the same period, Horton introduced the concept of the infiltration capacity and described it as "the maximum rate at which rain can be absorbed by a given soil when in a given condition" (Horton 1933). He used this concept to estimate the excess precipitation over infiltration and the resultant surface runoff (Horton 1940). In addition to Horton's infiltration theory, Green and Ampt (1911) proposed a physical-based model for infiltration that has been widely used in rainfall-runoff modeling. They applied a simplified concept of infiltration and developed a mathematical equation based on hydraulic conductivity and porosity. Philip (1957) developed another popular infiltration formula by solving the Richard's equation under certain conditions. These mathematical methods for infiltration have been used in rainfall-runoff modeling to estimate the surface runoff by abstracting infiltration from precipitation. The resultant surface runoff sometimes is referred to as the Hortonian overland flow. Table 2-1 below gives some common methods for infiltration estimation.

Table 2-1: Equations for Infiltration

Infiltration Equations	Formulas	Coefficients
Horton's Equation	$f(t) = f_c + (f_0 - f_c) \cdot e^{-k \cdot t} k$	f_0 : Initial rate f_c : Constant rate k : Decay constant t : Time
Phillip's Equation	$f(t) = \frac{1}{2} \cdot S \cdot t^{-0.5} + K$	S : Sorptivity K : Hydraulic conductivity
Green-Ampt Equation	$f(t) = K \cdot \left[\frac{\psi \cdot \Delta\theta}{F(t)} + 1 \right]$	ψ : Soil suction head θ : Soil moisture content K : Hydraulic conductivity F : Cumulative infiltration

Source: Chow et al. 1988

There are methods to quantify other abstractions such as evaporation and transpiration, interception, depression storage, etc. For instant, Thornthwaite and Holzman (1939) developed one of the earliest equations for evaporation based on the humidity gradient between land surface and the air, and wind speed across the land surface. This aerodynamic method assumes no energy supply limitation for evaporation. Another method, called the Energy Balance Method, describes the evaporation rate based on energy balance and assumes no vapor transport limitation. However evaporation is controlled by both processes: aerodynamics and energy supply. Therefore, it is

appropriate to develop a combination formula that integrates both processes. Penman (1948) proposed the first combination method for evaporation and its simplified formula was derived by Priestley and Taylor later (1972). Table 2-2 lists some common equations that are used in hydrological water quality models.

Table 2-2: Equations for Evaporation

ET Equations	Formulas	Coefficients
Thornthwaite-Holzman Equation	$E_a = B \cdot (e_{as} - e_a)$	B : Vapor transfer coefficient e_{as} : Vapor pressure at surface e_a : Ambient vapor pressure in air
Energy Balance Method	$E_r = 0.0353 \cdot R_n$	R_n : Net radiation
Penman Evaporation Equation	$E = \frac{\Delta}{\Delta + \gamma} \cdot E_r + \frac{\gamma}{\Delta + \gamma} \cdot E_a$	γ : Psychrometric constant Δ : Gradient of Saturated Vapor pressure at temperature T_a E_a : Evaporation rate from the aerodynamic method E_r : Evaporation rate from net radiation
Priestley-Taylor Equation	$E = 1.3 \cdot \frac{\Delta}{\Delta + \gamma} \cdot E_r$	γ : Psychrometric constant Δ : Gradient of Saturated Vapor pressure at temperature T_a E_r : Evaporation rate from net radiation

Source: Chow et al. 1988

In addition to the Hortonian method, another widely-used method to account for these abstractions from precipitation is called the SCS curve number method, developed by the Soil Conservation Service (SCS) (Mockus 1972). It assumes the ratio of actual surface retention to the potential retention to be the same as the ratio between direct runoff and potential runoff. The parameters required to calculate the surface runoff are precipitation and curve numbers (Equation 2-1), which are tabulated by SCS based on surface land use and coverage, soil type, and hydrological conditions. Although this approach was developed to estimate the daily runoff from daily rainfall, it has been used in rainfall-runoff models to estimate the infiltration and surface runoff in continuous hydrological simulations.

Equation 2-1: SCS Curve Number Equation

$$P_e = \frac{(P - 0.2 \cdot S)^2}{P + 0.8 \cdot S}$$

$$\text{where } S = \frac{1000}{CN} - 10$$

Where P: Precipitation (inch) and CN: Curve Number

2.1.2 Groundwater Hydrology

Henry Darcy (1856) introduced one of the fundamental equations in groundwater hydrology. He developed the empirical equation that relates water movement in porous saturated media to the hydraulic gradient. Modified formulas were developed by Dupuit to estimate steady flow in an unconfined aquifer and by Thiem to estimate the steady flow in a confined aquifer (Freeze and Cherry 1979). Based on the analogy between heat flow and water flow, Theis (1935) derived an equation for unsteady flow in a confined aquifer and provided the basis for quantitative groundwater hydrology. Jacob (1943) proposed an "effective average rate of precipitation" method to determine the contribution of precipitation to groundwater flow in streams. Later, Hantush and Jacob introduced a solution to predict drawdowns for a two-layer aquifer system (Freeze and Cherry 1979). These formulas have been used in watershed modeling to account for the contribution from groundwater.

2.1.3 Open Channel Hydrology

Early in 1871, Barre de Saint-Venant introduced the continuity equation and momentum equations to estimate the flow in an open channel (Table 2-3) (Chow, et al. 1988). These equations provide the foundation for distributed flow routing methods such as the kinematic wave, diffusion wave, and dynamic wave method. These methods have been used to estimate the spatial and temporal distribution of the flow at an outlet with known hydrographs. Lighthill and Whitham (1955) introduced the kinematic wave theory to flow routing in a long river, and this has been widely used to predict overland flow, channel flow, and other hydrological processes. Another popular kinematic wave equation is called the Muskingum-Cunge method that is applied to linear hydrological storage routing (Cunge 1969).

In addition to the distributed routing methods, there are lumped flow routing methods based on the storage-outflow relationship. Lumped flow routing doesn't consider the spatial variances in a system. Some examples include the modified Puls method (Chow

1951), the Muskingum method (Chow, et al. 1988) and linear reservoir method (Chow, et al. 1988).

Although the concepts and components of rainfall-runoff modeling were under development and improvement for a long time, rainfall-runoff modeling was made possible in the 1960s due to the development of digital computers. Crawford and his colleagues (1966) developed the Stanford Watershed Model that led to the Hydrological Simulation Program–Fortran (HSPF), which probably represents the first attempt to simulate different hydrological components in one system entity. During the same period, the Hydrological Engineering Center (1986) of the U.S. Army Corps of Engineers introduced HEC-1 to estimate the flood hydrograph. Since then, several rainfall-runoff models have been developed and distributed to the public. These include AGNPS, ANSWERS, GLEAMS, HSPF, PRMS, SWAT, SWMM, HEC-HMS and WEPP. A brief review of these public domain hydrological models is given below.

Table 2-3: Summary of Saint-Venant Equations

Continuity Equation

Conservation Form

$$\frac{\partial Q}{\partial x} + \frac{\partial A}{\partial t} = 0$$

Nonconservation Form

$$V \cdot \frac{\partial y}{\partial x} + y \cdot \frac{\partial V}{\partial x} + \frac{\partial y}{\partial t} = 0$$

Q : Flow Rate (L^3T^{-1})
A : Cross Section Area (L^2)
V : Flow Velocity at Point 1 (LT^{-1})
y : Water Depth (L)

Momentum Equation

Conservation Form

$$\frac{1}{A} \cdot \frac{\partial Q}{\partial t} + \frac{1}{A} \cdot \frac{\partial}{\partial t}\left(\frac{Q^2}{A}\right) + g \cdot \frac{\partial y}{\partial x} - g \cdot (S_0 - S_f) = 0$$

Local Acceleration Term | Convective Acceleration Term | Pressure Force Term | Gravity Force Term | Friction Force Term

Q : Flow Rate (L^3T^{-1})
A : Cross Section Area (L^2)
S_0 : Channel Bottom Slope (L/L)
S_f : Friction Slope (L/L)

Nonconservation Form

$$\frac{\partial V}{\partial t} + V \cdot \frac{\partial v}{\partial x} + g \cdot \frac{\partial y}{\partial x} - g \cdot (S_0 - S_f) = 0$$

Kinematic Wave
Diffusion Wave
Dynamic Wave

V : Flow Velocity at Point 1 (LT^{-1})
y : Water Depth (L)
S_0 : Channel Bottom Slope (L/L)
S_f : Friction Slope (L/L)

Source: Chow, et al. 1988

The Agricultural Non-Point-Source Pollution Model (AGNPS) (Young, et al. 1994) is an event-oriented distributed mathematical model developed by the United States Department of Agriculture (USDA) in the late 1980s. It describes a watershed as square grid cells with areas around 0.4-16 hectares. Twenty-two coefficients are used to characterize the hydrology, sediment erosion and nutrient loads in each grid. The flow and pollutants are routed through cells in a stepwise fashion to estimate the flow and pollutant loads at a watershed outlet. In the hydrological module, the SCS Curve Number method is used to estimate the surface runoff volume while the Smith algorithm is used to estimate the peak flow rates. However, AGNPS doesn't account for subsurface flows, common phenomena in agricultural land areas. The Modified Universal Soil Loss Equation (MUSLE) is applied to calculate sediment erosion from a single storm event. The sediment transport capacities are estimated by a modified stream power equation for five particle groups. AGNPS considers the transport of nitrogen, phosphorus and chemical oxygen demand (COD), which are further divided into two groups: soluble and particulate. The sediment-associated pollutants are related to the total sediment yield while the soluble pollutants account for the contribution from rainfall, fertilizer, and leaching. In 1998, AGNPS was modified into AnnAGNPS to expand its application to continuous multi-event systems. It has also been linked to Geographic Resources Analysis Support System (GRASS GIS) (GRASS Development Team 2005).

Areal Nonpoint Source Watershed Environment Response Simulation (ANSWERS) is a distributed continuous watershed-scale model. Originally, it was designed to simulate single storm events (Beasley, et al. 1980). The latest version ANSWERS 2000 has the capability to describe continuous hydrological events on non-urban areas (Bouraoui 1994). In contrast to lumped models, ANSWERS is a distributed parameter model which describes a watershed as homogeneous grid cells with uniform soil properties, slopes, land use, management practice, etc. Different characteristics among neighbor grids represent the heterogeneity of a watershed. This feature allows ANSWERS to identify the critical areas within a watershed as well as evaluate the impact of BMP implementation. The model simulates overland flow, infiltration, and channel flow within each grid by using physically-based equations. It simulates erosion and transport of particles with

various sizes. Because channel erosion isn't included (Bouraoui 1994), the model might under-predict the sediment erosion from land surfaces. The model describes the transport and interaction of both dissolved and sediment-associated nutrients. These include four nitrogen species (stable organic N, active organic N, nitrate and ammonium) and four phosphorus species (stable mineral P, active mineral P, soil organic P and labile P).

The Groundwater Loading Effects of Agricultural Management Systems (GLEAMS) model is another continuous field-scale model developed by USDA (Knisel and Davis 1999). As an extension of Chemicals, Runoff and Erosion from Agricultural Management Systems (CREAMS), GLEAMS is designed to estimate the "edge-of-field and root-of-bottom loadings of water, sediment, pesticides, and plant nutrients for complex climate-soil-management interactions" (Knisel and Davis 1999). It has three basic components: hydrology, sediment yield and chemical transport. In the hydrology part, a modified SCS Curve Number method is used to estimate the surface runoff volume and an empirical equation is applied to estimate the peak flow by using the hydraulic slope. MUSLE is adapted to calculate sediment erosion while a modified Yalin equation is used to estimate the sediment transport capacity. The nutrient transport part is further divided into the plant nutrient part and the pesticide part. GLEAMS can simulate up to 366p esticides simultaneously. It not only considers the surface transport of pesticides due to runoff and sediment, but also the movement within and through the root zones. In the plant nutrient part, it simulates the nitrogen and phosphorus cycles in the soil layers by estimating the transformation between organic and mineral nitrogen and phosphorus. It also considers the contribution of agricultural activities to the nutrient loadings, such as fertilizer application, animal waste application, and tillage.

Hydrological Simulation Program–Fortran (HSPF) is a conceptual lumped hydrological model designed to simulate various hydrological and associated water quality components in a watershed (Bicknell, et al. 2001). The origin of the model, called the Stanford Watershed Model (SWM), was developed in the 1960s. After being continuously updated, it is now the core program of the United States Environmental Protection Agency (USEPA) Better Assessment Science Integrating Point and Nonpoint Sources (BASINS) package. Different from single event simulation models, HSPF

describes a continuous series of hydrological events by using intensive rainfall and other meteorological data, such as temperature, solar radiation, wind speed, potential evaporation, and cloud cover. Based on hydrological characteristics, HSPF defines two types of land segments. The pervious land segments describe comprehensive hydrological and water quality processes that occur in forest, agricultural or other permeable land areas. Theoretical and empirical equations are applied to simulate moisture allocation among surface flow, interflow and baseflow. It also describes the sediment erosion, transportation and deposition on the land surfaces. Two methods are provided to simulate the water quality constituents: a simple relationship with water and sediment yield, or a detailed agricultural chemical approach. Impervious land segments describe water movement, sediment transport and water quality in a much simpler system based on similar concepts. Because pervious and impervious land areas are mixed-distributed, the model has limited capability to identify critical areas in a watershed. The runoff, along with associated water quality components, is passed to the reach section, where transport and fate in well-mixed streams and rivers are described. Diverse water quality constituents, including DO, carbonaceous biochemical oxygen demand (CBOD), nitrogen, phosphorus, algae and phytoplankton, can be simulated.

The Precipitation Runoff Modeling System (PRMS) (Leavesley, et al. 1983) is a distributed-parameter hydrological model designed to simulate the hydrographs of daily flows as well as single storm events. It defines watersheds as a series of homogeneous response units based on soil property, slope, vegetation, elevation, etc. It is developed in a modular fashion in order to "evaluate the impacts of various combinations of precipitation, climate, land-use or surface-water runoff" (Leavesley et al. 1983). For each grid, water balance and energy balance are performed on a daily basis. Then the contributions from each grid are area-weighted to produce the daily flow at the watershed outlet. PRMS considers sediment detachment and transport processes in interrill as well as rill areas, which are responsible for almost all sediment and sediment-associated pollutant movement (Carey and Simon 1984). It applies the Smith method and Hjelmfelt, Piest and Saxon method for rainfall detachment and flow detachment, respectively. The transport capacity is assumed to be linear relative to the detachment capacity. There is no

water quality module in PRMS. However, it has been linked to DAFLOW and MODFLOW in the Modular Modeling System (MMS) package, which provides an integrated watershed-modeling framework (Leavesley, et al. 1996).

Soil and Water Assessment Tool (SWAT) is a continuous physically-based watershed scale model (Neitsch, et al. 2002), another core model in the EPA BASINS package. The original model, called Simulator for Water Resources in Rural Basins (SWRRB), was developed in the 1980s. It is designed to simulate the long-term impact of management strategies on water quality issues on a relatively large-scale watershed. Based on land uses, soil properties and other information, watersheds are delineated into several subbasins. In each subbasin, daily precipitation and other meteorological data are applied to simulate hydrological processes on different soil layers, including snowfall and melting, surface runoff, infiltration, evaporation, subsurface flow, and groundwater flow. The model provides two equations to estimate surface runoff: SCS curve number and Green & Ampt infiltration method. A modified rational method is used to calculate runoff volumes and peak runoff rates that would be used to estimate sediment erosion. SWAT uses the MUSLE to estimate the long-term sediment erosion and yields. It simulates various chemical and biological processes to estimate nutrient cycles in soil layers, which include transformation and interaction among five nitrogen forms and six phosphorus forms, respectively. The results, along with surface runoff and sediment, are passed to the stream network that simulates the flow and water quality components in reservoirs or main channels. Different routing approaches can be applied to flow, sediment, nutrient and pesticide routing in reservoirs and main channels, which provide SWAT the flexibility to simulate diverse features.

Storm Water Management Model (SWMM) is a dynamic model designed to simulate water quality in urban areas (Huber and Dickinson 1988). It was developed in the early 1970s. After continuous updating over the years, it now has the capability to simulate either single storm events or continuous hydrological processes. It defines watersheds as homogeneous subcatchments with uniform land properties. Various hydrological processes in pervious and impervious land areas are simulated in the runoff module. Three methods (Horton, Green & Ampt, and Curve Number) are provided to estimate

flow distribution over different soil profiles in pervious areas. Rainfall interception and evaporation are accounted for in the depression storage. SWMM includes a flexible hydraulic module to represent diverse structure facilities in storm sewers and combined sewer systems, such as storage/treatment units, flow dividers, pumps, weirs, and orifices. In the transport module, three flow routing methods are available to link the surface runoff to the conveyance systems. As for the water quality aspect, SWMM has the capability to handle any user-defined pollutants associated with runoff. It simulates three activities that impact the pollutant loads in the land surface. These are buildup, washoff and street cleaning. It accounts for the routing through the pipe/channel network by using mass balance equations. In the storage-treatment module, SWMM considers the reduction of water quality concentrations in operation or storage units. It has been used to simulate water quality control facilities such as Best Management Practices (BMP).

The Hydrological Modeling System (HEC-HMS) is a physical based hydrological model developed by the Hydrological Engineering Center (HEC) of the U.S. Army Corps of Engineers (2000). It is designed for both event and long-term continuous simulations. Watersheds are depicted as any combination of six hydrological elements that include subbasin, river reach, reservoir, source and sink, junction, and diversion. It provides four methods to describe the observed precipitation events and four methods to produce hypothetic storm precipitation data that could be used to estimate direct runoff volumes. Subbasins are categorized into pervious and directly-linked impervious land areas, and three hydrological components (direct flow, base flow and flow losses) are simulated. Four methods are provided to estimate the cumulative losses due to evaporation, infiltration, interception, storage, etc. These are initial and constant-rate, deficit and constant-rate, SCS curve number, and Green & Ampt methods. Base flows are estimated by using the constantly varying method, exponential recession method or linear reservoir model. Given the upstream hydrographs, HEC-HMS applies five routing methods to solve the momentum and continuity equations to estimate the downstream hydrographs. These are the lag method, the kinematic wave method, the Muskingum-Cunge method, the Muskingum method, and the modified Puls method. These functions provide great flexibility to simulate or predict hydrological events. However, the current version of

HEC-HMS does not simulate snowfall and melting processes, which limits its application in areas receiving snow. The model does not simulate any water quality components.

Water Erosion Prediction Project (WEPP) is a process-based distributed parameter model, which was developed by the USDA Agriculture Research Service in the 1980s (Flanagan and Nearing 1995). The model is designed to estimate soil erosion from agricultural activities. It describes a watershed as a series of hillslopes that are linked by channels. WEPP consists of twelve components that simulate the hydrology and sediment processes in a watershed. The weather component generates the daily climate information by using a stochastic model. The hydrology component has several process modules including infiltration, overland flow hydraulics, water balance, subsurface hydrology, hillslope erosion and deposition. The Green & Ampt equation and the kinematic wave method are used in the hydrological components to estimate the surface flow volumes and flow rates. Both interrill and rill sediment movement are considered under the erosion component. Soil detachment capacity is based on hydraulic shear stress and transport capacity is estimated by a simplified Yalin equation. The model has the capability to represent the spatial variance of sediment erosion and transport, which allows the capture of critical areas in a watershed that contribute mostly to the sediment yields. WEPP does not have a water quality component.

2.2 *Receiving Water Quality Models*

Receiving water quality models are used to simulate the transport and fate of pollutants in receiving waterbodies, such as streams, rivers, lakes, reservoirs and estuaries.

One type of receiving water quality model describes the processes in the mixing zone when point source pollutants are discharged into receiving waters. A typical example is CORMIX (Jirka, et al. 1991). It analyzes turbulent buoyant jet mixing patterns that describe the flow and pollutant characteristics in discharge plumes. The model has the capability to predict the mixing behavior of various discharge patterns, such as power plant cooling water, desalinization plants and municipal wastewater. Other mixing zone models include Plume and Visual Plume (Frick, et al. 2001).

Unlike mixing zone models, the other type is capable of describing the transport and movement of pollutants further downstream. These are sometimes called “far-field” models (Novotny 2002). Usually they assume the system is mixed and there is no spatial difference in contaminant concentration in a defined volume. They could be one-, two- or three-dimensional. Because the natural system is described in a broader region, they are often applied to simulate the water quality on a waterbody scale. The following is a review of this type of receiving water quality models.

The early modeling effort can be traced back to the 1920s when the Ohio River Commission performed a comprehensive survey to investigate the pollution and self-recovery mechanism of the Ohio River. In this investigation, one of the most significant water quality models, the Streeter-Phelps equation, was created (Streeter and Phelps 1925). The equation described the variation of DO with water movement downstream. The model considered two significant processes that controlled the overall DO balance in the river system. One was the degradation of dissolved and suspended organic materials that were discharged from sewage plants, and the other was the atmospheric reaeration. These two opposing processes were combined to estimate the DO deficit. The authors applied a first-order differential equation to describe the natural system and provided an analytical solution to describe the DO balance over time. The results showed that when dissolved and suspended organic materials entered the river, they were consumed by organisms and thus reduced the DO concentrations in the river. However, the concentration gradient between water and atmosphere was another driving force and atmospheric oxygen entered the river system in order to compensate for the DO deficit. There was a critical point when biochemical oxygen demand (BOD) decay and reaeration were in balance and the DO deficit was at its highest. After this point, the river eventually recovered to the unpolluted condition. A classic plot, known as the DO sag curve, was developed.

In the 1960s, the Delaware Estuary Comprehensive Study (DECS) was undertaken to investigate possible solutions to water quality problems in the Delaware Estuary (Udall, et al. 1966). In this study, the classic Streeter-Phelps model was extended to a more comprehensive one. The Delaware Estuary was mathematically represented as a

30-segment system. BOD and DO mass balance equations were written for each section. These differential equations were solved simultaneously and the results successfully described the DO variation along the estuary. The model had the capability to simulate the impact of time-dependent waste loads discharged at different locations. And it represented the real system more closely by using spatially- and temporally-varying decay and reaeration rates. The model was expanded to simulate other water quality components such as chlorides and coliform bacteria. Another significant application of the model was to execute it for various scenarios, such as changing loads at multiple locations. These scenarios provided a rapid assessment of alternative management strategies for pollution control and helped the decision makers to evaluate the different approaches.

Due to the successful applications of mathematical models in water quality simulation, government agencies and other scientific groups began to increasingly use this new technology. Model applications were no longer restricted to DO and BOD simulations. In the 1960s, a consulting company called Water Resources Engineers, Inc (WRE 1968) and a group at the Massachusetts Institute of Technology (Huber, et al. 1972) applied heat energy principles to impoundment systems and developed the first mathematical scheme to describe vertical changes of temperature in one-dimensional reservoir models. Later on, these models were extended to simulate other water quality components such as DO and nutrients. In 1972, the Tennessee Valley Authority (TVA 1972) released a comprehensive report and developed better formulae to represent air-water heat exchanges. These empirical equations have been widely used in other water quality models such as CE-QUAL-W2.

The mathematical models were extended to estimate the trophic state of a waterbody because the extensive nutrient loadings into lakes and reservoirs altered the chemical and biological characteristics dramatically and aroused significant environmental concerns. In the 1970s, QUAL I was developed to simulate stream temperature and water quality constituents such as DO and BOD. EPA specified it as the basis to develop other advanced water quality models. QUAL II, an updated version released a few years later, had the capability to describe the impact of nutrient loads on the DO balance in a more

complicated stream. Due to its flexibility and good documentation, QUAL II was adopted and improved by other agencies, such as the Southeast Michigan Council of Governments (SEMCOG) and the National Council of the Paper Industry for Air and Stream Improvement (NCASI). They adopted numerical solutions to simulate oxygen demand, nutrient cycle, advection, and dispersion, which enhanced the simulation capabilities and extended the application of QUAL II. In 1987, USEPA, NCASI and Tufts University performed a cooperative program and developed QUAL2E, which has been "widely used for waste load allocations, discharge permit determinations, and other conventional pollutant evaluations in the United States" (Brown and Barnwell 1987).

QUAL2E is a steady-state one-dimensional water quality model available from the USEPA. It applies a finite difference approach to solve mass transport equations simultaneously. It is suitable for describing dendritic stream systems with point discharge/withdrawal or distributed loads/losses. Although algae are simulated as chlorophyll *a*, the model provides more accurate prediction of DO by including algae, nutrient and DO interaction. In addition, it is able to simulate fifteen water quality constituents, including nitrogen, phosphorus, coliform and CBOD. Typical applications of QUAL2E include stream assimilative capacity, waste load allocation studies and diurnal response to climatology (Brown and Barnwell 1987). Currently, it is included in the BASINS package as an in-stream water quality model.

Unlike simple steady-state water quality models, hydrodynamic and water quality models describe the spatial and temporal characteristics of rivers, lakes, reservoirs and estuaries. The fundamental mechanisms behind the models are the conservation of mass, energy and momentum (Equation 2-2).

Equation 2-2: Conservation Equation (Source: Martin and McCutcheon (1999)

$$Accumulation = \pm Transport \pm Sources/Sinks$$

$$\text{Where : } Accumulation = \underbrace{\frac{\Delta\left[\left(\rho \cdot c_p \cdot T\right) \cdot V\right]}{\Delta t}}_{Heat}, \underbrace{\frac{\Delta\left[(\rho) \cdot V\right]}{\Delta t}}_{Water\ Mass}, \underbrace{\frac{\Delta\left[(C) \cdot V\right]}{\Delta t}}_{Constituent\ Mass}, \text{ or } \underbrace{\frac{\left[(\rho \cdot u) \cdot V\right]}{\Delta t}}_{Momentum}$$

The conservation of mass states that "all the materials can neither be created nor destroyed, but merely transferred or transformed" (Martin and McCutcheon 1999). In water quality models, it is applied to write the mass balance equations or advection-dispersion equations for water quality constituents. Conservation of water mass forms the basis for the continuity equation, which is applied to estimate flow volume.

Conservation of energy states that "the energy associated with matter entering any system plus the net energy added is equal to the energy leaving the system, or the net work done by the system, and the change in energy within the system" (Martin and McCutcheon 1999). It is the theory behind the heat balance for temperature estimation in water quality modeling. It helps to simulate thermal stratification and related mixing energy in lakes and reservoirs. In water quality models, temperature is normally used as a measure for heat energy.

The conservation of momentum states "momentum can neither be created nor destroyed, but merely transferred or transformed" (Martin and McCutcheon 1999). Unlike mass and energy, momentum is a vector quantity. It has both magnitude and direction. The conservation of momentum indicates that momentum is conserved in all three coordinate axes (*x, y* and *z*). It is applied to estimate the flow velocity and direction.

To simulate the changes of energy, mass and momentum, the water system is normally defined by a series of control volumes. A control volume is "an object for analysis separated from all other objects by a known or defined boundary" (Martin and McCutcheon 1999). A control volume with open boundary allows the transport of mass, energy and momentum either into or out of the system. The size of a control volume varies. It ranges from nearly 500^3 m^3 for large-scale systems to 50^3 m^3 for smaller ones (Martin and McCutcheon 1999), depending on system characteristics. If variables are expressed as instantaneous terms in a control volume, six basic equations can be written for conservation of mass, energy and momentum (Table 2-4).

Table 2-4: Equations for Flow and Transport Written In Term of Instantaneous Variables

Continuity	$\frac{\partial u}{\partial x}+\frac{\partial v}{\partial y}+\frac{\partial w}{\partial z}=q$
Constituent Transport	$\frac{\partial C}{\partial t}=-\frac{\partial(uC)}{\partial x}-\frac{\partial(vC)}{\partial y}-\frac{\partial(wC)}{\partial z}+\frac{\partial}{\partial x}(D_m\frac{\partial C}{\partial x})+\frac{\partial}{\partial y}(D_m\frac{\partial C}{\partial y})+\frac{\partial}{\partial z}(D_m\frac{\partial C}{\partial z})\pm Sources/Sinks$
Momentum	
x-direction	$\frac{\partial u}{\partial t}=-\frac{\partial(uu)}{\partial x}-\frac{\partial(vu)}{\partial y}-\frac{\partial(wu)}{\partial z}+\frac{\partial}{\partial x}(\psi\frac{\partial u}{\partial x})+\frac{\partial}{\partial y}(\psi\frac{\partial u}{\partial y})+\frac{\partial}{\partial z}(\psi\frac{\partial u}{\partial z})+g_x$
y-direction	$\frac{\partial v}{\partial t}=-\frac{\partial(uv)}{\partial x}-\frac{\partial(vv)}{\partial y}-\frac{\partial(wv)}{\partial z}+\frac{\partial}{\partial x}(\psi\frac{\partial v}{\partial x})+\frac{\partial}{\partial y}(\psi\frac{\partial v}{\partial y})+\frac{\partial}{\partial z}(\psi\frac{\partial v}{\partial z})+g_y$
z-direction	$\frac{\partial w}{\partial t}=-\frac{\partial(uw)}{\partial x}-\frac{\partial(vw)}{\partial y}-\frac{\partial(ww)}{\partial z}+\frac{\partial}{\partial x}(\psi\frac{\partial w}{\partial x})+\frac{\partial}{\partial y}(\psi\frac{\partial w}{\partial y})+\frac{\partial}{\partial z}(\psi\frac{\partial w}{\partial z})+g_z$
Equation of State	$\rho=f(C,T)$

Source: Martin and McCutcheon. 1999.

Where:

u : Instantaneous Velocity Along x Axis (LT^{-1})
v : Instantaneous Velocity Along y Axis (LT^{-1})
w : Instantaneous Velocity Along z Axis (LT^{-1})
C : Concentration (M/L^3)
T : Temperature
ρ : Density (M/L^3)
Dm : Diffusion Coefficient (L^2T^{-1})
ψ : Kinematic Viscosity of Water (L^2T^{-1})

Due to the mathematical challenges in solving these equations, in the late 19th century, Reynolds proposed a simplified method to split the instantaneous velocities into two parts: mean values and the fluctuation from the mean values. By substituting instantaneous velocities with these two components, the motion and constituent transport equations are simplified because the average of the fluctuation values are zero by definition. This simplified approach is known as the Reynolds average equations and is widely used in water quality models such as CE-QUAL-W2. Table 2-5 shows the simplified six basic motion and transport equations.

These equations could be used in three-dimensional, or two-dimensional systems if variation of velocity in one axis is assumed to be negligible compared to the other two physical axes. For example, for a long, narrow waterbody, flow variation could be assumed to be relatively small along the lateral (y) axis. The simplified equations for this case are shown in Table 2-6.

Table 2-5: Reynolds Averaged Equations of Flow and Transport

Continuity	$\frac{\partial u}{\partial x}+\frac{\partial v}{\partial y}+\frac{\partial w}{\partial z}=q$
Constituent Transport	$\frac{\partial C}{\partial t}=-\frac{\partial (uC)}{\partial x}-\frac{\partial (vC)}{\partial y}-\frac{\partial (wC)}{\partial z}-\frac{\partial}{\partial x}\overline{u'C'}-\frac{\partial}{\partial y}\overline{v'C'}-\frac{\partial}{\partial z}\overline{w'C'}+\frac{\partial}{\partial x}(D_m\frac{\partial C}{\partial x})+\frac{\partial}{\partial y}(D_m\frac{\partial C}{\partial y})+\frac{\partial}{\partial z}(D_m\frac{\partial C}{\partial z})\pm Sources/Sinks$
Momentum	
x-direction	$\frac{\partial u}{\partial t}=-\frac{\partial (uu)}{\partial x}-\frac{\partial (vu)}{\partial y}-\frac{\partial (wu)}{\partial z}-\frac{\partial}{\partial x}\overline{u'u'}-\frac{\partial}{\partial y}\overline{v'u'}-\frac{\partial}{\partial z}\overline{w'u'}+\frac{\partial}{\partial x}(\psi\frac{\partial u}{\partial x})+\frac{\partial}{\partial y}(\psi\frac{\partial u}{\partial y})+\frac{\partial}{\partial z}(\psi\frac{\partial u}{\partial z})+g_x$
y-direction	$\frac{\partial v}{\partial t}=-\frac{\partial (uv)}{\partial x}-\frac{\partial (vv)}{\partial y}-\frac{\partial (wv)}{\partial z}-\frac{\partial}{\partial x}\overline{u'v'}-\frac{\partial}{\partial y}\overline{v'v'}-\frac{\partial}{\partial z}\overline{w'v'}+\frac{\partial}{\partial x}(\psi\frac{\partial v}{\partial x})+\frac{\partial}{\partial y}(\psi\frac{\partial v}{\partial y})+\frac{\partial}{\partial z}(\psi\frac{\partial v}{\partial z})+g_y$
z-direction	$\frac{\partial w}{\partial t}=-\frac{\partial (uw)}{\partial x}-\frac{\partial (vw)}{\partial y}-\frac{\partial (ww)}{\partial z}-\frac{\partial}{\partial x}\overline{u'w'}-\frac{\partial}{\partial y}\overline{v'w'}-\frac{\partial}{\partial z}\overline{w'w'}+\frac{\partial}{\partial x}(\psi\frac{\partial w}{\partial x})+\frac{\partial}{\partial y}(\psi\frac{\partial w}{\partial y})+\frac{\partial}{\partial z}(\psi\frac{\partial w}{\partial z})+g_z$
Equation of State	$\rho=f(C,T)$

Source: Martin and McCutcheon 1999.

Table 2-6: Reynolds Average Equations for a Two Dimensional System Assuming Lateral (y-Axis) Homogeneity

Continuity	$\frac{\partial u}{\partial x}+\frac{\partial w}{\partial z}=q$
Constituent Transport	$\frac{\partial C}{\partial t}=-\frac{\partial (uC)}{\partial x}-\frac{\partial (wC)}{\partial z}-\frac{\partial}{\partial x}\overline{u'C'}-\frac{\partial}{\partial z}\overline{w'C'}+\frac{\partial}{\partial x}(D_m\frac{\partial C}{\partial x})+\frac{\partial}{\partial z}(D_m\frac{\partial C}{\partial z})\pm Sources/Sinks$
Momentum	
x-direction	$\frac{\partial u}{\partial t}=-\frac{\partial (uu)}{\partial x}-\frac{\partial (wu)}{\partial z}-\frac{\partial}{\partial x}\overline{u'u'}-\frac{\partial}{\partial z}\overline{w'u'}+\frac{\partial}{\partial x}(\psi\frac{\partial u}{\partial x})+\frac{\partial}{\partial y}(\psi\frac{\partial u}{\partial y})+\frac{\partial}{\partial z}(\psi\frac{\partial u}{\partial z})+g_x$
y-direction	----
z-direction	$\frac{\partial w}{\partial t}=-\frac{\partial (uw)}{\partial x}-\frac{\partial (ww)}{\partial z}-\frac{\partial}{\partial x}\overline{u'w'}--\frac{\partial}{\partial z}\overline{w'w'}+\frac{\partial}{\partial x}(\psi\frac{\partial w}{\partial x})+\frac{\partial}{\partial y}(\psi\frac{\partial w}{\partial y})+\frac{\partial}{\partial z}(\psi\frac{\partial w}{\partial z})+g_z$
Equation of State	$\rho=f(C,T)$

Source: Martin and McCutcheon 1999.

Analytical solutions provide a quick check for numerical solutions, and some typical examples include Euler's method, Heun's method, and the Runge-Kutta method. Because hydrodynamic and water quality models involve a series of differential equations, the analytical approach is rarely used.

The more popular approaches include finite difference and finite element. Finite difference is the analog of the derivative, and the difference approximations include forward, backward and centered difference. Because the hydrodynamic models involve both spatial and temporal variables, they are mixed to solve complicated equations. For example, the forward-time/centered space (FTCS) method applies forward difference in time variables and centered difference in spatial variables, while the forward time/backward space (FTBS) method applies forward difference in time variables and backward difference in spatial variables.

The finite element approach defines the system as "finite elements" (segments or elements that are small in relation to the physical size of the system), which are connected with each other through nodal points. The continuous quantities over the elements are represented by assembling quantities at discrete points. It has the capability to represent waterbodies with greatly complex geometries.

For water quality models of rivers and streams, flow characteristics are essential to the systems. The Chezy equation and the Manning Equation are among the most widely used empirical approaches to estimate the flow velocities that don't vary over time (Table 2-7). For channels with varying depths or cross sections in space, the Bernoulli energy equation is able to estimate the relationship between flow velocity and energy losses due to structures and irregular channels. Unsteady flow methods are used to predict dynamic flow conditions when flows are varying over time and space (Table 2-7). Flow velocities are predicted by solving the continuity and momentum equations simultaneously. In order to reduce the complexity involved, some terms of the momentum equations are ignored during calculation. The simplified methods include the kinematic wave method, diffusion method and quasi-steady method.

Table 2-7: Hydraulic Methods for Different Flows

Steady, uniform flow

Manning's Equation

$$U = \frac{\delta}{n} \cdot R^{2/3} \cdot S^{1/2}$$

δ : Unit Conversion ($L^{1/3}T^{-1}$)
n : Manning Roughness (unitless)
R : Hydraulic Radius (L)
S : Channel Slope (L/L)

Chezy's Equation

$$U = C_z \cdot \sqrt{R \cdot S}$$

$$Where: C_z = \sqrt{2g / C_D}$$

C_z : Chezy Coefficient (LT^{-2})
C_D : Drag Coefficient (unitless)
R : Hydraulic Radius (L)
S : Channel Slope (L/L)

Steady, Nonuniform Flow

Bernoulli Equation

$$\frac{U_1^2}{2g} + h_1 = \frac{U_2^2}{2g} + h_2 + \frac{n^2}{\delta^2 \cdot R^{4/3}} \cdot U^2 \cdot \Delta x$$

U_1 : Flow Velocity at Point 1 (LT^{-1})
U_2 : Flow Velocity at Point 2 (LT^{-1})
h_1 : Water Surface Elevation at Point 1 (L)
h_2 : Water Surface Elevation at Point 2 (L)
δ : Unit Conversion ($L^{1/3}T^{-1}$)
R : Hydraulic Radius (L)
n : Manning Roughness (unitless)
Δx : Channel Length Between Point 1 and Point 2 (L)

Unsteady flow

Continuity Equation

$$\frac{\partial Q}{\partial x} + \frac{\partial A}{\partial t} = 0$$

Q : Flow Rate (L^3T^{-1})
A : Cross Section Area (L^2)

Momentum Equation

$$\frac{\partial U}{\partial t} + U \cdot \frac{\partial U}{\partial x} + g \cdot \frac{\partial \gamma}{\partial x} - g \cdot (S_0 - S_f) = 0$$

Kinematic Wave
Diffusion Wave
Dynamic Wave

U : Flow Velocity at Point 1 (LT^{-1})
γ : Water Depth (L)
S_0 : Channel Bottom Slope (L/L)
S_f : Friction Slope (L/L)

Source: Chow, et al. 1988

In water quality models for lakes and reservoirs, thermal stratification and mixing mechanisms are of concern because they affect water quality in different limnetic zones. There are two commonly-used methods to estimate the surface water temperature. One is based on the heat exchange at the water surface. In general, the heat flux at the water surface is considered to be the summation of solar radiation, back radiation from the water surface, atmospheric radiation, evaporation heat loss and conduction. Either physically- or empirically-based equations are used to estimate the contribution from each energy source or sink. The resultant net thermal energy flux provides water surface temperature information. The other method, called the equilibrium temperature method, is simpler in concept. It assumes that the surface water temperature tends to approach an equilibrium temperature based on meteorological conditions. So, if the water surface temperature is less than the equilibrium temperature, there will be a heat gain in the water system, and vice versa. Because analytical methods use more-direct calculation processes, the equilibrium method requires less computation time and storage space.

In addition to the QUAL series, there are other receiving water quality models. Those in the public domain include WASP, CE-QUAL-W2, EFDC/HEM3D, and RAM series.

The Water Quality Analysis Simulation Program (WASP) is a dynamic water quality model that can simulate the transport and fate of conventional and toxic contaminants in water columns as well as benthic segments (Wool, et al. 2003). By applying the compartment approach, the model allows the application on one-, two- or three-dimensional spaces. The model provides the linkage between hydrodynamic models and water quality models. The hydrodynamic model DYNHYD5 originated from the Dynamic Estuary Model (Feigner and Harris 1970). After several updates, the current version applies the finite difference approach to solve the one-dimensional continuity equation and momentum equations. The results allow the prediction of water velocities, water heads, flows and volumes, which can be used in water quality models to calculate the mass transport and contaminant concentrations. In addition to DYNHYD5, WASP provides linkages to RIVMOD, a one-dimensional river hydrodynamic model, as well as SED3D, a three-dimensional lake hydrodynamic model. WASP6 includes two kinetic

water quality models, EUTRO4 and TOXI4. EUTRO can simulate conventional pollutants such as DO, nitrogen, phosphorus, CBOD, and phytoplankton. It considers the interaction and transport between waterbodies and benthic layers and has also been used to investigate the eutrophication and nutrient loading to lakes and reservoirs. TOXI4 can simulate the transport and transformation of toxic materials, such as metals and organic chemicals. This module is used to simulate Polychlorinated Biphenyls (PCB), kepone and volatile organic pollutants.

CE-QUAL-W2 is a two-dimensional hydrodynamic and water quality model sponsored by the U.S. Army Corps of Engineers (Cole and Wells 2003). It describes the longitudinal and vertical variations of flow and water quality characteristics while assuming homogeneity along the lateral direction. Such considerations make the model capable of describing water quality gradients in relatively long and narrow waterbodies such as rivers, reservoirs, estuaries and lakes. Waterbodies are defined using variable grid spacing. Six governing equations (the continuity equation, momentum equations for x- and z-axis, free surface equation, state equation and hydrostatic pressure equation) are written for each grid. A finite difference method with numerical schemes is applied to solve these equations for each grid at each time step. The results describe the spatial and temporal variance of the surface elevation, horizontal velocity, vertical velocity and constituent concentrations. The model simulates diverse conventional water quality constituents, such as temperature, DO, CBOD, nutrients, algae, etc. The latest version of CE-QUAL-W2 is able to simulate multiple algae groups as well as epiphyton/periphyton groups. These improvements increase its capability to represent the nutrient cycles and eutrophication.

HEM3D is a three-dimensional hydrodynamic and water quality model. Its concept is similar to that of WASP, which links a hydrodynamic model to a water quality model. A model called the Environmental Fluid Dynamics Code (EFDC) was originally developed for the Chesapeake Bay estuarine system. It defines the waterbodies as orthogonal curvilinear horizontal grids and sigma-stretched vertical grids (Hamrick 1996), which allows the model to represent irregular shoreline configurations. A second order accurate spatial finite difference method is used to solve the governing momentum equations and a

finite difference scheme with an internal-external mode splitting procedure is used for time integration. This allows the model to describe physical processes like flow circulation, tide and vertical mixing driven by wind. The momentum equations are dynamically integrated with two transport-transformation equations (Eulerian and Lagrangian), which describe the spatial and temporal distribution of temperature, salinity and sediment. Later, a water quality model (TMP-VIMS), which was developed mostly from the 3-D Chesapeake Bay water quality model CE-QUAL-ICM (Park, et al. 1995), was included. The resultant model is known as HEM3D, which simulates the spatial and temporal distribution of twenty one water quality constitutes that include DO, CBOD, three suspended algae groups, nutrients, and silica. It also includes a sediment process module to describe nutrient fluxes between water layers and sediment layers. These features not only allow HEM3D to predict the eutrophication level of waterbodies, but also to predict the long-term impact of upstream nutrient loadings.

The RMA series are one-, two-, or three-dimensional hydrodynamic and water quality models originally developed by Resource Management Associates (RMA) and currently maintained by U.S. Army Corps of Engineers Waterways Experiment Station (WES). RMA2 (King, et al. 2001) is a two dimensional, vertically averaged hydrodynamic model to estimate the surface elevation and horizontal velocity of free-surface flow systems. The depth-averaged mass balance and momentum equation are solved by the finite element method using the Galerkin method of weighted residuals. The Gaussian approach and a nonlinear finite difference method are used to perform spatial and temporal integration. RMA4 (King, et al. 2003) applies similar hydrodynamic concepts for flow estimation. However, it has the capability to estimate the transport and fate of up to six conservative or non-conservative constituents. RMA10 is a multiple-dimensional hydrodynamic model that can perform either steady-state or dynamic simulation for flow velocity, salinity and sediment transport. The finite element method is applied to solve the governing equations. RMA11 is designed to accept the flow velocity and depth data generated by RMA2 or RMA10 as input data. These inputs are used to estimate the transport and fate of water quality constituents such as DO, BOD, ammonia, nitrate, phosphate, algae, and suspended solids. The RMA series models are widely used to

estimate the hydrodynamic and constituent fate in surface waters and have been incorporated into the Surface Water Modeling System (SMS).

2.3 *Linked Models*

In the early period of water quality model development, most models were designed to handle one particular system. For example, QUAL2E was developed to estimate the DO and BOD variation along a stream at steady state while HSPF was created to simulate the hydrological processes on land surfaces. So there are groundwater models, surface water models, hydrological models, river models, etc. Each of them simulates different compartments in the interrelated natural system and represents the impacts from surroundings as boundary conditions and initial conditions. The assumption behind these model applications is that each watercourse is independent and isolated from surrounding systems. This allows the representation of specific characteristics associated with individual waterbodies.

One reason for this was the limitation of computer resources. There was inadequate storage and memory to perform simulation for complex systems. However, this has become less and less important due to improvement in computation techniques and resources. Although these models have the capability to predict and evaluate water quality in individual waterbodies, they cannot address the interaction between different waterbodies and surroundings. Thus they have limited applications in complex and multi-purpose management programs.

The digital revolution of the late twentieth century in personal computers allowed sufficient memory and storage space to perform high-resolution calculations. This made mathematical simulation possible for complex and interdependent systems. At the same time, more and more attention has been paid to integrated watershed management. Such programs address the natural system from a big-picture point of view and treat a watershed as a single entity. Individual waterbodies and processes in a watershed are regarded as components of a larger system. The behavior of each waterbody and interaction between various processes help to shape the whole system. When water

quality models play a role in these management programs, it requires the consideration of how to represent such a complex condition correctly. A single model application might not be appropriate. For example, a watershed model is designed to estimate the hydrological processes over the land as well as through different soil layers. Most watershed models provide stream routing functions to estimate flow distribution into receiving waterbodies, which are generally assumed to be rivers or streams. However, these simulations might not be as accurate as those done by special river or stream models.

When the management objective is the water quality in the receiving streams, the application of a watershed model might not be able to give predictions as accurately as those from stream models. On the other hand, when a stream model is applied to perform simulation for streams, it actually isolates the streams from the surrounding system and the decision-makers end up treating the system piece by piece instead of as an interdependent system.

Such dilemmas give rise to considerations of linked model application. In this case, modelers can select an appropriate watershed model to estimate the hydrological processes in the system and link it to a stream model that estimates the receiving stream water quality. Thus, the physical and chemical processes described by the individual models in a linked model application represent the inter-linkage in the natural system. Model applications can be regarded as an analytical tool in integrated watershed management strategies.

Linked model applications are particularly helpful to represent a more complex natural system. A good example is the linkage of surface water models with groundwater models. Interaction between groundwater and surface water has been intensively studied (Freeze and Cherry 1979). In some areas, surface water quality is highly related to the groundwater system, and vice versa. In some modeling applications, a state-of-the-art groundwater model, MODFLOW, has been linked to other surface water models to account for the interaction between groundwater and surface water (Jobson and Harbaugh 1999; Ramireddygari, et al. 2000; Sophocleous, et al. 1999; Swain and Wexler 1996). It

has also been linked with an open channel flow model called UNET (Walton, et al. 2000). The coupled model, called MODNET, has been applied in the south Florida region to estimate the transient flow between aquifer and streams. Table 2-8 gives some examples of integrated model applications that link two or more models.

Table 2-8: Linked Model Applications

Locations	Models	Applications
— (Swain and Wexler 1996)	MODFLOW→BRANCH	To integrate groundwater and surface water models
— (Jobson and Harbaugh 1999)	DADLOW→MODFLOW	To couple surface water and groundwater model applications
Back Bay Watershed, MS (MDEQ 2002)	NPSN→WASP	For Fecal Coliform TMDL program
Ballona Creek watershed, CA (Burian, et al. 2001)	CIT→SWMM	To Estimate atmospheric deposition and storm water washoff of nitrogen species
Black Rock Forest, NY (Engel, et al. 2002)	SPA→TOPMODEL	To estimate plant-water relations in a forest catchment
Bluegrass Watershed, Iowa (Tim, et al. 1995)	ARC/INFO→AGNPS	To evaluate the effectiveness of BMPs
Brandywind Creek Watershed, DE (USEPA 2001)	HSPF→EFDC	To update flow and sediment transport routines in HSPF
Calaveras River Watershed, CA (Anderson, et al. 2000)	MM5*→HEC-HMS	To predict the reservoir inflows resulting from watershed runoff
Cooper River, SC (Conrads and Roehl Jr. 1999)	BRANCH→BLTM	To simulate stream temperature and DO
Coosa River Basin, GA (GDNR 2003)	LSPC→EFDC	For chlorophyll *a* TMDL program
Dade County, FL (Walton, et al. 2000)	MODFLOW↔UNET	To couple open channel and groundwater model applications
Estero-Imperial-Cocohatchee Watershed, FL (Christierson, et al. 2001)	MIKE SHE→MIKE 11	For flood management
Grande Ronde River Basin, OR (Chen, et al. 1998b)	SHADE→HSPF	Simulation of stream temperature on a watershed scale
Higginsville River Basin, MI (Leung, et al. 2001)	SWAT→ Finite Element Lake Model	Simulation of atrazine transport
Ipswich River Basin, MA (Zarriello, et al. 2001)	STRMDEPL→HSPF	Estimation of groundwater contribution to stream flow
Klamath River, OR (Campbell, et al. 2001)	MODSIM→HEC-5Q	DO and temperature simulation.
Lahn-Dill Hill-Country, Germany (Weber, et al. 2001)	ProLand→SWMM ProLand→ELLA	Estimation of land use effect on agricultural economics, ecology and hydrology.
Lake Gaston, VA (Gatling, et al. 2000)	SWMM→QUAL2E	To control water flow and TSS in the lake
Lower Arkansas River Basin, CO (Dai and Labadie 2001)	MODSIM↔QUAL2E	Estimation of irrigation return flow
Lake Waco-Bosque River Basin, TX (Flowers, et al. 2001)	SWAT→HSPF	To evaluate phosphorus control strategies
Mill Creek, KS (York, et al. 2002)	ATMOS→VOS-MOD	A coupled aquifer–land surface–atmosphere model
Nepean-Hawkesbury River, Sydney, Australia (Perrens, et al. 1991)	TIDEWAY→HSPF	River system and catchment hydrology simulation
Norris and Melton Hill Reservoirs, TN	ADYN-RQUAL→CE-QUAL-W2	Linkage of two reservoirs for temperature and DO simulation

(Hadjerioua, et al. 2001)		
Northern Tampa Bay, FL (Ross, et al. 2004)	HSPF↔MODFLOW	Integrated surface/groundwater simulate
Rattlesnake Creek Basin, KS (Sophocleous, et al. 1999)	SWAT → MODFLOW	Simulation of surface water, groundwater and stream interaction
Salt Creek, IL (Ishii, et al. 1998)	HSPF→FEQ**	Real-time streamflow simulation
Tamil Nadu, India (Selvarajan, et al. 1995)	CAPSIM→ASIM→SAHEL	Evaluation of groundwater recharge through percolation ponds
Texas Rivers (Lizarraga 1996)	QUALTX→DAFLOW/BLTM	TMDL evaluation for Texas rivers.
Townbrook Watershed, NY (Cerucci and Conrad 2003)	SWAT→REMM	Investigation of impact of riparian buffer on sediment and phosphorus load reduction
Wet Walnut Creek Watershed, KS (Ramireddygari, et al. 2000)	MODFLOW→POTYLDR	Integration of groundwater and surface water models

*Full Equation Model, a dynamic-wave routing model sponsored by USGS
** PSU/NCAR mesoscale model for precipitation forecas

Another benefit of a linked model application is the ability to address multidisciplinary management objectives. Water quality models are not only used to simulate straightforward water quality problems such as water quality standards violations and eutrophication, but they are used in more complex management applications. For example, the Chesapeake Bay watershed is a multi-state watershed and all states within the watershed have some level of responsibility for water quality issues in the Bay. It is important and necessary to identify the contribution from each potential source, so that each state or jurisdiction is able to set allocation targets based on the overall pollution reduction goal. This program, called the Tributary Strategy, had been carried out in the Bay since 2000 (Chesapeake Bay Program Office 2000). The Bay model has been used to determine the contributions from potential sources and thus provide pollution reduction goals for each of them. It provides a scientific framework for stakeholder groups to understand and contribute to the pollution reduction program.

Zhen et al. (2004) coupled a modified AGPNS to an optimization algorithm called the scatter search methodology. The linked model application helped to identify the optimal location and configuration for storm BMPs based on the long-term storm evaluation within the studied watershed.

Another trend in modeling applications is to link water quality models with ecological models. The purposes of such linked model applications are to estimate water quality impact on ecological systems and associated costs and benefits that are of more concern to stakeholders and more understandable by the public. For instance, a probability network model was developed to estimate the nitrogen TMDL for the Neuse River Estuary (Borsuk, et al. 2003). The model integrated an oxygen concentration module, a benthic oxygen demand module and a shellfish survival model. Thus the output of the model not only indicated the impact of nitrogen loads to DO and Chlorophyll *a*, but also its impact on shellfish survival. Such ecological considerations provided a scientific approach to TMDL decisions.

Saito et al. (2001) applied CE-QUAL-W2 to simulate the impact of the new temperature control operation on Shasta Lake, California. The predicted phytoplankton production generated by CE-QUAL-W2 was fed into a food web-energy transfer model that applied stable isotope analysis with an optimization procedure for diet proportion. The results from the interdisciplinary application addressed the impact of the new dam operation on various fish species, which could not be achieved by stand-alone models.

Anderson et al. (1997) applied linked models to investigate salmon survival, growth and migration in the Sacramento River and San Francisco Bay/Delta system. RAM-2 was used to simulate the hydrodynamic characteristics in the system, which provided flow information for RAM-11 to perform the water quality estimation. The output from the combined RAM-2 and RAM-11 was fed into an ecological model called RMATRK, which had the capability to estimate spatial and temporal distribution of salmon as well as their population. This integrated model application allowed investigation of the impact of flow, temperature and salinity on the aquatic ecosystem, which was represented by salmon distribution in this case.

Water quality models are also linked with decision support systems (DSS), which integrate hydrological, social, economic and ecological information into one system. It helps the decision makers to evaluate alternative scenarios with respect to all these considerations. For example, Bosch et al. (2003) linked HSPF to a statistical model to evaluate the hydrological and economic impact of land use changes on the Back Creek Basin, Virginia. Hydrological responses to various land use scenarios were simulated by HSPF. The statistical economic model evaluated the impact of land use changes on land values, tract development costs, as well as tax revenues. The results indicated the environmental and economic tradeoff of different residential development scenarios. It provided the best available information and helped decision makers to make desired profit while still protect the environment.

Cerucci et al. (2003) estimated potential efficiency and budget to install riparian buffers along a watershed in New York. SWAT and REMM were applied to simulate pollutant loads from agricultural areas with or without buffers. The resultant pollution loads were

used by a riparian decision support system (RDSS) to estimate the cost and width of the riparian buffer zones.

Chen et al. (1999) proposed a decision support system to estimate TMDL for the Catawba River Basin of South and North Carolina. A modified Integrated Lake-Watershed Acidification Study model (ILWAS) was used to simulate hydrology, nonpoint source load and water quality. This information was fed into a total maximum daily load (TMDL) module that estimated the TMDL under different control levels. A consensus module helped stakeholders to reach an agreement of watershed management plans.

Geographic Information System (GIS) has been widely used with watershed model applications. It links map products with water resource management and provides variables that are difficult to obtain through traditional approaches. It improves database storage and organization by incorporating diverse databases, such as digital elevation model (DEM) products, State Soil Geographic (STATSGO) products and land use maps. It helps to determine watershed characteristics as well as stream morphology (Miller, et al. 2003) that can be used by other models. For example, ArcView has been used with HSPF to predict the long-term impact of urbanization on surface water runoff (Brun and Band 2000). Smith et al. (1992) linked GIS with a sediment erosion and transport model to predict sediment yield for major single storm events in North Reelfood Creek Watershed, Tennessee. Lunetta et al. (2003) applied GIS analysis to identify waterbodies as salmon habitats in Oregon and Washington. The results provided management guidance for salmon habitat preservation and restoration efforts. Dymond et al. (2004) developed a GIS based spatial decision support system (SDSS) for Back Creek watershed in Virginia. They applied GIS as a user interface to manage different spatial and temporal information. Hydrological, economic and ecological models were integrated into one system to provide a full estimation of the impact of alternative development scenarios.

Recognizing the benefits of integrated model applications in water resource management, government agencies and other research groups have been involved in developing such all-in-one models. Generally, such integrated models are designed for technical and

non-technical people to address multi-disciplinary water resource management decisions. A common user interface provides a straightforward way to manage disparate data and operate individual processes in an integrated system. It also provides a framework to integrate scientific models with management models such as economic, social and ecological models. The results from these complex model applications would offer the best available information for decision makers. Some examples include Better Assessment Science Integrating Point and Nonpoint Sources (BASINS), Watershed Modeling System (WMS), Surface Water Modeling System (SMS), Modules Modeling System (MMS) and TMDL Modeling Toolbox (Table 2-9).

Table 2-9: Integrated Model Frameworks

	Sponsors	System Delineation	Watershed Models	Receiving Water Models	Other Models	Applications
BASINS	USEPA	Automatic and Manual	HSPF, SWAT	QUAL2E	PLOAD	Free to the public
WMS	DoD	Automatic	HEC-1 (HEC-HMS) TR-20 TR-55 Rational Method, NFF MODRAT HSPF	HEC-RAS CE-QUAL-W2	GSSHA	Free to DoD and USEPA employees
SMS	DoD	Automatic	—	ADCIRC STWAVE CGWAVE RMA2 RMA4 SED2D RMA10-WES FESWMS HIVEL2D	—	Free to DoD employees
MMS	USGS	Automatic	PRMS	DAFLOW TOPFLOW	User defined modules	Free to the public
Toolbox	USEPA	Automatic and Manual	LSPC WAMView SWMM	EPDRiv1 QUAL2K CONCEPTS EFDC WASP	—	Free to the public

BASINS is an EPA sponsored "multipurpose environmental analysis system for use by regional, state, and local agencies in performing watershed and water quality based studies" (USEPA 2004b). It was designed to meet three objectives: "(1) to facilitate examination of environmental information, (2) to provide an integrated watershed and

modeling framework, and (3) to support analysis of point and nonpoint source management alternatives" (USEPA 2004b). It integrates a national environmental database and a GIS database to provide input data for water quality models. It also provides utilities to manage output information. It includes two watershed delineation functions (manual and automatic). There are four models inside the BASINS package: an in-stream water quality model (QUAL2E), two watershed water quality models (HSPF and SWAT) and a simplified nonpoint source annual loading model (PLOAD). BASINS is free to the public.

Watershed Modeling System (WMS) is sponsored by the Department of Defense. It is "a comprehensive graphical modeling environment for all phases of watershed hydrology and hydraulics" (EMS-I Inc. 2002b). It integrates a group of models behind a GIS-based interface. It provides input and output utilities to facilitate database management. It includes a drainage module that provides an automatic watershed delineation function based on digital elevation, land use and soil data. The hydrological models include HEC-1 (HEC-HMS), TR-20, TR-55, Rational Method, NFF, MODRAT, and HSPF. The hydraulic models include HEC-RAS and CE-QUAL-W2. A two dimensional hydrological model called GSSHA is also included in WMS to simulate the interaction between surface water and groundwater. Users have great flexibility to combine appropriate models for specific objectives. It is free to employees of the Department of Defense, USEPA, or onsite contractors of these agencies.

Surface-Water Modeling System (SMS) is another model package sponsored by the Department of Defense. It is a "comprehensive software package that facilitates the understanding and management of coastal and inland waterways and wetland areas" (EMS-I Inc. 2002a). It includes an automatic mesh/grid generation to create two- and three-dimensional finite element meshes and finite difference grids for systems. It provides a graphic interface to integrate various hydraulic and coastal models, which include ADCIRC, STWAVE, CGWAVE, RMA2, RMA4, SED2D, RMA10-WES, FESWMS, and HIVEL2D. These models have the capabilities to simulate surface elevation and flow velocities for one-, two-, or three-dimensional systems. They are suitable for both steady-state and dynamic systems. It is applied to simulate contaminant

migration, salinity intrusion, sediment transport, etc. SMS is free to employees of the Department of Defense.

Modules Modeling System (MMS) is "an integrated system of computer software that has been developed to provide the research and operational framework needed to support the development, testing, and evaluation of physical-process algorithms and to facilitate the integration of user-selected sets of algorithms into an operational model" (Leavesley, et al. 1996). The complex model system, developed by the US Geological Survey, provides a GIS-based common user interface to facilitate pre-process and post-process components. Models are available through a module library, which includes a variety of mathematical formulae for water, energy and biogeochemical processes. Users have the flexibility to represent systems of interest by combining any processes. It allows the users to build their own models by using existing models. Currently, DAFLOW, TOPFLOW and PRMS are included in the module library. MMS also allows users to write their own modules by using preferred algorithms. A watershed delineation function for distributed parameter models is included. MMS is free to the public.

TMDL Modeling Toolbox is another model sponsored by USEPA (USEPA 2004a). It includes components from two other complex model applications: Watershed Characterization System (WCS) and Watershed Assessment Model (WAMView). WCS provides users initial data of the watershed characteristics such as watershed boundaries, land uses, soil data, environmental monitoring data, etc. This information can be quickly analyzed and used to generate a watershed characteristics report. In addition, WCS has some extensions that can be used in TMDL programs, which include a sediment budget model, mercury-loading model and LSPC/HSPF. Besides assessment tools, Toolbox provides three watershed models and five receiving water models. They are LSPC, WAMView, SWMM, EPDRiv1, QUAL2K, CONCEPTS, EFDC and WASP. All these models are integrated into a GIS-based interface. Users have the flexibility to combine desired models to perform estimation of TMDL for streams, lakes and estuaries.

2.4 *References*

Anderson, J.D., Orlob, G.T. and King, I.P. (1997). *Linking Hydrodynamic, Water Quality, and Ecological Models to Simulate Aquatic Ecosystem Response to Stress: Case Study of Juvenile Salmon Migration in the Sacramento River and San Francisco Bay/Delta System*. Environmental and Coastal Hydraulics: Protecting the Aquatic Habitat, American Society of Civil Engineers, New York.

Anderson, M.L., Chen, Z.Q., Kavvas, M.L. and Feldman, A. (2000). Coupling HEC-HMS with Atmospheric Models for the Prediction of Watershed Runoff. *Building Partnerships - 2000 Joint Conference on Water Resource Engineering and Water Resources Planning & Management*, Virginia.

Beasley, D. B., Huggins, L.F. and Monke, E.J. (1980). ANSWERS: A Model for Watershed Planning. *Transactions of the ASAE*, **23**(4), 938-944.

Bicknell, B.R., Imhoff, J.C., Kittle, J.L., Jobes, T.H. and Donigian, A.S. (2001). *Hydrological Simulation Program-Fortran HSPF Version 12 User's Manual*, U.S. Environmental Protection Agency, National Exposure Research Laboratory, Athens, Georgia.

Borsuk, K.E., Stow, C.A. and Reckhow, K.H. (2003). Integrated Approach to Total Maximum Daily Load Development for Neuse River Estuary using Bayesian Probability Network Model (Neu-BERN). *Journal of Water Resources Planning and Management*, **129**(4), 271-282.

Bosch, D.J., Lohani, V.K., Dymond, R.L., Kibler, D.F. and Stephenson, K. (2003). Hydrological and Fiscal Impacts of Residential Development: A Virginia Case Study. *Journal of Water Resources Planning and Management*, **129**(2), 107-114.

Bouraoui, F. (1994). *Development of a Continuous, Physically-Based, Distributed Parameter, Nonpoint Source Model*, Ph.D. Dissertation, Virginia Polytechnic Institute and State University, Blacksburg. Virginia.

Brown, L. C. and Barnwell, T. O. (1987). *The Enhanced Stream Water Quality Models QUAL2E and QUAL2E-UNCAS: Documentation and User Manual*, Environmental Resources Laboratory, Environmental Protection Agency, Athens, Georgia.

Brun, S.E. and Band, L.E. (2000). Simulating Runoff Behavior in an Urbanizing Watershed. *Computers, Environment and Urban Systems*, **24**(1), 5-22.

Burian, S.J., Streit, G.E., McPherson, T.N., Brown, M.J. and Turin, H.J. (2001). Modeling the Atmospheric Deposition and Stormwater Washoff of Nitrogen Compounds. *Environmental Modelling & Software*, **16**(5), 467-479.

Campbell, S.G., Hanna, R.B., Flug, M. and Scott, J.F. (2001). Modeling Klamath River System Operations for Quantity and Quality. *Journal of Water Resources Planning and Management*, **127**(5), 284-294.

Carey, W.P. and Simon, A. (1984). *Physical Basis and Potential Estimation Techniques for Soil Erosion Parameters in the Precipitation-Runoff Modeling System (PRMS)*, U.S. Geological Survey, Nashville, Tennessee.

Cerucci, M. and Conrad, J.M. (2003). The Use of Binary Optimization and Hydrologic Models to Form Riparian Buffers. *Journal of the American Water Resources Association*, **39**(5), 1167-1180.

Chen, C.W., Herr, J., Ziemelis, L., Goldstein, R.A. and Olmsted, L. (1999). Decision Support System for Total Maximum Daily Load. *Journal of Environmental Engineering*, **125**(7), 653-659.

Chen, Y.D., Carsel, R.F., McCutcheon, S.C. and Nutter, W.L. (1998). Stream Temperature Simulation of Forested Riparian Areas: I. Watershed-Scale Model Development. *Journal of Environmental Engineering*, **124**(4), 304-315.

Chesapeake Bay Program Office. (2000). *Geology of the Chesapeake*, Chesapeake Bay Program Office, Annapolis, Maryland.

Chow, V.T. (1951). A Practical Procedure of Flood Routing. *Civil Engineering And Public Works Review*, **46**(452), 586-588.

Chow, V.T., Maidment, D.R. and Mays, L.W. (1988). *Applied Hydrology*, McGraw-Hill Inc., New York.

Christierson, B., Dabbs, C., Soerensen, H. and Kjelds, J. (2001). An Integrated Flood Management Model for the Estero-Imperial-Cocohatchee Watershed. *Urban Drainage Modeling*, Reston, Virginia.

Cole, T. M. and Wells, S. A. (2003). *CE-QUAL-W2: A Two-Dimensional Laterally Averaged, Hydrodynamic and Water Quality Model, Version 3.2 User Manual*. U.S. Army Corps of Engineers, Washington, D.C.

Conrads, P.A. and Roehl Jr., E.A. (1999). Comparing Physics-Based and Neural Network Models for Simulating Salinity, Temperature, and Dissolved Oxygen in a Complex, Tidally Affected River Basin. *Proceedings of the 1999 South Carolina Environmental Conference*, Myrtle Beach, South Carolina.

Crawford, N.H. and Linsley, R.K. (1966). *Digital Simulation in Hydrology: Stanford Watershed Model IV*. Stanford University, Palo Alto. California.

Cunge, J.A. (1969). On the Subject of a Flood Propagation method (Muskingum Method). *Journal of Hydraulics Research*, **7**(2), 205-230.

Dai, T. and Labadie, J.W. (2001). River Basin Network Model for Integrated Water Quantity/Quality Management. *Journal of Water Resources Planning and Management*, **127**(5), 295-305.

Darcy, H. (1856). *The Public Fountains of the City of Dijon (translation of les fontaines publiques de la Ville de Dijon)*, Patricia Bobeck (translator), Kendall/Hunt Publishing Company, Dubuque, Iowa (2004).

Dymond, R.L., Regmi, B., Lohani, V.K. and Dietz, R. (2004). Interdisciplinary Web-Enabled Spatial Decision Support System for Watershed Management. *Journal of Water Resources Planning and Management*, **130**(4), 290-300.

EMS-I Inc. . (2002a). *SMS8.1-Overview*. South Jordan, Utah.

EMS-I Inc. (2002b). *WMS7-Overview*. South Jordan, Utah.

Engel, V.C., Stieglitz, M.M., Williams, M. and Griffin, K.L. (2002). Forest Canopy Hydraulic Properties and Catchment Water Balance: Observations and Modeling. *Ecological Modelling*, **154**(3), 263-288.

Feigner, K.D. and Harris, H.S. (1970). *Documentation Report- FWQA Dynamic Estuary Model*, U.S. Department of Interior, Federal Water Quality Administration, Washington D.C.

Flanagan, D.C. and Nearing, M.A. (1995). *USDA Water Erosion Prediction Project Hillslope Profile and Watershed Model Documentation*, USDA-ARS National Soil Erosion Research Laboratory, West Lafayette, Indiana.

Flowers, J.D., Hauck, L.M. and Kiesling, R. (2001). *USDA: Lake Waco-Bosque River Initiative: Water Quality Modeling of Lake Waco Using CE-QUAL-W2 for Assessment of Phosphorus Control Strategies*, Texas Institute for Applied Environmental Research, Texas.

Freeze, A.R. and Cherry, J.A. (1979). *Groundwater*, Prentice-Hall, Inc, New Jersey.

Frick, W.E., Roberts, P.J.W., Davis, L.R., Keyes, J., Baumgartner, D.J. and George, K.P. (2001). *Dilution Models for Effluent Discharges, 4th Edition (Visual Plumes) Draft*, U.S. Environmental Protection Agency, Athens, Georgia.

Gatling, L.A., Kardash, A.O. and Yoon, J. (2000). Spatiotemporal Water Quality Modeling of Pipeline Water Intake Lake Gaston, Virginia. *Building Partnerships - 2000 Joint Conference on Water Resource Engineering and Water Resources Planning & Management*, Virginia.

Georgia Department of Natural Resources (2003). *Draft: Total Maximum Daily Load Evaluation for the Little River Embayment in the Coosa River Basin for Chlorophyll α.*, Georgia.

GRASS Development Team. (2005). *Geographic Resources Analysis Support System (GRASS) Programmer's Manual*. Trento, Italy.

Green, W.H. and Ampt, G.A. (1911). Studies on Soil Physics, Part I: The Flow of Air and Water Through Soil. *Journal of Agricultural Science*, **4**(1), 1-24.

Hadjerioua, B., Lindquist, K.F. and Siler, V. (2001). Linking TVA's Norris and Melton Hill Reservoirs Water Quality: CE-QUAL-W2 Models. *World Water Congress 2001, Bridging the Gap: Meeting the World's Water and Environmental Resources Challenges*, Florida.

Hamrick, J.M. (1996). *User's Manual for the Environmental Fluid Dynamics Computer Code*, Virginia Institute of Marine Science, Virginia.

Horton, R. E. (1933). The Role of Infiltration in the Hydrological Cycle. *Transactions of the American Geophysical Union*, **14**, 446-460.

Horton, R. E. (1940). An Approach Toward A Physical Interpretation of Infiltration-Capacity. *Soil Science Society of America*, **5**, 399-417.

Huber, W.C., Harleman, D.R.F. and Ryan, P.J. (1972). Temperature Prediction in Stratified Reservoirs. *Proceedings of American Society of Civil Engineers, Journal of Hydraulics Division*, **98**(4), 645-666.

Huber, W.C. and Dickinson, R.E. (1988). *Storm Water Management Model User's Manual, Version 4*, U.S. Environmental Protection Agency, Athens, Georgia.

Hydrological Engineering Center. (1986). *HEC-1 Flood Hydrograph Package: User's Manual*. Davis, California.

Hydrocomp Inc. (1978). *The Occoquan Basin Computer Model Calibration, Verification and User's Manual*. Georgia, USA.

Ishii, A.L., Charlton, T.J., Ortel, T.W. and Vonnahme, C.C. (1998). Operational Modeling System with Dynamic-Wave Routing. *Water Resources and the Urban Environment: Proceedings of the 25th Annual Conference on Water Resources Planning and Management*, Illinois.

Jacob, C.E. (1943). Correlation of Ground-Water Levels and Precipitation on Long Island New York. *Transactions, American Geophysical Union*, **25**, 564-573.

Jirka, G.H., Doneker, R. L. and Barnwell, T.O. (1991). CORMIX: An Expert System for Mixing Zone Analysis. *Water Science and Technology*, **24**(6), 267-274.

Jobson, H.E. and Harbaugh, A.W. (1999). *Modifications to the Diffusion Analogy Surface-Water Flow Model (DAFLOW) for Coupling to the Modular Finite-Difference Ground-Water Flow Model (MODFLOW)*. U.S. Geological Survey, Virginia.

King, L., Donnell, B.P., Letter, J.V., McAnally, W.H., Thomas, W.A. and LaHatte, C. (2001). *Users Guide to RMA2 WES Version 4.5*, U.S. Army Corps of Engineers, Vicksburg, Mississippi.

King, L., Letter, J.V. and Donnell, B.P. (2003). *Users Guide to RMA4 WES Version 4.5* U.S. Army Corps of Engineers, Vicksburg, Mississippi.

Knisel, W.G. and Davis, F.M. (1999). *GLEAMS Groundwater Loading Effects of Agricultural Management Systems, Version 3.0 User Manual*, U.S. Department of Agriculture, Tifton, Georgia.

Leavesley, G., Restrepo, P.J., Markstrom, S.L., Dixon, M. and Stannard, L.G. (1996). *The Modular Modeling System (MMS): User's Manual*. U.S. Geological Survey, Denver, Colorado.

Leavesley, G.H., Lichty, R.W., Troutman, B.M. and Saindon, L.G. (1983). *Precipitation-Runoff Modeling System: User's Manual*, U.S. Geological Survey, Denver, Colorado.

Leung, K.S., R.L., Segar Jr. and Burr, S.A. (2001). Atrazine Transport Modeling in a Rural Missouri Watershed. *Bridging the Gap: Meeting the World's Water and Environmental Resources Challenges Proceedings of the World Water and Environmental Resources Congress*, Florida.

Lighthill, M. J. and Whitham, G.B. (1955). On Kinematic Waves, I: Flood Movement in Long Rivers. *Proceedings of the Royal Society of London*, **229**, 245-252.

Lizarraga, J. (1996). *Using QUALTX and DAFLOW/BLTM to Simulate Water Quality in Texas Rivers*. U.S. Geological Survey, Maryland.

Lunetta, R.S., Cosentino, B.L., Montgomery, D.R., Beamer, E.M. and Beechie, T.J. (2003). *Watershed-Based Evaluation of Salmon Habitat*. GIS for Water Resources and Watershed Management, Taylor & Francis Group, New York.

Martin, J.L. and McCutcheon, S.T. (1999). *Hydrodynamics and Transport for Water Quality Modeling*, CRC Press. Inc., Florida.

Mississippi Department of Environmental Quality. (2002). *Fecal Coliform TMDL for the Back Bay of Biloxi and Biloxi Bay: Coastal Streams Basin, Harrison and Jackson Counties, Mississippi.*, Mississippi.

Miller, S.N., Guertin, D.P. and Goodrich, D.C. (2003). *Deriving Stream Channel Morphology Using GIS-Based Watershed Analysis*. GIS for Water Resources and Watershed Management, Taylor & Francis Group, New York.

Mockus, V. (1972). *National Engineering Handbook: Estimation of Direct Runoff from Storm Rainfall*. Soil Conservation Service, Portland, Oregon.

Mulvaney, T.J. (1850). On the Use of Self-Registering Rain and Flood Gauges in Making Observation of the Relations of Rainfall and of Flood Discharges in a Given Catchment. *Proceedings of the Institution of Civil Engineers*, **4**, 18-31.

Neitsch, S.L., Arnold, J.R., Kiniry, J.R., Williams, J.R. and King, W.K. (2002). *Soil and Water Assessment Tool Theoretical Documentation Version 2000*. Texas Water Resources Institute, College Station, Texas.

Novotny, V. (2002). *Water Quality: Diffuse Pollution and Watershed Management*, 2nd Edition. John Wiley & Sons Inc., New Jersey.

Northern Virginia Planning District Commission. (1994). *Mission Statement for the Occoquan Basin Model Upgrade*. Annandale, Virginia.

Northern Virginia Planning District Commission. (1987). *Reverification of Occoquan Basin Computer Model: Post Audit No.2 With 1982-1984 Monitoring Data*. Virginia.

Park, K., Kuo, A.Y., Shen, J. and Hamrick, J.M. (1995). *A Three-Dimensional Hydrodynamic-Eutrophication Model (HEM-3D): Description of Water Quality and Sediment Process Submodels*, Virginia Institute of Marine Science, College of William and Mary, Virginia.

Penman, H.L. (1948). Natural Evaporation from Open Water, Bare Soil and Grass. *Proceedings of the Royal Society of London*, **193**, 120-146.

Perrens, S., Druery, B., Plastrier, B., Nielsen, J., Greentree, G.S. and Fisher, I. (1991). Nepean-Hawkesbury River Water Quality Modeling. *International Hydrology & Water Resrouces Symposium*, Australia.

Philip, J.R. (1957). The Theory of Infiltration: 1. The Infiltration Equation and Its Solution. *Soil Science*, **83**(5), 345-357.

Priestley, C.H.B. and Taylor, R.J. (1972). On the Assessment of Surface Heat Flux and Evaporation Using Large-Scale Parameters. *Monthly Weather Review*, **100**, 81-92.

Ramireddygari, S.R., Sophocleous, M.A. , Koelliker, J.K., Perkins, S.P. and Govindaraju, R.S. . (2000). Development and Application of a Comprehensive Simulation Model to Evaluate Impacts of Watershed Structures and Irrigation Water Use on Streamflow and

Groundwater: the Case of Wet Walnut Creek Watershed, Kansas, USA. *Journal of Hydrology*, **236**(3-4), 223-246.

Ross, M., Geurink, J., Aly, A., Tara, P., Trout, K. and Jobes, T. (2004). *Integrated Hydrological Model (IHM) Volume I: Theory Manual*. Tampa Bay Water and Southwest Florida Water Management District, Florida.

Saito, L., Johnson, B.M., Bartholow, J. and Hanna, R.B. (2001). Assessing Ecosystem Effects of Reservoir Operations Using Food Web-Energy Transfer and Water Quality Models. *Ecosystem*, **4**(2), 105-125.

Selvarajan, M., Bhattacharya, A.K. and Penning de Vries, F.W.T. (1995). Combined Use of Watershed, Aquifer and Crop Simulation Models to Evaluate Groundwater Recharge Through Percolation Ponds. *Agricultural Systems*, **47**(1), 1-24.

Sherman, L.K. (1932). Streamflow from Rainfall by the Unit-Graph Method. *Engineering News Review*, **108**, 501-505.

Smith, R.H., Sahoo, S.N. and Moore, L.W. (1992). A GIS Based Synthetic Watershed Sediment Routing Model. *Water Resources Planning and management: Saving a Threatened Resource, In Search of Solutions: Proceedings of the Water Resources Sessions at Water Forum NY*, New York.

Sophocleous, M.A., Koelliker, J.K., Govindaraju, R.S., Birdie, T., Ramireddygari, S.R. and Perkins, S.P. (1999). Integrated Numerical Modeling for Basin-Wide Water Management: The Case of the Rattlesnake Creek Basin in South-Central Kansas. *Journal of Hydrology*, **214**(1-4), 179-196.

Streeter, H.W. and Phelps, E.R. (1925). *A Study of the Pollution and Natural Purification of the Ohio River*, United States Public Health Service, Washington D.C.

Swain, E.D. and Wexler, E.J. (1996). *A Coupled Surface-Water and Ground-Water Flow Model (MODBRANCH) for Simulation of Stream-Aquifer Interaction*. U.S. Geological Survey Techniques of Water-Resources Investigations, U.S. Geological Survey, Virginia.

Tennessee Valley Authority. (1972). *Heat and Mass Transfer Between a Water Surface and the Atmosphere*, Tennessee Valley Authority, Tennessee.

Theis, C.V. (1935). The Relation Between the Lowering of the Piezometric Surface and The Rate and Duration of Discharge of a Well Using Groundwater Storage. *Transaction, American Geophysical Union*, **16**, 519-524.

Thornthwaite, C.W. and Holzman, B. (1939). The Determination of Evaporation from Land and Water Surfaces. *Monthly Weather Review*, **67**(1), 4-11.

Tim, U.S., Jolly, R. and Liao, H. (1995). Impact of Landscape Feature and Feature Placement on Agricultural Non-Point-Source-Pollution Control. *Journal of Water Resources Planning and Management*, **121**(6), 463-470.

U.S. Army Corps of Engineers. (2000). *Hydrological Modeling System HEC-HMS Technical Reference Manual*. Davis, California.

Udall, S.L., Quigley, J.M., McLeman, E.L., Geismar, E.V. and Thomann, R.V. (1966). *Delaware Estuary Comprehensive Study: Preliminary Report and Findings*, U.S. Department of the Interior, Philadelphia, Pennsylvania.

U.S. Environmental Protection Agency (2001). *One-Dimensional Hydrodynamic/Sediment Transport Model for Stream Networks*. Washington D.C.

U.S. Environmental Protection Agency. (2004a). *About BASINS 3.0-A Powerful Tool for Managing Watersheds*. Washington D.C.

U.S. Environmental Protection Agency. (2004b). *TMDL Modeling Toolbox Overview*. Washington D.C.

Walton, R., Wexler, E.J., Chapman, R. and Welter, D. (2000). MODNET: An Integrated Groundwater/Open-Channel Flow Model. *Building Partnerships - 2000 Joint Conference on Water Resource Engineering and Water Resources Planning & Management*, Virginia.

Water Resources Engineers, Inc. (1968). *Prediction of Thermal Energy Distribution In Streams and Reservoirs*, Water Resources Engineers, Inc.

Weber, A., Fohrer, N. and Moeller, D. (2001). Long-term Land Use Changes in a Mesoscale Watershed Due to Socio-Economic Factors — Effects on Landscape Structures And Functions. *Ecological Modelling*, **140**(1-2), 125-140.

Wool, T.A., Ambrose, R.B., Martin, J.L. and Cormer, E.A. (2003). *Water Quality Analysis Simulation program (WASP) Version 6.0 Draft: User's Manual*. U.S. Environmental Protection Agency, Atlanta, Georgia.

York, J.P., Person, M., Gutowshi, W.J. and Winter, T.C. (2002). Putting Aquifers into Atmospheric Simulation Models: An Example from the Mill Creek Watershed, Northeastern Kansas. *Advances in Water Resources*, **25**(2), 221-238.

Young, R.A., Onstad, C.A., Bosch, D.D. and Anderson, W.P. (1994). *AGricultural Non-Point Source Pollution Model, Version 4.03 AGNPS User's Guide*, U.S. Department of Agriculture, Washington, D.C.

Zarriello, P.J., Barlow, P.M. and Duda, P.B. (2001). Simulating the Effects of Ground-Water Withdrawals on Streamflow in a Precipitation Runoff Model. *Bridging the Gap: Meeting the World's Water and Environmental Resources Challenges*, Virginia.

Zhen, X.Y., Yu, S.L. and Lin, J.Y. (2004). Optimal Location and Sizing of Stormwater Basins at Watershed Scale. *Journal of Water Resources Planning and Management*, **130**(4), 339-347.

Chapter 3. The Hydrological Calibration and Validation of a Linked Watershed-Reservoir Model for the Occoquan Watershed, Virginia

3.1 *Summary*

Runoff models such as HSPF and reservoir models such as CE-QUAL-W2 are used to model water quality in watersheds. Often, the models are independently calibrated to observed data. When models are linked by using the model output from an upstream model as input to a downstream model, the physical reality of a continuous watershed, where the overland and waterbody portions are parts of the whole, is better represented. There are some additional challenges in the calibration of such linked models, because the aim is to simulate the entire system as a whole, rather than piecemeal. When public entities are charged with model development, one of the driving forces is to use publicly-available models. This paper describes the use of two such models, HSPF and CE-QUAL-W2, in the linked modeling of the Occoquan Watershed located in northern Virginia, USA. The description of the process is provided, and results from the hydrological calibration and validation are shown. The Occoquan Model consists of six HSPF and two CE-QUAL-W2 applications, linked in a complex way, to simulate two major reservoirs and the associated drainage areas. The linked model was calibrated for a three-year period and validated for a two-year period. The results show that a successful calibration can be achieved using the linked approach, with moderate additional effort. Overall flow balances based on the three-year calibration period at four stream stations showed agreement ranging from –3.95% to +3.21%. Flow balances for the two reservoirs, compared via the daily water surface elevations, also showed good agreement (R^2 values of 0.937 for Lake Manassas and 0.926 for Occoquan Reservoir), when missing (un-monitored) flows were included. The models were adequately validated to represent the general watershed behavior. One of the advantages of using the linked approach is to develop a direct linkage between upstream activities and downstream water quality. This make it easier for decision makers to evaluate the alternative watershed management plan

and for the public to understand the decision making process. The successful calibration on hydrology would provide a solid base for further model application.

3.2 *Introduction*

The modeling of watersheds for water quality (WQ) is typically performed using runoff models such as Hydrological Simulation Program–Fortran (HSPF) (Bicknell, et al. 2001) and Soil and Water Assessment Tool (SWAT) (Neitsch, et al. 2002), whereas WQ modeling for receiving waterbodies uses models such as Water Quality Analysis Simulation Program (WASP) (Wool, et al. 2003) and CE-QUAL-W2 (Cole and Wells 2003). When public entities are charged with model development, one of the driving forces is to use publicly-available models. When a watershed drains to a single waterbody, this process is fairly straightforward. In cases where there is more than one major waterbody in a watershed, a decision must be made as to how to best represent the physical reality in the entire watershed, even when the focus is principally on the WQ in the most-downstream waterbody.

The Occoquan Watershed (Watershed) is such a system. The most-downstream waterbody is the Occoquan Reservoir (Reservoir). However, in one of the sub-watersheds draining to the Reservoir, there is another significant waterbody called Lake Manassas (Lake). Both waterbodies serve as drinking water sources.

This paper describes the hydrological calibration and validation of a linked model for the Occoquan Watershed. Linkage here is defined as the output of an upstream submodel being used as input to the next downstream submodel (i.e., serial linkage). The calibration of models linked in such a fashion presents some challenges that are different from those encountered when submodels are independently calibrated using observed data, rather than outputs from upstream submodels, as inputs. Specifically, the Occoquan model (Model) consists of six HSPF and two CE-QUAL-W2 submodels linked together. The initial calibration of the linked model is for the years 1993-95, with a validation period of 1996-97. Land-use data are updated every five years; therefore the model years were “centered” on 1995, when a land-use data update was issued. Similarly, the next

five-year period, 1998-2002, spanning the land-use update for 2000, will be used for an updated model in the future.

The major aims of this study are to better understand, from a modeling perspective, the hydrologic processes occurring in the Watershed, and to establish a good flow simulation for further investigation of water quality trends in the Watershed and receiving waterbodies. This paper describes the general process of calibrating a model linked in such a complex way, and reports on the hydrological calibration and validation of the Model. Due to length considerations, the calibration of the WQ component of the Model will be reported separately.

3.2.1 Study Area

The Occoquan Watershed is a 1,515 km^2 basin located in northern Virginia, USA (Figure 3-1), and the mouth of the Watershed is located about 50 km southwest of Washington D.C.

The Watershed is hydrologically divided into two major sub-watersheds: the Occoquan River sub-watershed and the Bull Run sub-watershed. In the southern part of the Watershed lies the Occoquan River sub-watershed, with two principal streams, Cedar Run and Broad Run, and two principal waterbodies, Lake Manassas and Lake Jackson (Figure 3-1). Below Lake Manassas, Broad Run, as well as other small tributary streams, runs eastward until it confluences with Cedar Run just above Lake Jackson. Below Lake Jackson lies the Occoquan River, which is part of the headwaters of the Reservoir. The total drainage area of the Occoquan River is approximately 880 km^2 (OWML 1998).

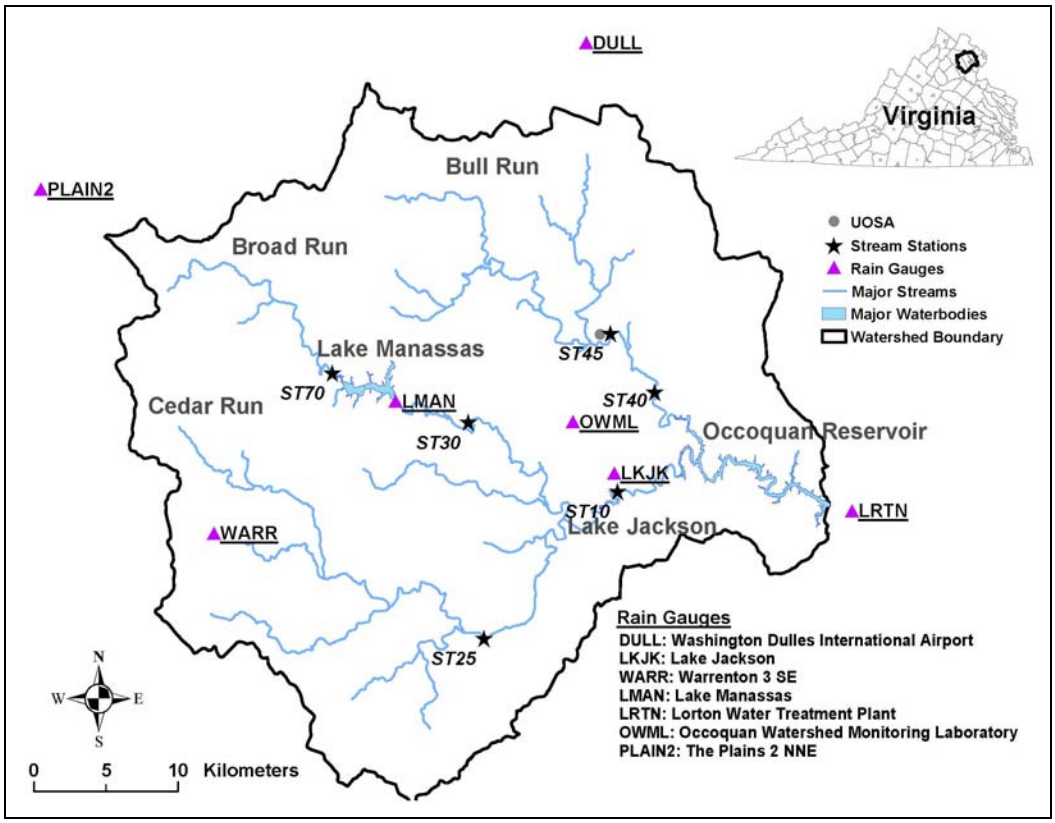

Figure 3-1: Location of Occoquan Watershed in Virginia, USA, Showing Main Tributaries, Main Waterbodies, Stream Stations and Rain Stations Used in This Study

The northern part of the Watershed comprises the Bull Run sub-watershed. The Upper Occoquan Sewage Authority (UOSA) water reclamation facility (WRF) discharges into Bull Run about 10 km above the point where Bull Run forms the other headwater of the Reservoir (Figure 3-1). The UOSA WRF discharge is an important component of the water quality management of the Reservoir (Randall and Grizzard 1995). Much of the Bull Run sub-basin is rapidly urbanizing and drains close to 471 km^2, about a third of the Watershed (OWML 1998). Several small tributary streams scattered around the Watershed make up the remaining 164 km^2 drainage area. These include Sandy Run and Hooes Run (Figure 3-2).

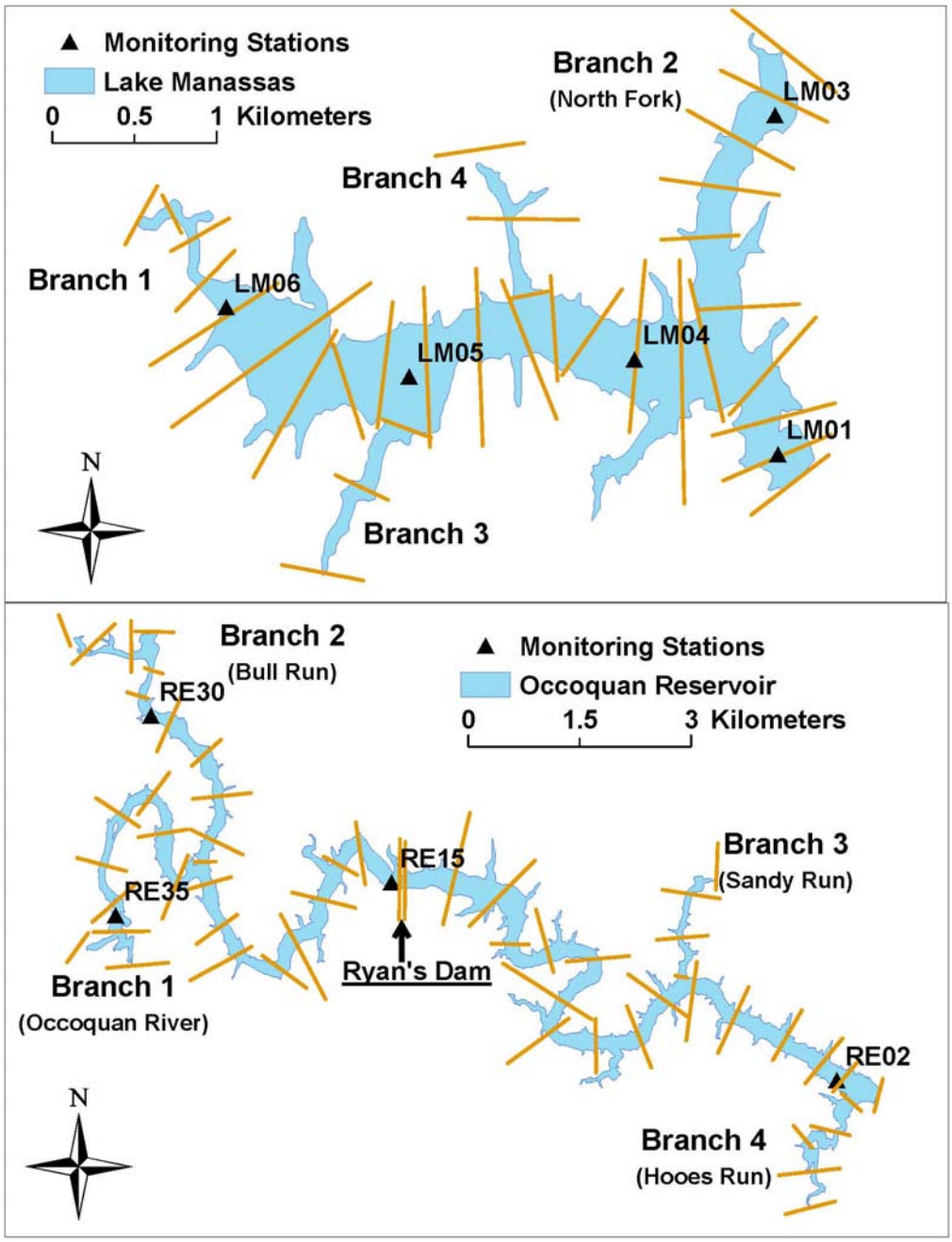

Figure 3-2: Segmentation of Lake Manassas and Occoquan Reservoir and Selected Monitoring Stations

There are two major drinking water sources within the Watershed. One is the Occoquan Reservoir, which is part of the major drinking water supply for 1.3 million northern Virginia residents served by Fairfax Water (FW). It is also a major recreation site. It was created in 1950 when a 10-meter low head dam was constructed at the mouth of the

Occoquan River (OWML 1998). In 1957, a higher dam, called the Upper Occoquan Dam, was built approximately 900 m upstream from the lower dam. In 1980, the dam elevation was extended by 0.6 m, increasing the storage capacity to 31.4×10^6 m^3 and the safe yield to 2.5×10^5 m^3 per day (which includes the discharge from UOSA) (OWML 1998). Other characteristics of the Reservoir are listed in Table 3-1.

The other major waterbody, Lake Manassas, is located in the upper part of the Watershed. It serves as the principal drinking water supply for the City of Manassas and is also used for recreational purposes. Three golf courses are located on its north shore (Robert Trent Jones, Virginia Oaks, and Par 3). The Lake was created by the damming of Broad Run in the late 1960s. In 1997-98, an inflatable bladder was added to increase the dam height by 1.52 m, although the pool elevation was not increased (by inflation of the bladder) until 2000 (Johnston 2005). The storage capacity without the bladder is 15.4×10^6 m^3 (Eggink 2001) with a safe yield of 6.4×10^4 m^3 per day (Black & Veatch 2000). Other characteristics of the Lake are listed in Table 3-1.

Table 3-1: Summary of Occoquan Reservoir and Lake Manassas Characteristics

Waterbody Characteristics	Occoquan Reservoir	Lake Manassas
Volume (m^3)	31.4×10^6	15.4×10^6
Surface Area (ha)	616	282
Length (m)	2.25×10^4	5.97×10^3
Mean Depth (m)	5.1	5.5
Maximum Depth (m)	20	15
Mean Width (m)	150	353
Maximum Width (m)	275	724
Safe Yield (m^3/day)	2.5×10^5*	6.4×10^4
Average Inflow (m^3/day)	1.6×10^6*	1.3×10^5
Dam Crest Height above Mean Sea Level (m)	37.2	86.7
Hydraulic Residence Time (day)	19.6	118.5

*Includes daily discharge from UOSA WRF of 79,760 m^3/day (1993-97 average)

3.2.1.1 Water Quality Issues

Summertime eutrophication was observed in the Reservoir in the late 1960s. At the time, eleven small publicly-owned treatment works (POTWs) had discharges in the Watershed. The Virginia State Water Control Board (VSWCB) commissioned Metcalf & Eddy Inc. to investigate the water quality issues. The study showed that the eleven POTWs were the primary cause of the eutrophication (Metcalf & Eddy 1970). Based on the recommendations from the study, VSWCB developed the management plan for the

Watershed and the Reservoir in 1971, known as the "Occoquan Policy" (VSWCB 1971). The policy called for the elimination of the poorly-performing POTWs and the construction of a state-of-the-art advanced wastewater treatment plant. As a consequence of this, UOSA began operations in 1978. Initially, UOSA had a treatment capacity of 28,400 m^3/day, and currently it is at 204,400 m^3/day. While this has substantially improved the water quality of the Reservoir, eutrophication is still an issue and FW uses copper compounds to control algae growth during summer months.

Lake Manassas has been nutrient enriched for a considerable time, and the limiting nutrient is phosphorus (Eggink 2001; Laufer 1986; OWML 1991, 1996). It has high biological productivity and copper compounds were applied for at least fourteen years (1982-1995), typically four times a year (Eggink 2001).

3.2.2 Model History

The Occoquan Model effort started in the late 1970s. In 1977-78, a mainframe model, named the Occoquan Basin Computer Model (Hydrocomp Inc. 1978), was developed from a modified version of the Hydrocomp Simulation Programming (HSP) and Nonpoint Source Model (NPS). The modified HSP simulated hydrological processes while NPS estimated sediment erosion and other nonpoint source loads. Later, receiving water sub-models were added to represent the Lake and the Reservoir as two-layer, single-segment waterbodies. The model was used to estimate the runoff potential and nonpoint pollution generation based on the projected land use development (NVPDC 1979). After the UOSA WRF went into operation, the model was modified in 1982 to account for the presence of UOSA. The discharge from UOSA was represented as a point source input in the model.

In 1994, a PC (personal computer) version of the Occoquan model was proposed to replace the mainframe model to provide an "up-to-date defensible tool to review future conditions and the consequent requirements that may be indicated" (NVPDC 1994). The improvement included two parts. First, after a review of watershed models available in the public domain, HSPF was proposed to replace NPS/HSP as the pollutant loading and

transport model. Second, a more complex hydrodynamic reservoir model, CE-QUAL-W2 (W2), was proposed to replace the simple two-layer single-segment reservoir model for the Reservoir. The applications of these models were proposed to be linked in a serial manner. The overall objective was to improve mathematical representation of the reality and thus to enhance the accuracy of reservoir responses to alternative control strategies (Stein, et al. 1998). This modeling effort was not completed until 2003.

Starting in 2004, more improvements have been implemented. Firstly, W2 was applied to fully represent the characteristics of the Lake. In the model update begun in 1994, the two-layer single-segment water quality model for the Lake then existing in the original Occoquan Basin Computer Model was not converted to a better hydrodynamic water quality model as was proposed for the Reservoir. Instead, it was further simplified in the 1994 linked model application and was represented as a completely-mixed lake under HSPF. Such simplification cannot fully represent the physical, chemical and biological processes in the Lake. The 2004-05 updates improved this situation by using W2 for the Lake. The resultant model is a complex linked model application (Figure 3-3). As a further improvement, the Watershed and waterbodies have been represented at finer scales (Figures 3-2 and 3-3). The watershed delineation was performed based on more accurate and updated geographic information. Finer watershed and waterbody segmentation were adopted to allow better representation of the hydrologic and hydrodynamic activities.

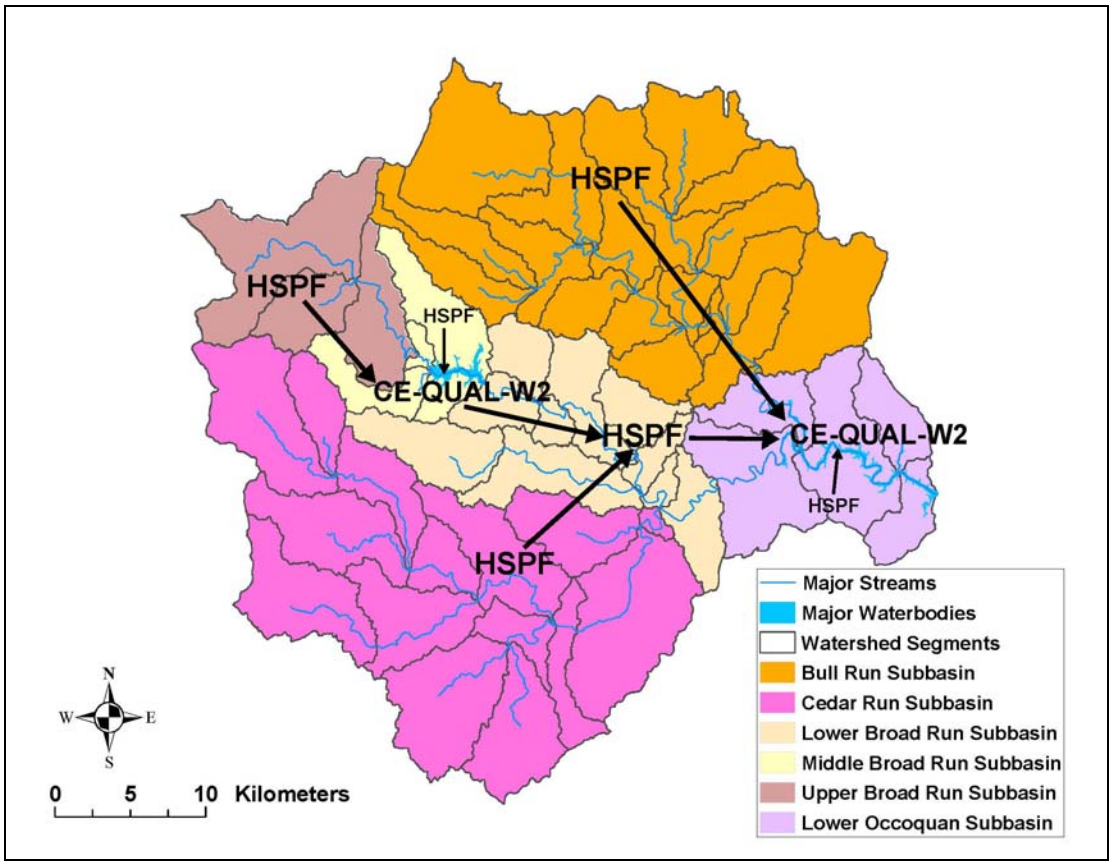

Figure 3-3: Occoquan Watershed Model Application Schema and Watershed Segmentation

3.3 *Model Description*

3.3.1 HSPF and CE-QUAL-W2

Hydrological Simulation Program–Fortran (HSPF) is a conceptual lumped hydrological model designed to simulate various hydrological processes and associated water quality components in a watershed (Bicknell, et al. 2001). After being continuously updated since the 1960s, it is now the core program of the U.S. Environmental Protection Agency (EPA) Better Assessment Science Integrating Point and Nonpoint Sources (BASINS) package. HSPF simulates hydrologic and water quality processes in pervious and impervious land surface, streams and well-mixed impoundments. It has been widely applied in watersheds with diverse geographic characteristics (Albek, et al. 2004; Hayashi, et al. 2001). HSPF is commonly used to evaluate the impacts of flow diversions, land use changes (Brun and Band 2000), and point and nonpoint source treatment plans (Rahman and Salbe 1995). It has been used in the Chesapeake Bay program to evaluate

the impacts of nutrient and sediment reduction plans (Cerco, et al. 2002). The model itself has been used with other models, such as SHADE (1998a; Chen, et al. 1998b) and MODFLOW (Ross, et al. 2004).

CE-QUAL-W2 is a two-dimensional hydrodynamic and water quality model developed by the U.S. Army Corps of Engineers (Cole and Wells 2003). It describes longitudinal and vertical variations of flow and water quality characteristics while assuming homogeneity along the lateral direction. The model is capable of describing water quality gradients in relatively long and narrow waterbodies such as rivers, reservoirs, estuaries and lakes. There are more than 1,000 applications worldwide (Wells 2005), including those to predict impacts of management plans on water quality and ecosystems (Bowen and Hieronymus 2003; Gunduz, et al. 1998; Sullivan, et al. 2003). The model has also been used with other models, such as an ecological model (Saito, et al. 2001) and ANDYN-RQUAL (Hadjerioua, et al. 2001).

3.3.2 Approach Used for the Linked Occoquan Model

In HSPF, land segments and reaches are used to represent a watershed. Based on different hydrological characterizations, HSPF defines two types of land segments: PERLND and IMPLND (Bicknell, et al. 2001). PERLND describes comprehensive hydrological and water quality activities that occur in forest, agricultural or other permeable land areas. PWATER in PERLND is the core section of HSPF where the water budget is allocated among surface flow, interflow, baseflow and moisture storage. Due to the geographic location of the Watershed, the SNOW section is turned on to simulate early spring storms due to snow accumulation and melting. IMPLND describes water movement and associated water quality in impervious land areas such as paved urban surfaces. The IWATER section under IMPLND is included to account for interception, detention and evaporation from impervious land surfaces. Because infiltration is negligible in impervious areas, the hydrologic simulation formulas are much simpler than those in PERLND.

Processes in receiving streams and well-mixed impoundments are described in the RCHRES unit. The processes in land segments are connected to reaches by a network routine to represent a watershed as an entity. The HYDR section in RCHRES is used to simulate hydraulic behavior in the streams using a storage volume relation defined in FTABLEs. Contributions from precipitation and evaporation are also considered for RCHRES. Because HSPF assumes reaches to be completely mixed and unidirectional, RCHRES is suitable for simulating processes in streams, rivers and well-mixed lakes and ponds. However, this assumption becomes restrictive when applied on watersheds where water flows drain into receiving waterbodies such as reservoirs (stratification) and estuaries (complex flow and stratification). It is inappropriate to represent those waterbodies as RCHRES segments because processes such as thermal stratification and tides cannot be described in HSPF.

To overcome the limitations of HSPF, one approach is to represent those complex waterbodies with models that have the capability to describe them in an appropriate way. In this study, the two major waterbodies in the Watershed were modeled by W2. In W2, waterbodies are defined by a series of control volumes with vertical layers in each longitudinal segment. Dam processes are represented by allowing water withdrawal based on outlet geometry, upstream density gradient, or specified outflow. The structures and functions of HSPF and W2 are further described elsewhere (Bicknell, et al. 2001; Chen, et al. 1998b; Cole and Wells 2003; Donigian and Crawford 1976).

In this study, HSPF is linked with W2 for the modeling of the Watershed. The schema in Figure 3-3 shows the HSPF and W2 submodels used, and how they are linked. In general, three modules in HSPF (PERLND, IMPLND, and RCHRES) are used for the water budget calibration, which account for all the inflows as either outflows or changes in storage. Runoff from the Middle Broad Run and Lower Occoquan subbasins are assumed to drain directly into the Lake and the Reservoir, respectively, and only PERLND and IMPLND processes are used in these submodels. The output from these submodels serves as input (as distributed tributaries along the waterbodies) for the W2 submodels. Output from the Lake Manassas W2 application is used as input to the Lower Broad Run HSPF application. Thus, the six HSPF submodels (Cedar Run, Upper Broad Run, Middle Broad

Run, Lower Broad Run, Bull Run, and Lower Occoquan) and two W2 submodels (Lake Manassas and Occoquan Reservoir) are linked, and the entire Model can be calibrated to the basin outlet at the Occoquan Dam.

While the final calibration of the Model is done at the Occoquan Dam, initial and intermediate calibrations are performed for the submodels using the observed data from monitoring stations shown in Figures 3-1 and 3-2. Calibration is started with those submodels at the most upstream end of the linked Model (Cedar Run, Upper Broad Run, and Bull Run) by comparing simulated flow rates with those recorded at stations ST25, ST70 and ST45, respectively (Figure 3-1). Output from the Upper and Middle Broad Run submodels are used as input to the Lake Manassas W2 submodel, which is calibrated next with water surface elevations at LM01 (Figure 3-2). Output from it is routed via the Lower Broad Run submodel (ST30), which also receives the output from the Cedar Run submodel. Lake Jackson, at the confluence of the Lower Broad Run and Cedar Run subbasins, is a small lake, and is modeled as a completely mixed lake under HSPF. Just downstream from Lake Jackson is the Occoquan River arm of the Reservoir, and this is part of the mainstem of the W2 model for the Reservoir. Output from the Bull Run submodel forms the Bull Run branch of the Reservoir W2 model at a point near station ST40 (Figure 3-1). Finally, the Occoquan Reservoir submodel is calibrated using the Occoquan Dam as the outlet. In calibrating the latter, a finer calibration of the entire Model (all submodels) is performed in a feedback loop fashion.

The principal water budget variable in W2 is the water surface elevation (WSE), which is highly dependent on the waterbody bathymetry and boundary conditions. To enhance simulation accuracy, input flow includes all available water budget information, such as simulated upstream flows from HSPF, distributed flow from HSPF, precipitation and evaporation. Other flows, such as the daily water withdrawal, power generation (the Reservoir only), bypass, and flows that don't go over the dam, are obtained principally from the water treatment plants and are included as specified outflows. Because the waterbody submodels used simulated HSPF flows, rather than observed flows, as input, some flow anomalies (both in timing and quantity) were noticed when observed flows over the dams were used as specified outflows. These differences are to be expected even

in well-calibrated HSPF applications, but could be substantial enough on certain days to make a meaningful difference in observed and simulated WSE values. Observed WSE data are daily averages collected using pressure transducers at the Lake Manassas dam. At the Occoquan dam, these data are gathered manually once per day using a staff gauge. Therefore, there are bound to be differences due to both the HSPF simulation and the limits on gauged and ungauged flows. To resolve these issues, a modification was made to the W2 code to incorporate elevation-discharge relationships for computing flow over each dam. This modification worked well, and a successful calibration was achieved.

3.3.3 Watershed and Reservoir Segmentation

The process of watershed delineation and segmentation was performed using EPA BASINS software based on local geographic characteristics. The boundaries of watershed segments were defined based on the physical characteristics of the Watershed, such as topography, geography, land use, soil properties, etc. Some site-specific features were included in this process. For example, a relatively small segment was added to account for the contribution from the UOSA WRF. Some additional segments were added to prepare the Model to be used when future development plans are implemented. This process resulted in the 1,515 km^2 watershed being divided into 56 land (HSPF) segments with an average size of 27.0 km^2 each (Figure 3-3). The physical characteristics of these land segments and reaches are listed in Table 3-2. Middle Broad Run and Lower Occoquan have relatively short drainage paths and are assumed to drain directly into the receiving waterbodies.

Table 3-2: Characteristics of Sub-Watersheds of the Occoquan Watershed and Their Reaches

	Cedar Run	Bull Run	Upper Broad Run	Middle Broad Run	Lower Broad Run	Lower Occoquan
Surface Area (km^2)	501.72	470.56	126.21	63.02	189.33	163.81
Number of Segments	15	20	3	3	10	5
Average Segment Size (km^2)	33.44	23.52	42.07	20.00	18.93	32.76
Average Elevation (m)	304.3	261.2	524.0	411.0	254.2	257.8
Average Slope (%)	16.7	19.3	34.9	18.4	16.2	30.5
Average Reach Length (m)	24.6	21.5	19.3	0.1	21.7	0.1
Average Reach Slope (%)	2.5	3.3	5.2	4.2	2.1	1.8
Average Reach Width (m)	10.2	8.1	11.9	7.4	7.3	10.3
Average Reach Depth (m)	0.5	0.4	0.6	0.4	0.4	0.5

The hydrodynamics and water quality in the Lake and the Reservoir were simulated by W2. The original bathymetric data were determined from survey data collected using a global positioning system and depth sounding technique. The data were processed using SURFER (Golden Software Inc. 2002) to determine the sizes of the computational grids.

The modeled region of the Lake extends from just downstream of station ST70 to the dam, a distance of 5.97 km. For modeling purposes, it is divided into four branches: the mainstem, North Fork, and two unnamed arms, and has a total of 29 active computational segments (Figure 3-2). The segment length varies from 173 m to 568 m. There are 4 to 28 computational layers, each 0.5 m thick. The orientation of each segment relative to the north was determined based on the stream centerline. The average width of the top layers is 297.2 m.

The Reservoir encompasses streams from approximately downstream of the Lake Jackson dam (station ST10 in Figure 3-1) on the Occoquan River arm and from approximately station ST40 on the Bull Run arm (Figure 3-1). This W2 model includes four branches: Occoquan River (mainstem, Branch 1), Bull Run (Branch 2), Sandy Run (Branch 3) and Hooes Run (Branch 4), and has a total of 69 active computational segments. The average segment length is 583 m with a maximum of 838 m (segment 55 at the very upstream end of Bull Run) and a minimum of 74 m (Segment 32, at Ryan's Dam, a submerged feature with a narrow vertical opening). There are from 1 to 39 computational layers, each 0.5 m thick. The average width of the top layers is 149.7 m, about half of that for the Lake.

3.4 *Data Sources*

3.4.1 Meteorological Data

Both models, especially HSPF, require intensive meteorological data to simulate hydrological behavior (Table 3-3). The Washington Dulles International Airport weather station (Dulles station) maintained by the National Oceanic and Atmospheric Administration (NOAA) is the major weather station near the Watershed and provides hourly time series of cloud cover, wind speed, wind direction, air temperature and dew point temperature. Because potential evapotranspiration (ET) data required by HSPF were not directly available, the modified Penman Pan empirical method (Kohler, et al. 1955) was used to estimate potential ET from maximum daily air temperature, minimum daily air temperature, average daily dew point temperature, total daily wind movement and total daily solar radiation obtained from the Dulles station. In W2, evaporation is accounted for through a user defined formula (Cole and Wells 2003). Hourly solar radiation data for the Dulles station were obtained from the Integrated Surface Irradiance Study (ISIS) performed by NOAA's Air Resources Laboratory (Hicks, et al. 1996). ISIS started in August 1995, and solar radiation data for the period prior to that were estimated from Hamon's empirical function (Hamon, et al. 1954). The estimated data were compared to the ISIS solar radiation data and correlated well, with an R^2 of 0.994. Thus, estimated solar radiation data were used up to the end of 1995, and ISIS data were used afterwards.

Table 3-3: Meteorological Data Series for HSPF and CE-QUAL-W2

	HSPF Version 12	CE-QUAL-W2 Version 3.2
Air Temperature	Required	Required
Cloud Cover	Required	Required
Dew Point Temperature	Required	Required
Potential Evapotranspiration	Required	Not Required
Precipitation	Required	Required
Solar Radiation	Required	Optional
Wind Speed	Required	Required
Wind Direction	Not Required	Required

One of the most important meteorological time series is precipitation, which is provided by seven rain gauge stations (Figure 3-1). Except at Warrenton, these rain gauge stations collected precipitation data on an hourly basis. The Warrenton gauge only had daily data,

and these were distributed to hourly time series based on data from the neighboring station at The Plains 2.

3.4.2 Land Use Data

Land use data were obtained from the Northern Virginia Regional Commission (NVRC), which performs a land use survey every five years using the aerial-photography technique. The land use data of 1995 were initially classified into fourteen land use categories, which were then consolidated into nine categories based on imperviousness and soil properties. These are forest, pasture, high tillage cropland, low tillage cropland, townhouse/garden apartment, low density residential, medium density residential, industrial/commercial, and institutional. The purpose of doing this was to reduce the complexity of the HSPF applications without significantly affecting simulation results. The summary of areas and land use categories for subbasins are shown and described in Table 3-2 and Figure 3-4. The Bull Run subbasin and Lower Occoquan subbasin are highly urbanized, with more than 30% and 50%, respectively, of land area falling into the urban land type, while agricultural activities are more dominant in the Cedar Run and Broad Run subbasins. The average coverage of forest in the entire Watershed was around 50% in the mid 1990s.

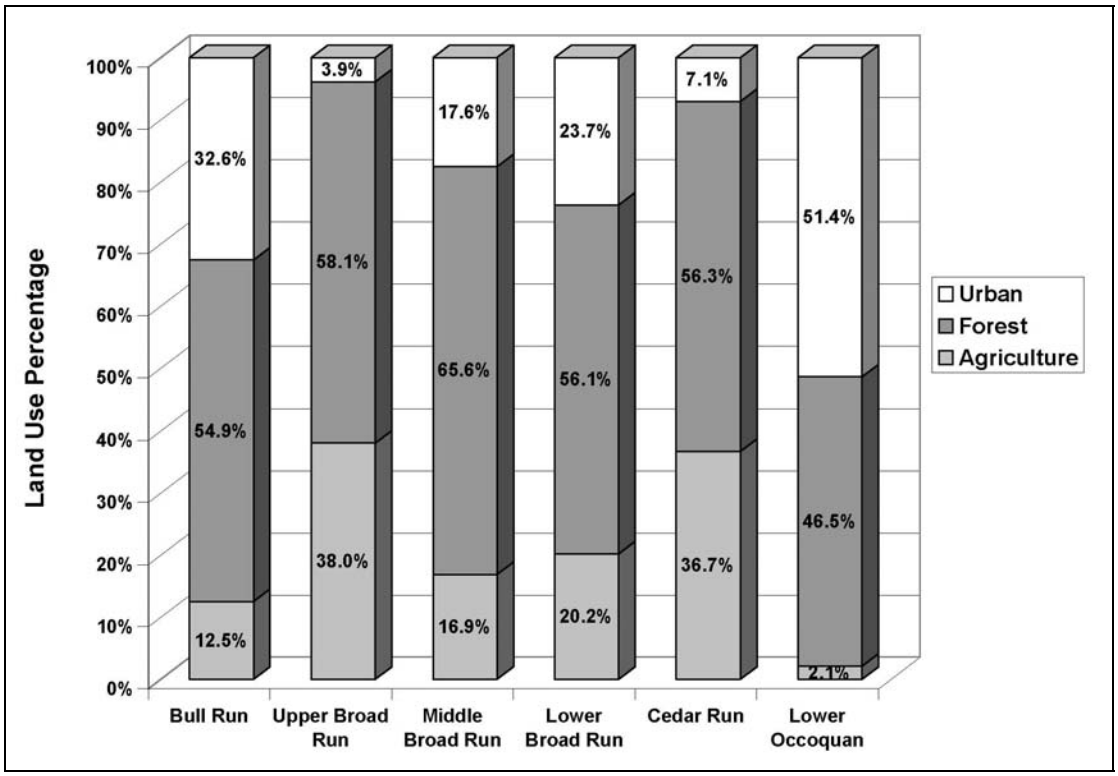

Figure 3-4: Land Use Characteristics of Subbasins in the Occoquan Watershed

3.4.3 Initial and Boundary Conditions

In HSPF, initial hydrologic variables include moisture storage in interception, upper zone, lower zone, surface flow, interflow and active groundwater flow. At first, these were assigned reasonable values and the submodels were run through a one-year simulation. The initial values were then adjusted based on the values at the end of the simulation.

W2 requires initial water surface elevation in each segment to start velocity calculations. They were set to be the values of the observed data on the starting date.

Time-varying boundary conditions for W2 include upstream flow, tributary flow, distributed tributary flow, and water withdrawal. Water quality inputs for each of these flows, as well as for rainfall, are also required, but are not discussed here because water quality is not addressed in this paper. For the Lake, upstream flow data were based on daily stream flow time series obtained from the Upper Broad Run subbasin HSPF application, as calibrated against observed flows. Flows from ungauged small tributaries

along the Lake were supplied by the Middle Broad Run HSPF submodel. Water withdrawal data were provided by the water treatment plant of the City of Manassas. However, those records were only available from October 1995 to February 1997. Investigation of those data indicated that water withdrawal by the water treatment plant was fairly constant. Missing water withdrawal records were filled in using the average value. Other withdrawal data, such as by golf courses, were not known. Those missing flows were estimated by a W2 utility called WaterBalance, which determines a water balance based on the discrepancy between observed and simulated water surface elevations.

A similar approach was adopted for the Reservoir. Daily upstream flows into the two major branches of the Reservoir are provided by the HSPF applications for the Bull Run and Lower Broad Run subbasins, respectively, which were calibrated against observed data. For Hooes Run and Sandy Run, runoff from their drainage land segments is estimated by the Lower Occoquan HSPF submodel. Other ungauged tributary flows are also supplied by the Lower Occoquan HSPF application. Daily water withdrawals from the Reservoir and water usage for power generation and bypass were provided by Fairfax Water.

3.4.4 Calibration Criteria

Because there is no single accepted test to determine whether or not a model is calibrated, both graphical and statistical methods were applied to evaluate model performance. In addition to traditional statistical measures such as mean values, several other statistical methods were also used.

The percentage difference (PD) between simulated and observed data is defined below:

$$PD = \frac{100 \cdot (Y - X)}{X}\%$$

where *X* is the observed flow rate, and *Y* is the simulated flow rate. Donigian (2002) suggested a value in the range of 10-15% for a good hydrology/flow calibration of HSPF (Table 3-4).

Table 3-4: General Calibration/Validation Targets or Tolerance for HSPF Applications

	% Difference Between Simulated and Recorded Values		
	Very Good	Good	Fair
Hydrology/Flow	<10	10-15	15-25
Sediment	<20	20-30	30-45
Water Temperature	<7	8-12	13-18
Water Quality/Nutrients	<15	15-25	25-35
Pesticides/Toxic	<20	20-30	30-40

Source: Donigian (2002)

The standard coefficient of determination (R^2) is also used to evaluate model performance. Donigian (2002) suggested a value greater than 0.8 for a good hydrology/flow calibration based on monthly flow comparison (Table 3-4).

3.5 *Results and Discussion*

The hydrological calibration performance is evaluated by comparing simulated and observed flow data, which are collected on a continuous basis at various stations maintained by the Occoquan Watershed Monitoring Laboratory (Figure 3-1). Some other aspects of calibration, including the statistics used, are described here. There is no single accepted statistical test to determine whether or not a model is calibrated. Thus, in addition to traditional statistical measures such as mean and median values, several other statistical methods were used to evaluate the model calibration.

3.5.1 Model Calibration

For calibrating the HSPF submodels, the parameter estimation program PEST (Watermark Numerical Computing 2004) was used to accelerate the calibration process and to provide an initial calibrated parameter set. The coefficients were then manually fine-calibrated to account for variance among different land uses. Daily flows measured

at four principal stream stations were used and compared with the model outputs. For the W2 applications, the WSE was the primary calibration parameter. The WaterBalance utility, mentioned earlier, was used to account for missing flows. The average water balance flow correction for the Lake and the Reservoir were 0.005 and 0.18 m^3/s respectively, accounting for 0.2 and 0.9 % of the average outflows. Calibration of the overall water balance for the Model was focused on obtaining well-calibrated inflow and tributary flow data from HSPF, obtaining accurate withdrawal data from water treatment plants, and providing well-estimated missing flow data.

Table 3-5 indicates the seven primary parameters for rainfall-runoff calibration. The values used in the HSPF submodels fall into the recommended value ranges (USEPA 2000). The ranges of individual parameter values correspond to the land use differences and seasonal fluctuation in each segment. For example, LZETP represents the ET capability of the lower zone and is a function of vegetation. Thus, monthly values were used for each subbasin to adjust for seasonal variation. The differences among individual subbasins reflect the physical variations in the watershed. For instance, 67% of soil in the Upper Broad Run subbasin is categorized as B for SCS (Soil Conservation Society) hydrological soil group, which features a moderate rate of infiltration capability. SCS hydrologic soil group C is the dominant soil in the Lower Broad Run subbasin, which accounts for more than 90% of the total area. The calibrated INFILT values are in agreement with the difference in soil characteristics in these two subbasins, indicating that the Lower Broad Run subbasin expresses a slower infiltration rate.

Table 3-5: Principal Hydrologic Calibration Parameters in HSPF Applications

HSPF Parameters	Recommended Value Range*	Cedar Run Subbasin	Bull Run Subbasin	Upper Broad Run Subbasin	Middle Broad Run Subbasin	Lower Broad Run Subbasin	Lower Occoquan Subbasin
AGWRC	0.92-0.99	0.92	0.92	0.92	0.92	0.98	0.92
INFILT	0.01-0.25	0.11-0.16	0.10-0.15	0.13-0.18	0.05-0.10	0.05-0.10	0.1-0.15
INTFW	1.0-3.0	3.0	2.0	3.0	3.0	3.0	2.0
IRC	0.5-0.7	0.5	0.5	0.5	0.5	0.7	0.5
LZSN	3.0-8.0	5.0	5.0	3.8	4.5	5.0	5.0
UZSN	0.1-1.0	0.50-0.67	0.43-0.67	0.50-0.72	0.50-0.72	0.50-0.66	0.50-0.66
LZETP	0.2-0.7	0.50-0.70	0.27-0.70	0.50-0.80	0.50-0.80	0.40-0.60	0.40-0.60

*USEPA (2000)

The water budget of four major subbasins for the 1993-95 simulation periods is shown in Table 3-6. The principal component of water input to the Watershed is precipitation. The

Bull Run subbasin has another inflow source, the UOSA WRF discharge, which accounts for 5.0% of its total flow. The average annual precipitation over the studied years was around 110 cm. The years 1993 and 1994 are normal water years, while 1995 represents a dry period with much less precipitation (85.9 cm). Water losses consist of three parts. Based on the total volumes in the whole simulation period, approximately 35% of precipitation became water runoff, and 62% turned into evapotranspiration back to the hydrological cycle. The rest percolated into the deep aquifer and became lost from the system. The slight discrepancy between input and outflow is due to various contributions from individual land uses.

Table 3-6: Water Balance for Each Subbasin in HSPF Applications

	Cedar Run Subbasin		Bull Run Subbasin		Upper Broad Run Subbasin		Lower Broad Run Subbasin	
	Mean (cm)	Percentage (%)	Mean (cm)	Percentage (%)	Mean (cm)	Percentage (%)	Mean (cm)	Percentage (%)
Inputs								
Precipitation	118.2	100.0	117.5	95.0	114.8	100.0	108.8	100.0
Point Discharge			6.2	5.0				
Outflow								
Runoff	39.5	33.7	40.0	32.8	41.0	35.9	37.9	35.3
Deep Groundwater Losses	1.7	1.4	3.8	3.1	2.2	1.9	2.6	2.4
Evapotranspiration	76.1	64.9	78.2	64.1	71.1	62.2	67.0	62.4

Figure 3-5 displays the yearly total flow volumes for the 1993-95 period for different locations in the Watershed. Overall, the annual water balances were replicated well by the HSPF applications and the percentage differences (PD) based on the total flow volumes from the three-year simulation period ranged from –3.95% to +3.21% (Table 3-7). The PD values of the annual flows ranged from –5.84% to +6.26% for various stations during the three-year simulation period except for ST70 in 1995, where it was +21.14%. The relatively large error at ST70 in 1995 is due to three high precipitation events, one in July and two in November. The July 1995 high precipitation event is recorded in the precipitation time series and shows its influence in the simulated data. However, the observed stream flow rate at ST70 does not show correspondingly high flows for those events. It is assumed that this precipitation event was local to the gauge and didn't widely affect the Upper Broad Run subbasin. For the two closely-spaced high precipitation events in November 1995, the HSPF submodel produced more runoff than was recorded.

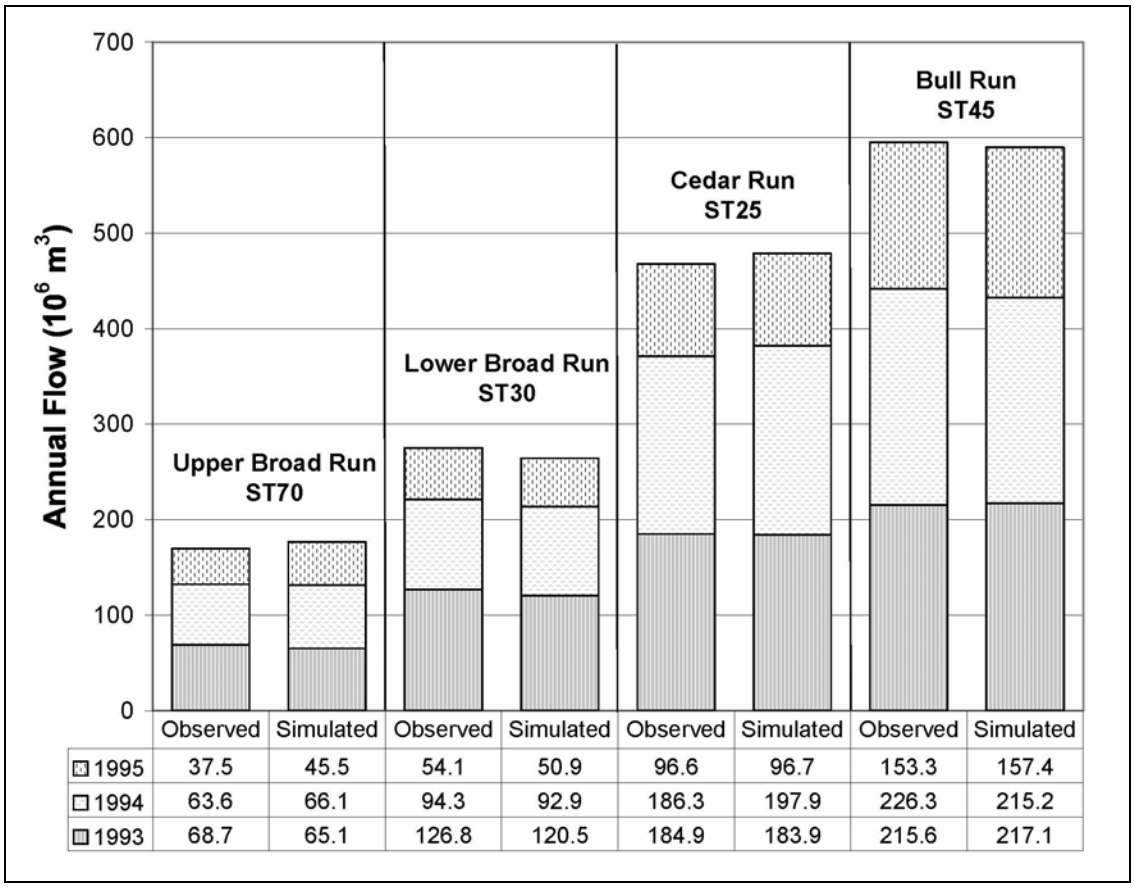

Figure 3-5: Comparison of Annual Total Flow at Selected Stream Stations for Model Calibration

Table 3-7: Comparison of Annual and Three-Year Total Flow Volumes at Various Stream Stations

	Percentage Difference of Annual Flow Volume (%)			
Station	1993	1994	1995	1993-95
ST25	–0.52	+6.26	+0.09	+2.30
ST70	–5.15	+3.96	+21.14	+3.21
ST30	–4.94	–1.54	–5.84	–3.95
ST45	+0.73	–4.89	+2.70	–0.90

The good agreement between observed and simulated data not only indicates that HSPF submodels were well-calibrated to capture the principal hydrological characteristics in those subbasins, but also proves the validity of the linkage between the two different types of water quality models: the watershed model HSPF and the receiving waterbody model W2. ST30 is the stream station located downstream of the Lake, and in terms of model applications, it received the Lake outflow provided by W2. Even though flow balances were generally under-predicted (Figure 3-5), the percentage differences were in a reasonable range of –5.84% to –1.54% (Table 3-7). The calibration of water balance at

ST30 not only depended on calibrating the Lower Broad Run HSPF submodel, but also relied on the calibration of the Lake Manassas W2 submodel as well as the Upper and Middle Broad Run HSPF submodels. Flows contributed by the Upper Broad Run subbasin and Lake Manassas make up approximately 80% of the streamflow at ST30, and therefore the impact of the upstream submodels on the calibration of the Lower Broad Run (ST30) submodel is significant.

The hydrologic performance of the coupled model application was further investigated using the daily and monthly flow comparisons for the Upper Broad Run (ST70) and Lower Broad Run subbasins (ST30) (Figures 3-6 and 3-7). The submodels clearly captured the rapid changes in stream flows throughout the simulation years, although a few extreme events were not so well-reproduced. They showed high performance in the hydrologic simulation for both subbasins with R^2 values based on the monthly flows of 0.896 and 0.885, respectively (Table 3-8). R^2 values for daily average stream flows are, as expected, less than those of monthly flow, because the simulation accuracy of HSPF is positively related to the length of the aggregation interval (Hayashi, et al. 2001; Laroche, et al. 1996). The results indicated that the hydrological responses in the Lower Broad Run subbasin were well-captured by the linked modeling approach.

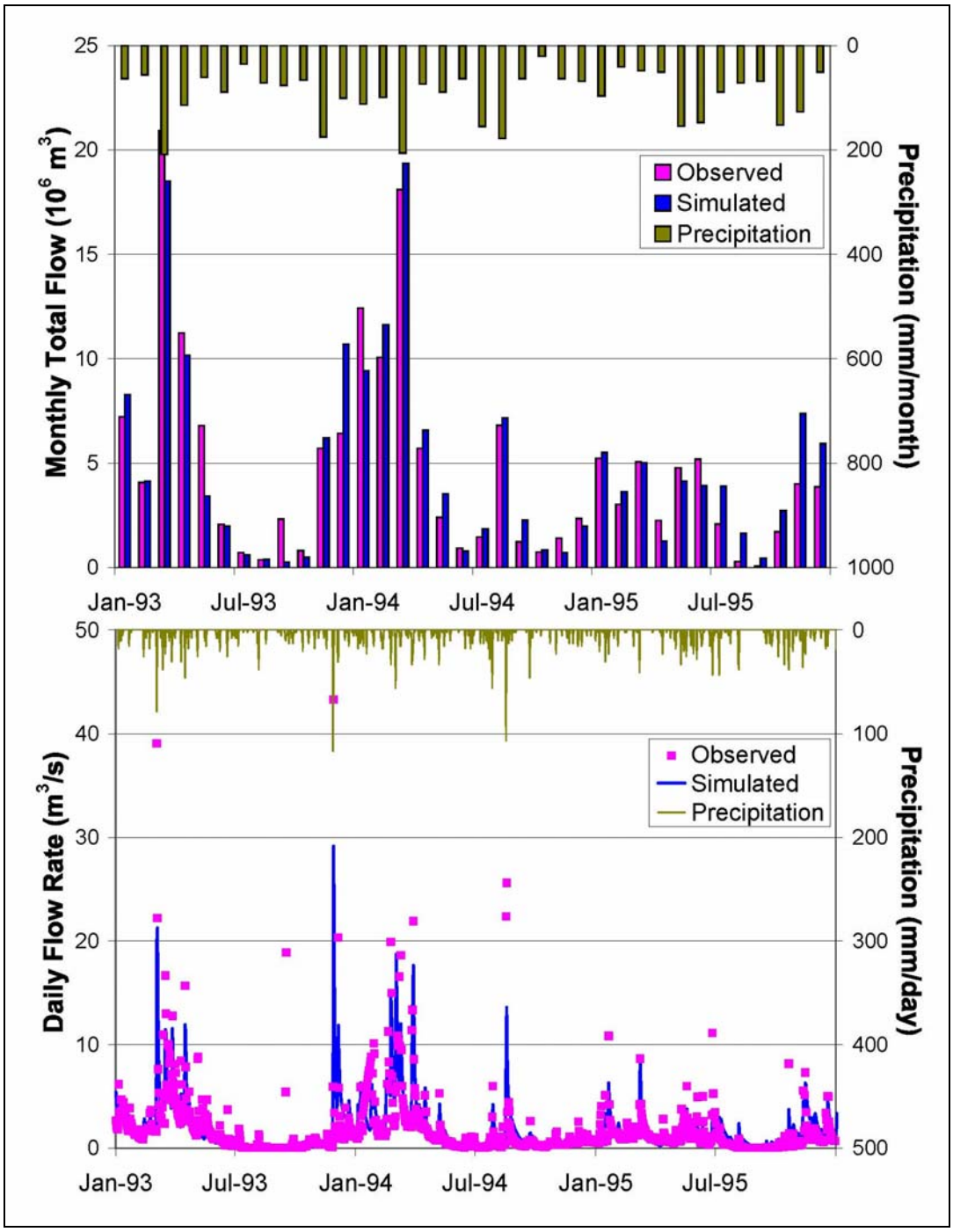

Figure 3-6: Comparison of Monthly (Top) and Daily (Bottom) Flow at Station ST70 in the Upper Broad Run Subbasin

Table 3-8: Comparison between Simulated and Observed Flow at Principal Stream Stations

Subbasins	Daily Mean Flow Rate (m^3/s)			Monthly Mean Runoff (10^6 m^3)			R^2*		Probability Values	
	Obs.**	Sim.***	PD**** (%)	Obs.	Sim.	PD (%)	Daily Flow Rate	Monthly Flow Rate	Monthly Flow Rate	
									T Test	Wilcoxon
Cedar Run (ST25)	4.944	5.057	+2.3	12.99	13.29	+ 2.3	0.523	0.857	0.050	0.065
Bull Run (ST45)	6.292	5.352	–14.9	17.61	16.02	–9.0	0.503	0.815	0.005	0.365
Upper Broad Run (ST70)	1.880	1.870	–0.6	4.98	4.55	–8.6	0.632	0.896	0.557	0.266
Lower Broad Run (ST30)	2.888	2.898	–0.3	7.59	7.62	+0.3	0.460	0.885	0.012	0.065

* R^2 is calculated using a zero intercept.
** Obs. stands for Observed values.
*** Sim. stands for Simulated values.
**** PD stands for Percentage Difference.

When comparing the statistics for flows at four stations (Table 3-8), it can be seen that daily flow rates were well-simulated for the Cedar Run, Upper Broad Run and Lower Broad Run subbasins, with absolute percent differences of 2.3% or less. The PD for Bull Run was –14.9%. This relatively large difference is due to several high precipitation events that were not captured adequately by the simulation. The PDs based on monthly runoff comparisons varied from –9.0% to +2.3%.

The R^2 values for daily flow rates at various stations were in the range of 0.460-0.632. Because small shifts in the timing of storms, specially those that span the midnight boundary between one day and the next, can impact the daily correlations adversely, while being quite acceptable from a watershed modeling perspective, these correlation coefficients are often low. When the aggregation period was increased to a month, the R^2 values ranged from 0.815 to 0.896, showing good correlation. The relatively small errors in percentage difference and large values of monthly R^2 indicated that the Model represented hydrologic activities well.

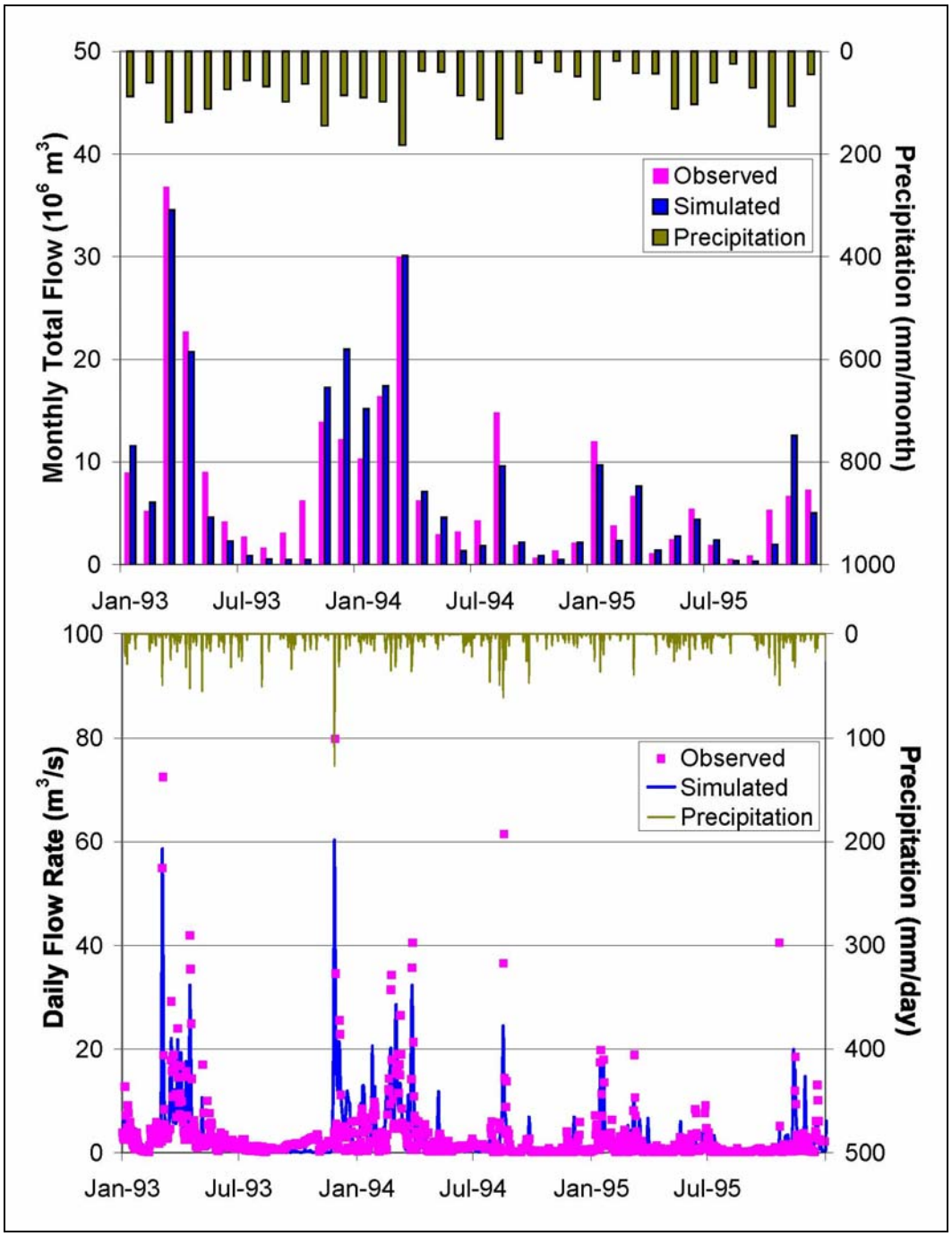

Figure 3-7: Comparison of Monthly (Top) and Daily (Bottom) Flow at Station ST30 in the Lower Broad Run Subbasin

This conclusion is also supported by other statistics (Table 3-8). Although quantile-quantile plots (not shown) indicated that simulated and observed flow rates came from a population with similar distributions, they were not normally distributed, as expected for flow. Thus, log-transformations were performed before paired t-tests were

applied. The results showed that, for Cedar Run and Upper Broad Run, simulated and observed data sets have similar mean values, with probability (P) values greater than 0.05. However, for Lower Broad Run, the discrepancies occurred due to July-October 1993, when no overflows were observed at Lake Manassas (Figure 3-7). With contribution only from the relatively small drainage area below the Lake and up to ST30, the submodel didn't capture some flow events observed at ST30 during those dry periods. Although those months affected the difference between simulated and observed monthly mean values, they had little impact on annual flow comparisons, because the flows in these months were low. A similar explanation applied to Bull Run during low flow months of 1993 (July, August and October) and 1994 (October). The results from non-parametric testing (Wilcoxon signed-rank test) confirmed that simulated and observed monthly flow data were highly related and showed no significant differences in terms of median values at all four stations. From these statistical tests, it was concluded that the model simulation results had excellent agreement with observed data.

Figures 3-8 and 3-9 present the comparison of WSEs at the Lake and the Reservoir, including the three-year calibration and two-year validation periods. In both cases, observed data were measured at the dams. It can be seen that the agreement between observed and simulated values is excellent (the R^2 values were 0.937 and 0.926, respectively). Although the input flow data used were those generated by HSPF applications, rather than those observed at the monitoring stations, W2 demonstrated its ability to capture both the dry periods and flooding events in the three-year simulation period. This well-simulated water budget for Lake Manassas provided a solid base for a good performance by the next downstream HSPF submodel (the Lower Broad Run subbasin).

These results indicate that it is possible to obtain a good hydrology calibration of a complex linked model by using fairly simple intermediate calibration steps, followed by an overall calibration. While the traditional method of calibrating individual models to observed data works well, this approach demonstrates that with some additional effort the models can be linked, all observed data are used in calibration (although some are used only in the intermediate steps), and an excellent overall model can be the result.

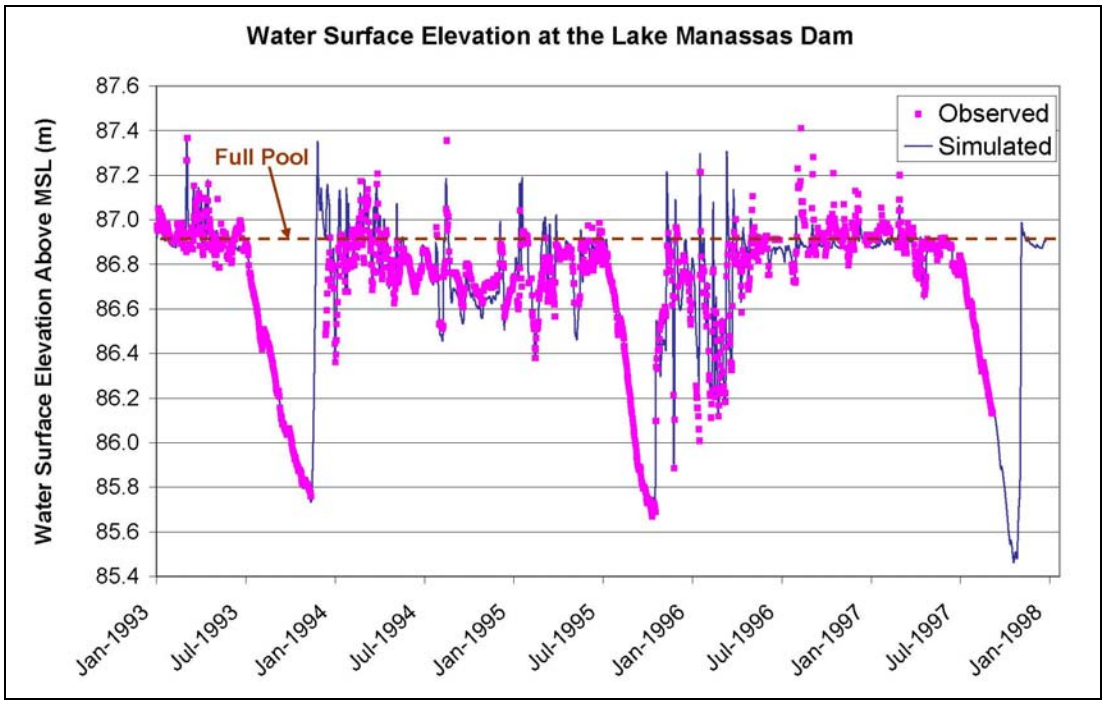

Figure 3-8: Comparison of Water Surface Elevation at Lake Manassas for Model Calibration and Validation

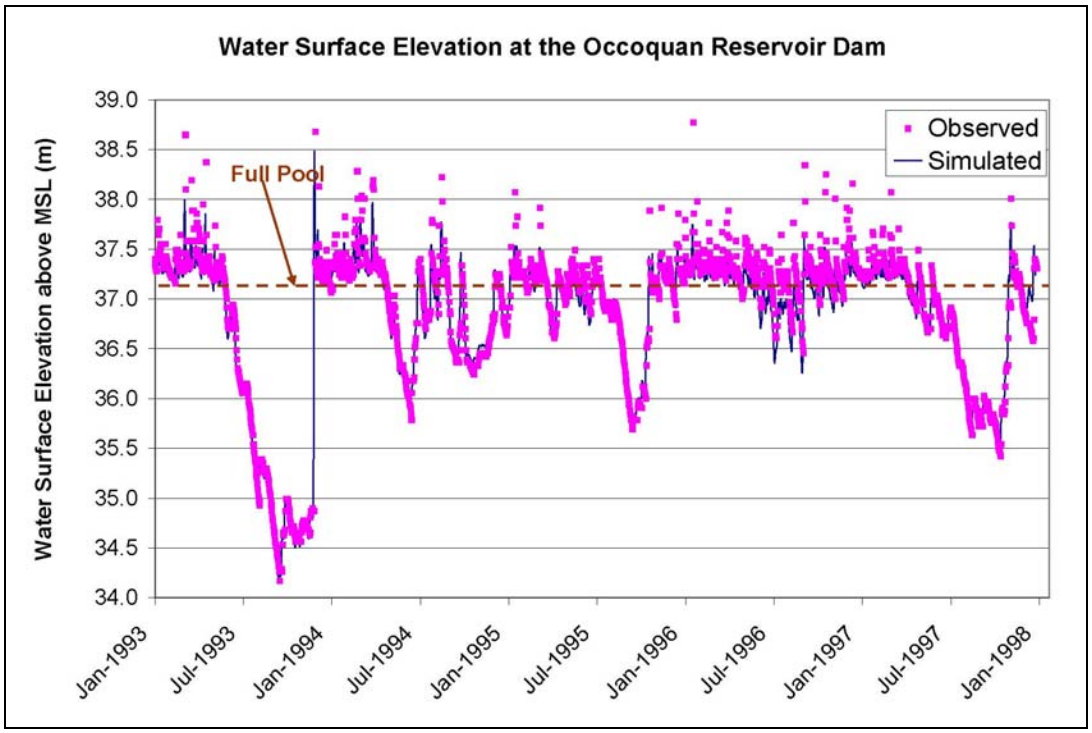

Figure 3-9: Comparison of Water Surface Elevation at Occoquan Reservoir for Model Calibration and Validation

3.5.2 Model Validation

Simulated and observed stream flows for the years 1996 and 1997 were used for model validation. Compared with the 51-year average, the year 1996 was an extremely wet year with an annual precipitation of 45.13 inches (Table 3-9). The year 1997 was a relatively dry year and shared a similar annual precipitation volume with the year 1995. Both the calibration and validation period were combinations of wet and dry years and are considered suitable for model calibration and validation purposes. Stream flows for these two validation years were simulated using the same 1995 land use as for the calibration period, along with the 1996 and 1997 meteorological data.

Table 3-9: Rainfall Summary (1993-1997)

	Rainfall (inches)				
Year	Spring	Summer	Fall	Winter	Total
1993	14.03	7.11	12.23	8.65	42.02
1994	9.90	17.87	5.44	9.25	42.46
1995	7.45	7.50	12.02	6.84	33.81
1996	11.41	11.60	12.81	9.31	45.13
1997	7.76	6.43	10.97	5.34	30.50
Average (1951-2002)	10.37	11.61	9.74	8.16	39.88

As in the model calibration process, the hydrological validation was also performed at four levels: annual water balance, monthly flow rates, daily flow rates, and individual storms. The results shown here include both calibration and validation periods so that model validation can be seen in context. Table 3-10 and Figure 3-10 indicate relatively high discrepancies for the simulation year 1996 because the model under-predicted some closely-spaced storm events due to continuous low-intensity-precipitation events. However, the model reproduced the annual flow balance of the year 1997 fairly well with the percentage differences based on annual flow comparison ranging from −17.2 to +21.0% for four principal monitoring stations. According to the scale used by Donigian (2002), these are simulated as “fair” to “very good” (see Table 3-4).

Table 3-10: Model Performance in Predicting Annual Flow Volumes at Various Stream Stations, 1993-1997

		ST25 Cedar Run	ST70 Upper Broad Run	ST30 Lower Broad Run	ST45 Bull Run
Calibration	1993	–0.5* Very Good*	–5.2 Very Good	–4.9 Very Good	+0.7 Very Good
	1994	+6.3 Very Good	+4.0 Very Good	–1.5 Very Good	–4.9 Very Good
	1995	+0.1 Very Good	+21.1 Fair	–5.8 Very Good	+2.7 Very Good
Validation	1996	–58.6 Poor	–39.1 Poor	–42.4 Poor	–31.8 Poor
	1997	+21.0 Fair	+8.5 Very Good	–17.2 Fair	+8.0 Very Good
Summary	1993-1995	+2.3	+4.0	–4.0	–0.9
	1993-1997	–19.9	+8.2	–16.4	–9.0

*Numbers are percent differences from observed data (%), and ratings are as based on Table 3-4

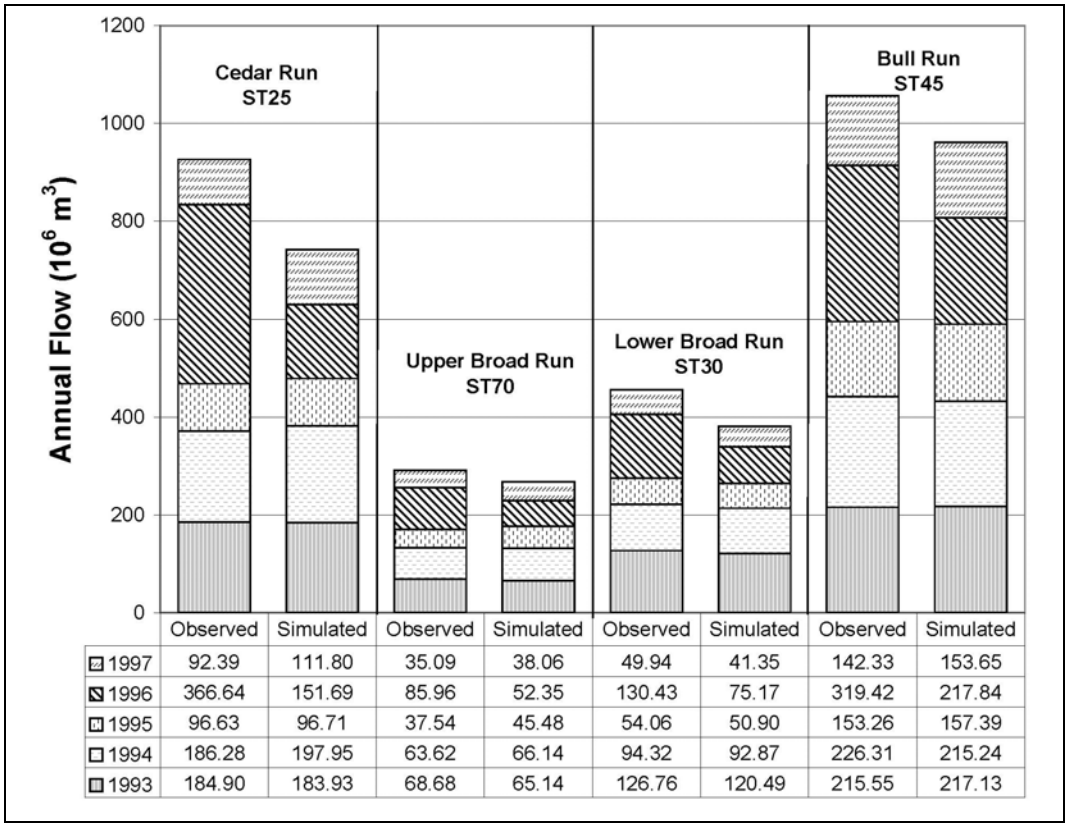

	Observed	Simulated	Observed	Simulated	Observed	Simulated	Observed	Simulated
1997	92.39	111.80	35.09	38.06	49.94	41.35	142.33	153.65
1996	366.64	151.69	85.96	52.35	130.43	75.17	319.42	217.84
1995	96.63	96.71	37.54	45.48	54.06	50.90	153.26	157.39
1994	186.28	197.95	63.62	66.14	94.32	92.87	226.31	215.24
1993	184.90	183.93	68.68	65.14	126.76	120.49	215.55	217.13

Figure 3-10: Comparison of Annual Flow Balance at Selected Stream Stations for Model Calibration and Validation

Compared with the calibration period (1993~1995), the validation period showed relatively weaker correlations between simulated and observed data, which were due to the discrepancies in the year 1996 (Table 3-11). The statistical analysis for the whole five-year simulation period shows generally good correlations between simulated and observed flow rates with R^2 values in the range of 0.594~0.791 for monthly data. Although the linked model was not well validated under extremely wet years, the model output is useful as it can provide adequate representation of the general watershed behavior.

Table 3-11: R^2 Values based on Daily and Monthly Comparison of Flow Rates at Various Stream Stations for Model Calibration and Validation

		ST25 Cedar Run	ST70 Upper Broad Run	ST30 Lower Broad Run	ST45 Bull Run
Monthly	Calibration	0.857	0.896	0.885	0.815
	93~95	Very Good*	Very Good	Very Good	Good
	Validation	0.382	0.389	0.724	0.728
	96~97	Poor	Poor	Fair	Fair
	Summary	0.594	0.746	0.791	0.774
	93~97	Poor	Good	Good	Good
Daily	Calibration	0.523	0.632	0.460	0.503
	93~95	Poor	Fair	Poor	Poor
	Validation	0.211	0.298	0.298	0.444
	96~97	Poor	Poor	Poor	Poor
	Summary	0.205	0.419	0.405	0.455
	93~97	Poor	Poor	Poor	Poor

*Ratings are based on Table 3-4

The poor performance of the model for daily flow rates (Table 3-11) is probably due to the timing shift between observed and simulated data. The timing and duration of a simulated storm might be advanced or delayed by some hours (typically one to three hours), compared to observed data, due to the uncertainty related to meteorological data and the model itself. This can shift HSPF-predicted flows from one day to the next across the midnight divide.

The HSPF submodels showed their capability of capturing the general trend of the temporal and spatial distribution of daily flow rates (Figure 3-11). Even though the submodels were capable in capturing both small and large storm events, they missed some closely-spaced storm events caused by continuous low-intensity-precipitation events. This helps to explain the relatively large discrepancies in the extremely wet year 1996.

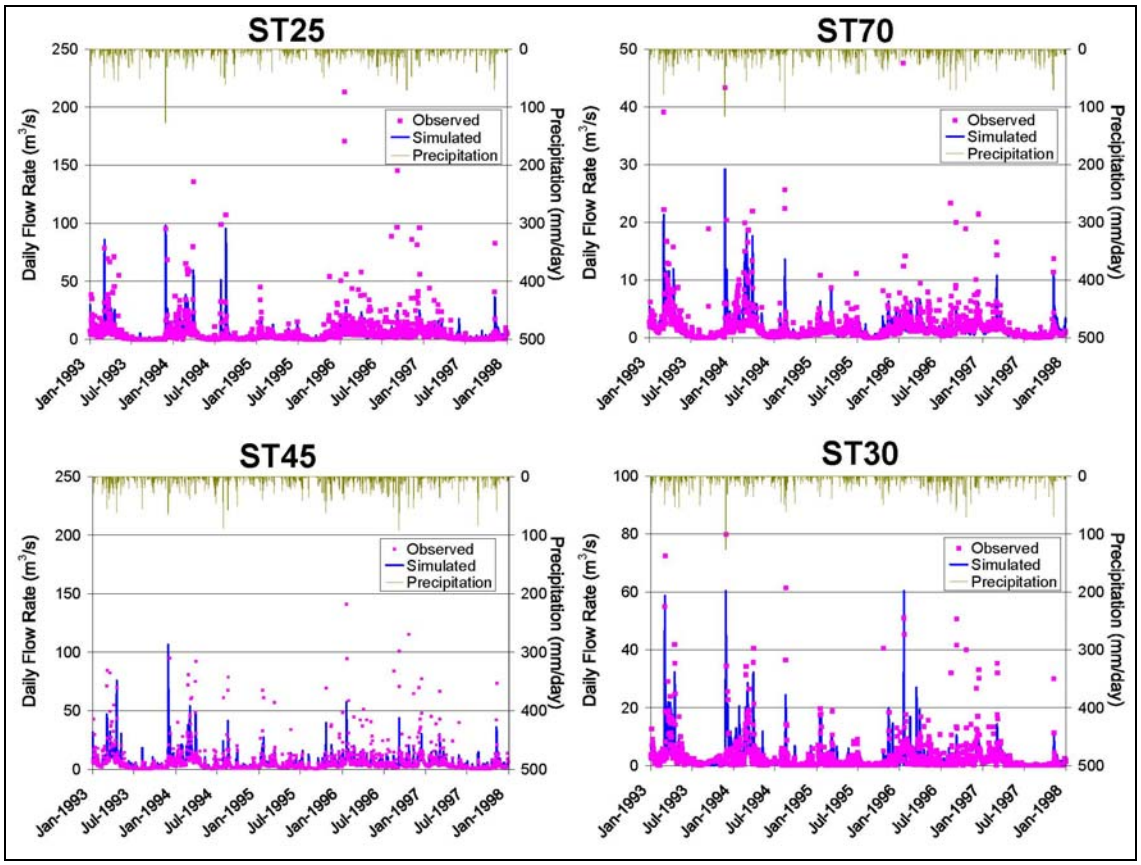

Figure 3-11: Daily Flow Rates Comparison at Four Principal Stations for Model Calibration and Validation

The water surface elevation was well validated (Figures 3-8 and 3-9) for the Lake and the Reservoir. In the validation period, the R^2 values based on daily comparisons were 0.921 and 0.949 for the Lake and the Reservoir, respectively. At Lake Manassas, the observed data were missing from 09/10/1997 to 12/31/1997 due to station reinstallation and the W2 submodel filled the period with reasonable estimates, which were confirmed by the flow comparison at ST30, the station downstream of the lake. A W2 utility called WaterBalance was used to estimate the missing flows based on simulated and observed flow volumes. It indicated that the average water balance flow correction for both waterbodies was less than 0.005 m^3/s for the five-year simulation period (1993-1997).

3.6 *Conclusions*

A complex linked model, using six applications of HSPF and two of CE-QUAL-W2, was created for the Occoquan Watershed. The procedure used in the model development and calibration was described. The hydrological calibration of this linked model was performed successfully, and, in spite of one very wet year, the validation was reasonably good, thus indicating that linked models can be adequately calibrated with moderate additional effort. The advantages of doing this are twofold: (i) the model behaves more as a single entity and forces the modeler to look at approaches to calibration that benefit the overall model rather than the individual components, and (ii) the resultant linked model is more easily accepted by managers and the general public because it can be more readily seen to represent a natural system which is not unlinked. The latter advantage can often have greater weight than the former in many situations (management decision-making, public information dissemination, to name two), because it focuses attention on the model without leaving an impression that something might be inapt in how the natural system was represented by submodels that are not linked.

3.7 *References*

Albek, M., Ögeütveren, U.B. and Albek, E. (2004). Hydrological Modeling of Seydi Suyu Watershed (Turkey) with HSPF. *Journal of Hydrology*, **285**, 260-271.

Bicknell, B.R., Imhoff, J.C., Kittle, J.L., Jobes, T.H. and Donigian, A.S. (2001). *Hydrological Simulation Program-Fortran HSPF Version 12 User's Manual*, U.S. Environmental Protection Agency, National Exposure Research Laboratory, Athens, Georgia.

Black & Veatch Corporation. (2000). *Safe Yield of Lake Manassas*. Manassas, Virginia.

Bowen, J.D. and Hieronymus, J.W. (2003). A CE-QUAL-W2 Model of Neuse Estuary for Total Maximum Daily Load Development. *Journal of Water Resources Planning and Management*, **129**(4), 283-294.

Brun, S.E. and Band, L.E. (2000). Simulating Runoff Behavior in an Urbanizing Watershed. *Computers, Environment and Urban Systems*, **24**(1), 5-22.

Cerco, C.F., Linker, L., Sweeney, J., Shenk, G. and Butt, A.J. (2002). Nutrient and Solid Controls in Virginia's Chesapeake Bay Tributaries. *Journal of Water Resources Planning and Management*, **128**(3), 179-189.

Chen, Y.D., Carsel, R.F., McCutcheon, S.C. and Nutter, W.L. (1998a). Stream Temperature Simulation of Forested Riparian Areas: I. Watershed-Scale Model Development. *Journal of Environmental Engineering*, **124**(4), 304-315.

Chen, Y.D., Carsel, R.F., McCutcheon, S.C. and Nutter, W.L. (1998b). Stream Temperature Simulation of Forested Riparian Areas: II. Model Application. *Journal of Environmental Engineering*, **124**(4), 316-328.

Cole, T. M. and Wells, S. A. (2003). *CE-QUAL-W2: A Two-Dimensional Laterally Averaged, Hydrodynamic and Water Quality Model, Version 3.2 User Manual*. U.S. Army Corps of Engineers, Washington, D.C.

Donigian, A.S. (2002). Watershed Model Calibration and Validation: The HSPF Experience. *National TMDL Science and Policy Specialty Conference 2002*, Phoenix, Arizona.

Donigian, A.S. and Crawford, N.H. (1976). *Modeling Nonpoint Pollution from the Land Surface*. U.S. Environmental Protection Agency, Environmental Research Laboratory, Athens, Georgia.

Eggink, J. (2001). *An Exploration of the Limnological Dynamics of Lake Manassas*, Master's Thesis, Virginia Polytechnic Institute and State University, Falls Church, Virginia.

Golden Software, Inc. (2002). *Surfer 8: Contouring and 3D Surface Mapping for Scientists and Engineers User's Guide*. Golden, Colorado.

Gunduz, O., Soyupak, S. and Yurteri, C. (1998). Development of Water Quality Management Strategies for the Proposed Isikli Reservoir. *Water Science and Technology*, **37**(2), 369-376.

Hadjerioua, B., Lindquist, K.F. and Siler, V. (2001). Linking TVA's Norris and Melton Hill Reservoirs Water Quality: CE-QUAL-W2 Models. *World Water Congress 2001, Bridging the Gap: Meeting the World's Water and Environmental Resources Challenges*, Florida.

Hamon, R.W., Weiss, L.L. and Wilson, W.T. (1954). Insolation as an Empirical Function of Daily Sunshine Duration. *Monthly Weather Review*, **82**(6), 141-146.

Hayashi, S., Murakami, S., Watanabe, M. and Xu, B. (2001). HSPF Simulation of Runoff and Sediment Loads in the Upper Changjiang River Basin, China. *Journal of Environmental Engineering*, **137**(7), 801-815.

Hicks, B.B., DeLuisi, J.J. and Matt, D.R. (1996). The NOAA Integrated Surface Irradiance Study (ISIS)-A New Surface Radiation Monitoring Program. *Bulletin of the American Meteorological Society*, **77**(12), 2857-2864.

Hydrocomp Inc. (1978). *The Occoquan Basin Computer Model Calibration, Verification and User's Manual*. Georgia, USA.

Johnston, J. (2005). Personal Communication. Manassas, Virginia.

Kohler, M.A., Nordenson, T.J. and Fox, W.E. (1955). *Evaporation from Pans and Lakes*. U.S. Weather Bureau.

Laroche, A.M., Gallichand, J., Lagace, R. and Pesant, A. (1996). Simulating Atrazine Transport with HSPF in an Agricultural Watershed. *Journal of Environmental Engineering*, **122**(7), 622-630.

Laufer, S.M. (1986). *Nutrient Dynamics in the Lake Manassas (Virginia) Watershed*, Master's Thesis, Polytechnic Institute and State University, Blacksburg, Virginia.

Metcalf & Eddy Inc. (1970). *The Occoquan Reservoir Study*. Boston, Massachusetts.

Neitsch, S.L., Arnold, J.R., Kiniry, J.R., Williams, J.R. and King, W.K. (2002). *Soil and Water Assessment Tool Theoretical Documentation Version 2000*. Texas Water Resources Institute, College Station, Texas.

Northern Virginia Planning District Commission. (1979). *Assessments of Water Quality Management Strategies With the Occoquan Basin Computer Model*. Annandale, Virginia.

Northern Virginia Planning District Commission. (1994). *Mission Statement for the Occoquan Basin Model Upgrade*. Annandale, Virginia.

Occoquan Watershed Monitoring Laboratory. (1991). *Water Quality Assessment for Lake Manassas, Virginia*. Manassas, Virginia.

Occoquan Watershed Monitoring Laboratory. (1996). *An Updated Water Quality Assessment for Lake Manassas, Virginia*. Manassas, Virginia.

Occoquan Watershed Monitoring Laboratory. (1998). *An Updated Water Quality Assessment for the Occoquan Reservoir and Tributary Watershed: 1973-1997*. Manassas, Virginia.

Rahman, M. and Salbe, I. (1995). Modelling Impacts of Diffuse and Point Source Nutrients on the Water Quality of South Creek Catchment. *Environment International*, **21**(5), 597-603.

Randall, C.W. and Grizzard, T.J. (1995). Management of the Occoquan River Basin: A 20-Year Case History. *Water Science and Technology*, **32**(5-6), 235-243.

Ross, M., Geurink, J., Aly, A., Tara, P., Trout, K. and Jobes, T. (2004). *Integrated Hydrological Model (IHM) Volume I: Theory Manual*. Tampa Bay Water and Southwest Florida Water Management District, Florida.

Saito, L., Johnson, B.M., Bartholow, J. and Hanna, R.B. (2001). Assessing Ecosystem Effects of Reservoir Operations Using Food Web-Energy Transfer and Water Quality Models. *Ecosystem*, **4**(2), 105-125.

Stein, S.M., Goulet, N., Kammer, T., Waye, D. and Saffarinia, K. (1998). Occoquan Water Supply Protection Tool. *International Water Resources Engineering Conference: Proceedings*, Reston, Virginia.

Sullivan, A.B., Jager, H.I. and Myers, R. (2003). Modeling White Sturgeon Movement in a Reservoir: The Effect of Water Quality and Sturgeon Density. *Ecological Modeling*, **167**(1), 97-114.

U. S. Environmental Protection Agency, Office of Air Quality. (2000). *Meteorological Monitoring Guidance for Regulatory Modeling Applications*. *EPA-454/R-99-005*, Washington, D.C.

Virginia State Water Control Board. (1971). *A Policy for Waste Treatment and Water Quality Management in the Occoquan Watershed*. Richmond, Virginia.

Wells, S. (2005). Personal Communication. Portland, Oregon.

Watermark Numerical Computing. (2004). *PEST: Model-Independent Parameter Estimation, User's Manual 5th Edition*. Brisbane, Australia.

Wool, T.A., Ambrose, R.B., Martin, J.L. and Cormer, E.A. (2003). *Water Quality Analysis Simulation program (WASP) Version 6.0 Draft: User's Manual*. U.S. Environmental Protection Agency, Atlanta, Georgia.

Chapter 4. Temperature and Dissolved Oxygen Calibration and Validation of a Linked Model for the Occoquan Watershed, Virginia

4.1 *Summary*

The Occoquan Watershed is a 1,515 km^2 basin located in northern Virginia and contains two principal waterbodies: the Occoquan Reservoir and Lake Manassas. Both waterbodies are principal drinking water supplies for local residents and experience eutrophication and summer algae growth. They are continuously threatened by new development from the rapid expansion of the greater Washington D.C. region. The Occoquan model, consisting of six HSPF and two CE-QUAL-W2 submodels linked in a complex way, has been developed to simulate hydrology and water quality activities in these two major reservoirs and the associated drainage areas. This paper describes the application of the linked model to simulate the spatial and temporal distribution of temperature and dissolved oxygen (DO) in the watershed and reservoirs. The models were calibrated for a three-year simulation period and validated for a two-year simulation period based on more than 8,000 field measurements. The results show that a successful calibration can be achieved using the linked approach, with moderate additional effort. The results showed strong correlation between simulated and observed values and the R^2 values based on daily data were 0.882 or greater for temperature and 0.487 or greater for DO at various steam stations. The differences of seasonal temperatures and DO concentrations at various stream stations ranged from –1.87 °C to +0.38 °C and from –0.53 mg/L to +1.75 mg/L, respectively. The hydrodynamic differences between the two waterbodies, as well as spatial and temporal variations of temperatures and DO concentrations in them, were well reproduced by the W2 submodels. The differences of the average surface temperatures were less than 0.42 °C and 1.38 °C for Lake Manassas and the Occoquan Reservoir, respectively, and the differences in surface DO concentrations were less than 1.25 mg/L and 1.42 mg/L, respectively. The model was adequately validated to represent the general trend of temperature and DO in the watershed and waterbodies. The good calibration and validation of the linked model

provide a direct linkage between upstream activities and downstream water quality, and thus facilitate the ongoing DO TMDL project, which will evaluate alternative watershed management plans to meet the TMDL goal.

4.2 *Introduction*

Temperature and dissolved oxygen (DO) are two fundamental factors in natural aquatic systems. Due to urbanization and associated increase of imperviousness, stream temperature and water quality have been greatly modified (Schueler 1994). According to the U.S. Environmental Protection Agency (USEPA 2002), thermal modification and low DO are ranked as the fourth and sixth reasons, respectively for impairment of streams and rivers. In Virginia, approximately 53% of assessed waterbodies are impaired due to organic enrichment and low DO concentrations (VA DEQ 2004). The Occoquan Reservoir is listed as an impaired waterbody due to low DO concentrations in bottom waters and a total maximum daily loads (TMDL) project is scheduled to be completed before 2010 (VA DEQ 2004).

Because water quality problems result from various factors, including those related to DO dynamics, water quality models have been widely used to determine the key processes that control temperature and DO dynamics, so that alternative management scenarios can be evaluated. Examples include watershed models, such as Hydrological Simulation Program–Fortran (HSPF) (Bicknell, et al. 2001) and Soil and Water Assessment Tool (SWAT) (Neitsch, et al. 2002), and receiving waterbody models, such as Water Quality Analysis Simulation Program (WASP) (Wool, et al. 2003) and CE-QUAL-W2 (W2) (Cole and Wells 2003). One of the difficult challenges with simulation of temperature and DO in watershed models is insufficient description of physical, chemical and biological processes in the receiving waterbodies. For example, HSPF assumes receiving streams and reservoirs to be well mixed and unidirectional, thus thermal stratification would not be appropriately reproduced. SWAT ignores the impact of solar radiation and wind speed, and assumes air temperature to be the only factor determining stream water temperature. On the other hand, receiving water quality models such as W2 and WASP require time-varying boundary inputs that drive these models during the course of a

simulation. They usually include inflows, outflows, temperature, water quality data, and meteorological data. However, these boundary conditions, with the possible exception of meteorological data, are normally not monitored at a frequency to provide a sufficient temporal description of the driving forces. These shortcomings in common modeling applications can be overcome by linking watershed models to receiving waterbody models. This approach provides a more accurate representation of the real world and allows integration of downstream water quality to upstream land activities. In addition, it can be applied to complicated watersheds that have more than one major waterbody. However, few researches have adopted this approach because of insufficient data support and the complications involved with linking two or more state-of-the-art water quality models.

Described in this paper are the calibration and validation of temperature and DO in the Occoquan Watershed as well as two principal waterbodies, using a complex linked model that consists of six HSPF and two W2 applications. The main objectives of this paper are to 1) provide a good calibration of water temperature and DO in the streams;
2) demonstrate the capture of thermal stratification and DO depletion in the reservoirs;
3) provide a solid calibrated model for the DO TMDL development. The initial calibration of the linked model was for the years 1993-95, with a validation period of 1996-97, a total five-year period spanning the land-use data update issued in 1995. Land-use data are updated every five years. Due to length limitations, separate papers will provide discussion on hydrology(Xu, et al. 2006), nutrient transport and fate, and algae dynamics.

4.2.1 Study Area

The Occoquan Watershed (Watershed) is a 1,515 km^2 basin in northern Virginia (Figure 4-1). It contains three major tributaries: Cedar Run, Broad Run and Bull Run, and two major waterbodies: Occoquan Reservoir (Reservoir) and Lake Manassas (Lake).

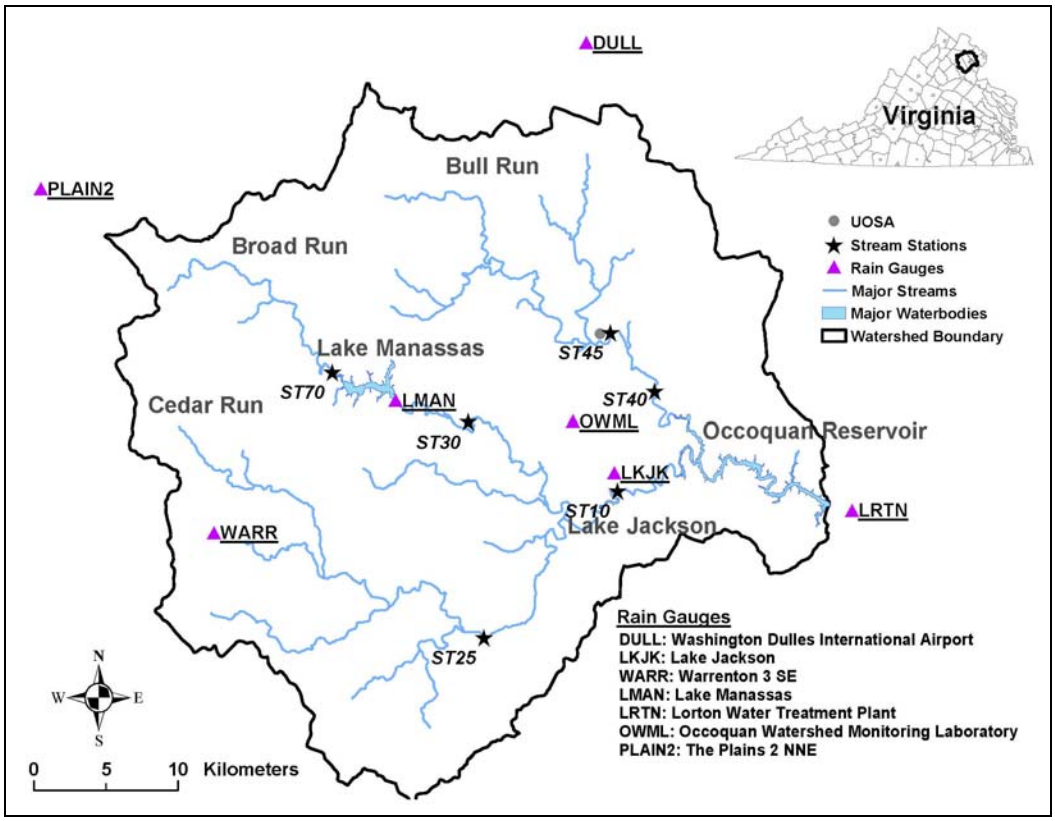

Figure 4-1: Location of Occoquan Watershed in Virginia, USA, Showing Main Tributaries, Main waterbodies, Stream Stations and Rain Stations Used in This Study

The Reservoir is part of the drinking water supply for 1.2 million northern Virginia residents and is a major recreation site. It receives flows from two principal tributaries, Occoquan River and Bull Run. The Upper Occoquan Sewage Authority (UOSA) water reclamation facility discharges into Bull Run, which is an important component of the water quality management of the Reservoir (Randall and Grizzard 1995). Flows over the Occoquan dam drain into the Potomac River after running approximately 8 km southeast. The total capacity of the Reservoir is 31.4×10^6 m^3 and the safe yield is 2.5×10^5 m^3/d (which includes the discharge from UOSA) (OWML 1998). The surface area at the maximum elevation of 36.6 m above mean sea level is 616 hectare. The average depth of the Reservoir is 5.1 m with a maximum of approximately 20.0 m near the dam. The average residence time is 19.6 days. Based on Wetzel's (2001) classification of the trophic status of lakes, the Reservoir is mesotrophic with the limiting nutrient being orthophosphate phosphorus (Randall and Grizzard 1995). Copper compounds are used to control algae growth during summer months.

Lake Manassas is another major waterbody in the Watershed. It serves as the principal drinking water supply for the City of Manassas and is used for recreational purposes. The total drainage area is approximately 189 km^2. Three golf courses are located on the north shore (Robert Trent Jones, Virginia Oaks, and Par 3). The City of Manassas withdraws water from three water intakes at the dam (primarily from the top intake) for municipal service. During dry periods, the golf courses withdraw water from the surface. The natural storage capacity of the Lake is 15.4×10^6 m^3 and the safe yield is 6.37×10^4 m^3/d. The surface area at the maximum elevation of 86.9 m above mean sea level is 282 hectare. The average depth is 5.5 m with a maximum depth of approximately 15.0 m near the dam. Lake Manassas is classified as an eutrophic waterbody and the limiting nutrient is phosphorus (Eggink 2001). It has high biological productivity and copper compounds were applied for at least fourteen years (1982-1995), typically four times a year.

4.3 *Model Description*

HSPF divides simulated watersheds into three blocks and simulates processes occurring in: (1) pervious land areas (PERLND); (2) impervious land areas (IMPLND); and (3) well-mixed streams and reservoirs (RCHRES) (Bicknell, et al. 2001). The heat budget is simulated in the section PWTGAS under the module PERLND, IWTGAS under IMPLND, and HTRCH under RCHRES. For pervious land segments, PWTGAS computes water temperatures based on the assumption that the water temperatures from each outflow are equal to the soil temperatures of the layer from which the flow is generated, except that water temperatures cannot be less than freezing. Because extensive measured soil temperature data are not available, the section PSTEMP is applied to calculate soil temperatures for surface, upper, lower and groundwater layers of a pervious land segment, based on which the water temperatures are estimated. For impervious land segments, IWTGAS applies a similar method with PWTGAS to estimate the surface runoff temperature. The heat content from PERLND and IMPLND are then supplied to HTRCH to determine water temperatures in the well-mixed streams and reaches. In HTRCH, the heat budget method is applied to estimate six important heat components to determine the net heat exchange at the water surface. These are shortwave solar radiation,

longwave radiation, conduction-convection, evaporative heat loss, heat content of precipitation, and bed conduction. The water temperatures are then determined by the heat content in a defined amount of water. The parameters in HTRCH generally play a key role in water temperature calibration, and some important ones are listed in Table 4-1.

Table 4-1: Key Parameters for Temperature and DO Simulation in HSPF

Parameter	Definition	Unit	Typical Values	Values Used
CFSAEX	Ratio of radiation at water surface to gage radiation value. Also accounts for the shading of the waterbody	—	0-1.0*	0.9-1.0
KATRAD	Longwave radiation coefficient	—	9.0**	6.5-10
KCOND	Conduction-convection heat transfer coefficient	—	1-20*	6.12
KEVAP	Evaporation coefficient	—	1-5*	2.24
REAK	Empirical coefficient for aeration equation	hr^{-1}	0.08-0.971**	0.2
KBOD20	BOD decay rate at 20 ºC	hr^{-1}	0.0004-0.04**	0.004-0.04
KODSET	BOD settling rate	ft/hr	0.0004-0.06**	0.027-0.05
BENOD	Benthic oxygen demand at 20 ºC	$mg \cdot m^2/hr^{-1}$	0.0917-1833**	10
KATM20	Nitrification rate at 20 ºC	hr^{-1}	0.004-0.008**	0.01-0.05

*Bicknell et al. 2001
**Bowie et al. 1985

In HSPF, DO in surface runoff is calculated as a direct function of water temperature in PWTGAS of PERLND and IWTGAS of IMPLND by the following equation (Bicknell, et al. 2001):

$$SODOX = (14.652 + SOTMP \cdot (-0.41022 + SOTMP \cdot (0.007991 - 0.000077774 \cdot SOTMP))) \cdot ELEVGC$$

where: SODOX is DO concentration in surface runoff (mg/L)
SOTMP is surface outflow temperature (ºC)
ELEVGC is the correction factor for elevation above sea level.

DO concentrations in interflow and active groundwater flows are supplied as monthly variables.

Section OXRX of the RCHRES module estimates DO concentrations in mixed streams, which receive the DO inputs from upland segments. It determines oxygen balance from several processes including reaeration, decay of organic matter and benthal oxygen demand. In addition, the oxygen balance can be adjusted by other processes such as nitrification, photosynthesis, and algae respiration, if applied. Some key parameters that affect the oxygen balance are listed in Table 4-1.

W2 is a two-dimensional hydrodynamics and water quality model suitable for long and narrow waterbodies, such as reservoirs and lakes (Cole and Wells 2003). The mechanism of the heat budget simulation in W2 is similar to that in HTRCH of HSPF. It applies the energy budget accounting method to estimate the contribution from each heat component. However, components such as shortwave radiation, longwave radiation, evaporation heat loss, and heat conduction are estimated from different empirical equations. In addition, a user-specified wind speed function is included to account for impacts from wind stress. This function affects evaporation heat loss and surface heat conduction calculation and plays an important role in the overall heat balance. Due to the geographic locations of the waterbodies, the icing function is applied, which not only affects water temperature but also oxygen concentrations.

W2 provides comprehensive calculations for DO simulation. It considers oxygen consumption processes such as nitrification, decomposition of both dissolved and particulate organic matter, and respiration and photosynthesis of algal species. The model supports a wide range of reaeration formulas, including nine for river systems, fourteen for lakes and reservoirs, and three for estuaries. In addition, W2 provides equations to predict the oxygen entrainment at dams and weirs and allows users to select appropriate equations to fit specific considerations. Both aerobic and anaerobic processes are included to not only allow the capture of oxygen saturation in surface water but also the oxygen depletion in metalimnetic and hypolimnetic layers. Detailed descriptions of both models can be found elsewhere (Bicknell, et al. 2001; Chen, et al. 1998b; Cole and Wells 2003; Donigian and Crawford 1976).

4.3.1 Linked Model Approach

The Occoquan model is a complex linked model application, which includes six HSPF and two W2 submodels. The schema of the linked model approach, as well as the watershed segmentation, is shown in Figure 4-2. The Watershed is divided into six subbasins, with a total of 56 land (HSPF) segments. The average segment size is 27.0 km^2.

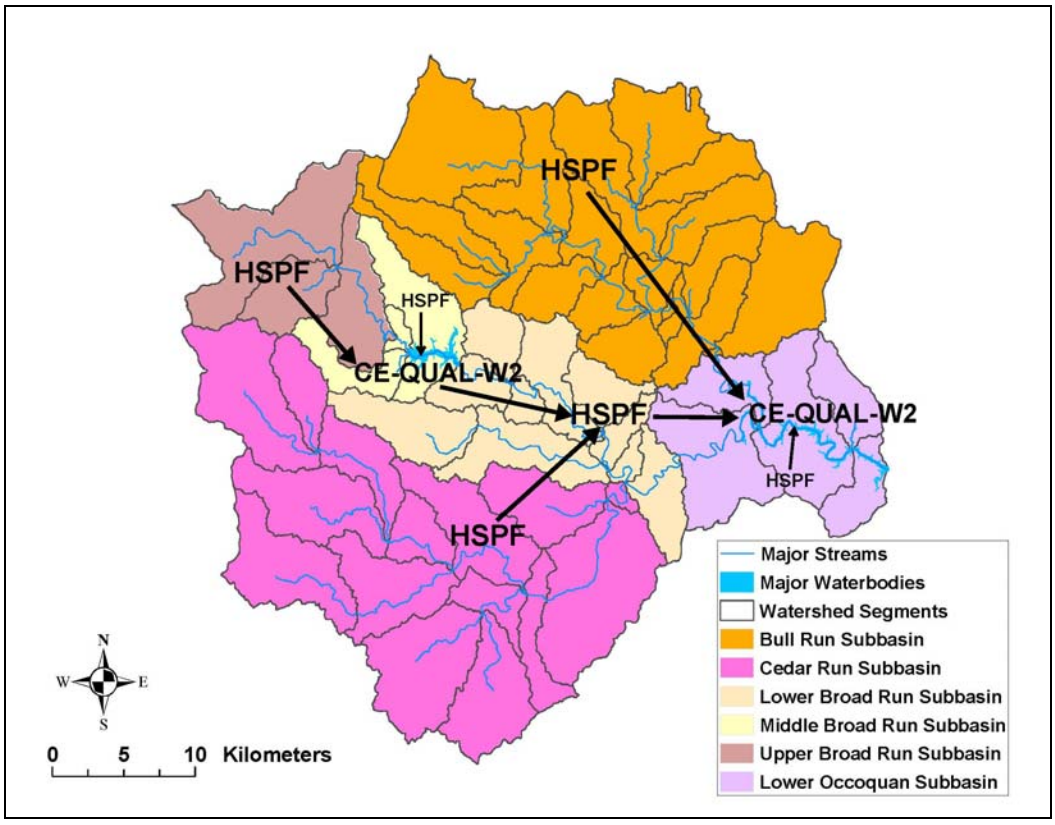

Figure 4-2: Occoquan Watershed Model Application Schema and Watershed Segmentation

The bathymetries of the Lake and the Reservoir are shown in Figure 4-3. For modeling purposes, the Lake is divided into four branches and has a total of 29 active computational segments with lengths ranging from 173 m to 568 m. There are 4 to 28 computational layers, each 0.5 m thick. The Reservoir is also divided into four branches with a total of 69 computational segments. The average segment length is 583 m with a minimum of 74 m (Segment 32, at Ryan's Dam, a submerged feature with a narrow vertical opening) and a maximum of 838 m. There are from 1 to 39 computational layers, each 0.5 m thick. A detailed description of the model development, watershed segmentation and waterbody segmentation can be found elsewhere(Xu, et al. 2006).

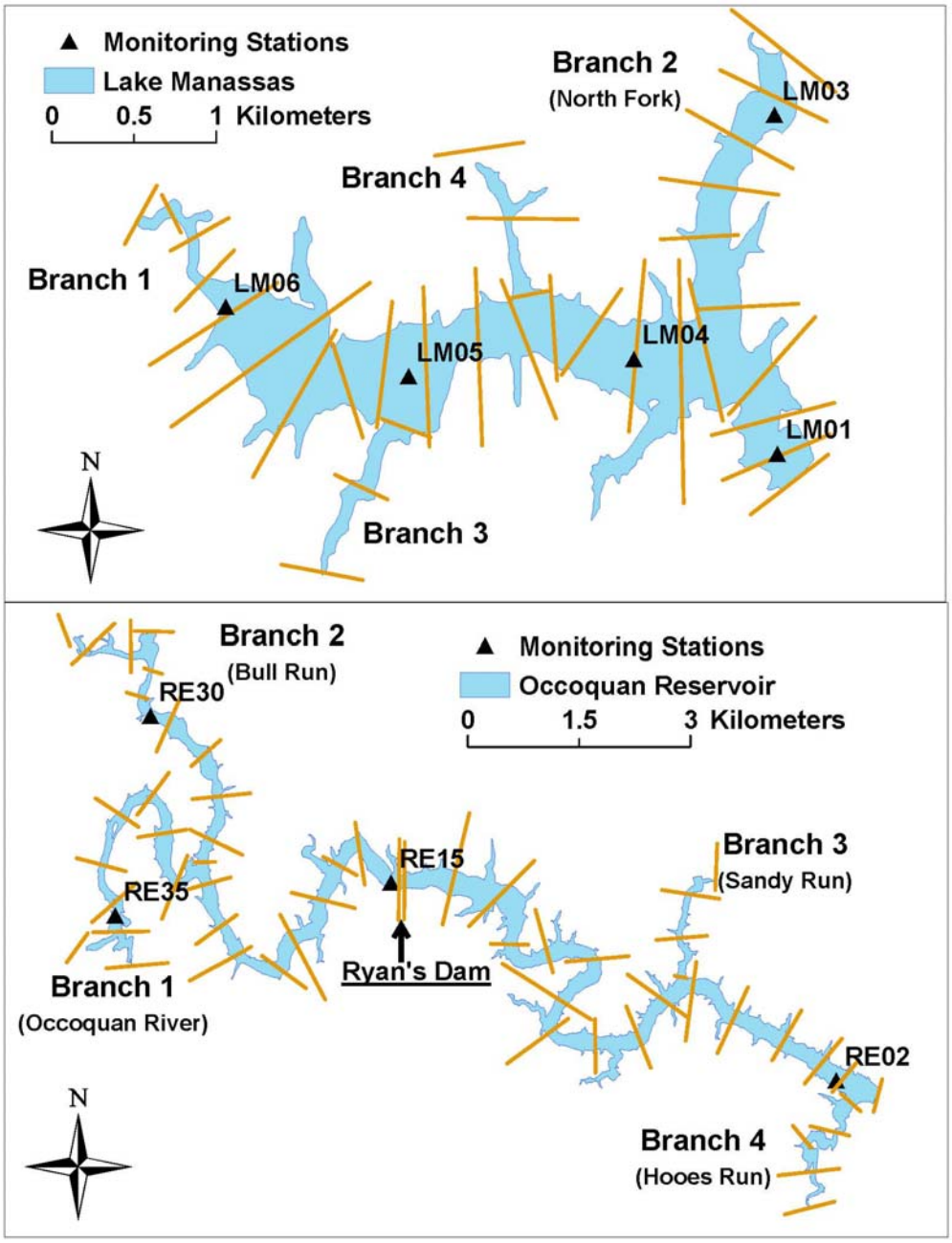

Figure 4-3: Segmentation of Lake Manassas and Occoquan Reservoir and Selected Monitoring Stations

4.3.2 Boundary Conditions

In this model application, the boundary conditions required by W2, such as inflows, temperature, and DO data, are provided by upstream HSPF submodels. For example, in the Lake W2 submodel, the Upper Broad Run HSPF submodel not only provides daily

time series inputs of direct inflows, but also temperature, DO and other water quality concentrations (Figure 4-2). The ungauged distributed tributary flows along the Lake and associated water quality are estimated by the Middle Broad Run HSPF submodel. The outputs from the Lake W2 submodel serve as inputs for the Lower Broad Run HSPF submodel. Similarly, the Lower Broad Run HSPF application, including the contribution from the Cedar Run subbasin, provides flows and water quality time series for the Occoquan River branch of the Reservoir. The input time series of the Bull Run branch are provided by the Bull Run HSPF submodel. The Lower Occoquan HSPF submodel provides the ungauged distributed tributary flows and associated water quality along the Reservoir. Thus, six HSPF and two W2 submodels are linked together to fully represent the hydrology and water quality activities in the Watershed and two principal waterbodies.

4.3.3 Initial Conditions

The initial temperatures and DO concentrations in HSPF submodels were first assigned reasonable values. Then the submodels were run through a one-year simulation. The initial values were then adjusted based on the values at the end of the simulation.

The initial values for temperature and DO concentrations in W2 submodels were set to be the same with the observed data available at the beginning of the simulation period at the stations closest to the dams.

4.3.4 Observed Data

At stream stations (Figure 4-1), the temperature and DO data are available on a monthly basis during the winter season and on a weekly basis during other seasons. Here, the seasons are defined as winter (December, January, February), spring (March, April, May), summer (June, July, and August), and fall (September, October, November). For the Lake and the Reservoir stations (Figure 4-3), in-pool depth profile data of temperature and DO are collected on a monthly basis during the winter season and on a weekly basis during other seasons.

4.3.5 Calibration Criteria

Because there is no single accepted test to determine whether or not a model is calibrated, both graphical and statistical methods were applied to evaluate model performance. In addition to traditional statistical measures such as mean values and the standard coefficient of determination (R^2), several other statistical methods were also used.

The percentage difference (PD) between simulated and observed data is defined below:

$$PD = \frac{100 \cdot (Y - X)}{X}\%$$

where X is the observed temperature or DO concentration, and Y is the simulated temperature or DO concentration. Donigian (2002) suggested a value in the range of 15-25% for a good water quality/nutrient calibration and 8-12% for a good temperature calibration of HSPF.

The absolute mean error (AME) indicates how far the simulated values are from the observed data and is given by the following equation:

$$AME = \frac{\sum |\text{Predicted} - \text{Observed}|}{\text{Number of Observations}}$$

The root mean square (RMS) indicates the spread of how far the computed values deviate from the observed values and is given by the following equation:

$$RMS = \sqrt{\frac{\sum (\text{Predicted} - \text{Observed})^2}{\text{Number of Observations}}}$$

4.4 *Results and Discussion*

When interpreting temperature and DO results from W2, several important points should be considered. Firstly, W2 assumes uniform temperature and DO concentrations in each computational grid. However, observed data are normally collected at one specific point

within a waterbody. Secondly, although the observed data are normally taken around noon, the exact times vary from 10:00 a.m. to 2:00 p.m. They are compared with the model output at noon. Thirdly, the computed temperatures and DO concentrations in the computational cells close to the headwaters are subject to large daily variations depending on how rapidly inflows, outflows, and meteorological inputs change. Thus, in this linked model application, the results of stations near headwaters of a waterbody rely on the performance of upstream submodels.

Similarly, several points need to be considered when interpreting the results from HSPF. Firstly, HSPF assumes streams and reaches to be well mixed and unidirectional, thus it only provides a single value for temperature and DO concentration in a particular segment. In reality, they vary along streams and the observed data are collected at specific stream locations. Secondly, observed data, which are normally taken around noon, are compared with model outputs based on daily averages. Finally, the channel geometric and hydraulic characteristics were estimated from the local digital elevation model because extensive field measurements were not available. This might have little impact on overall watershed simulation, but might impact the heat budget on a local basis. Therefore, the simulated outputs from W2 and HSPF applications are expected to contain inaccuracies, and there are bound to be differences between observed and simulated data.

4.4.1 Model Calibration

Table 4-2 provides the daily and seasonal comparisons of temperatures at five principal stream stations. Results from ST25 and ST70 are used to evaluate HSPF performance of the Cedar Run and Upper Broad Run subbasins. ST30 is located downstream of the Lake and is used to evaluate the overall model performance up to this point, including the Lake. ST40, located at approximately 5 km downstream of UOSA, is used to evaluate the performance of the Bull Run subbasin. ST10 is located downstream of Lake Jackson and is used to evaluate the joint performance of the Cedar Run and Broad Run subbasins. In addition, ST10 and ST40 are stations at the headwaters of the Reservoir, where HSPF

submodels were linked to the Reservoir W2 submodel, in terms of the linked model application.

Table 4-2: Daily and Seasonal Temperature Comparisons at Various Stream Stations in the Occoquan Watershed

		ST25	ST70	ST30	ST10	ST40
R2 for Daily Values		0.930	0.933	0.882	0.934	0.957
Spring	Observed (ºC)	13.92	12.82	13.63	14.65	14.58
	Simulated (ºC)	14.25	12.96	11.85	14.00	13.89
	Difference (ºC)	+0.33	+0.14	–1.78	–0.65	–0.69
	PD* (%)	+2.37	+1.09	–13.06	–4.44	–4.73
Summer	Observed (ºC)	24.23	23.71	24.14	25.47	25.20
	Simulated (ºC)	24.61	24.09	24.03	25.20	24.75
	Difference (ºC)	+0.38	+0.38	–0.11	–0.27	–0.45
	PD* (%)	+1.57	+1.60	–0.46	–1.06	–1.79
Fall	Observed (ºC)	13.87	13.70	13.62	16.59	15.84
	Simulated (ºC)	13.44	13.23	13.48	14.72	14.00
	Difference (ºC)	–0.43	–0.47	–0.14	–1.87	–1.84
	PD* (%)	–3.10	–3.43	–1.03	–11.27	–11.62
Winter	Observed (ºC)	2.47	3.67	3.39	3.67	3.27
	Simulated (ºC)	1.72	4.01	1.96	2.54	1.91
	Difference (ºC)	–0.75	+0.34	–1.43	–1.13	–1.36
	PD* (%)	–30.36	+9.26	–42.18	–30.79	–41.59

* PD: Percentage Difference

Overall, HSPF reproduced the spatial and temporal distribution of stream temperatures fairly accurately and the R^2 values based on daily data are 0.882 or greater for five principal stream stations. The lack of observed temperature data from the UOSA discharge helps to explain the general under-prediction of temperature at station ST40. The differences of seasonal average temperature ranged from –1.87 ºC to +0.38 ºC for all seasons. Although the stream temperatures were not well reproduced in winter months, the submodels were well calibrated in other seasons, according to the scale used by Donigian (Donigian 2002) (see Table 3-4) and the absolute PD values were 12% or less for most sites (less than 5%, actually, for all but three cases). The increase of temperatures from upstream stations (ST25 and ST70) to downstream stations (ST10, ST30 and ST40) was noticeable, and this is due to the increase of stream paths and resultant increased exposure to solar radiation.

Similarly, the observed DO concentrations follow a seasonal pattern, which was well reproduced by the model predictions. The lowest DO concentrations were found during the summer season when stream temperatures were highest (Table 4-3). The differences

of seasonal average DO concentrations ranged from –0.53 mg/L to +1.75 mg/L and the observed and simulated DO showed strong correlations with R^2 based on daily values ranging from 0.487 to 0.725. Overall, the stream DO concentrations were very well calibrated (Donigian 2002) (see Table 3-4) and the absolute PD values were less than 15% for most sites.

Table 4-3: Daily and Seasonal DO Comparisons at Various Stream Stations in the Occoquan Watershed

		ST25	ST70	ST30	ST10	ST40
R^2 for Daily Values		0.639	0.700	0.487	0.725	0.577
Spring	Observed (mg/L)	9.75	10.90	10.34	10.30	10.79
	Simulated (mg/L)	10.22	10.46	10.88	10.51	10.81
	Difference (mg/L)	+0.47	–0.44	+0.54	+0.21	+0.02
	PD* (%)	+4.82	–4.04	+5.22	+2.04	+0.19
Summer	Observed (mg/L)	6.42	7.88	7.54	7.90	8.66
	Simulated (mg/L)	7.66	7.48	7.49	8.34	8.60
	Difference (mg/L)	+1.24	–0.40	–0.05	+0.44	–0.06
	PD* (%)	+19.31	–5.08	–0.66	+5.57	–0.69
Fall	Observed (mg/L)	7.86	9.44	8.68	9.32	10.28
	Simulated (mg/L)	9.61	9.30	8.53	9.92	10.70
	Difference (mg/L)	+1.75	–0.14	–0.15	+0.60	+0.42
	PD* (%)	22.26	–1.48	–1.73	+6.44	+4.09
Winter	Observed (mg/L)	12.00	13.10	12.68	12.60	12.81
	Simulated (mg/L)	13.63	13.00	12.15	13.70	13.80
	Difference (mg/L)	+1.63	–0.10	–0.53	+1.10	+0.99
	PD* (%)	+13.58	–0.76	–4.18	+8.73	+7.73

* PD: Percentage Difference

A closer investigation was performed for ST30, a stream station located downstream of the Lake (Figure 4-1), which, in terms of the modeling application, received the inputs generated by the Lake W2 submodel. The results indicated a strong correlation between simulated and observed temperatures with an R^2 value of 0.882 (Table 4-2). The seasonal temperature variations were also captured well with differences ranging from –1.78 ºC to –0.11ºC. The temperatures were generally under-predicted, and this is probably related to the under-prediction of surface temperature at LM01 (Table 4-4), a station near the Lake dam. Although the simulated and observed DO concentrations showed a relatively weak correlation (R^2 value of 0.487), the seasonal trend was well reproduced by the model and the seasonal differences ranged from –0.53 mg/L to +0.54 mg/L (Table 4-3). The good calibration of temperature and DO concentrations at this station not only indicates the good performance of upstream submodels (the Lake W2, the Upper Broad Run, and

Middle Broad Run HSPF submodels), but also proves the validity of the linkage between the two different types of water quality models.

Table 4-4: Comparison between Simulated and Observed Daily Temperature and DO at Lake Manassas Stations

		LM01	LM03	LM04	LM05	LM06
Temperature						
Surface	R^2	0.986	0.976	0.985	0.984	0.956
	Difference (ºC)	–0.12	–0.20	–0.17	–0.42	–0.31
Bottom	R^2	0.835	0.935	0.854	0.940	0.963
	Difference (ºC)	+0.51	–0.47	–0.25	–0.71	–0.18
DO						
Surface	R^2	0.559	0.521	0.535	0.532	0.529
	Difference (mg/L)	–0.50	–0.27	–0.72	–0.99	–1.25
Bottom	R^2	0.855	0.828	0.921	0.898	0.608
	Difference (mg/L)	+1.10	+1.11	+0.20	+0.46	+1.65

The results from the W2 submodels show a good simulation of the spatial trends of surface temperatures in the waterbodies (Figure 4-4). The absolute differences at surface layers are less than 0.42 ºC and 1.38 ºC for the Lake and Reservoir, respectively (Tables 4-4 and 4-5). The general under-prediction of surface temperatures in the two waterbodies is partially related to meteorological data. The surface temperatures are affected primarily by surface heat and wind mixing. These data were derived from meteorological data obtained from the Washington Dulles International Airport weather station that is located approximately 28 km away for the Lake and 35 km from the Reservoir. This might partially explain the discrepancies in surface temperature simulation. The R^2 values based on daily surface temperatures at various in-lake stations were greater than 0.956 and 0.945 for the Lake and the Reservoir, respectively (Tables 4-4 and 4-5), showing strong correlations between simulated and observed data.

Table 4-5: Comparison between Simulated and Observed Daily Temperature and DO at Occoquan Reservoir Stations

		RE02	RE15	RE30	RE35
Temperature					
Surface	R^2	0.975	0.975	0.954	0.945
	Difference (ºC)	–0.91	–0.95	–1.38	–0.55
Bottom	R^2	0.796	0.676	0.825	0.811
	Difference (ºC)	–1.41	+0.95	–0.91	+1.12
DO					
Surface	R^2	0.238	0.210	0.145	0.218
	Difference (mg/L)	+0.22	–1.42	–1.24	–1.61
Bottom	R^2	0.825	0.730	0.362	0.651
	Difference (mg/L)	+0.22	+0.39	–0.25	+1.30

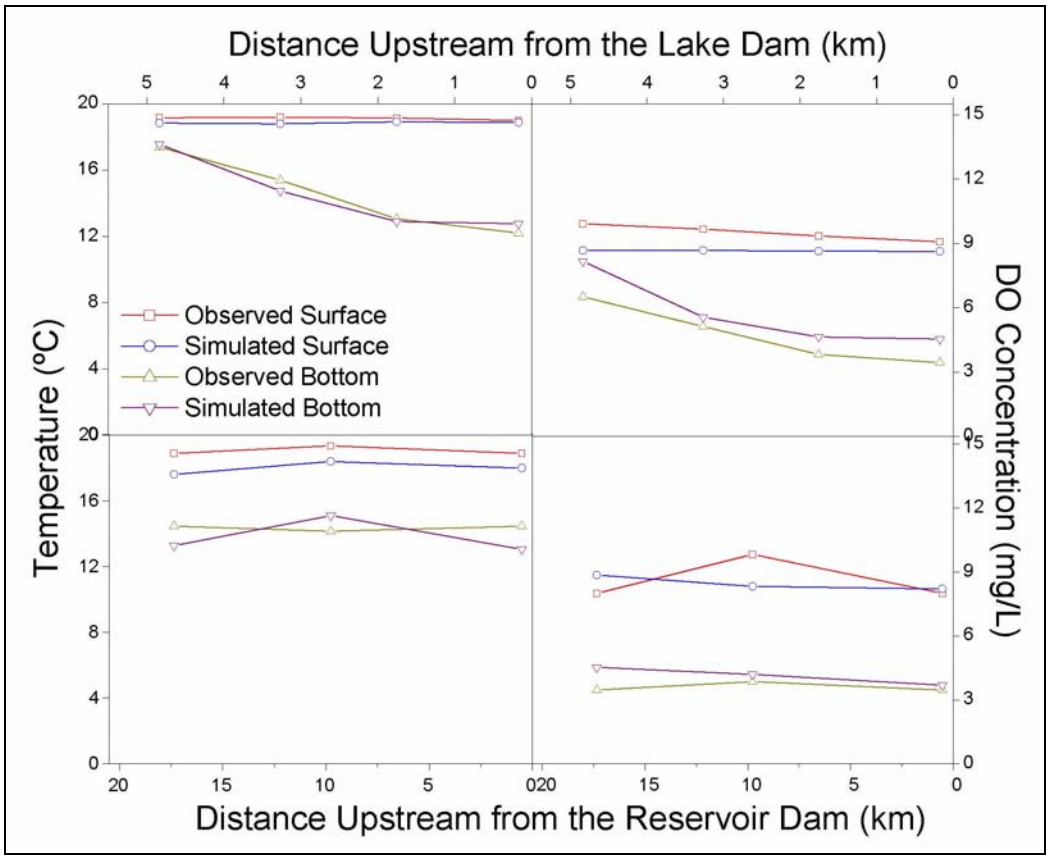

Figure 4-4: Comparison of Surface and Bottom Temperature (Left) and Dissolved Oxygen (Right) Concentrations along the Mainstems of Lake Manassas (Top) and Occoquan Reservoir (Bottom)

It also can be seen that these two waterbodies show different bottom temperature trends (Figure 4-4). The observed temperatures in the bottom layers of the Lake tend to decrease as water flows towards the dam, while the temperatures remain fairly constant along the bottom layers of the Reservoir. This indicates the differences in hydrodynamic characteristics of these two waterbodies due to lake morphology and boundary conditions. The W2 submodels demonstrated the capability to reproduce different hydrodynamics conditions. Although the simulated and observed bottom temperatures showed weaker correlations than the surface ones, the R^2 values based on daily bottom temperatures at various in-lake stations were still 0.835 and 0.676 or better for the Lake and the Reservoir, respectively (Tables 4-4 and 4-5).

Sensitivity analysis indicated that temperature simulation was sensitive to inflow conditions. Therefore, a closer investigation was performed for stations close to the headwaters (LM05 of the Lake and RE30 and RE35 of the Reservoir), which received

inputs generated by upstream HSPF submodels. In the Lake, the small differences between simulated and observed temperatures at LM05 (0.42 ºC for surface and 0.71 ºC for bottom) (Table 4-4) are mainly results of the good performance of the upstream submodel: the Upper Broad Run HSPF submodel. This was confirmed by the results at ST70 (the seasonal differences ranged from –0.47 ºC to +0.38 ºC) (Table 4-2). This helps to confirm the validity of the linkage between the two different types of water quality models: the watershed model HSPF and the receiving waterbody model W2. The differences at the Reservoir headwaters were relatively large, which were partially due to the differences at ST10 and ST40 (Table 4-2). For Branch 1 (RE35), the differences are –0.55 ºC and +1.22 ºC for surface and bottom layers, respectively. For Branch 2 (RE30), those differences are –1.38 ºC and –0.91ºC, respectively (Table 4-5).

The W2 submodels also captured the general trends of DO concentrations in the Lake and Reservoir (Figure 4-4). Although the bottom DO concentrations were generally over-predicted by less than 1.65 mg/L and 1.30 mg/L for the Lake and the Reservoir, respectively, the simulated and observed bottom DO showed high correlations and the R^2 values based on daily data were greater than 0.608 for the Lake and 0.651 for the Reservoir (Tables 4-4 and 4-5). The exception was at RE30 (bottom DO R^2 of 0.362), which represented the water quality of the Bull Run branch. For surface DO, although the results indicated strong correlations at stations in the Lake (R^2 values greater than 0.521), the surface DO concentrations in the Reservoir were not well captured (R^2 values from 0.145 to 0.238). In the current study, only one algae species was modeled in the Reservoir W2 submodel when the observed species count data suggest three dominant algae species. Thus the timing and magnitude of algae growth were not well captured. Because the surface DO dynamics are closely related to algae growth, this might cause the DO discrepancies especially during summer months. The absolute differences of average surface DO concentrations at various stations were less than 1.25 mg/L and 1.61 mg/L for the Lake and the Reservoir, respectively.

Further analysis was performed for stations near the dams (RE02 for the Reservoir and LM01 for the Lake). This is because the surface conditions at these stations generally represent the water quality flowing downstream over the dams. In addition, it also

provides information on water quality into the water treatment plant of the City of Manassas, because the plant withdraws waters primarily from the top intake. This consideration does not apply to the Reservoir because Fairfax Water withdraws water primary from the middle intake at the dam.

The W2 submodels demonstrated the ability to capture the seasonal variation patterns for temperature and DO (Figure 4-5, which includes the validation period). Both surface and bottom temperatures followed seasonal patterns that were well reproduced by the W2 submodels. The development of metalimnion zones during summer thermal stratification and discontinuity during spring and fall turnover were captured well. It also can be seen that during summer months the differences between surface and bottom temperatures were smaller at RE02 (the Reservoir) than LM01 (the Lake), although the water at RE02 is approximately 5 m deeper than LM01. This is probably due to two reasons. Firstly, the Reservoir has a smaller average retention time (19.6 days) than the Lake (118.5 days), and thus experiences greater turbulence and flushing rates than the Lake. Therefore, more mixing in the Reservoir reduces the temperature differences between surface and bottom layers, and thus limits the development of thermal stratification. This is also confirmed by results from other location in the Reservoir (Figure 4-4). In addition, the aeration system implemented at the bottom (near the dam) in the Reservoir generated more turbulence and thus reduced the thermal gradient between the surface and bottom layers. This might also partially explain the under-prediction of the bottom temperature at RE02 (Table 4-5).

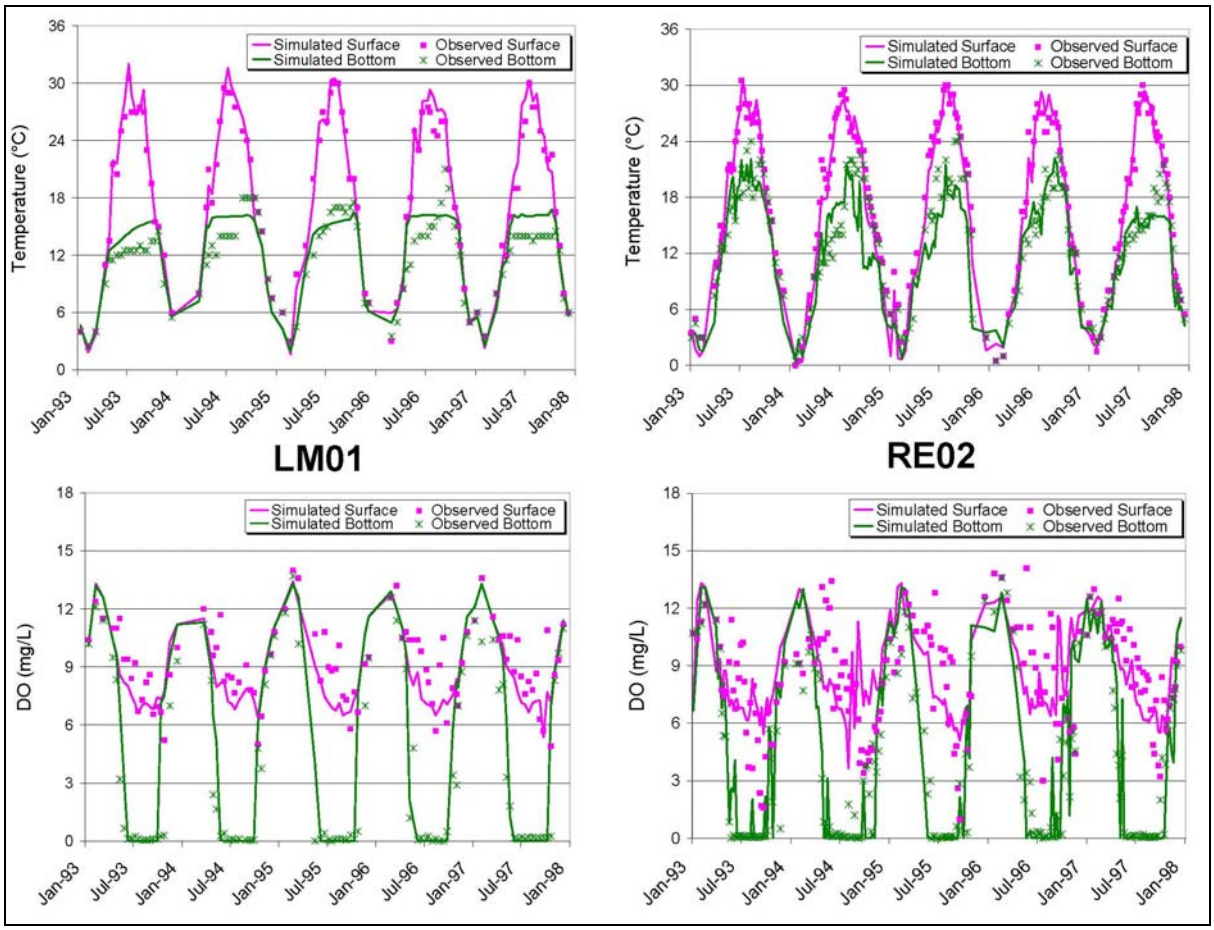

Figure 4-5: Surface and Bottom Simulated and Observed Temperature and Dissolved Oxygen Concentrations at Stations near Lake Manassas and Occoquan Reservoir Dams for Model Calibration and Validation

The observed surface DO concentrations also followed a seasonal pattern, with the lowest concentrations during summers when temperatures were highest and algae were most active (Figure 4-5). This was well reproduced by the model. However, the surface DO concentrations in the Reservoir were generally under-predicted during later spring and summer seasons. This is probably related to algal dynamics and may be improved by including multiple algae species in the W2 submodel. The bottom DO patterns were also well-reproduced. The timing and duration of the onset of bottom oxygen depletion, the development of the hypolimnetic anoxia zone, and the increase in DO during fall overturn were well-simulated by the W2 submodels.

The vertical variations of temperature and DO concentrations at LM01 and RE02 were also investigated (Figure 4-6). Although the vertical stratification during summer months

was generally reproduced by the W2 submodels, the degree of stratification was quite different in the two waterbodies. The Lake showed clear boundaries of epilimnion, metalimnion, and hypolimnion. However, the Reservoir did not show strong stratification and the differences among thermal layers were not as obvious as those in the Lake, which has been explained above. The statistical analysis indicated that the AME values for summer months are in the range of 1.13 ºC ~2.24 ºC for the Lake and 0.58~1.99 ºC for the Reservoir during the three-year simulation period (Table 4-6). Most discrepancies were due to the over-prediction of temperatures in the lower layers.

The vertical distributions of DO concentrations indicated that the oxygen depletion in the hypolimnion zone of the Lake was captured by the W2 submodel. However, the submodel tended to over-predict the DO concentrations in the metalimnion. This is probably due to the oxygen produced by the algae with relatively slow settling rates. The Reservoir W2 submodel did not reproduce the DO vertical distribution as well as the Lake. The DO AME values for summer months ranged from 1.04 mg/L to 3.22 mg/L, which were higher than those of the Lake (0.53 mg/L to 1.77 mg/L). The discrepancies were mainly due to the over-prediction at the metalimnion zones in summer months, which are possibly related to the insufficient description of algae/nutrient/DO dynamics by the model (Cole and Tillman 2001; Giorgino and Bales 1997). Currently only one lumped algae group was simulated in the Reservoir, although the algae count data show three dominant algae species. This might be improved by including multiple algae species in future simulations.

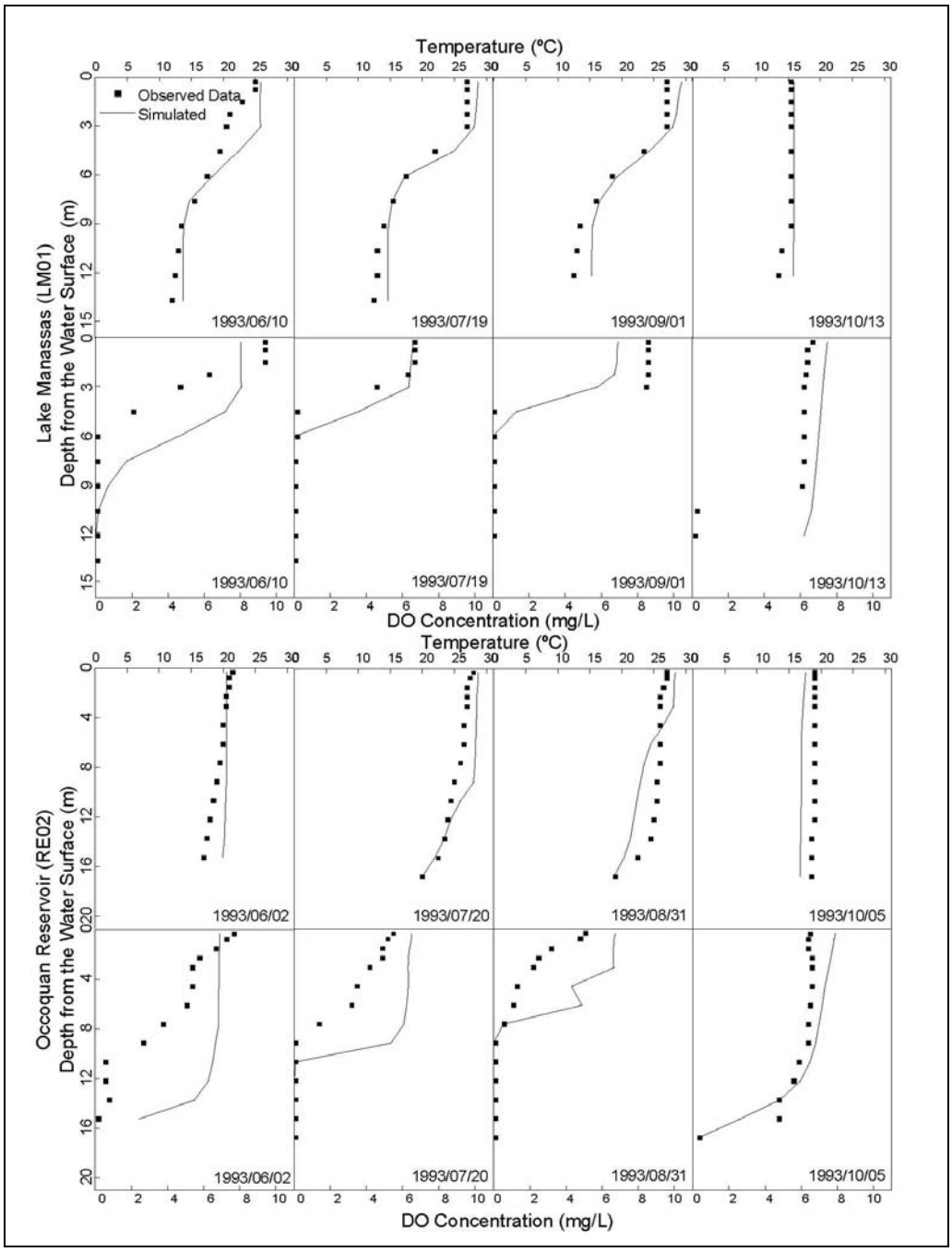

Figure 4-6: Comparison of Vertical Profiles of Temperature and Dissolved Oxygen at Stations near the Dams of Lake Manassas (Top) and Occoquan Reservoir (Bottom)

Table 4-6: Statistical Analysis of Summer Temperature and DO Concentrations at the Stations Near Lake Manassas and Occoquan Reservoir Dams

Lake Manassas					Occoquan Reservoir				
Date	Temperature		DO		Date	Temperature		DO	
	AME	RMS	AME	RMS		AME	RMS	AME	RMS
06/10/93	1.88	2.46	1.76	2.38	06/02/93	1.17	1.52	2.51	3.14
07/19/93	1.37	1.55	0.53	1.12	07/20/93	1.38	1.62	1.43	2.14
09/01/93	1.53	1.69	0.96	1.34	08/31/93	1.99	2.22	1.45	2.19
06/08/94	1.18	1.40	0.85	1.42	06/01/94	1.41	1.54	2.55	3.17
07/07/94	1.95	2.10	0.93	1.38	07/19/94	0.87	1.01	2.22	2.83
08/31/94	2.24	2.42	1.77	2.80	08/30/94	1.65	1.94	1.62	2.02
06/07/95	1.13	1.23	1.20	1.93	06/01/95	1.55	1.84	3.22	3.92
07/19/95	1.88	2.19	1.22	1.72	07/18/95	1.69	1.94	2.49	3.23
08/30/95	1.20	1.51	0.58	0.80	08/19/95	0.58	0.84	1.04	1.50

4.4.2 Model Validation

Simulated and observed temperature and DO concentrations for the years 1996 and 1997 were used for model validation. Both the calibration and validation periods were combinations of wet and dry years and are considered suitable for model calibration and validation purposes. The simulated output for these two validation years were generated using the same land use as for the calibration period (the year 1995), and the 1996 and 1997 meteorological data.

The results shown here include both the calibration and validation periods so that model validation can be seen in context. For the validation period, the simulated and observed temperature and DO at the stream stations indicate high correlations and R^2 values (Table 4-7) are greater than 0.627 for temperature and 0.516 for DO. The exception was at ST45, which was probably due to the lack of temperature and DO information for the UOSA discharge.

Table 4-7: R^2 Values based on Daily Comparison of Temperature and DO at Principal Stations for Model Calibration (1993-1995) and Validation (1996-1997)

		1993~1995	1996~1997	1993~1997
ST25	Temperature	0.930	0.709	0.829
	DO	0.639	0.568	0.605
ST70	Temperature	0.933	0.911	0.924
	DO	0.700	0.607	0.646
ST30	Temperature	0.882	0.637	0.767
	DO	0.487	0.522	0.492
ST45	Temperature	0.751	0.577	0.685
	DO	0.386	0.248	0.334
ST10	Temperature	0.934	0.638	0.815
	DO	0.725	0.557	0.650
ST40	Temperature	0.957	0.627	0.827
	DO	0.577	0.516	0.540

Figures 4-7 and 4-8 show comparisons of daily temperature and DO at four monitoring stations for the 5-year calibration and validation period. During the validation period, the submodels reproduced the seasonal variation for temperature and DO fairly well.

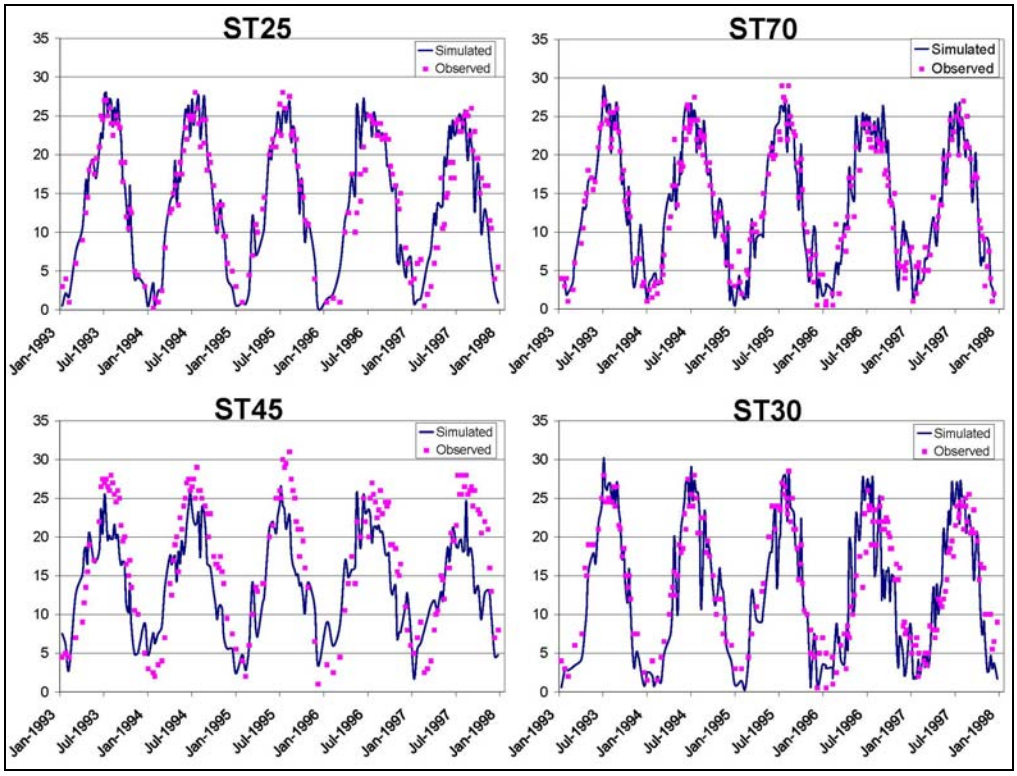

Figure 4-7: Comparison of Daily Temperature (ºC) at Four Principal Stream Stations in the Occoquan Watershed for Model Calibration (1993-1995) and Validation (1996-1997)

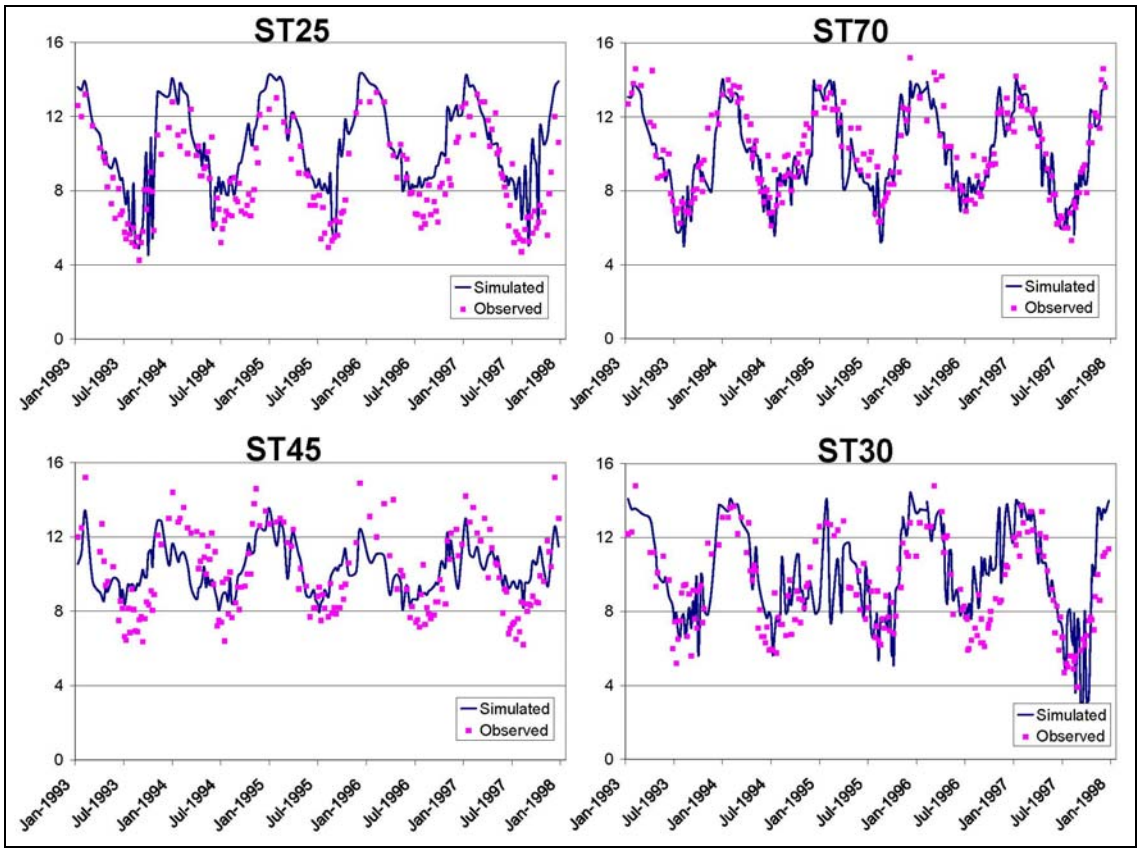

Figure 4-8: Comparison of Daily DO Concentrations (mg/L) at Four Principal Stream Stations in the Occoquan Watershed for Model Calibration (1993-1995) and Validation (1996-1997)

The temperature and DO concentrations were also validated for the Lake and the Reservoir stations. The R^2 values indicated that the Lake W2 submodel was well validated, and simulated and observed values showed strong correlations at various stations (R^2 values greater than 0.820 for temperature and greater than 0.556 for DO) (Table 4-8). The W2 submodel also captured the seasonal fluctuations of temperature and DO, including summer thermal gradients, fall turnover, and bottom DO depletion (Figure 4-5).

The W2 submodel for temperature of the Occoquan Reservoir was also considered to be well validated and the R^2 values were greater than 0.824 (Table 4-9). Both calibration and validation results indicated weak correlation of surface DO concentrations, which is perhaps due to algae simulation. However, the seasonal patterns in the Reservoir were captured (Figure 4-5).The bottom DO concentrations were well validated with the R^2 values equal to 0.521 or greater.

Table 4-8: R^2 Values based on Daily Comparison of Temperature and DO at Lake Manassas Stations for Model Calibration (1993-1995) and Validation (1996-1997)

	LM01	LM03	LM04	LM05	LM06
Temperature					
Surface (Calibration)	0.986	0.976	0.985	0.984	0.956
Surface (Validation)	0.977	0.975	0.984	0.983	0.951
Bottom (Calibration)	0.835	0.935	0.854	0.940	0.963
Bottom (Validation)	0.821	0.952	0.820	0.953	0.941
Dissolved Oxygen					
Surface (Calibration)	0.559	0.521	0.535	0.532	0.529
Surface (Validation)	0.625	0.556	0.596	0.646	0.630
Bottom (Calibration)	0.855	0.828	0.921	0.898	0.608
Bottom (Validation)	0.897	0.803	0.879	0.864	0.685

Table 4-9: R^2 Values based on Daily Comparison of Temperature and DO at Occoquan Reservoir Stations for Model Calibration (1993-1995) and Validation (1996-1997)

	RE02	RE15	RE30	RE35
Temperature				
Surface (Calibration)	0.975	0.975	0.954	0.945
Surface (Validation)	0.979	0.973	0.947	0.944
Bottom (Calibration)	0.796	0.676	0.825	0.811
Bottom (Validation)	0.890	0.824	0.853	0.842
Dissolved Oxygen				
Surface (Calibration)	0.238	0.210	0.145	0.218
Surface (Validation)	0.184	0.162	0.434	0.348
Bottom (Calibration)	0.825	0.730	0.362	0.651
Bottom (Validation)	0.823	0.857	0.521	0.587

4.5 *Conclusions*

A complex linked model, using six applications of HSPF and two of CE-QUAL-W2, was applied to simulate the temperature and DO in the Occoquan Watershed. The linked model not only successfully simulated the temporal and spatial distribution of temperature and DO in the upland streams, but also captured thermal stratification, spring and fall turnover, and DO depletion in the waterbodies. The linked model was adequately validated to capture the general trend of temperature and DO in the watershed and two principal waterbodies.

One of the noteworthy features of this study was the application of the linked water quality models. By linking the state-of-the-art watershed model HSPF with reservoir model CE-QUAL-W2, the model represents the real world more as a single entity and forces the modeler to look at approaches to calibration that benefit the overall model

rather than the individual components. Moreover, this approach develops a direct cause-and-effect linkage between upstream activities and downstream water quality, although it requires extra effort to develop and calibrate the linked model. This coupled approach allows the assessment of thermal stress on stream habitat due to urbanization, and allows prediction of possible impairment to fish communities. This advantage of the linked model approach benefits the ongoing TMDL project, where various nutrient reduction scenarios and/or land development scenarios are required to evaluate their impacts on DO concentrations in the Occoquan Reservoir. Therefore, instead of using assumed loading reduction rates, W2 could use the boundary conditions corresponding with these scenarios to predict the water quality variations and propose appropriate approaches to achieve the management goal set by the TMDL process.

4.6 *References*

Bicknell, B.R., Imhoff, J.C., Kittle, J.L., Jobes, T.H. and Donigian, A.S. (2001). *Hydrological Simulation Program-Fortran HSPF Version 12 User's Manual*, U.S. Environmental Protection Agency, National Exposure Research Laboratory, Athens, Georgia.

Chen, Y.D., Carsel, R.F., McCutcheon, S.C. and Nutter, W.L. (1998). Stream Temperature Simulation of Forested Riparian Areas: I. Watershed-Scale Model Development. *Journal of Environmental Engineering*, **124**(4), 304-315.

Cole, T. M. and Wells, S. A. (2003). *CE-QUAL-W2: A Two-Dimensional Laterally Averaged, Hydrodynamic and Water Quality Model, Version 3.2 User Manual*. U.S. Army Corps of Engineers, Washington, D.C.

Cole, T.M. and Tillman, D.H. (2001). *Water Quality Modeling of Allatoona and West Point Reservoirs Using CE-QUAL-W2*. U.S. Army Engineer Research and Development Center, Vicksburg, Mississippi.

Donigian, A.S. (2002). Watershed Model Calibration and Validation: The HSPF Experience. *National TMDL Science and Policy Specialty Conference 2002*, Phoenix, Arizona.

Donigian, A.S. and Crawford, N.H. (1976). *Modeling Nonpoint Pollution from the Land Surface*. U.S. Environmental Protection Agency, Environmental Research Laboratory, Athens, Georgia.

Eggink, J. (2001). *An Exploration of the Limnological Dynamics of Lake Manassas*, Master's Thesis, Virginia Polytechnic Institute and State University, Falls Church, Virginia.

Giorgino, M.J. and Bales, J.D. (1997). *Rhodhiss Lake, North Carolina: Analysis of Ambient Conditions and Simulation of Hydrodynamics, Constituent Transport and Water-Quality Characteristics, 1993-1994*. U.S. Geological Survey, Raleigh, North Carolina.

Neitsch, S.L., Arnold, J.R., Kiniry, J.R., Williams, J.R. and King, W.K. (2002). *Soil and Water Assessment Tool Theoretical Documentation Version 2000*. Texas Water Resources Institute, College Station, Texas.

Occoquan Watershed Monitoring Laboratory. (1998). *An Updated Water Quality Assessment for the Occoquan Reservoir and Tributary Watershed: 1973-1997*. Manassas, Virginia.

Randall, C.W. and Grizzard, T.J. (1995). Management of the Occoquan River Basin: A 20-Year Case History. *Water Science and Technology*, **32**(5-6), 235-243.

Schueler, T. R. (1994). The Importance of Imperviousness. *Watershed Protection Techniques*, **1**(3), 100-111.

U.S. Environmental Protection Agency. (2002). *National Water Quality Inventory 2000 Report*. *EPA-841-R-02-001*, Washington, D.C.

Virginia Department of Environmental Quality. (2004). *Final 2004 305(b)/303(d) Water Quality Assessment Integrated Report*. Richmond, Virginia.

Wetzel, R.G. (2001). *Limnology: Lake and River Ecosystems*, Third Edition. Academic Press, San Diego, California.

Wool, T.A., Ambrose, R.B., Martin, J.L. and Cormer, E.A. (2003). *Water Quality Analysis Simulation program (WASP) Version 6.0 Draft: User's Manual*. U.S. Environmental Protection Agency, Atlanta, Georgia.

Xu, Z., Godrej, A.N. and Grizzard, T.J. (2006). The Hydrological Calibration of a Linked Watershed-Reservoir Model for the Occoquan Watershed, Virginia. *In Preparation*.

Chapter 5. Modeling Soluble Inorganic Nitrogen Transport and Fate, and the Impact of Land Use Changes in the Occoquan Watershed Using a Linked Model Application

5.1 *Summary*

The Occoquan Watershed is a 1,515 km^2 basin located in northern Virginia and contains two principal waterbodies: the Occoquan Reservoir and Lake Manassas. Both of them are principal drinking water supplies for local residents and experience eutrophication and summer algae growth. They are continuously threatened by new development from the rapid expansion of the greater Washington D.C. region. The Occoquan model, consisting of six HSPF and two CE-QUAL-W2 submodels linked in a complex way, has been developed and applied to simulate the hydrology and water quality activities of the two major reservoirs and the associated drainage areas. This paper describes the application of the linked model to simulate the transport and fate of ammonium-nitrogen (NH4-N) and oxidized nitrogen (Ox-N) in the watershed and reservoirs. The models were calibrated for a three-year simulation period and validated for a two-year simulation period based on more than 12,000 field measurements. The results show that a successful calibration can be achieved using the linked approach, with moderate additional effort. The percentage difference values of load comparison based on the three-year study period ranged from −3.95 to +10.22% for NH4-N loads and from −11.89 to +6.10% for Ox-N loads. The differences of average simulated and observed NH4-N concentrations in flow over the dams were equal to or less than 0.01 mg/L for both Lake Manassas and Occoquan Reservoir. The differences of average Ox-N concentrations in flow over the dams were equal to or less than 0.01 mg/L for Lake Manassas and 0.07 mg/L for Occoquan Reservoir. The model was adequately validated to capture the nitrogen load production from the drainage areas and temporal distribution of nitrogen species in the waterbodies. Because the linked watershed-reservoir water quality model approach provides a direct cause-effect relationship between upstream activities and downstream water quality, the model was then used to predict the impact of alternative land use

scenarios on water quality changes in the Occoquan Reservoir. The model predicted that the annual NH4-N loads would be doubled due to future urban expansion. Although the changes of land use patterns also suggest increases in Ox-N loads from drainage areas, the impact on the Occoquan Reservoir water quality is masked by a wastewater treatment plant that accounts for a significant portion of oxidized nitrogen loads into the Occoquan Reservoir. The increases of external nitrogen loads lead to nutrient enrichment in the Occoquan Reservoir. The NH4-N and Ox-N concentrations in the flow over the Occoquan Reservoir dam would be increased by 100% and 43%, respectively, due to future urbanization.

5.2 *Introduction*

Excess nutrient flux into streams, lakes and reservoirs is a leading source of waterbody impairment in the USA (USEPA 2002). Large amounts of biologically available nutrients, primarily nitrogen (N) and phosphorus, enhance the nutrient status of waterbodies and trigger lake eutrophication. Common indicators of eutrophication include dissolved oxygen depletion, water transparency decrease, undesired growth of algae and aquatic weeds, and fish kills (Wetzel 2001). These problems will eventually lead to degradation of ecological systems and threaten the public health.

Although it is clear that these issues are related to increased external nutrient fluxes due to human activities, the knowledge of the quantification of these sources, especially diffuse sources, and their effect on aquatic systems is needed to better understand the transport and fate of nutrients in watersheds, so that nutrient reduction programs can be better implemented to prevent undesired consequences to aquatic ecosystems. Therefore, a total maximum daily loads (TMDL) program is required under the Clean Water Act (40.C.F.R.§130.7.) for each impaired waterbody to improve water quality by reducing point and nonpoint source loadings.

Water quality problems such as nutrient enrichment, eutrophication, and degradation of aquatic ecosystems relate to various factors and N cycling is one of them. Because of the complication of N dynamics, water quality models have been widely used to determine

the key processes that control N transport and fate, so that alternative N load reduction plans can be evaluated. Examples include the Water Quality Analysis Simulation Program (WASP) (Borsuk, et al. 2003), CE-QUAL-W2 (W2) (Bowen and Hieronymus 2003), and Neu-BERN (Borsuk, et al. 2003). External N loads from point and/or nonpoint sources are fed into these models as boundary conditions. However, these are normally not monitored at a frequency to provide a sufficient description of driving forces. Moreover, diffuse pollution, a major contributor of the excess loadings to receiving waterbodies, is hard to quantify by using traditional engineering techniques. Thus numerical methods have been applied to estimate the temporal changes of external N fluxes (McIsaac, et al. 2002). When investigating the impact of alternative management plans, N load reduction scenarios were developed by reducing the inflow N concentrations (Bowen and Hieronymus 2003; Imteaz, et al. 2003). Although this approach does answer the questions on the potential impact of external N load reduction on aquatic systems, it does not provide a practical guide to implement those load reduction programs and thus does not fully answer the management questions posed by TMDL programs.

Watershed models are also used in TMDL programs, such as spatially referenced regression model (SPARROW) (McMahon, et al. 2003), Soil and Water Assessment Tool (SWAT) (Jayakrishnan, et al. 2005), and Hydrological Simulation Program–Fortran (HSPF) (Merrill, et al. 2002). One of the difficult challenges regarding simulation of N dynamics in watershed models is insufficient description of the physical characteristics of receiving waterbodies as well as associated processes. For example, although HSPF considers several different routines to simulate soluble inorganic nitrogen (SIN) in reaches, it assumes streams and reservoirs to be well-mixed (Bicknell, et al. 2001). Thus, it cannot fully represent the spatial distribution of inorganic N due to phytoplankton accumulation in the epilimnion and oxygen depletion in the hypolimnion. SWAT makes a similar assumption for reservoirs (Neitsch, et al. 2002). In addition, it assumes no transformation or degradation of nutrients in channels.

These shortcomings in common modeling applications can be overcome by linking watershed models to receiving waterbody models (DePinto, et al. 2004). This approach provides a more accurate representation of the real world and allows integration of the downstream water quality to upstream land activities. In addition, it can be applied to complicated watersheds that have more than one major waterbody. However, few researchers have adopted this approach because of insufficient data availability and complications involved with linking more than two state-of-the-art water quality models.

In this paper, a complex linked model consisting of six HSPF and two W2 applications is applied to simulate SIN dynamics in the Occoquan Watershed as well as its receiving waterbodies: Occoquan Reservoir and Lake Manassas. While the objectives of the research are broader, the main objectives of this paper are to 1) provide a good calibration of SIN detachment and transport in the drainage areas; 2) capture the temporal and spatial distribution of SIN in the reservoirs; 3) provide a solid calibrated model for further Dissolved Oxygen (DO) TMDL development due to the interrelation of algae/nutrient/DO dynamics; 4) evaluate the impacts of alternative land use scenarios on nitrogen loadings and water quality in the Occoquan Reservoir. The initial calibration of the linked model is for the years 1993-95, with a validation period of 1996-97; a total five-year period spanning a land-use data update issued in 1995. The years 1993, 1994 and 1996 had annual precipitation of 106.7 cm, 107.8 cm, 114.5 cm respectively, and are considered to be average-to-somewhat-wet years based on a 51-year average of 101.3 cm. The years 1995 and 1997 were dry years with total rainfalls of 85.9 cm and 77.5 cm respectively. Due to length limitations, separate papers will provide discussion on hydrologic activities (Xu, et al. 2006), DO and temperature, soluble inorganic phosphorus and algae activities.

5.2.1 Study Area

The Occoquan Watershed (Watershed) is a 1,515 km^2 basin in northern Virginia (Figure 5-1). It contains three principal tributaries—Cedar Run, Broad Run and Bull Run; and two major waterbodies—Occoquan Reservoir (Reservoir) and Lake Manassas (Lake).

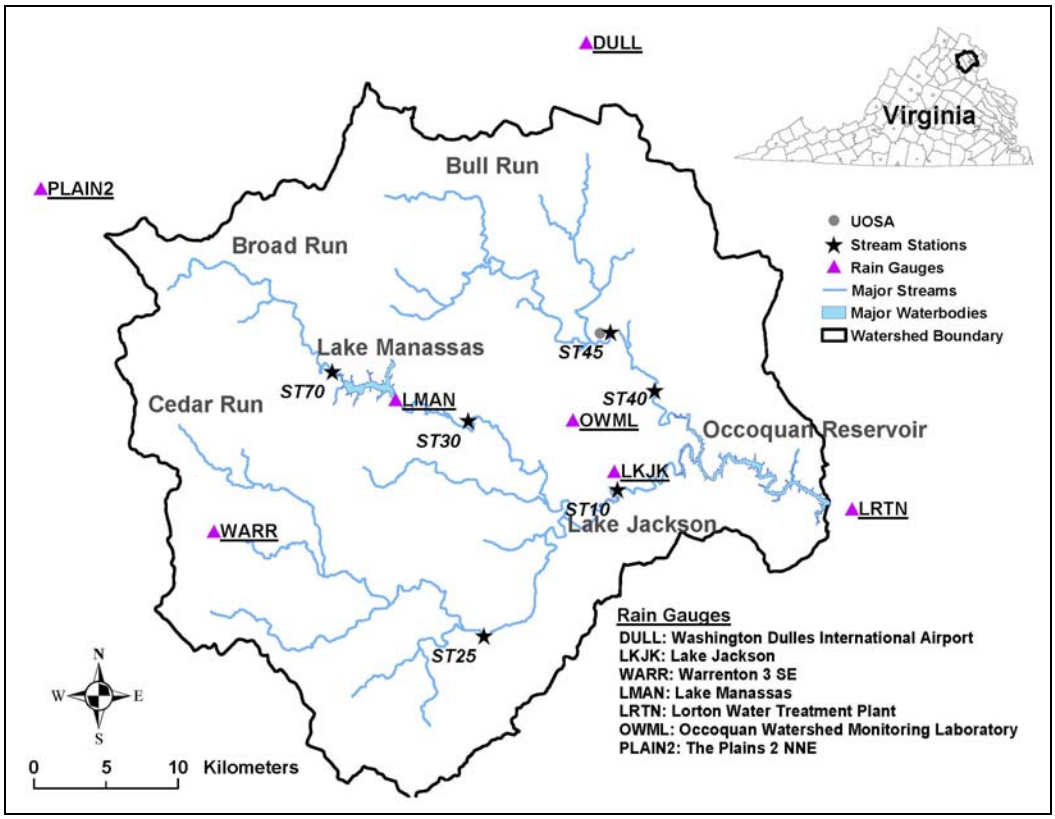

Figure 5-1: Location of Occoquan Watershed in Virginia, USA, Showing Main Tributaries, Main Waterbodies, Stream Stations and Rain Stations Used for This Study

The Reservoir is part of the drinking water supply for 1.2 million northern Virginia residents and is a major recreation site in the northern Virginia area. It receives flows from two principal tributaries: Occoquan River and Bull Run. The Upper Occoquan Sewage Authority (UOSA) water reclamation facility discharges into Bull Run. Its effluent is cooler than the water in the Reservoir during the warmer months and rich in nitrate-nitrogen. Thus, when this stream reaches the main body of the Reservoir, the nitrate-rich water flows toward the bottom due to density differences. This has a significant impact on water quality in the Reservoir and is an important component of the management of the Reservoir (Randall and Grizzard 1995). Flows over the Occoquan dam drain into the Potomac River after running approximately 8 km southeast. The total capacity of the Reservoir is 31.4×10^6 m^3 and the safe yield is 2.5×10^5 m^3/d (which includes the discharge from UOSA)(OWML 1998). The surface area at the maximum elevation of 36.6 m above mean sea level is 616 hectare. The average depth of the Reservoir is 5.1 m with a maximum depth of approximately 20.0 m near the dam. The

average residence time is 19.6 days. Based on Wetzel's (2001) classification of the trophic status of lakes, the Reservoir is mesoeutrophic with the limiting factor being orthophosphate phosphorus (Randall and Grizzard 1995). Copper compounds are used to control algae growth during summer months.

Lake Manassas is another major waterbody in the Watershed. It serves as the principal drinking water supply for the City of Manassas as well as for recreational purposes. The total drainage area is approximately 189 km^2. Three golf courses are located on the north shore (Robert Trent Jones, Virginia Oaks, and Par 3). The City of Manassas withdraws water from three water intakes at the dam (primarily the intake at the top) for municipal service. During dry periods, the golf courses withdraw water from the surface. The natural storage capacity of the Lake is 15.4×10^6 m^3 and the safe yield is 6.37×10^4 m^3/d. The surface area at the maximum elevation of 86.9 m above mean sea level is 282 hectare. The average depth is 5.5 m with a maximum depth of approximately 15.0 m near the dam. Lake Manassas is classified as an eutrophic waterbody and the limiting nutrient is phosphorus (Eggink 2001). It has high biological productivity and copper compounds were applied for at least fourteen years (1982-1995), typically four times a year.

5.3 *Model Description*

HSPF divides simulated watersheds into three blocks and simulates processes occurring in: (1) pervious land areas (PERLND); (2) impervious land areas (IMPLND); and (3) well-mixed streams and reservoirs (RCHRES) (Bicknell, et al. 2001). The nutrient loads carried by runoff from pervious land areas are the summation of loads from surface runoff, interflow and groundwater, and can be estimated using two different methods. One of the methods assumes simple relationships with water and/or sediment yield. An empirical factor, called washoff potency factor (POTFW), is used to relate the nutrient yield to sediment removal. N yields from land surfaces can also be assumed to be a function of water flow and storage quantity. During dry periods, HSPF assumes a linear relationship of N storage with a user-specific accumulation rate (ACQOP) and maximum storage capacity (SQOLIM). The N removal during wet periods is simulated based on an

exponential function, where a user-defined parameter called WSQOP is used to relate the washoff rate to the surface runoff rate. N fluxes in interflow and active groundwater are estimated by multiplying flow rates by user-specified concentrations.

The other method to estimate N loads from pervious land segments is under the NITR section, where transformation among nitrate-nitrogen, ammonium-nitrogen and organic nitrogen is simulated in each soil layer. Processes important to agricultural fields include plant uptake, fixation, immobilization, mineralization, denitrification, adsorption/desorption, and volatilization. Although this method provides a more process-oriented approach to simulate N cycling, it is suitable for agricultural areas where corresponding monitoring data are available. The approach for N fluxes from impervious land areas (IMPLND) is similar to the method in PERLND, where simple relationships with flow and sediment yield are used. In this model application, two inorganic nitrogen species: ammonium nitrogen (NH4-N) and oxidized nitrogen (Ox-N) were simulated under PERLND (the simple method) and IMPLND. The contribution from wet and dry atmospheric deposition was supplied as monthly fluxes for the entire studied watershed.

After the N fluxes are transported from pervious and impervious lands to the aquatic systems, several physical and biochemical processes take place under the RCHRES module to further simulate soluble inorganic N transformation in streams and reservoirs. These include advection, benthal release, ammonia ionization, ammonia vaporization, nitrification and denitrification, adsorption and desorption to inorganic sediment, deposition and scour of adsorbed nitrogen, and mineralization. In addition, processes related to consumption by plankton and benthic algae are addressed in separate modules.

W2, a two-dimensional hydrodynamic and water quality model, provides a detailed description of algae/nutrient/DO dynamics in long and narrow waterbodies such as lakes and reservoirs (Cole and Wells 2003). The simulated variables included temperature, DO, ammonium, nitrate+nitrite, orthophosphate phosphorus, BOD, organic matter and algae. The processes that affect sinks and sources of NH4-N include growth and respiration of algae, nitrification, denitrification, anaerobic release from the sediment, and decay of organic matter. Simulation of internal fluxes of nitrate and nitrite is relatively simpler

because it is not directly associated with decay of algae or organic matter. The biochemical reactions for Ox-N include photosynthesis of algae, nitrification, denitrification, and sediment diagenesis. Detailed descriptions of both models can be found elsewhere (Bicknell, et al. 2001; Chen, et al. 1998b; Cole and Wells 2003; Donigian and Crawford 1976).

5.3.1 Linked Model Approach

The Occoquan model is a complex linked model application, which includes six HSPF and two W2 submodels. The schema of the linked model approach, as well as the watershed segmentation, is shown in Figure 5-2. The Watershed is divided into six subbasins, with a total of 56 land (HSPF) segments. The average segment size is 27.0 km^2.

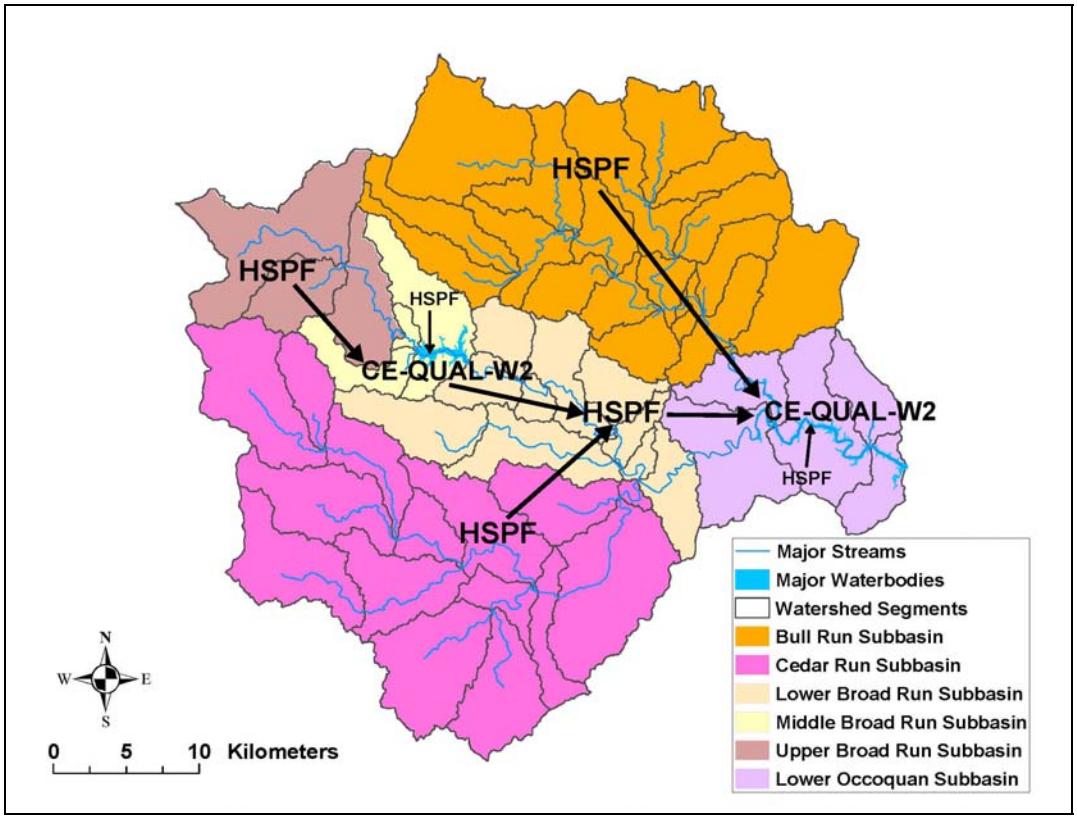

Figure 5-2: Occoquan Watershed Model Application Link Schema and Watershed Segmentation

The bathymetries of the Lake and the Reservoir are shown in Figure 5-3. For modeling purposes, the Lake is divided into four branches and has a total of 29 active

computational segments with lengths ranging from 173 m to 568 m. It has 4 to 28 computational layers, each 0.5 m thick. The Reservoir is also divided into four branches with a total of 69 computational segments. The average segment length is 583 m with a minimum of 74 m (Segment 32, at Ryan's Dam, a submerged feature with a narrow vertical opening) and a maximum of 838 m. There are from 1 to 39 computational layers, each 0.5 m thick. A detailed description of model development, watershed segmentation and waterbody segmentation can be found elsewhere (Xu, et al. 2006).

5.3.2 Boundary Conditions

In this model application, the boundary conditions required by W2, such as inflows, temperature and water quality data, are provided by upstream HSPF submodels (Figure 5-2). For example, in the Lake W2 submodel, the Upper Broad Run HSPF submodel not only provides daily time series inputs of direct inflows, but also SIN concentrations and other water quality components. The ungauged distributed tributary flows along the Lake and associated water quality are estimated by the Middle Broad Run HSPF submodel. The outputs from the Lake W2 submodel serve as inputs for the Lower Broad Run HSPF submodel. Similarly, the Lower Broad Run HSPF application, including the contribution from the Cedar Run subbasin, provides flows and water quality time-series for the Occoquan River branch of the Reservoir. The input time series for the Bull Run branch are provided by the Bull Run HSPF submodel. The Lower Occoquan HSPF application provides the ungauged distributed tributary flows as well as associated water quality along the Reservoir. Thus, six HSPF and two W2 submodels are integrated together to fully represent the hydrology and water quality activities in the Occoquan Watershed and two principal waterbodies.

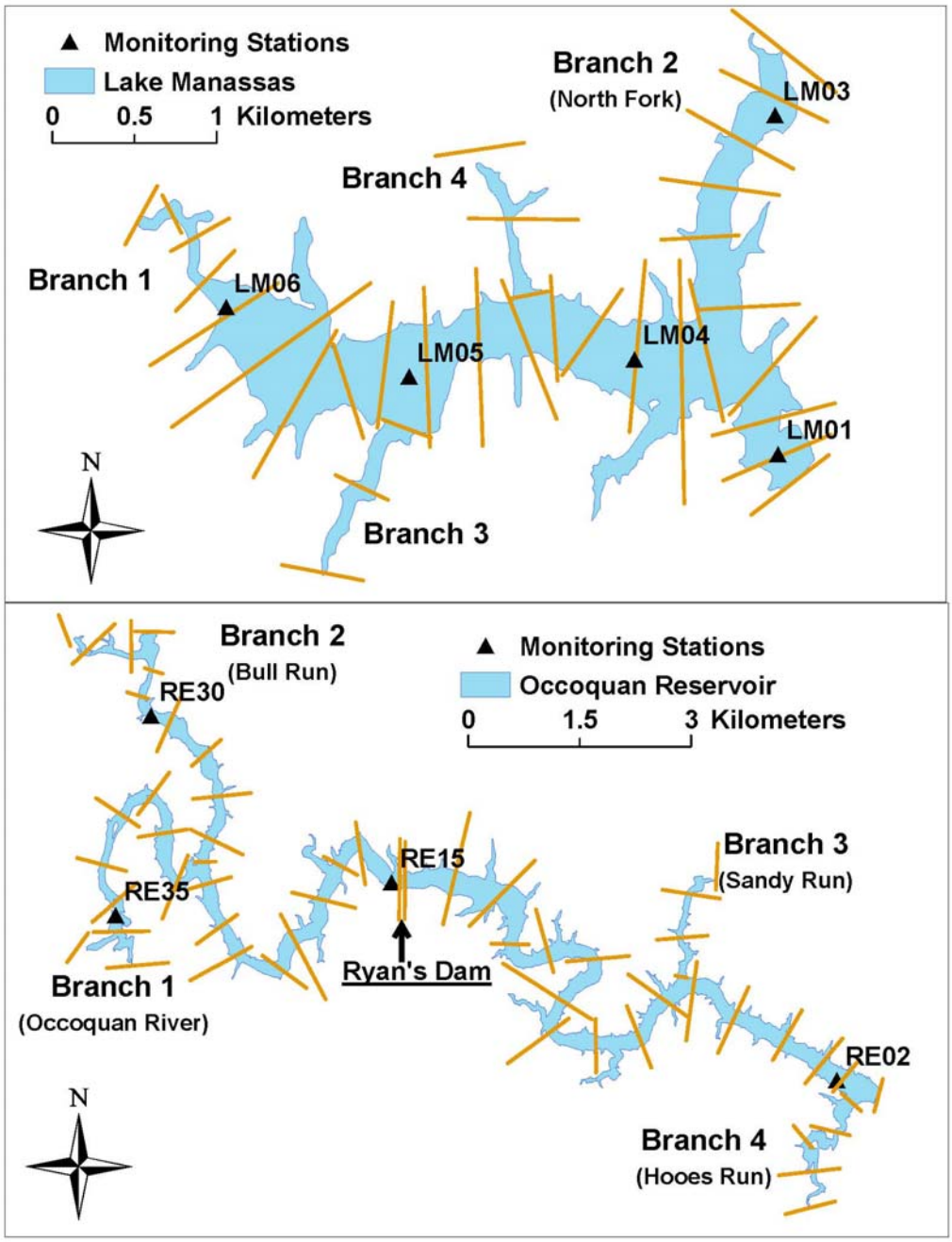

Figure 5-3: Segmentation of Lake Manassas (top) and Occoquan Reservoir (bottom), Showing Selected Monitoring Stations

5.3.3 Initial Conditions

The initial SIN concentrations in HSPF submodels were first assigned reasonable values. Then the submodels were run through a one-year simulation. The initial values were then adjusted based on the values at the end of the simulation.

The initial concentrations of SIN in W2 applications were set to be the same as observed data at the beginning of the simulation period at the stations closest to the dams.

5.3.4 Monitoring Data

For the stream stations (Figure 5-1), SIN data in base flow water quality samples were available on a biweekly basis during the winter season and on a weekly basis during other seasons. Composite flow-weighted storm water quality samples were also collected automatically for most storms. However, no automatic sample collection system was installed at ST10 due to the absence of stream flow measurements in the study period, and instead of composite flow-weighted samples, grab samples were collected during storm events.

For the Lake and the Reservoir (Figure 5-3) stations, near-surface and near-bottom water quality samples were available on a biweekly basis during the winter season and on a weekly basis during other seasons.

The monitored SIN components were nitrate-nitrogen, nitrite-nitrogen and ammonium-nitrogen. Samples were filtered through Whatman 934AH (1.5μm) filters before being analyzed by using standard EPA methods (1983).

5.3.5 Calibration Criteria

Because there is no single accepted test to determine whether or not a model is calibrated, both graphical and statistical methods are applied to evaluate the model performance. In addition to traditional statistical measures such as mean values and the standard coefficient of determination (R^2), several other statistical methods, such as paired t-test, were also used.

The percentage difference (PD) between simulated and observed data is defined below:

$$PD = \frac{100 \cdot (Y - X)}{X}\%$$

where *X* is the observed load or concentration, and *Y* is the simulated load or concentration. Donigian (2002) suggested a value based on an annual comparison in the range of 15-25% for a good water quality/nutrient calibration of HSPF.

5.4 *Results and Discussion*

The model results are presented in two sections. The first section describes the capability of the linked model to reproduce water quality conditions in the Watershed by comparing model results with the existing data for calibration (the January 1993 to December 1995 simulation period) and validation (the January 1996 to December 1997 simulation period). The second section describes the results of two land use development scenarios.

5.4.1 Current Case Simulation Results

5.4.1.1 Calibration

The simulated SIN loads from HSPF were compared with observed loads of individual storms, aggregated on both a monthly and an annual basis. Figures 5-4 and 5-5 show the annual load comparisons at four principal stream stations in the Watershed. According to the scale used by Donigian (2002), the results indicate good model performance and the PD values based on the three-year calibration period ranged from –3.95 to +10.22% for NH4-N and from –11.89 to +6.10% for Ox-N (Table 5-1). The absolute PD values based on annual loads are less than 25% for most sites (Table 5-1). The exceptions mostly occurred in the year 1995 (ST25 and ST70 for NH4-N, ST25 and ST30 for Ox-N). However, because 1995 was a dry year and produced less flow volumes, the annual NH4-N and Ox-N loads of 1995 are generally small compared to the other two simulation years (Figures 5-4 and 5-5), and thus have limited impact on the three-year totals. Although HSPF can address manure and fertilizer application under the Special Action block in the HSPF programs, the function was not used in this model application due to lack of records of application quantities and rates. This might partially explain the general under-prediction of oxidized nitrogen loads at the Cedar Run subbasin (ST25) where agricultural activities are significant.

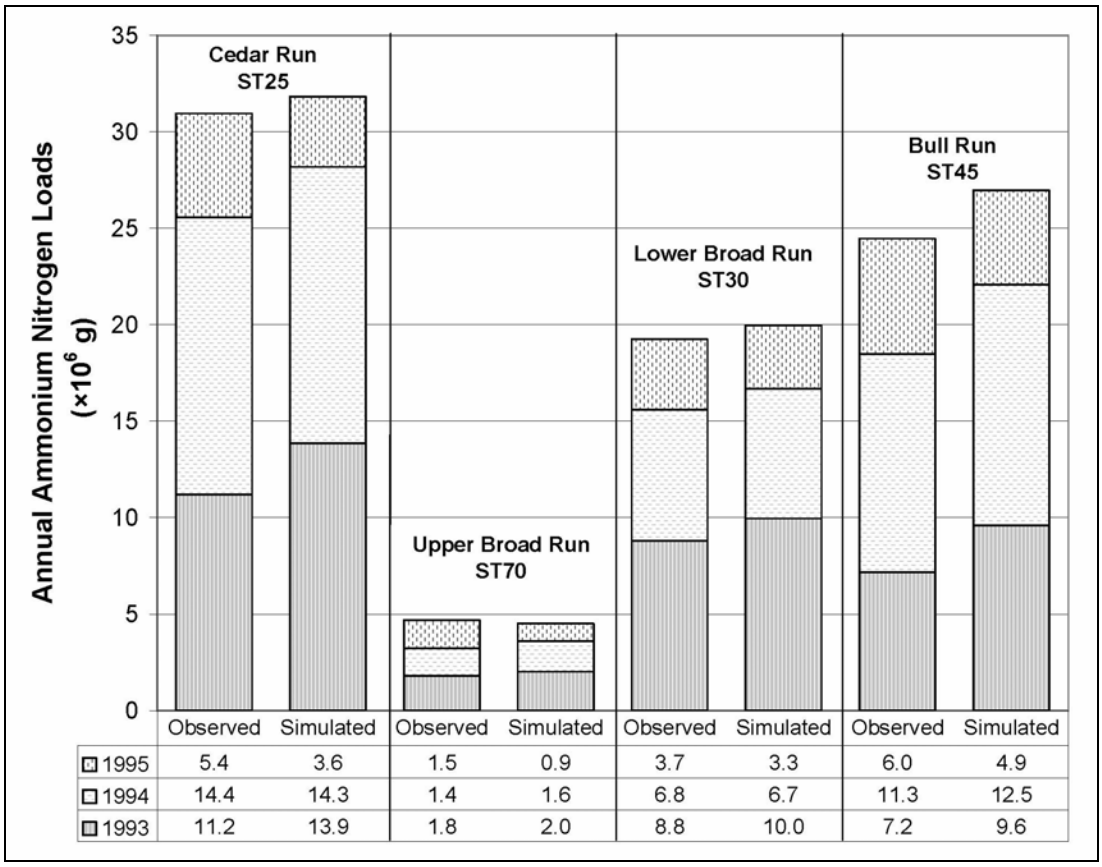

Figure 5-4: Comparison of Annual Ammonium Nitrogen Loads at Principal Stream Stations, 1993-95

Both annual and monthly loads of NH4-N and Ox-N show positive relationships with drainage areas except for Ox-N loads at ST45 (Figures 5-4 and 5-5, Table 5-2). This is because the nitrate-rich effluent from UOSA, located upstream of ST45, contributed approximately 75% of Ox-N loads at ST45.

Table 5-1: Comparison of Annual and Three-Year Totals of Soluble Inorganic Nitrogen Loads at Various Stream Stations

	Percentage Difference of Annual NH4-N Loads (%)				Percentage Difference of Annual Ox-N Loads (%)			
	1993	1994	1995	1993-95	1993	1994	1995	1993-95
ST25	+23.93	−0.44	−32.47	+2.79	−1.05	−6.48	−40.81	−11.89
ST70	+12.24	+9.27	−37.00	−3.95	−5.80	+12.76	+18.88	+6.10
ST30	+13.15	−0.80	−10.41	+3.74	−3.49	+4.63	−34.24	−5.37
ST45	+33.92	+10.05	−18.63	+10.22	+1.40	+1.18	−4.83	−0.74

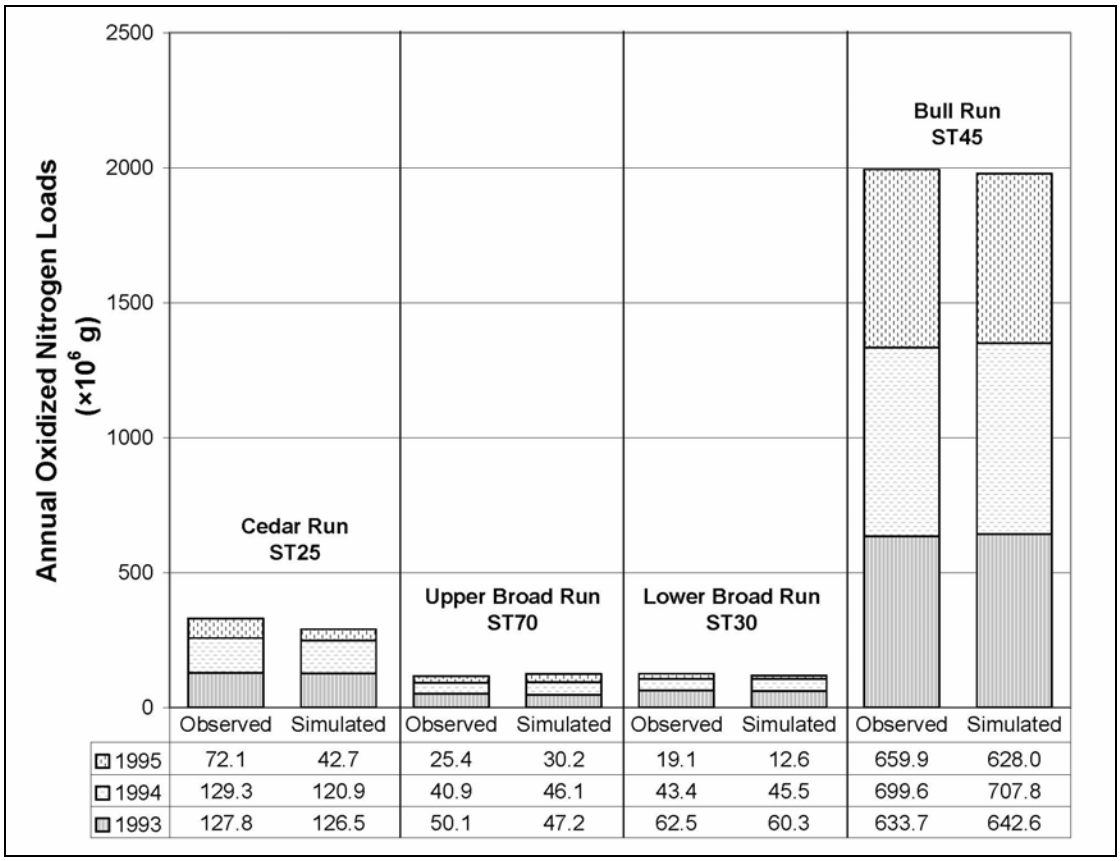

Figure 5-5: Comparison of Annual Oxidized Nitrogen Loads at Principal Stream Stations, 1993-95

Table 5-2: Comparison between Observed and Simulated Monthly Average Loads for NH4-N and Ox-N at Stream Stations

	Drainage Area	NH4-N				Ox-N			
	(km^2)	Observed ($\times 10^6$ g)	Simulated ($\times 10^6$ g)	PD* (%)	R^2	Observed ($\times 10^6$ g)	Simulated ($\times 10^6$ g)	PD* (%)	R^2
ST25	396	0.86	0.88	+2.3	0.225	9.14	8.06	–11.8	0.617
ST70	126	0.13	0.13	0.0	0.531	3.23	3.43	+6.1	0.887
ST30	228	0.53	0.55	+3.8	0.710	3.47	3.29	–5.2	0.843
ST45	373	0.68	0.75	+0.3	0.785	55.37	54.96	–0.7	0.606

*PD: Percentage Difference

The load analyses based on monthly average values also confirm the good match between observed and simulated loads with absolute PD values equal to or less than 3.8% for NH4-N and 11.8% for Ox-N (Table 5-2). The R^2 values based on monthly loads were 0.531 or greater for NH4-N and 0.606 for Ox-N, and thus indicated high correlations between simulated and observed values. The exception was NH4-N at ST25, which was due to the differences in 1993 and 1994. During November 27-28, 1993, a storm with a precipitation volume of 10.9-13.3 cm was recorded at seven rain gauge stations and was

confirmed by rapid responses in the hydrograph at ST25. The records indicated it as a major storm event that accounted for 85% of the flow volume of the whole month. However, no storm sample was collected and thus the event mean concentrations (EMCs) were missing. The missing pollutant loads were estimated from a regression relationship between storm flow volumes and EMCs developed for the 1990-1994 period. Even though this method provides a reasonable estimation of nutrient loads during missing storm events, the potential error associated with high flow events like this one could have significant impact on monthly, even annual, nutrient balances (Longabucco and Rafferty 1998). This might explain the over-prediction of NH4-N during November 1993. A similar reason applies to the over-prediction in July and August of 1994 when samples from three storm events were missing. The under-prediction of NH4-N loads in March 1994 was due to under-prediction of flow rates during a 5-day storm event. The R^2 of monthly loads at ST25 would be improved from 0.225 to 0.558 without those storms.

The empirical method to estimate the nutrient loads from missing storm events was also applied to the year 1995, where EMCs were developed based on the 1995-1999 period. The potential error associated with this method partially explained the relatively large differences between simulated and observed loads (Table 5-1). However, as mentioned earlier, the annual loads of the year 1995 were relatively small compared to the other two simulation years, thus they had limited impact on the comparison based on the three-year totals.

A closer investigation was performed for ST30, a stream station located downstream of the Lake (Figure 5-1), which, in terms of modeling application, received the inputs generated by the Lake W2 submodel. The results show good agreement between simulated and observed loads. The PD values based on annual loads ranged from –10.41% to +13.15% for NH4-N and from –34.24% to +4.63% for Ox-N (Table 5-1). The relatively large differences occurred in the year 1995, which has been explained above. The large R^2 values based on monthly comparison (0.710 for NH4-N and 0.843 for Ox-N) (Table 5-2) show strong correlations between simulated and observed loads. The good calibration of SIN at this station not only indicates the good performance of upstream submodel applications (the Lake W2, the Upper Broad Run and Middle Broad

Run HSPF submodels), but also proves the validity of the linkage between the two different types of water quality models.

Unlike most HSPF applications, the calibration procedure in this model application not only focused on nutrient loads, but also on nutrient concentrations. This is because the W2 submodels, which use the outputs of upstream HSPF submodels as inputs, perform the mass balances based on concentrations. The comparison of SIN concentrations was performed for stations located at the headwaters of the Reservoir (ST10 and ST40), where HSPF submodels were linked to the Reservoir W2 submodel. There were a total of 132 and 294 observed data samples for ST10 and ST40, respectively. Because less than ten grab storm samples were collected at ST10 during the three-year calibration period, they were not included in this analysis.

Tables 5-3 and 5-4 show the average concentrations at two stream stations located at the headwaters of the Reservoir. The results indicate that the absolute differences between average simulated and observed NH4-N concentrations were 0.01 mg/L at ST10 (baseflow) and 0.01 mg/L at ST40 (both baseflow and storms). The absolute differences between average simulated and observed Ox-N concentrations were 0.10 mg/L at ST10 (baseflow) and 1.94 mg/L and 1.39 mg/L at ST40 (baseflow and storms, respectively). It is notable that at ST40, the Ox-N concentrations in storm flows were generally smaller than those from base flow. This was because the UOSA effluent with an average Ox-N concentration of 22 mg/L was diluted by the upland storm runoff that has lower Ox-N concentrations.

Table 5-3: Comparison of NH4-N Baseflow and Stormflow Concentrations at Stream Stations at the Headwaters of the Occoquan Reservoir (ST10 and ST40)

	ST10		ST40			
	Baseflow		Baseflow		Storm Flow	
	Mean	SD*	Mean	SD*	Mean	SD*
Observed (mg/L)	0.06	0.05	0.02	0.02	0.04	0.03
Simulated (mg/L)	0.05	0.05	0.03	0.02	0.05	0.03
Difference (mg/L)	–0.01	–	+0.01	–	+0.01	–

*SD: Standard Deviation

Table 5-4: Comparison of Ox-N Baseflow and Stormflow Concentrations at Stream Stations at the Headwaters of the Occoquan Reservoir (ST10 and ST40)

	ST10		ST40			
	Baseflow		Baseflow		Storm Flow	
	Mean	SD*	Mean	SD*	Mean	SD*
Observed (mg/L)	0.20	0.21	6.88	4.20	2.11	1.51
Simulated (mg/L)	0.30	0.12	8.82	4.65	3.50	2.04
Difference (mg/L)	+0.10	–	+1.94	–	+1.39	–

*SD: Standard Deviation

The simulated baseflow Ox-N values at ST10 did not show as large a variation as observed data did (Table 5-4 and Figure 5-6). This was partially due to using fairly constant user-defined monthly concentration values in interflow and active groundwater. Because a significant portion of pollutants in base flows originated from interflow and active groundwater, the simulated base flow concentrations varied within a relatively small range. At ST40, NH4-N concentrations show a greater variation during storm events than in base flow events. This is because storm flow quality was affected by various factors such as precipitation duration and intensity, surface runoff and land uses. However, Ox-N concentrations at ST40 showed an opposite trend: greater variations during baseflow than storm flow. This is due to the dilution of nitrate-rich UOSA effluents by storm runoff that has lower Ox-N concentrations. The results also suggest good performance in capturing the seasonal trends for both base flow and storm events (Figure 5-6).

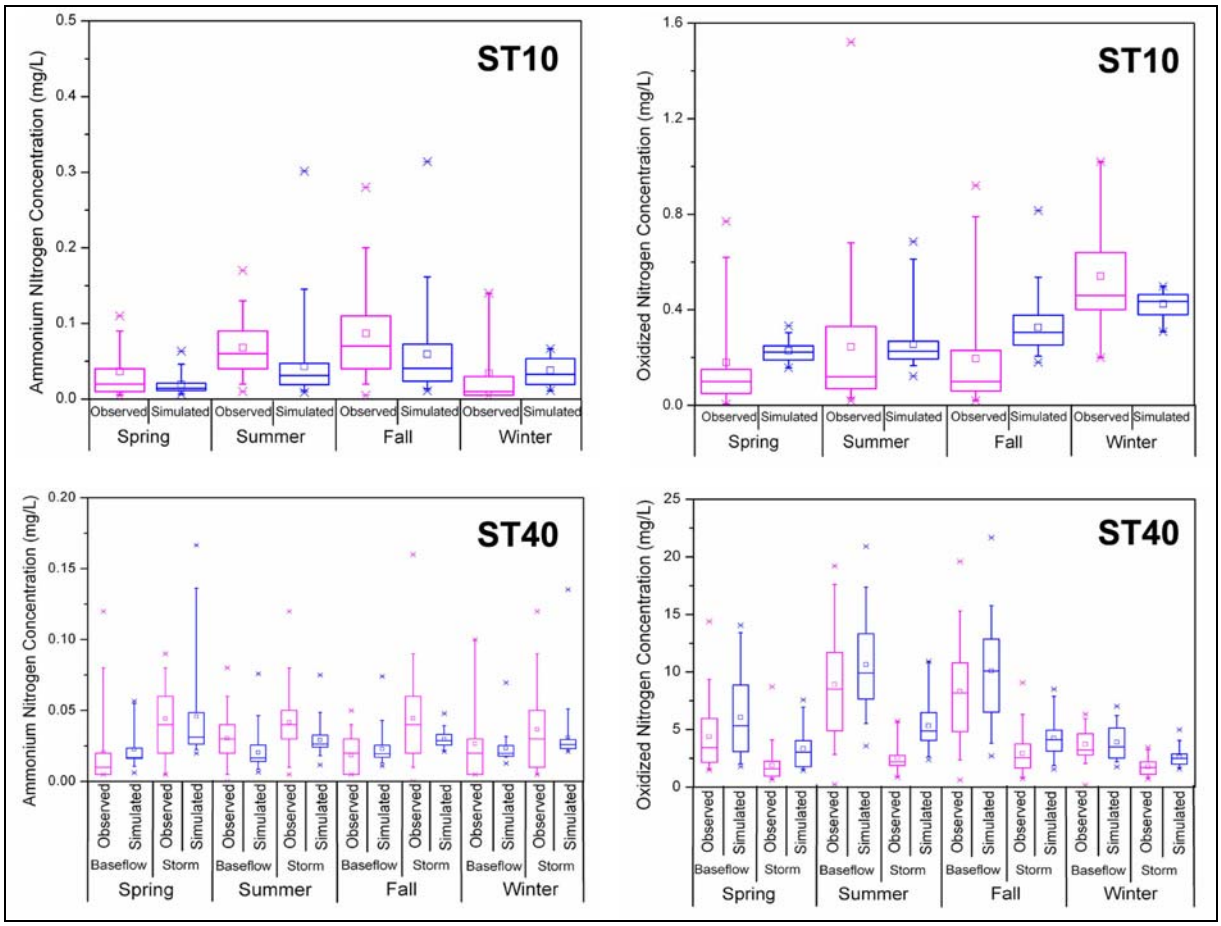

Figure 5-6: Seasonal Comparison of Baseflow and Stormwater NH4-N and Ox-N Concentrations at Stations near the Headwaters of the Occoquan Reservoir. Each box graphs the quartiles with the lower and upper edges representing the 25th and 75th percentiles, respectively. The midline is the median. The upper and lower points (asterisks) are the maximum and minimum values.

Figures 5-7 and 5-8 show the comparisons of average NH4-N and Ox-N concentrations along the mainstems of the Lake and the Reservoir as a function of distance upstream of the respective dams. The results indicate that the W2 submodels capture longitudinal distribution of SIN fairly well. In both waterbodies, the average concentrations of NH4-N tend to be similar among different sites in the surface layers, while increasing toward the dams in the bottom layers. At the various Lake stations, the absolute differences are equal to or less than 0.01 mg/L and 0.11 mg/L for surface and bottom NH4-N concentrations, respectively. Although the Reservoir W2 submodel reproduced the surface NH4-N concentrations fairly well (absolute differences are less than 0.02 mg/L for various sites), it under-predicted NH4-N concentrations along bottom layers except at the location close to the dam. W2 denitrifies a fraction of Ox-N to NH4-N and computes another fraction

that leaves the system (while not explicitly stated that it leaves as nitrogen gas, this is assumed). Therefore, the relatively high bottom NH4-N in the Reservoir might be related to denitrification accelerated by higher Ox-N concentrations due to UOSA effluent. Although this process is more likely to occur in the lacustrine zones than the riverine zones, W2 (Version 3.2) only allows a single value for each waterbody. This might partially explain the differences in NH4-N concentrations in the bottom layers in the Reservoir.

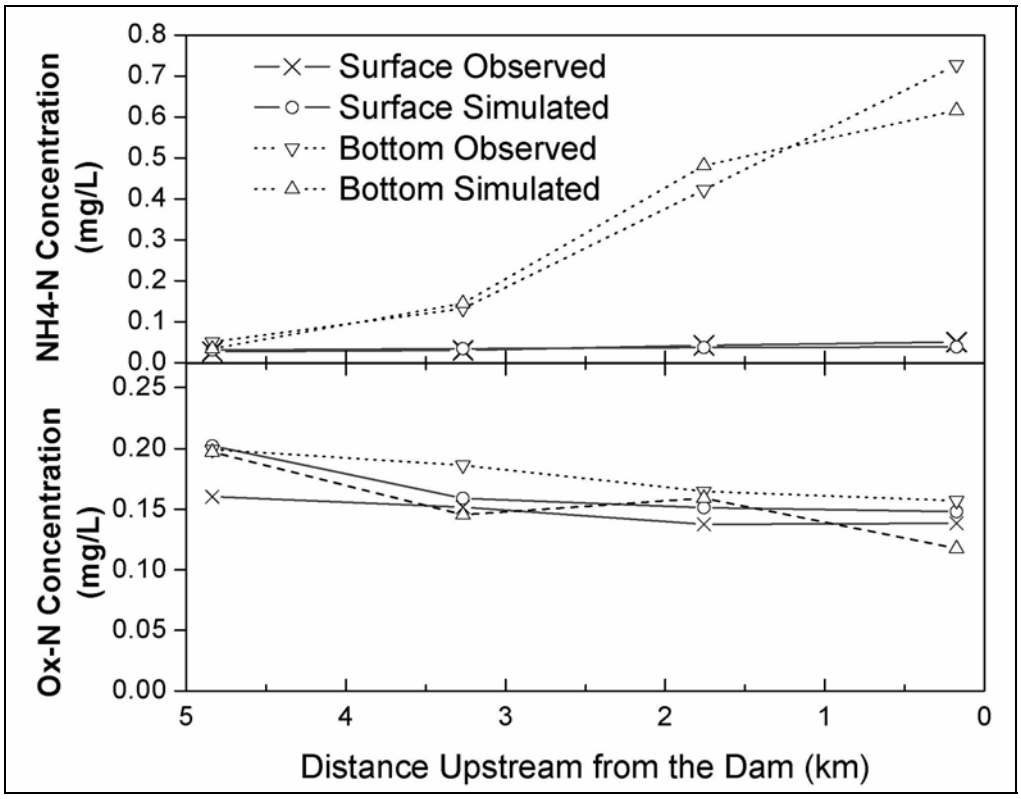

Figure 5-7: Comparison of Spatial Distributions of Ammonium Nitrogen and Oxidized Nitrogen along the Mainstem of Lake Manassas, 1993-95

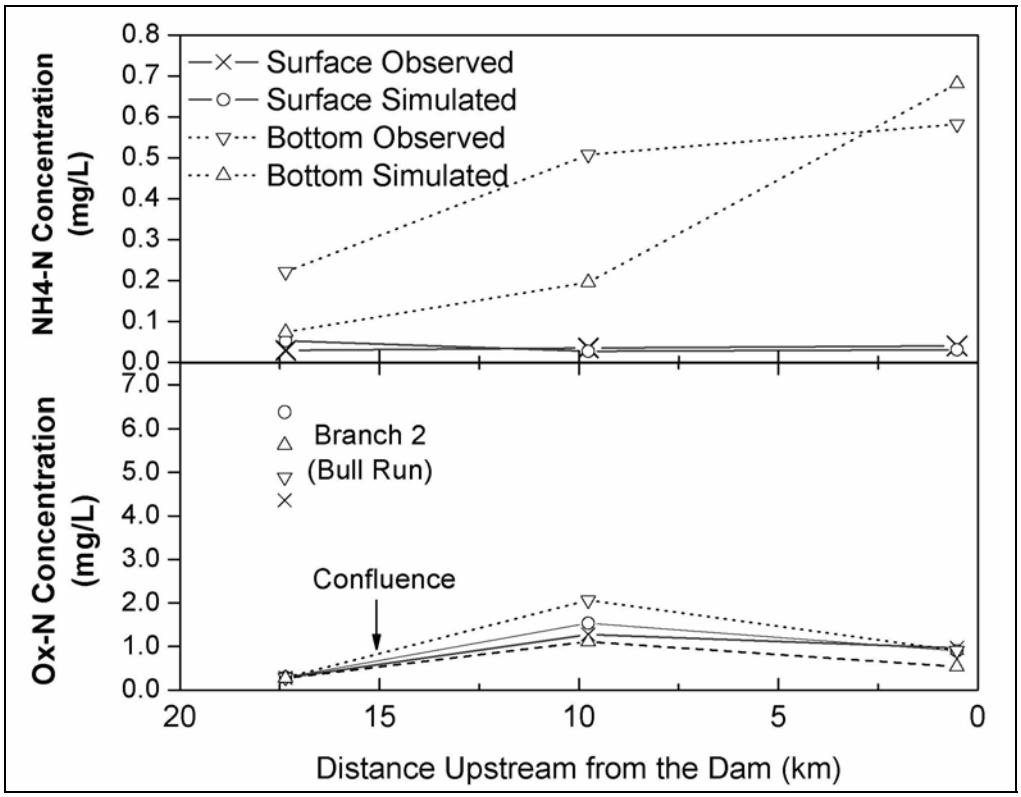

Figure 5-8: Comparison of Spatial Distributions of Ammonium Nitrogen and Oxidized Nitrogen along the Mainstem of the Occoquan Reservoir, 1993-95. (Ox-N values shown for Bull Run to illustrate the significant differences between the branches upstream of the confluence.)

In the Lake (Figure 5-7), differences between observed and simulated average surface Ox-N concentrations are less than 0.01 mg/L except for the location close to the headwater, which is over-predicted by 0.04 mg/L. This is probably due to over-prediction in the Upper Broad Run HSPF submodel (Table 5-1), which generated the inputs for the Lake W2 submodel. The near-bottom Ox-N was generally under-predicted by approximately 0.04 mg/L. The good agreement between simulated and observed NH4-N and Ox-N at surface layers of the Lake confirmed the good calibration of the Upper Broad Run HSPF submodel. It also provided a solid base for a good performance of the Lower Broad Run HSPF submodel.

In the Reservoir (Figure 5-8), the Ox-N concentrations in the Bull Run branch (Branch 2) were significantly higher than those in the Occoquan River (Branch 1). This is due to the contribution from UOSA nitrate-rich effluence. This explains the increase of the mainstem Ox-N concentrations after the confluence of Bull Run and Occoquan River (approximately 15 km upstream from the Reservoir dam). Although both surface and

bottom Ox-N concentrations from Branch 2 were over-predicted due to the over-prediction of the Bull Run HSPF submodel (Table 5-4, ST40), such differences between simulated and observed Ox-N concentrations were reduced after nitrate-rich flow from Branch 2 was mixed and diluted by the flow from Branch 1, which carried much lower nitrate concentrations. The differences in Ox-N concentrations near the Reservoir dam were 0.07 mg/L for surface and 0.37 mg/L for bottom (Table 5-5).

Table 5-5: Comparison of Surface and Bottom NH4-N and Ox-N Concentration at Monitoring Stations near the Lake Manassas (LM01) and Occoquan Reservoir (RE02) Dams

		LM01		RE02	
		Surface	Bottom	Surface	Bottom
NH4-N (mg/L)	Observed	0.05	0.73	0.04	0.58
	Simulated	0.04	0.62	0.03	0.82
	Difference	–0.01	–0.11	–0.01	+0.24
Ox-N (mg/L)	Observed	0.14	0.16	0.97	0.90
	Simulated	0.15	0.12	0.90	0.53
	Difference	+0.01	–0.04	–0.07	–0.37

Further investigations were performed for stations near the dams (RE02 for the Reservoir and LM01 for the Lake) (Tables 5-5 and 5-6). This is because the surface concentrations at these stations generally represent the water quality flowing downstream over the dams. In addition, it also provides information on water quality into the water treatment plant of the City of Manassas because the plant withdraws waters primarily from the top intake at the Lake Manassas dam. At LM01 (the Lake), the NH4-N concentrations were well reproduced by the W2 submodel and the differences were 0.01 mg/L and 0.11 mg/L for surface and bottom layers, respectively. The paired t-test results (Table 5-6) confirmed that there was no significant differences between observed and simulated data in term of the mean values with the probability values (p values) greater than 0.05. Although paired t-tests showed differences between the mean values of simulated and observed Ox-N concentration (p values less than 0.05), the differences were 0.01 mg/L for surface and 0.04 mg/L for bottom. The submodel also captured the seasonal nitrogen cycle in the Lake very well and correctly simulated both timing and magnitude of the seasonal cycle at both surface and bottom layers (Figure 5-9).

Table 5-6: Probability Values from Paired t-test Analysis at In-lake Monitoring Stations near the Lake Manassas (LM01) and Occoquan Reservoir (RE02) Dams

		LM01		RE02	
		Surface	Bottom	Surface	Bottom
NH4-N	Number of Samples	57	56	111	112
	Probability Value	0.31	0.07	0.38	<0.05
Ox-N	Number of Samples	57	57	112	113
	Probability Value	<0.05	<0.05	0.38	<0.05

At the RE02 station, although the bottom values are not well reproduced (p values less than 0.05), the simulated surface NH4-N and Ox-N concentrations show no significant differences with the observed values in term of the mean values (p values greater than 0.05) (Table 5-6). The average surface Ox-N concentrations were under-predicted by 0.07 mg/L, and large differences of Ox-N occurred in summer and fall months. The timing and magnitude of seasonal nitrogen cycles in the Reservoir is not well captured (Figure 5-9). This is likely related to algae simulation. In the current study, only one lumped algae species was modeled in the Reservoir W2 submodel although the observed species count data suggest three dominant algae species (blue green algae, green algae, and diatoms). The prediction of surface nitrogen concentrations would probably be improved in both timing and magnitude by including multiple algal species in the W2 submodels. The over-prediction of bottom NH4-N and under-prediction of bottom Ox-N in fall and summer months are possibly related to sediment diagenesis and denitrification.

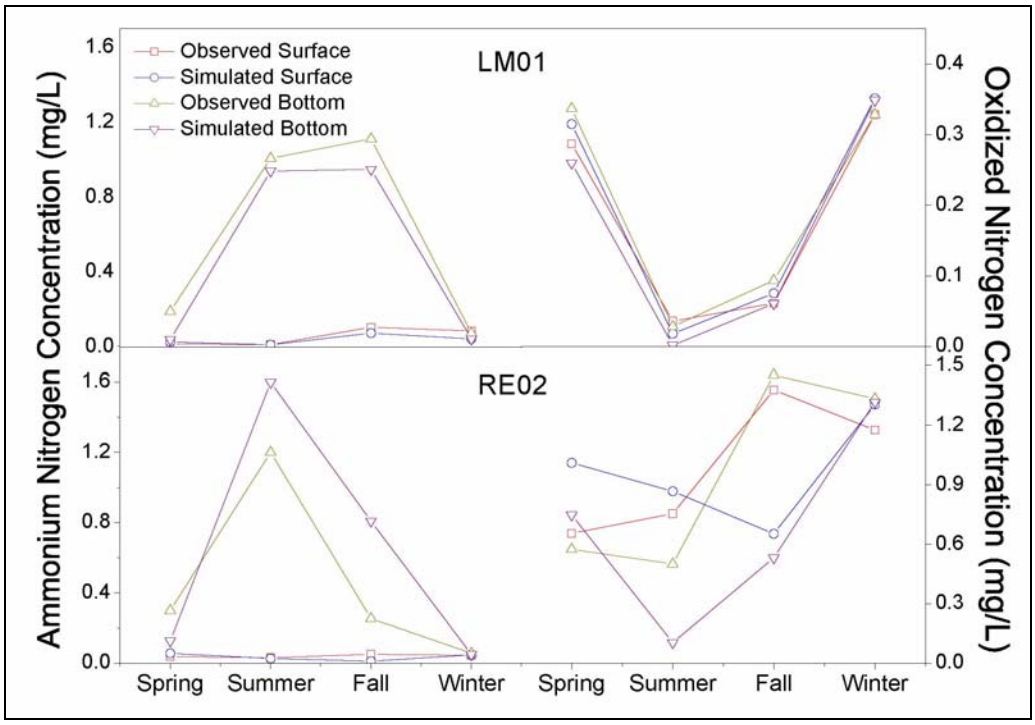

Figure 5-9: Comparison of Temporal Distributions of Ammonium Nitrogen (Left) and Oxidized Nitrogen (Right) at the Stations near the Dams of Lake Manassas (LM01) and Occoquan Reservoir (RE02), 1993-95

5.4.1.2 Validation

Simulated and observed nitrogen data for the years 1996 and 1997 were used for model validation. Both the calibration and validation periods were combinations of wet and dry years and are considered suitable for model calibration and validation purposes. Nutrient loads and concentrations for these two validation years were simulated using the same land use as for the calibration period (the year 1995) and the 1996 and 1997 meteorological data.

As done for model calibration, the validation of HSPF submodels was also performed on three levels: annual production, monthly production and individual storms. The results shown here include both calibration and validation periods so that model performance for two periods can be easily compared. Figures 5-10 and 5-11 show the annual nutrient load comparisons for the five-year simulation period including the two-year validation period. During the validation period, major discrepancies for the nutrient load production mainly occurred in the wet year 1996, where simulated nitrogen loads were greatly

under-predicted partially due to the difference in hydrologic systems (Xu, et al. 2006). The validation results of the relatively dry year 1997 are better with the percentage differences in the range of –32.4% ~ –0.6% for NH4-N and –33.5%~ +9.2% for Ox-N nitrogen (Table 5-7), which are considered to be "fair" or "very good" simulations, according to the scale used by Donigian (2002) (see Table 3-4).

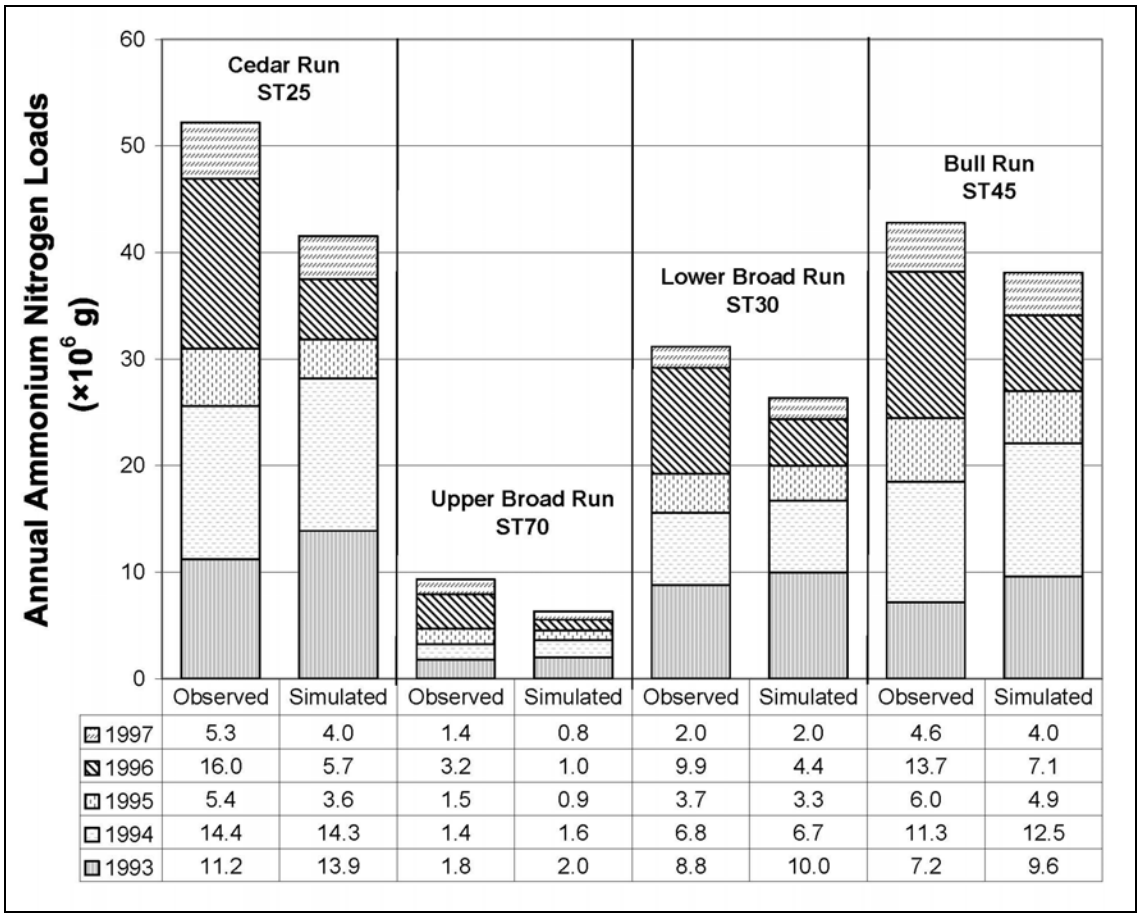

	Observed	Simulated	Observed	Simulated	Observed	Simulated	Observed	Simulated
1997	5.3	4.0	1.4	0.8	2.0	2.0	4.6	4.0
1996	16.0	5.7	3.2	1.0	9.9	4.4	13.7	7.1
1995	5.4	3.6	1.5	0.9	3.7	3.3	6.0	4.9
1994	14.4	14.3	1.4	1.6	6.8	6.7	11.3	12.5
1993	11.2	13.9	1.8	2.0	8.8	10.0	7.2	9.6

Figure 5-10: Comparison of Annual Ammonium Nitrogen Loads for Model Calibration and Validation

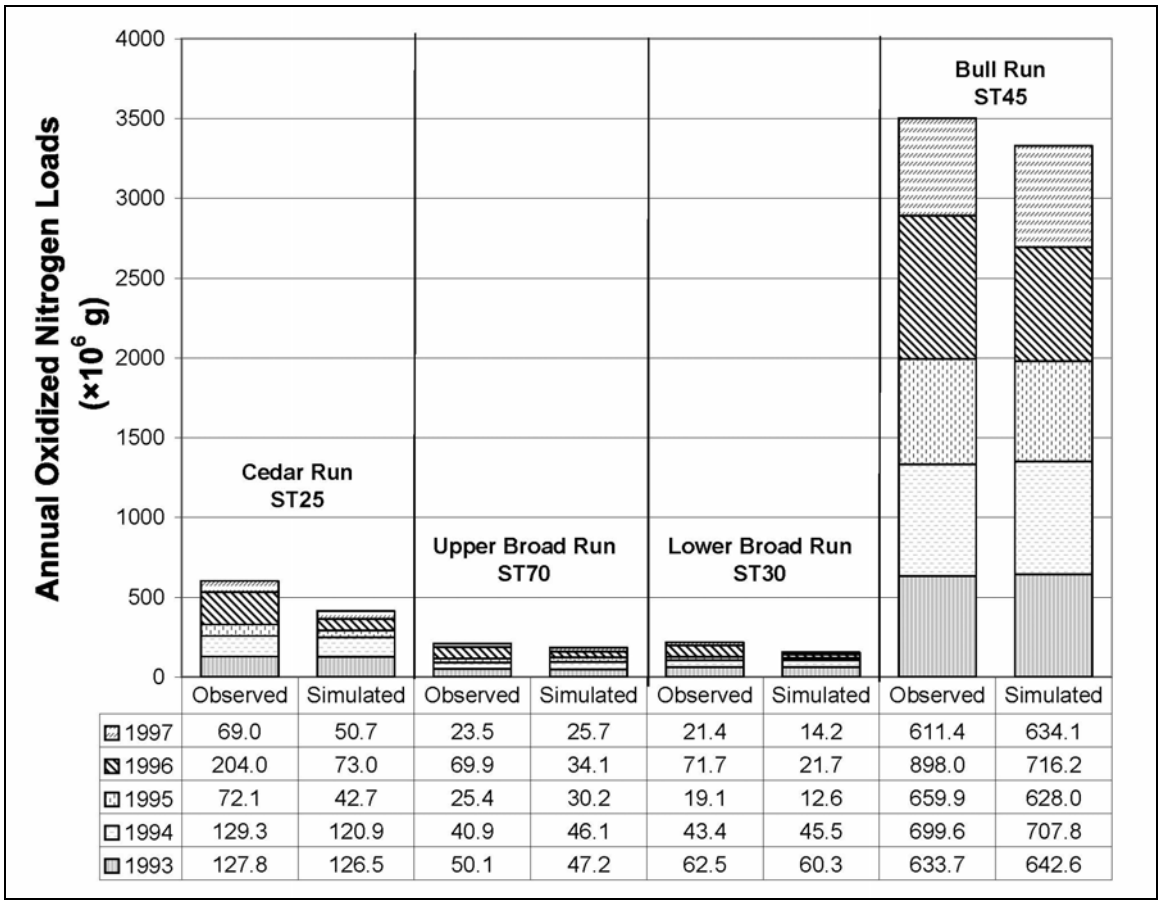

	Observed	Simulated	Observed	Simulated	Observed	Simulated	Observed	Simulated
1997	69.0	50.7	23.5	25.7	21.4	14.2	611.4	634.1
1996	204.0	73.0	69.9	34.1	71.7	21.7	898.0	716.2
1995	72.1	42.7	25.4	30.2	19.1	12.6	659.9	628.0
1994	129.3	120.9	40.9	46.1	43.4	45.5	699.6	707.8
1993	127.8	126.5	50.1	47.2	62.5	60.3	633.7	642.6

Figure 5-11: Comparison of Annual Oxidized Nitrogen Loads for Model Calibration and Validation

Table 5-7: Performance of the Occoquan Model in Simulating Annual Soluble Inorganic Nitrogen Loads at Various Stream Stations

		NH4-N				Ox-N			
		ST25	ST70	ST30	ST45	ST25	ST70	ST30	ST45
Calibration	1993	+23.9* Good*	+12.2 Very Good	+13.1 Very Good	+33.9 Fair	–1.1 Very Good	–5.8 Very Good	–3.5 Very Good	+1.4 Very Good
	1994	–0.4 Very Good	+9.3 Very Good	–0.8 Very Good	+10.5 Very Good	–6.5 Very Good	+12.8 Very Good	+4.6 Very Good	+1.2 Very Good
	1995	–32.5 Fair	–37.0 Poor	–10.4 Good	–18.6 Good	–40.8 Poor	+18.9 Good	–34.2 Fair	–4.8 Very Good
Validation	1996	–64.6 Poor	–44.3 Poor	–55.8 Poor	–48.0 Poor	–64.2 Poor	–51.2 Poor	–69.7 Poor	–20.2 Good
	1997	–23.0 Good	–32.4 Fair	–0.6 Very Good	–12.8 Very Good	–26.5 Fair	+9.2 Very Good	–33.5 Fair	+3.7 Very Good
Summary	1993-1995	+2.8	+2.4	+3.7	+10.2	–11.9	+2.4	–5.4	–0.7
	1993-1997	–20.4	–12.7	–15.5	–10.9	–31.3	–12.7	–29.3	–5.0

*Values are percent differences from observed data (%), and ratings are as per Table 3-4

Observed and simulated data for UOSA are also shown in Figures 5-12 and 5-13 for station ST45, as UOSA forms a significant component of the nitrogen load at this station, especially for the oxidized nitrogen. It can be seen that although the discrepancies for the validation year 1996 was the largest, the model captured the temporal fluctuations in validation year 1997.

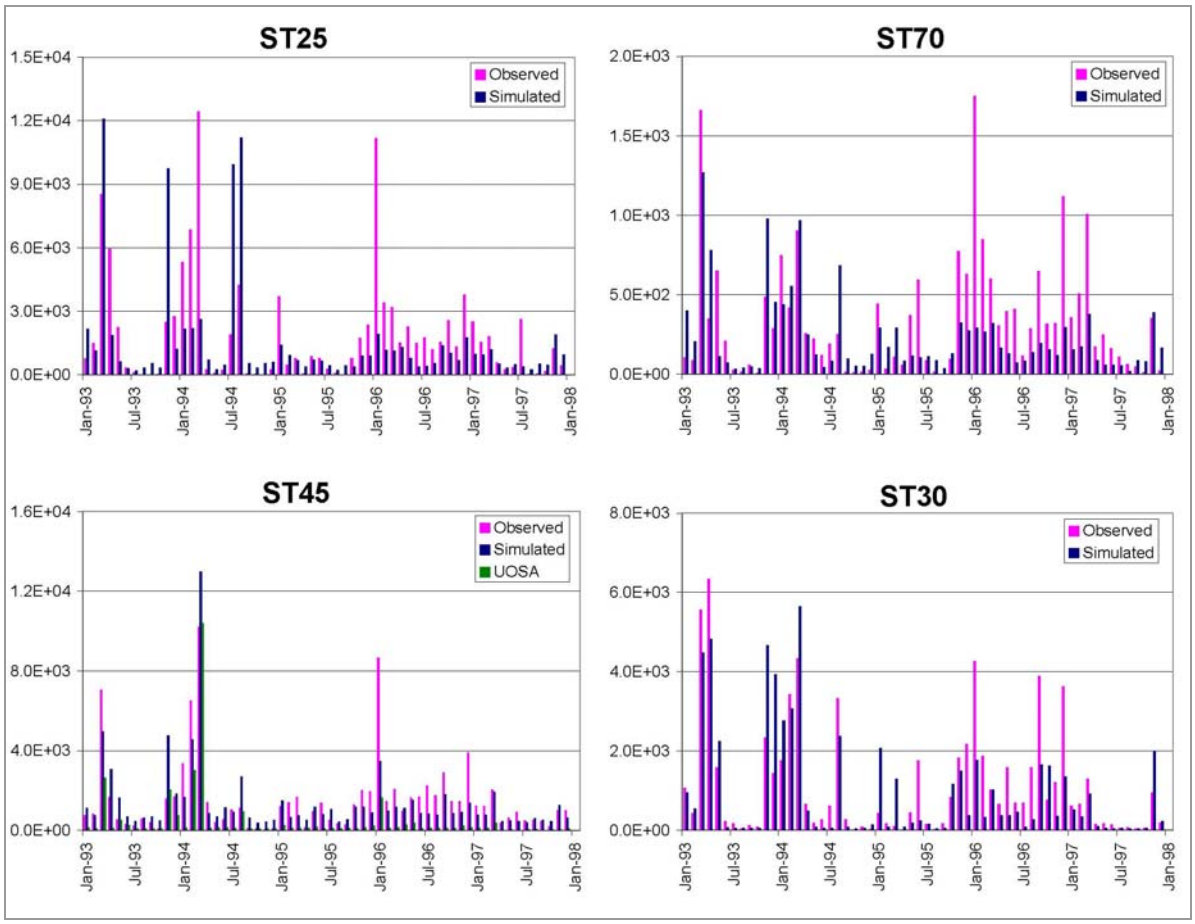

Figure 5-12: Comparisons of Monthly Ammonium Nitrogen Loads (lbs) at Four Principal Stream Stations in the Occoquan Watershed for Model Calibration (1993-1995) and Validation (1996-1997)

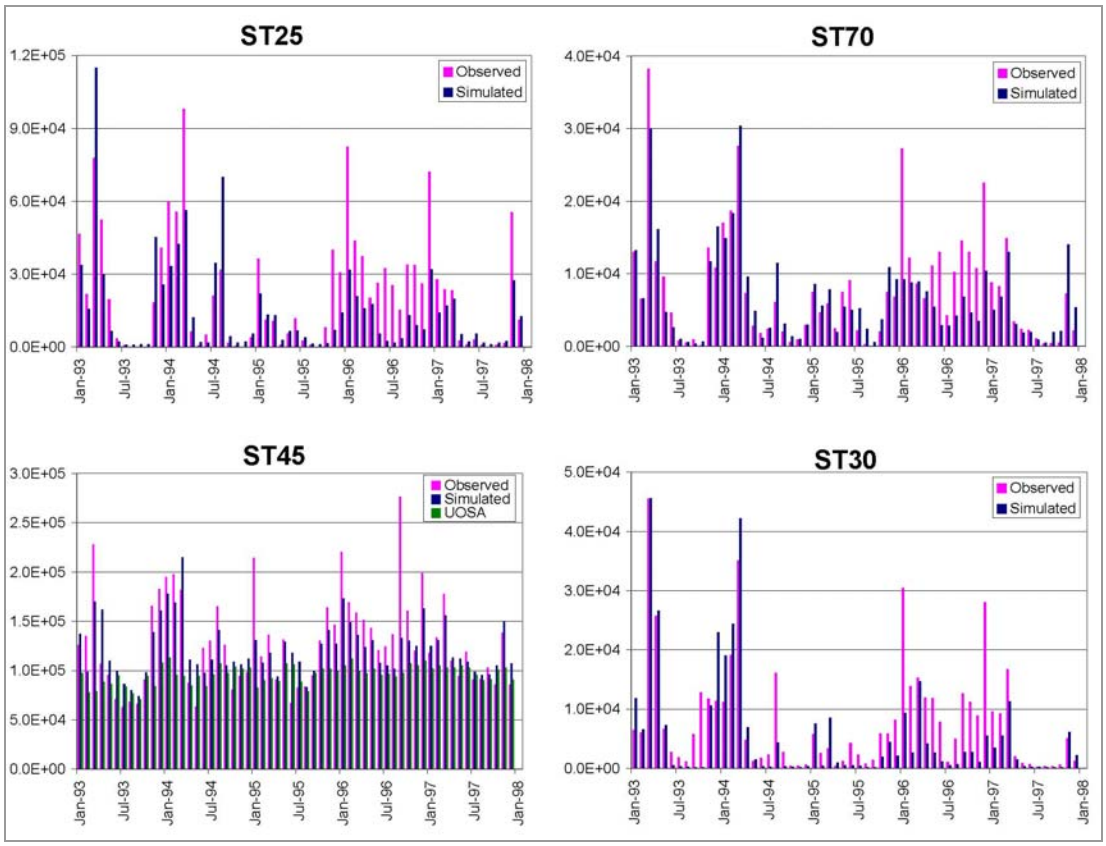

Figure 5-13: Comparisons of Monthly Oxidized Nitrogen Loads (lbs) at Four Principal Stream Stations in the Occoquan Watershed for Model Calibration (1993-1995) and Validation (1996-1997)

Tables 5-8 and 5-9 show the validation results from the Lake W2 submodel. The comparison of average NH4-N concentrations at major Lake Manassas stations indicated that the W2 submodel captured the spatial distribution of surface NH4-N concentrations fairly well. The differences at the bottom layer (–0.03 mg/L ~ +0.53 mg/L) are relatively large, especially at the LM01 stations.

The W2 submodel also captured the spatial distribution of Ox-N. In the validation period, the differences between observed and simulated concentrations are in the range of –0.09 mg/L ~ –0.04 mg/L for surface layers and –0.20 mg/L ~ –0.07 mg/L for bottom layers. The general under-prediction of Ox-N concentrations is possibly related to the under-prediction of the Upper Broad Run HSPF submodel, especially during the year 1996.

Tables 5-10 and 5-11 show the comparison of average surface and bottom NH4-N and Ox-N concentrations at major Occoquan Reservoir stations. The validation results show that the W2 submodel captured the spatial distribution of NH4-N as well as it did for the calibration period. Both surface and bottom NH4-N concentrations are well reproduced with the difference in the range of –0.02 mg/L ~ +0.01 mg/L and –0.13 mg/L ~ +0.28 mg/L, respectively.

The W2 submodel also captured the spatial distribution of Ox-N at the Occoquan Reservoir. The validation results indicated that the differences between observed and simulated concentrations are in the range of –0.51 mg/L ~ +0.74 mg/L for surface layers and –1.04 mg/L ~ +0.14 mg/L for bottom layers. These are comparable to the results obtained for the calibration.

Table 5-8: Comparison of Average Surface and Bottom NH4-N Concentrations (mg/L) at Major Lake Manassas Stations (1993-1997)

		LM01		LM03		LM04		LM05		LM06	
		Surface	Bottom	Surface	Bottom	Surface	Bottom	Surface	Bottom	Surface	Bottom
Calibration (1993-1995)	Observed	0.05	0.73	0.05	0.09	0.04	0.38	0.03	0.13	0.03	0.05
	Simulated	0.04	0.62	0.04	0.09	0.04	0.44	0.03	0.19	0.03	0.03
	Difference	–0.01	–0.11	–0.01	0.00	0.00	+0.06	0.00	+0.06	0.00	–0.02
Validation (1996-1997)	Observed	0.04	0.49	0.04	0.08	0.04	0.31	0.03	0.12	0.03	0.06
	Simulated	0.04	1.02	0.04	0.11	0.04	0.61	0.03	0.19	0.03	0.03
	Difference	0.00	+0.53	0.00	+0.03	0.00	+0.30	0.00	+0.07	0.00	–0.03

Table 5-9: Comparison of Average Surface and Bottom Ox-N Concentrations (mg/L) at Major Lake Manassas Stations (1993-1997)

		LM01		LM03		LM04		LM05		LM06	
		Surface	Bottom	Surface	Bottom	Surface	Bottom	Surface	Bottom	Surface	Bottom
Calibration (1993-1995)	Observed	0.14	0.16	0.12	0.14	0.14	0.20	0.15	0.19	0.16	0.20
	Simulated	0.15	0.12	0.17	0.17	0.15	0.16	0.16	0.15	0.20	0.20
	Difference	+0.01	–0.04	+0.05	+0.03	+0.01	–0.04	+0.01	–0.04	+0.04	0.00
Validation (1996-1997)	Observed	0.23	0.26	0.22	0.24	0.23	0.27	0.24	0.28	0.26	0.41
	Simulated	0.15	0.13	0.18	0.17	0.15	0.13	0.15	0.15	0.21	0.21
	Difference	–0.08	–0.13	–0.04	–0.07	–0.08	–0.14	–0.09	–0.13	–0.05	–0.20

Table 5-10: Comparison of Average Surface and Bottom NH4-N Concentrations (mg/L) at Major Occoquan Reservoir Stations (1993-1997)

		RE02		RE15		RE30		RE35	
		Surface	Bottom	Surface	Bottom	Surface	Bottom	Surface	Bottom
Calibration (1993-1995)	Observed	0.04	0.58	0.04	0.56	0.03	0.14	0.03	0.22
	Simulated	0.03	0.82	0.03	0.25	0.03	0.06	0.05	0.08
	Difference	–0.01	+0.24	–0.01	–0.30	–0.00	–0.08	+0.02	–0.14
Validation (1996-1997)	Observed	0.05	0.52	0.04	0.41	0.04	0.12	0.04	0.17
	Simulated	0.03	0.80	0.03	0.28	0.02	0.09	0.05	0.06
	Difference	–0.02	+0.28	–0.01	–0.13	–0.02	–0.03	+0.01	–0.11

Table 5-11: Comparison of Average Surface and Bottom Ox-N Concentrations (mg/L) at Major Occoquan Reservoir Stations (1993-1997)

		RE02		RE15		RE30		RE35	
		Surface	Bottom	Surface	Bottom	Surface	Bottom	Surface	Bottom
Calibration (1993-1995)	Observed	0.97	0.90	1.28	2.06	4.36	4.89	0.28	0.29
	Simulated	0.90	0.53	1.54	1.11	6.38	5.63	0.26	0.27
	Difference	–0.07	–0.37	+0.26	–0.95	+2.02	+0.74	–0.02	–0.02
Validation (1996-1997)	Observed	1.33	1.18	1.66	2.06	4.23	4.44	0.45	0.51
	Simulated	0.98	0.57	1.15	1.02	4.97	4.30	0.25	0.30
	Difference	–0.35	–0.61	–0.51	–1.04	+0.74	+0.14	–0.20	–0.21

Figure 5-14 shows that both the W2 submodels reproduce the temporal distribution of NH4-N and Ox-N concentrations. Although the Lake submodel tended to over-predict the bottom NH4-N concentrations during the validation period, it reproduced the seasonal variations fairly well. Otherwise, both W2 submodels are well validated for soluble inorganic nitrogen concentrations.

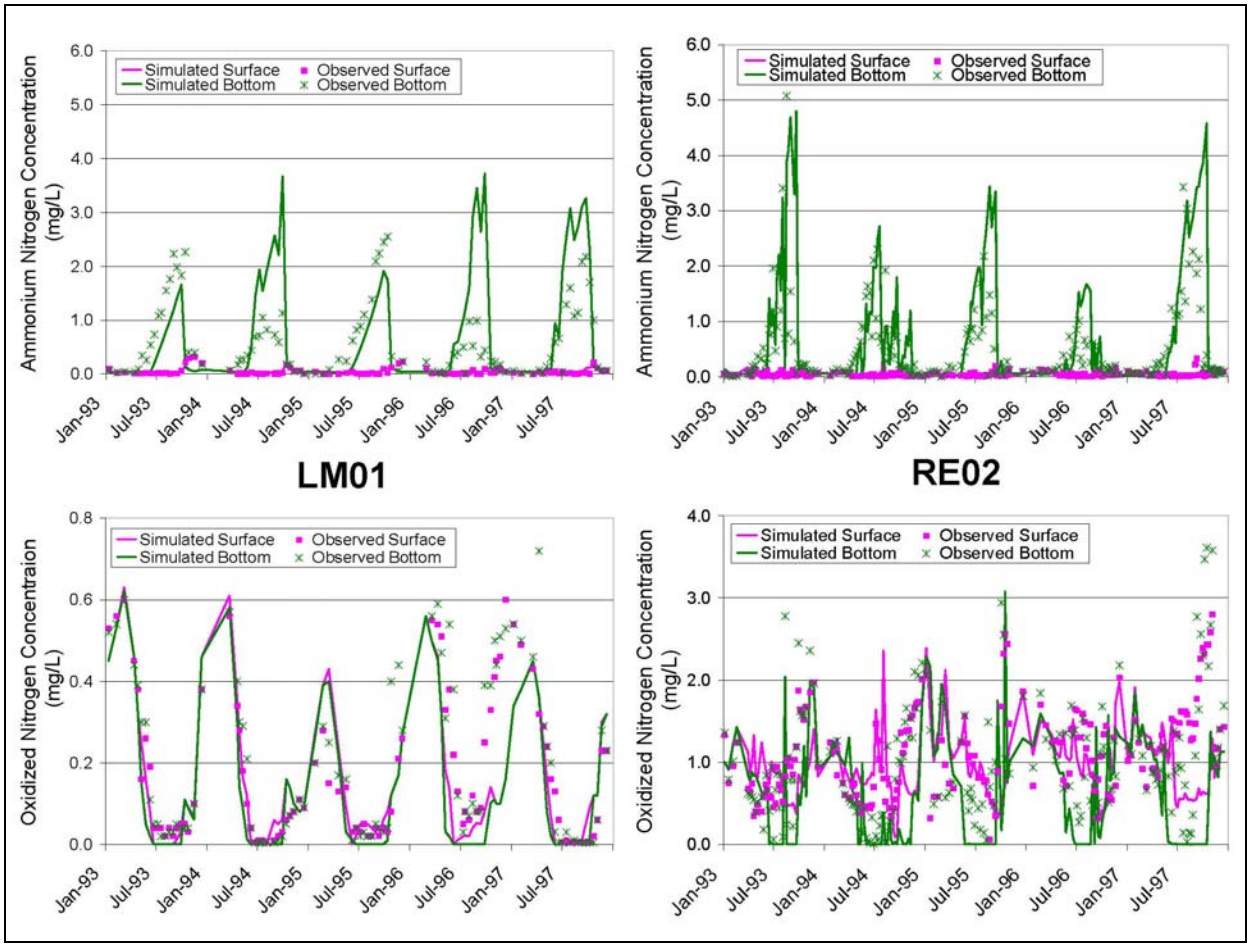

Figure 5-14: Comparison of Observed and Simulated Daily NH4-N and Ox-N Concentrations at LM01 and RE02 Stations for Model Calibration and Validation

5.4.2 Alternative Land Use Development Scenario Results

One of the advantages of linking watershed models to reservoir models is to develop a direct cause-effect relationship between upstream activities and downstream water quality. Therefore, W2 can use the boundary conditions corresponding with land development scenarios to predict the resultant water quality variation. This approach is different from that of most studies to quantify the nutrient load allocation to meet TMDL goals. Instead of reducing the inflow nutrient concentrations (Bowen and Hieronymus 2003; Imteaz, et al. 2003), alternative scenarios can be developed by investigating external nutrient load variation due to land development or best management practices (BMPs) implementation. Therefore, this approach can not only be used to investigate the impact of alternative land use development plans, but also can provide a practical guide of BMP implementation to meet the TMDL goals.

In this section, land use scenarios based on various time periods were developed and the impact of urbanization was investigated. The watershed segments, waterbody bathymetries, and all the input parameters, except the land use data, were the same as the current case (calibration). The land use changes developed for the two management scenarios are shown in Table 5-12.

Table 5-12: Percentage of Different Land Use Categories for Various Development Scenarios

	Current			Forest			Future		
	Agriculture	Forest	Urban	Agriculture	Forest	Urban	Agriculture	Forest	Urban
Cedar Run	36.7	56.3	7.1	0.0	100.0	0.0	36.7	28.2	35.3
Broad Run	25.6	58.3	16.1	0.0	100.0	0.0	25.6	29.2	43.3
Bull Run	12.5	54.9	32.6	0.0	100.0	0.0	12.5	28.2	60.1

5.4.2.1 Forest Scenario

One scenario (Forest) was developed wherein all the lands were assumed to be covered by forests. It represents the background condition with no impact from human activities before the Colonial history and can be used to evaluate the long-term impact of human activities on the water resources. The contribution of UOSA is eliminated in this scenario. With all the land areas covered by forests, natural processes such as organic matter decay and atmospheric deposition produce 16.6×10^6 g NH4-N and 266.3×10^6 g Ox-N per year (Table 5-13). As expected, these nutrient loads from the land segments are

much lower than the current condition (the Current case) and the model output suggests 11.9×10^6 g/year (71.5%) and 597.4 $\times10^6$ g/year (324.3%) increase of annual NH4-N and Ox-N load production, respectively, since the pre-Colonial period. They are the joint results from land development and UOSA operation. The nutrient loads from UOSA effluent are 3.7×10^6 g/year and 506.6×10^6 g/year for NH4-N and Ox-N respectively. UOSA was built to replace eleven major wastewater treatment plants that were responsible for serious eutrophication in the Reservoir during the 1960s. It applied advanced techniques to reduce nutrient loads into the Reservoir and studies have shown that the water quality in the Reservoir has been substantially improved since the operation of UOSA (Randall and Grizzard 1995). Although UOSA effluent accounts for 85% of Ox-N load increase, studies have shown its benefit to the Reservoir water quality. The nitrate-rich discharge has maintained the bottom sediment layers in an oxidized state to prevent the phosphorus release during anoxic conditions. Thanks to UOSA, the point source pollution has had insignificant impact on NH4-N enrichment in the Occoquan Reservoir. The analysis of land development since pre-Colonial days suggests that the coverage of forest has been halved and agricultural and urban development has been more dominant in the current condition. These changes on land use patterns account for more than 70% of NH4-N loads increases.

Table 5-13: Annual NH4-N and Ox-N Loads for Major Subbasins for Various Land Development Scenarios under 1993-1995 Flow and Weather Conditions

	Annual NH4-N loads ($\times10^6$ g)			Annual Ox-N loads ($\times10^6$ g)		
	Forest	Current	Future	Forest	Current	Future
Cedar Run	7.9	11.8	32.8	88.7	114.9	156.6
Broad Run	6.1	8.1	9.7	34.1	50.2	52.3
Bull Run	2.6	8.6	10.8	143.5	698.5	712.1
Total	16.6	28.5	53.3	266.3	863.6	921.0

Because land uses are not evenly spread across the watershed, the increase of nutrient loads due to land development varies in each subbasin. Figure 5-15 shows the NH4-N and Ox-N load production under the three different land use scenarios. The contribution from UOSA effluent is not included in this plot so that the changes of water quality due to land use development would not be masked by other factors. Although the background ammonium yields (Forest) is similar among different subbasins, background Ox-N yields are different. Overall, the Broad Run subbasin shows the smallest Ox-N yields in the

Forest scenario. This is possibly due to the catchment function of the Lake. The relatively high Ox-N yield in the Bull Run subbasin might be related to relatively high interflow and groundwater concentrations.

It is clear that different subbasins show different increase rates due to site characteristics. The Broad Run subbasin (Figure 5-15) shows the lowest increase of yield production for both NH4-N (10.3%) and Ox-N (5.1%) since the pre-Colonial period, where Lake Manassas probably traps these nutrients and reduces transport downstream. The Bull Run region shows the greatest increases in nitrogen load production (87.9% for NH4-N and 33.8% for Ox-N) due to its greater urbanization.

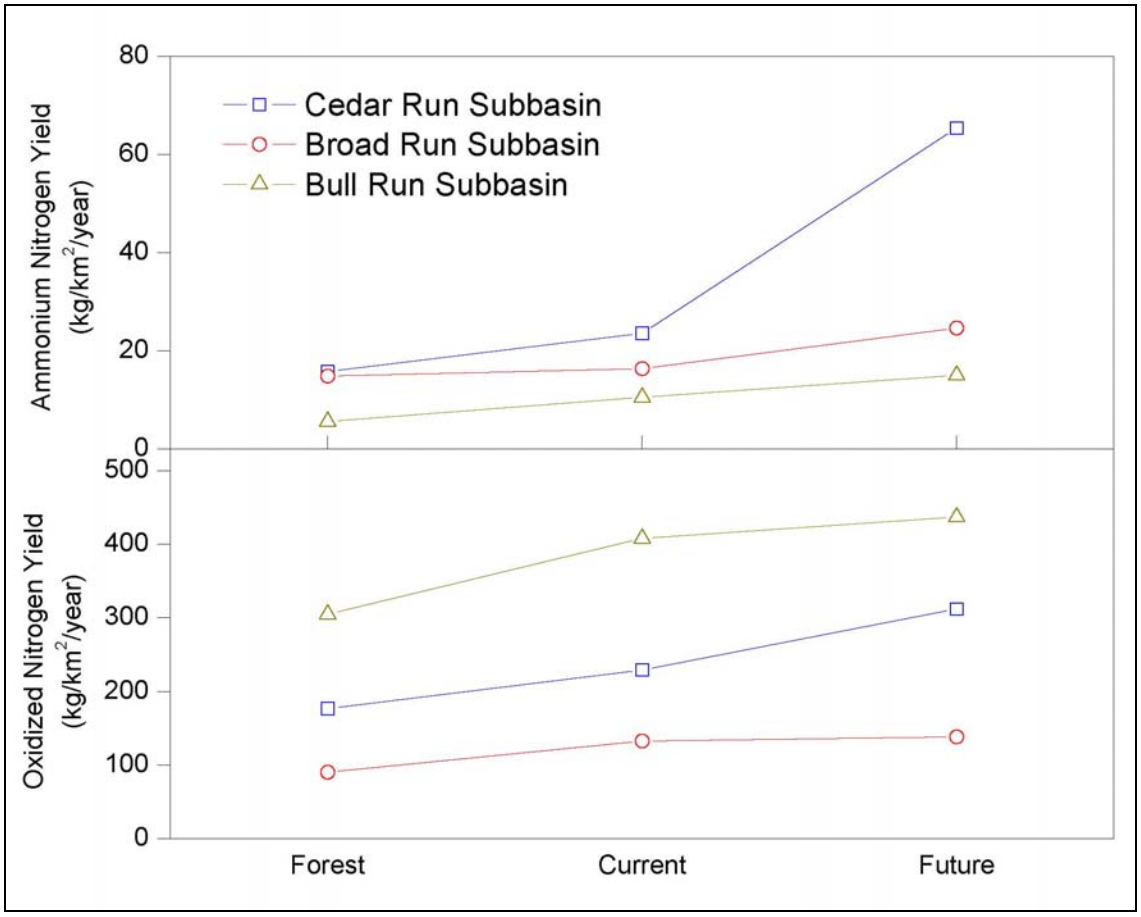

Figure 5-15: Comparison of the Impact of Different Land Development Scenarios on Simulated Ammonium Nitrogen and Oxidized Nitrogen Load Yields for 1993-95 Flow and Weather Conditions

The increases of external nitrogen loads since the pre-Colonial period lead to increases of nitrogen concentrations delivered to the Reservoir. On the other hand, if the land use pattern is restored from the Current scenario to the Forest scenario, the reduced nitrogen

loads would reduce the nitrogen concentrations into the Reservoir (Table 5-14). For Branch 1 (Occoquan River), the average concentrations would decrease by 40.0% and 27.8% for NH4-N and Ox-N, respectively. The water chemistry into Branch 2 (Bull Run) has shown more dramatic changes, which are the results of both land development and UOSA operation. The average concentrations of NH4-N and Ox-N would be reduced by 0.02 mg/L (66.7%) and 6.64 mg/L (88.4%), respectively, compared to the Current scenario.

Table 5-14: Comparison of Inflow NH4-N and Ox-N Concentrations into the Occoquan Reservoir for Various Land Development Scenarios

Scenarios	NH4-N				Ox-N			
	Branch 1		Branch 2		Branch 1		Branch 2	
	(mg/L)	PD* (%)	(mg/L)	PD* (%)	(mg/L)	PD* (%)	(mg/L)	PD* (%)
Current	0.05		0.03		0.36		7.51	
Forest	0.03	–40.0	0.01	–66.7	0.26	–27.8	0.87	–88.4
Future	0.09	+80.0	0.03	0.0	0.48	+33.3	7.70	+2.5

* Percentage Difference from the Current Scenario

Not surprisingly, if the land use pattern is restored from the Current scenario to the Forest scenario, decreases of external nitrogen loads from drainage areas will eventually lead to nutrient reduction in the Reservoir. Although the Reservoir W2 submodel results suggest a slight decrease of average NH4-N concentrations at the bottom layers near the dam (15.5%), the surface NH4-N increases by 0.01 mg/L (Table 5-15). This is likely related to algae dynamics. The decreases of external biological available nutrient would reduce the algae growth, and thus reduce the consumption of NH4-N, the nitrogen species preferred by algae. The seasonal patterns of in-lake NH4-N concentrations are shown in Figure 5-16, where spring and summer seasons show relatively greater consumption of NH4-N by algae. On the other hand, due to the elimination of UOSA, the in-lake Ox-N has been dramatically reduced.

Table 5-15: Comparison of NH4-N and Ox-N Concentrations at the Station near the Occoquan Reservoir Dam (RE02) for Various Land Development Scenarios

Scenarios	NH4-N				Ox-N			
	Surface		Bottom		Surface		Bottom	
	(mg/L)	PD* (%)	(mg/L)	PD* (%)	(mg/L)	PD* (%)	(mg/L)	PD* (%)
Current	0.03		0.84		0.90		0.53	
Forest	0.04	+33.3	0.71	–15.5	0.30	–66.7	0.22	–58.5
Future	0.06	+100.0	0.78	–7.1	1.29	+43.3	0.71	+34.0

* PD: Percentage Difference from the Current Scenario

5.4.2.2 Future Scenario

The second scenario (Future) was developed by converting 50% of the existing forested areas in each segment to residential and commercial development. This is based on the rapid urbanization in northern Virginia, which is ranked as one of the fastest-growing regions in the United States. The region has been, and will very likely continue to be, facing substantial residential and commercial development. This scenario represents the expansion of the current urban lands by about 141.2, 129.2, and 110.4 km^2 in the Cedar Run, Broad Run, and Bull Run subbasins, respectively. Although it is highly possible that UOSA would expand as population grows, the contribution from UOSA is assumed to be unchanged in this scenario so that the changes of water quality due to land use development would not be masked.

The results indicate that the projected land use development would almost double the annual NH4-N production to 53.3 $\times 10^6$ g/year, compared to the current condition (Table 5-13). However, annual Ox-N loads only show slightly increases (6.7%) because UOSA effluent dominates the loads. The Cedar Run subbasin shows the greatest increase in NH4-N (177.4%) and Ox-N (36.3%) production (Figure 5-15) because the dominant land use would shift from non-urban development to urban development. This suggests that BMPs must be incorporated into future land use development plans to reduce dramatic increases in nitrogen production.

On the other hand, the Bull Run subbasin appears to have slower yield increase rates, especially Ox-N, compared with the pre-Colonial period (Figure 5-15). The investigation of land uses in the Bull Run subbasin indicates an existing high urban development with more than 30% of the land categorized as urban. Therefore, future expansion does not result in a significant increase of Ox-N load production. Also, compared to UOSA, Ox-N loads generated from drainage areas only account for a small portion of Ox-N loads delivered to the Reservoir. Although the contribution from UOSA is assumed to be constant in this scenario, it is highly possible that the capacity and water chemistry from UOSA discharge will be changed with the plant expansion and possible application of

new treatment techniques. Therefore, scenarios based on these considerations might provide a more realistic forecast of water quality changes in the Reservoir.

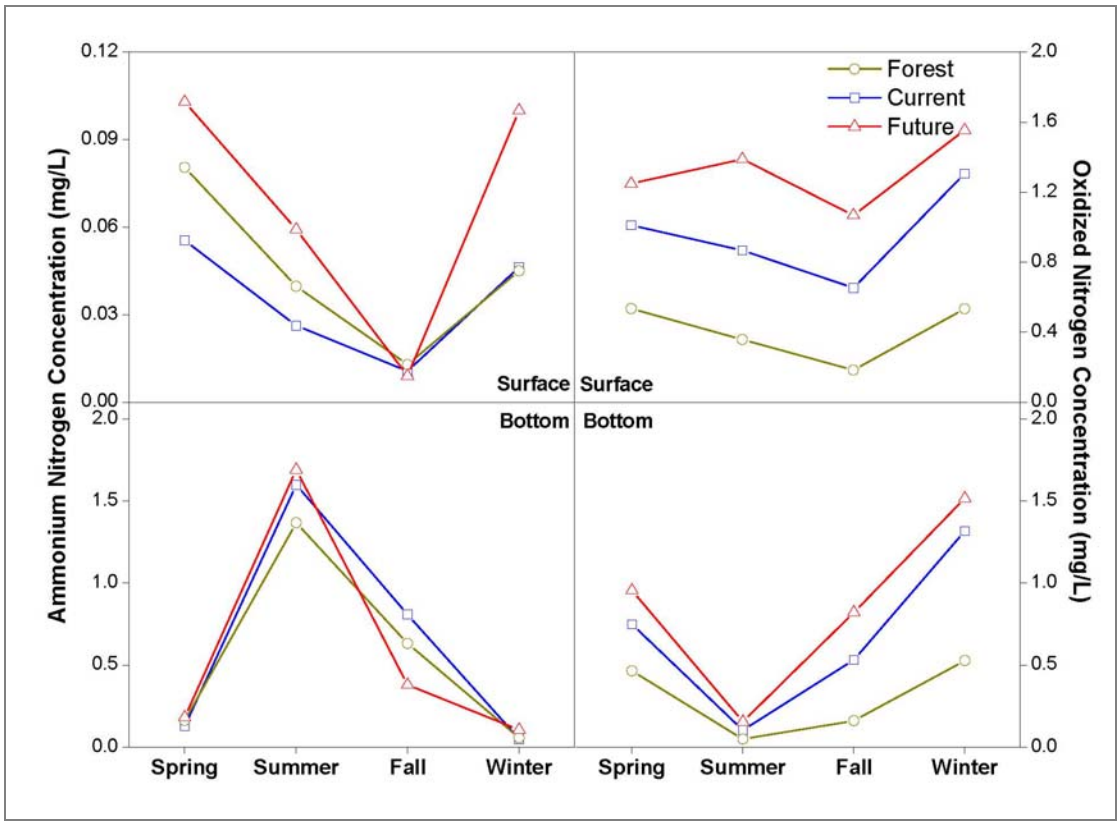

Figure 5-16: Comparison of Impact of Different Land Development Scenarios on Temporal Distributions of Ammonium Nitrogen (Left) and Oxidized Nitrogen (Right) at the Station near the Occoquan Reservoir Dam Using 1993-95 Flow and Weather Conditions

The dramatic change of the land use pattern in the Cedar Run subbasin due to urban expansion would increase NH4-N and Ox-N concentrations delivered into the Reservoir Branch 1 (Occoquan River) by 80.0% and 33.3%, respectively (Table 5-14). At the same time, the concentrations into Branch 2 (Bull Run) have shown no changes in NH4-N and a slightly increase (2.5%) in Ox-N.

As expected, the increase of external nutrient loads leads to the accumulation of nutrients in the Reservoir and the model results suggest a doubling of the surface NH4-N concentrations near the dam (Table 5-15). The high surface NH4-N concentrations would very likely stimulate algae growth and worsen the water quality issues due to oxygen depletion. However, the average bottom NH4-N concentration near the dam is suggested

by the model application to decrease by 0.06 mg/L. The seasonal pattern shown in Figure 5-16 indicates an unusual decrease of bottom NH4-N during the fall months. This might be related to the mixing of bottom water with surface water during fall turnover. Both surface and bottom Ox-N concentrations are increased by 43.3% and 34.0% respectively due to the increase of external loads. The increased bottom Ox-N would play an important role in preventing OP and metal releases from the sediment. As expected, future land use development would play an important role in the nutrient enrichment and eutrophication in the Reservoir.

5.5 *Conclusions*

A complex linked model, using six applications of HSPF and two of CE-QUAL-W2, was applied to simulate the transport and fate of soluble inorganic nitrogen species in the Occoquan Watershed. The linked model not only successfully simulated the detachment and transport of the inorganic nitrogen in the watershed, but also captured the temporal and spatial variations in the waterbodies, both for the calibration and validation periods.

There were several noteworthy features of this model application. One was the application of the linked water quality models. By linking the watershed model HSPF with the reservoir model CE-QUAL-W2, the resultant complex linked model provides a direct linkage between upstream activities and downstream water quality. Although the linked model requires extra effort for development and application, it has a great advantage when investigating the responses of water quality to alternative land use development plans. Many modeling studies have been implemented for similar purposes, especially for TMDL programs. The projected nutrient reduction scenarios were developed by arbitrarily reducing the inflow nutrient concentrations. However, both land use development and BMP implementation would very likely change both flow rates and nutrient concentrations. A simple change in nutrient concentrations would not fully predict the impact of these activities. In addition, it does not answer the question as to how to achieve these reductions and thus would be difficult to use to propose the management plans to meet the TMDL goals. These problems could be solved by using a linked water quality model approach described above. The scenarios of various land use

proposals, BMP implementation, and point source management could be incorporated into HSPF applications. Therefore, by using the boundary conditions provided by HSPF, W2 can predict the water quality variations corresponding with alternative scenarios. This approach provides decision makers a straightforward approach to assess the impact of point and nonpoint sources on the downstream water quality.

The results from the model application indicate the increases of ammonium nitrogen and oxidized nitrogen loads due to future urban expansion, which leads to nutrient enrichment and enhanced algae activity in the Reservoir. The nitrate-rich effluent from UOSA accounts for a significant portion of oxidized nitrogen loads into the Reservoir and thus poses an important role in the management of the Watershed. In this model application, the contribution from UOSA is assumed to be unchanged in the Future scenario so that the impact of land use changes will not be masked. However, due to the significance of this point source, future work that includes an expanded UOSA scenario will provide a more realistic prediction of water quality changes in the receiving waterbody due to human activities.

5.6 *References*

40.C.F.R.§130.7. Total Maximum Daily Loads (TMDL) and Individual Water Quality-Based Effluent Limitations. *Federal Register*, **40. C.F.R.**(§130.7).

Bicknell, B.R., Imhoff, J.C., Kittle, J.L., Jobes, T.H. and Donigian, A.S. (2001). *Hydrological Simulation Program-Fortran HSPF Version 12 User's Manual*, U.S. Environmental Protection Agency, National Exposure Research Laboratory, Athens, Georgia.

Borsuk, K.E., Stow, C.A. and Reckhow, K.H. (2003). Integrated Approach to Total Maximum Daily Load Development for Neuse River Estuary using Bayesian Probability Network Model (Neu-BERN). *Journal of Water Resources Planning and Management*, **129**(4), 271-282.

Bowen, J.D. and Hieronymus, J.W. (2003). A CE-QUAL-W2 Model of Neuse Estuary for Total Maximum Daily Load Development. *Journal of Water Resources Planning and Management*, **129**(4), 283-294.

Chen, Y.D., Carsel, R.F., McCutcheon, S.C. and Nutter, W.L. (1998). Stream Temperature Simulation of Forested Riparian Areas: I. Watershed-Scale Model Development. *Journal of Environmental Engineering*, **124**(4), 304-315.

Cole, T. M. and Wells, S. A. (2003). *CE-QUAL-W2: A Two-Dimensional Laterally Averaged, Hydrodynamic and Water Quality Model, Version 3.2 User Manual*. U.S. Army Corps of Engineers, Washington, D.C.

DePinto, J.V., Freedman, P.L., Dilks, D.M. and Larson, W.M. (2004). Models Quantify the Total Maximum Daily Load Process. *Journal of Environmental Engineering*, **130**(6), 703-713.

Donigian, A.S. (2002). Watershed Model Calibration and Validation: The HSPF Experience. *National TMDL Science and Policy Specialty Conference 2002*, Phoenix, Arizona.

Donigian, A.S. and Crawford, N.H. (1976). *Modeling Nonpoint Pollution from the Land Surface*. U.S. Environmental Protection Agency, Environmental Research Laboratory, Athens, Georgia.

Eggink, J. (2001). *An Exploration of the Limnological Dynamics of Lake Manassas*, Master's Thesis, Virginia Polytechnic Institute and State University, Falls Church, Virginia.

Imteaz, M.A., Asaeda, T. and Lockington, D.A. (2003). Modelling the Effects of Inflow Parameters on Lake Water Quality. *Environmental Modeling and Assessment*, **8**, 63-70.

Jayakrishnan, R., Srinivasan, R., Santhi, C. and Arnold, J. G. (2005). Advances in the Application of the SWAT Model for Water Resources Management. *Hydrological Processes*, **19**(3), 749-762.

Longabucco, P. and Rafferty, M.R. (1998). Analysis of Material Loading to Cannonsville Reservoir: Advantage of Event-Based Sampling. *Lake and Reservoir Management* **14**(2-3), 197-212.

McIsaac, G.F., David, M.B., Gertner, G.Z. and Goolsby, D.A. (2002). Relating Net Nitrogen Input in the Mississippi River Basin to Nitrate Flux in the Lower Mississippi River: A Comparison of Approaches. *Journal of Environmental Quality*, **31**, 1610-1622.

McMahon, C., Alexander, R.B. and Qian, S. (2003). Support of Total Maximum Daily Load Programs Using Spatially Referenced Regression Models. *Journal of Water Resources Planning and Management*, **129**(4), 315-329.

Merrill, L., Henry, T., Golliday, G., Pollison, D., Greene, R., Mirsajadi, H., Goman, W. and Morton, M. (2002). Nutrient and Dissolved Oxygen TMDL for Christina River

Basin. *Watershed 2002: WEF Specialty Conference Proceedings*, Fort Lauderdale, Florida.

Neitsch, S.L., Arnold, J.R., Kiniry, J.R., Williams, J.R. and King, W.K. (2002). *Soil and Water Assessment Tool Theoretical Documentation Version 2000*. Texas Water Resources Institute, College Station, Texas.

Occoquan Watershed Monitoring Laboratory. (1998). *An Updated Water Quality Assessment for the Occoquan Reservoir and Tributary Watershed: 1973-1997*. Manassas, Virginia.

Randall, C.W. and Grizzard, T.J. (1995). Management of the Occoquan River Basin: A 20-Year Case History. *Water Science and Technology*, **32**(5-6), 235-243.

U.S. Environmental Protection Agency. (1983). Methods for Chemical Analysis of Water and Wastes. U.S. Environmental Protection Agency, Cincinnati, Ohio.

U.S. Environmental Protection Agency. (2002). *National Water Quality Inventory 2000 Report*. *EPA-841-R-02-001*, Washington, D.C.

Wetzel, R.G. (2001). *Limnology: Lake and River Ecosystems*, Third Edition. Academic Press, San Diego, California.

Xu, Z., Godrej, A.N. and Grizzard, T.J. (2006). The Hydrological Calibration of a Linked Watershed-Reservoir Model for the Occoquan Watershed, Virginia. *In Preparation*.

Chapter 6. Modeling Phosphorus Transport and the Impact of Land Use Changes on Receiving Water Quality in the Occoquan Watershed by Using a Linked Model Application

6.1 *Summary*

The Occoquan Watershed is a 1,515 km^2 basin located in northern Virginia and contains two principal waterbodies: the Occoquan Reservoir and Lake Manassas. Both waterbodies are principal water supplies for local residents and experience eutrophication and summer algae growth. They are continuously threatened by new development from the rapid expansion of the greater Washington D.C. region. A complex linked model, which consists of six HSPF and two CE-QUAL-W2 submodels, was developed to simulate the hydrology and water quality activities in the watershed and to evaluate the impact of land use development on the water quality of the drinking water sources. This paper describes the application of the linked model to simulate phosphorus transport and fate in the watershed and reservoirs. The models were calibrated for a three-year simulation period and validated for a two-year period based on more than 8,000 field measurements. The results show that a successful calibration can be achieved using the linked approach, with moderate additional effort. The percentage difference (PD) values for three-year total loads ranged from –12.62% to –2.13% for four principal monitoring stream stations. The differences of surface orthophosphate phosphorus (OP) concentrations at various in-lake stations were 1 μg/L or less for Lake Manassas and 7 μg/L for Occoquan Reservoir. The model was adequately validated to capture the nutrient load production for drainage areas and the temporal distribution in the waterbodies. The advantage of the linked modeling approach is to represent the watershed and downstream waterbodies as a coupled system, instead of treating them as independent compartments. This allows integrating upstream activities to downstream water quality. Two land use scenarios were developed to evaluate impacts of land development on water quality. The results confirm the degradation of water quality due to urbanization and the increase of external OP loads due to future land development could result in a 65.0% increase of OP concentrations in the flow over the Occoquan Reservoir

dam. It also suggests a potential threshold of phosphorus loading production despite future land development.

6.2 *Introduction*

Phosphorus (P) is an essential nutrient for crops and aquatic organisms. However, excess amounts of phosphorus in lakes and reservoirs can enhance the nutrient status of waterbodies and trigger the undesired growth of algae and aquatic weeds, which eventually lead to dissolved oxygen depletion and fish kills (Wetzel 2001). For example, large amounts of P loads entering into the Chesapeake Bay play a significant role on eutrophication, oxygen depletion and increasing biomass production in the Bay (Boesch, et al. 2000) and a phosphorus load reduction program has been implemented. The improvement of water quality in the Bay will benefit boating, fishing and beach visiting (Morgan and Owens 2001).

Because of the potential impact on ecological systems, many researchers focus on aquatic P cycling processes, such as biological uptake, sediment release, adsorption and desorption, and release from organic matter. P is chemically reactive and the dynamics of P transport and fate within aquatic systems are complex, thus water quality models have been widely used to quantify the key processes as well as the impact on eutrophication (Chen, et al. 2002; Mostaghimi, et al. 1997; Wade, et al. 2001). The external nutrient loads from point and/or nonpoint sources are fed into these models as boundary conditions. However, those data are normally not monitored at a frequency to provide a sufficient description of driving forces. Moreover, diffuse pollution, a major contributor of excess P loadings to receiving waterbodies, is hard to quantify by using traditional engineering techniques. Thus both physical-based and empirical-based nonpoint source pollution models have been used to assess the temporal change of external P loadings to reservoirs and lakes. Some studies developed empirical relationships between P loads and sediment yield based on local physical characteristics and concerns (Garnier, et al. 2005; Jordan, et al. 2001). Others applied state-of-the-art models to estimate external P loads and linked them to receiving water quality models. For example, a watershed-scale model, Agricultural Nonpoint Source (AGNPS), has been applied to estimate nonpoint

source pollution loads, which were inputs to reservoir water quality models (Kao, et al. 1998; Mankin, et al. 2003; Martin and McCutcheon 1999; Young, et al. 1990). Although the model is capable of estimating external loads carried by runoff, it is a single-event model and thus does not account for base-flow yields.

On the other hand, watershed models have been applied to estimate the external P sources as well as their potential impact on ecological systems (Chun, et al. 2001; Francos, et al. 2001; Gassman, et al. 2002; Whittaker 2005). However, many of them have insufficient description of physical characteristics of receiving waterbodies as well as associated processes. For example, although Hydrological Simulation Program–Fortran (HSPF) contains several different routines to simulate soluble inorganic P in reaches, it assumes streams and reservoirs to be well mixed (Bicknell, et al. 2001). Thus, it cannot fully represent the spatial distribution of P due to phytoplankton accumulation in the epilimnion and sediment release due to oxygen depletion in the hypolimnion. Soil and Water Assessment Tool (SWAT) makes a similar assumption for reservoirs. In addition, it assumes no transformation or degradation of nutrients in channels (Neitsch, et al. 2002). Thus important processes associated with internal P loads are not fully addressed.

These common modeling limitations can be overcome by linking state-of-the-art watershed models to receiving water quality models. This approach provides a more accurate representation of the real world and allows integration of downstream water quality to upstream land activities. Thus the temporal and spatial changes of P loads due to land development and the resultant ecological impact on lakes and reservoirs can be investigated. However, due to insufficient data availability and the complications involved with linking two or more state-of-the-art models, few studies have adopted this approach.

In this research, six HSPF and two CE-QUAL-W2 (W2) applications were linked to simulate the Occoquan Watershed as well as its receiving waterbodies: Occoquan Reservoir and Lake Manassas. While the objectives of the research are broader, the main objectives of this paper are to 1) provide good spatial and temporal estimation of orthophosphate phosphorus (OP) loads generated from land areas; 2) provide a good

calibration of OP concentrations in the streams; 3) capture the temporal and spatial distribution of OP in the major waterbodies; 4) evaluate the impacts of alternative land use scenarios on OP loadings and water quality in the Occoquan Reservoir. The initial calibration of the linked model is for the years 1993-95, with a validation period of 1996-97; a total five-year period spanning a land-use data update issued in 1995. The years 1993, 1994 and 1996 had annual precipitation of 106.7 cm, 107.8 cm, 114.5 cm respectively, and are considered to be average-to-somewhat-wet years based on a 51-year average of 101.3 cm. The years 1995 and 1997 were dry years with total rainfalls of 85.9 cm and 77.5 cm respectively. A previous paper described the results obtained from a hydrologic analysis (Xu, et al. 2006). Other accompanying papers will provide results on dissolved oxygen, temperature, inorganic nitrogen, algae, and other water quality components in the watershed and the major waterbodies.

6.2.1 Study Area

The Occoquan Watershed (Watershed) is a 1,515 km^2 basin in northern Virginia (Figure 6-1). It contains three major tributaries: Cedar Run, Broad Run and Bull Run, and two major waterbodies: Occoquan Reservoir (Reservoir) and Lake Manassas (Lake). The Reservoir is part of the drinking water supply for 1.2 million northern Virginia residents and is a major recreation site. It receives flows from two principal tributaries: Occoquan River and Bull Run. The Upper Occoquan Sewage Authority (UOSA) water reclamation facility discharge to Bull Run is cooler than the water in the Reservoir during the warmer months, and is rich in nitrate-nitrogen. Thus, when this stream reaches the main body of the Reservoir, the nitrate-rich water flows toward the bottom due to density differences. This has a significant impact on water quality in the Reservoir and is an important component of the management of the Reservoir (Randall and Grizzard 1995). Flows over the Occoquan dam drain into the Potomac River after running approximately 8 km southeast. The total capacity of the Reservoir is 31.4×10^6 m^3 and the safe yield is 2.5×10^5 m^3/d (which includes the discharge from UOSA) (OWML 1998). The surface area at the maximum elevation of 36.6 m above mean sea level is 616 hectare. The average depth of the Reservoir is 5.1 m with a maximum depth of approximately 20.0 m near the dam. The average residence time is 19.6 days. Based on Wetzel's (2001)

classification of trophic status of lakes, the Reservoir is mesoeutrophic with the limiting factor being OP (Randall and Grizzard 1995). Copper compounds are used to control algae growth during summer months.

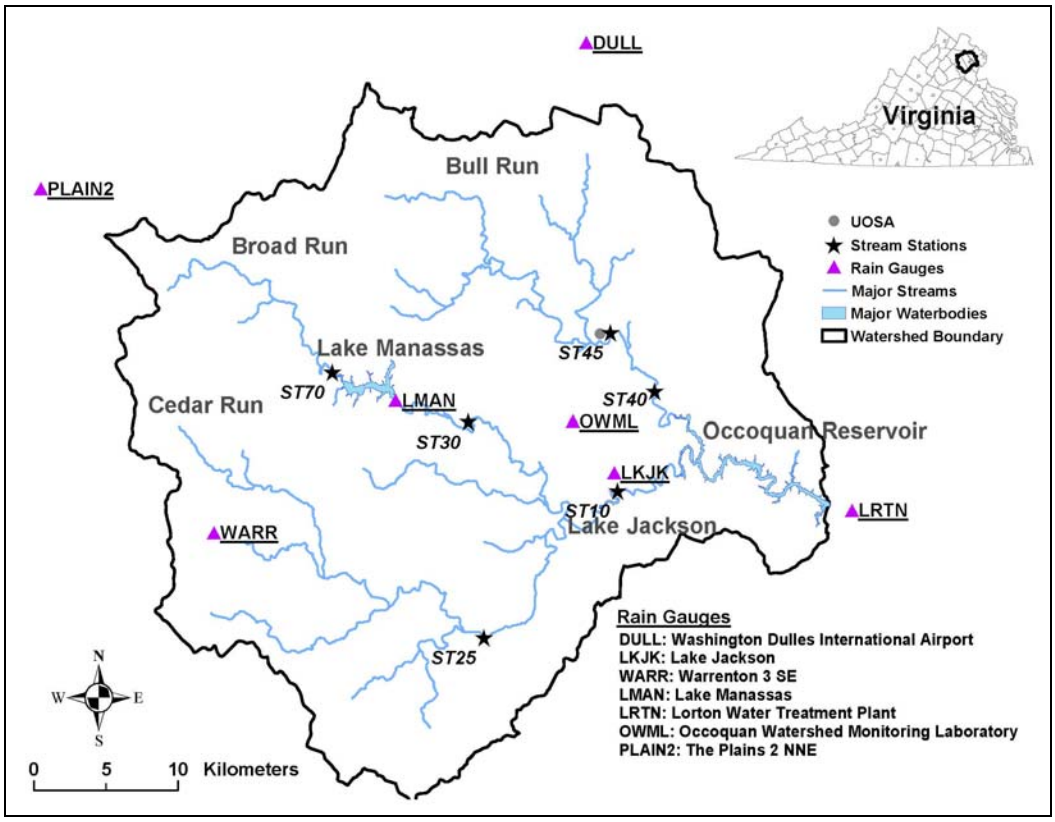

Figure 6-1: Location of Occoquan Watershed in Virginia, USA, Showing Main Tributaries, Main waterbodies, Stream Stations and Rain Stations Used in This Study

Lake Manassas is another major waterbody in the Watershed (Figure 6-1). It serves as the principal drinking water supply for the City of Manassas as well as for recreational purposes. Its total drainage area is approximately 189 km^2. Three golf courses are located on the north shore (Robert Trent Jones, Virginia Oaks, and Par 3). The City of Manassas withdraws water from three water intakes at the dam (primarily the top intake) for municipal service. During dry periods, the golf courses withdraw water from the surface. The natural storage capacity of the Lake is 15.4×10^6 m^3 and the safe yield is 6.37×10^4 m^3/d. The surface area at the maximum elevation of 86.9 m above mean sea level is 282 hectare. The average depth is 5.5 m with a maximum depth of approximately 15.0 m near the dam. Lake Manassas is classified as an eutrophic waterbody and the limiting nutrient is phosphorus (Eggink 2001). It has high biological productivity and

copper compounds were applied for at least fourteen years (1982~1995), typically four times a year.

6.3 *Model Description*

HSPF divides simulated watersheds into three blocks and simulates processes occurring in: (1) pervious land areas (PERLND); (2) impervious land areas (IMPLND); and (3) well-mixed streams and reservoirs (RCHRES) (Bicknell, et al. 2001). It provides two methods to estimate nutrient loads in pervious land segments. The total P loads in runoff are then the summation of loads from surface runoff, interflow and groundwater. One method assumes simple relationships with surface runoff and/or sediment yield. An empirical factor, called washoff potency factor (POTFW), is used to relate the nutrient yield to sediment removal. When P yields from land surfaces are assumed to be a function of water flow and storage quantity, two types of weather conditions are addressed. During dry periods, HSPF assumes a linear relationship of P storage with a user-specified accumulation rate (ACQOP) and maximum storage capacity (SQOLIM). The P removal during wet periods is simulated based on an exponential function, where a user-defined parameter called WSQOP is used to relate the washoff rate to the surface runoff rate. P fluxes in interflow and active groundwater are estimated by multiplying flow rates by user-specified nutrient concentrations. The other method of estimating P loads is under the PHOS section, which simulates transformation and movement between inorganic and organic P in different soil layers. Processes important to agricultural fields include plant uptake, immobilization, mineralization, and adsorption/desorption. Although the latter method provides a more process-oriented approach to simulate P cycling, it is suitable for agricultural areas where corresponding monitoring data are available. In this model application, the former method is used. The approach for P fluxes from impervious land areas (under the IMPLND module) is similar to the simple method used in PERLND, where simple relationships with flow and sediment yield are used. The contributions from wet and dry atmospheric deposition are supplied as monthly fluxes for the entire studied watershed.

After the P fluxes are transported from pervious and impervious lands to the aquatic systems, several physical and biochemical processes take place under the RCHRES module to simulate transformation of inorganic and organic P species in well-mixed streams and reservoirs. These include advection, benthal release, decay of organic matter, adsorption and desorption to inorganic sediment, deposition and scour of adsorbed phosphorus, and mineralization. In addition, processes related to consumption by plankton and benthic algae are addressed in separate modules.

W2, a two-dimensional hydrodynamic and water quality model (Cole and Wells 2003), provides a detailed description of algae/nutrient/dissolved oxygen dynamics in long and narrow waterbodies, such as lakes and reservoirs. The simulated variables include temperature, dissolved oxygen, ammonium, nitrate+nitrite, OP, biological oxygen demand, organic matter, and algae. The processes that affect sinks and sources of OP include growth and respiration of algae, anaerobic release from the sediment, decay of organic matter, adsorption, and settling. Detailed descriptions of both models can be found elsewhere (Bicknell, et al. 2001; Chen, et al. 1998b; Cole and Wells 2003; Donigian and Crawford 1976).

6.3.1 Linked Model Approach

The Occoquan model is a complex linked model application, which includes six HSPF and two W2 submodels. The schema of the linked model approach, as well as the watershed segmentation, is shown in Figure 6-2. The Watershed is divided into six subbasins, with a total of 56 land (HSPF) segments. The average segment size is 27.0 km^2.

The bathymetries of the Lake and the Reservoir are shown in Figure 6-3. For modeling purposes, the Lake is divided into four branches and has a total of 29 active computational segments with lengths ranging from 173 m to 568 m. There are 4 to 28 computational layers, each 0.5 m thick. The Reservoir is also divided into four branches with a total of 69 computational segments. The average segment length is 583 m, with a minimum of 74 m (Segment 32, at Ryan's Dam, a submerged feature with a narrow vertical opening) and a maximum of 838 m. There are from 1 to 39 computational layers,

each 0.5 m thick. A detailed description of model development, watershed segmentation, and waterbody segmentation can be found elsewhere (Xu, et al. 2006).

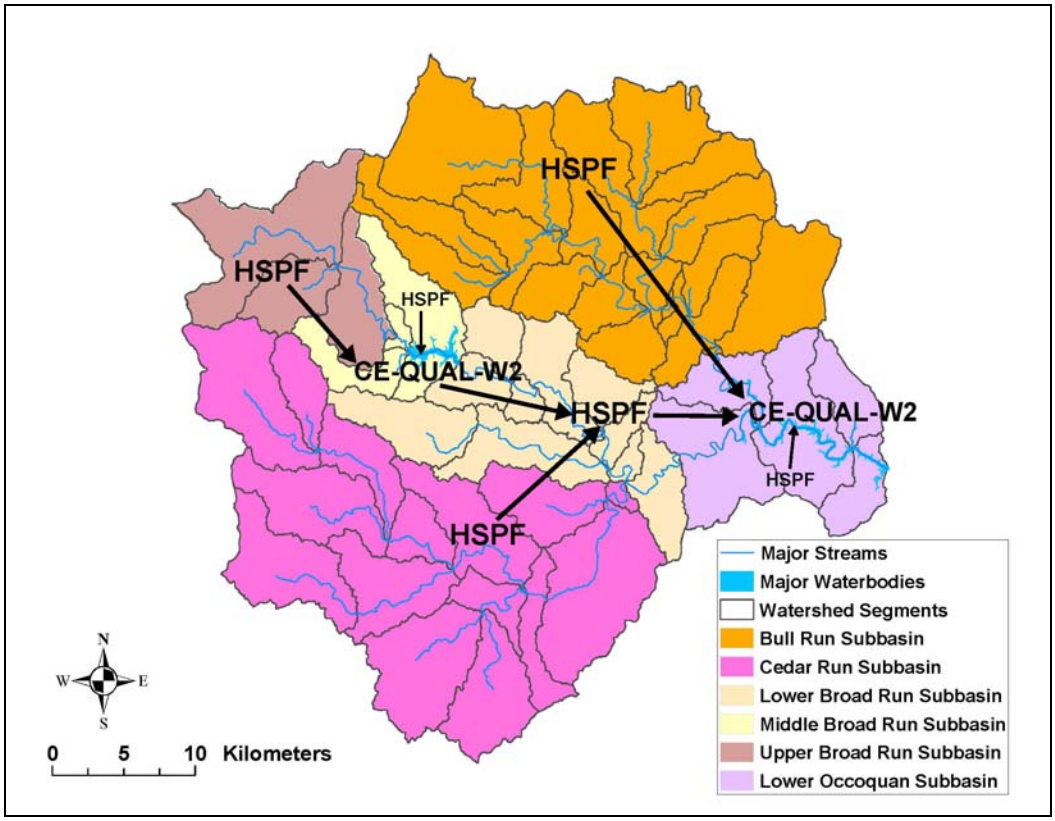

Figure 6-2: Occoquan Watershed Model Application Schema and Watershed Segmentation

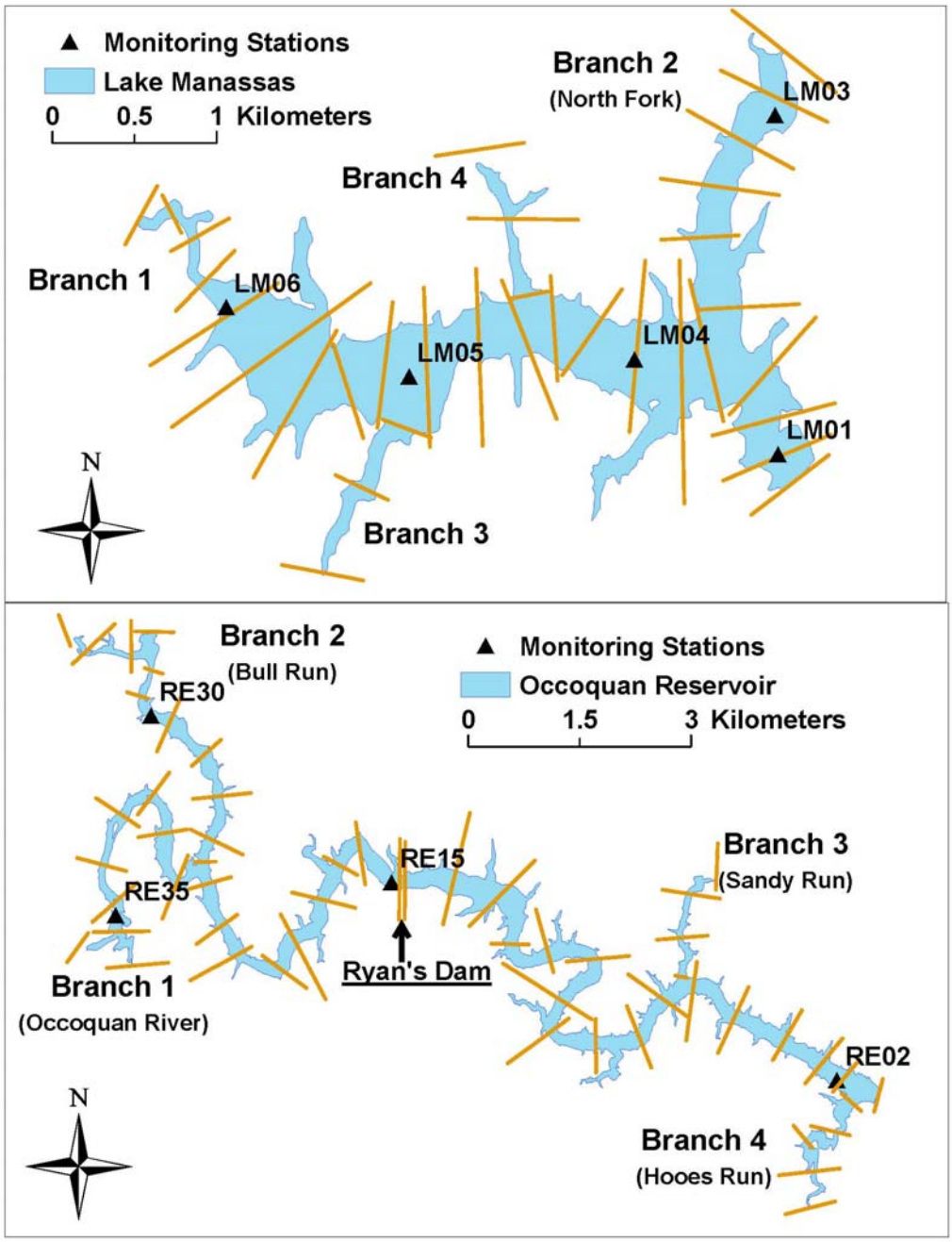

Figure 6-3: Segmentation of Lake Manassas and Occoquan Reservoir and Selected Monitoring Stations

6.3.2 Boundary Conditions

In this model application, the boundary conditions required by W2, such as inflows, temperature and water quality data, are provided by upstream HSPF submodels. For example, in the Lake W2 submodel, the Upper Broad Run HSPF submodel not only provides daily time series inputs of direct inflows, but also OP concentrations and other water quality components. The ungauged distributed tributary flows along the Lake and associated water quality are estimated by the Middle Broad Run HSPF submodel. The outputs from the Lake W2 submodel serve as inputs for the Lower Broad Run HSPF submodel (Figure 6-2). Similarly, the Lower Broad Run HSPF submodel, including the contribution from the Cedar Run subbasin, provides flows and water quality time-series for the Occoquan River branch of the Reservoir. The input time series of the Bull Run branch are provided by the Bull Run HSPF submodel. The Lower Occoquan HSPF application provides the ungauged distributed tributary flows and associated water quality along the Reservoir. Thus, six HSPF submodels and two W2 submodels are linked to represent hydrology and water quality activities in the Watershed and the two waterbodies.

6.3.3 Initial Conditions

The initial OP concentrations in HSPF submodels were first assigned reasonable values. Then the submodels were run through a one-year simulation. The initial values were then adjusted based on the values at the end of the simulation.

The initial concentrations of OP in W2 applications were set to be the same as the observed values at the very beginning of the simulation period at the stations near the dams.

6.3.4 Monitoring Data

For the stream stations (Figure 6-1), OP data in base flow water quality samples are available on a biweekly basis during the winter season and on a weekly basis during other seasons. Composite flow-weighted storm water quality samples are also collected automatically and analyzed for most storms. However, no automatic sample collection

system was installed at ST10 due to the absence of stream flow measurements during the study period, and, instead of composite flow-weighted samples, grab samples were collected during storm events.

For the Lake and the Reservoir (Figure 6-3) stations, near-surface and near-bottom water quality samples are available on a biweekly basis during the winter season and on a weekly basis during other seasons. Samples for OP were filtered through Whatman 934AH (1.5μm) filters before being analyzed using EPA standard methods (1983).

6.3.5 Calibration Criteria

Because there is no single accepted test to determine whether or not a model is calibrated, both graphical and statistical methods were applied to evaluate model performance. In addition to traditional statistical measures such as mean values and the standard coefficient of determination (R^2), several other statistical methods, such as t-test, were also used.

The percentage difference (PD) between simulated and observed data is defined below:

$$PD = \frac{100 \cdot (Y - X)}{X}\%$$

where X is the observed load or concentration, and Y is the simulated load or concentration. Donigian (2002) suggested a value based on annual comparison in the range of 15-25% for a good water quality/nutrient calibration of HSPF (see Table 3-4).

6.4 *Results and Discussion*

The model results are presented in two sections. The first section describes the capability of the linked model to reproduce water quality conditions in the Watershed by comparing model results with the existing data for calibration (the January 1993 to December 1995 period) and validation (the January 1996 to December 1997 period). The second section describes the results of two land use development scenarios.

6.4.1 Current Case Simulation Results

6.4.1.1 Calibration

The observed daily OP loads used to evaluate model performance are estimated by multiplying flow rates by OP concentrations. Although daily flow rates are automatically recorded at principal stations, daily baseflow concentrations were not available for the three-year simulation period and thus load estimation have to be made when measurements were not taken. Flow-weighted storm samples are automatically collected for most storms. However, there are bound to be some missing flow events due to unexpected situations such as equipment failure. Because the precision of the load estimation depends on the calculation estimates made for the periods without sampling, two empirical methods were developed to estimate loads for baseflow and storm events, respectively. A daily-flow-data integration method (Johnston 2005) was used to fill in missing baseflow concentrations by assuming a linear relationship on the baseflow sampling array. Although this method provides a good estimation of baseflow loads, it only partially incorporates missing stormflow loads by interpolating daily concentration values. To estimate the event mean concentrations (EMCs) for missing storms more accurately, empirical regression relationships between storm flow volumes and EMCs were developed for different time frames (1986~1989, 1990~1994 and 1995~1999). Even though this method provides a reasonable estimation of nutrient loads during storm events, the potential error associated with high flow events could have significant impacts on monthly, even annual, nutrient balances (Longabucco and Rafferty 1998).

The simulated OP loads from HSPF were compared with observed loads of individual storms, aggregated on both a monthly and an annual basis. Figure 6-4 and Table 6-1 provide the comparison of OP loads at principal monitoring sites. The results show good model performance. R^2 values based on monthly loads are 0.520 or greater, except at ST30. Percentage difference (PD) values for three-year totals range from −12.62% to −2.13% for four principal stream monitoring stations. Although HSPF can address manure and fertilizer application under the Special Action block of the HSPF program, this function was not used in this model application due to lack of records on application quantities and rates. This might partially explain the overall under-prediction of

phosphorus loads, especially in those portions of the watershed where the agricultural activities are significant (Cedar Run and Broad Run).

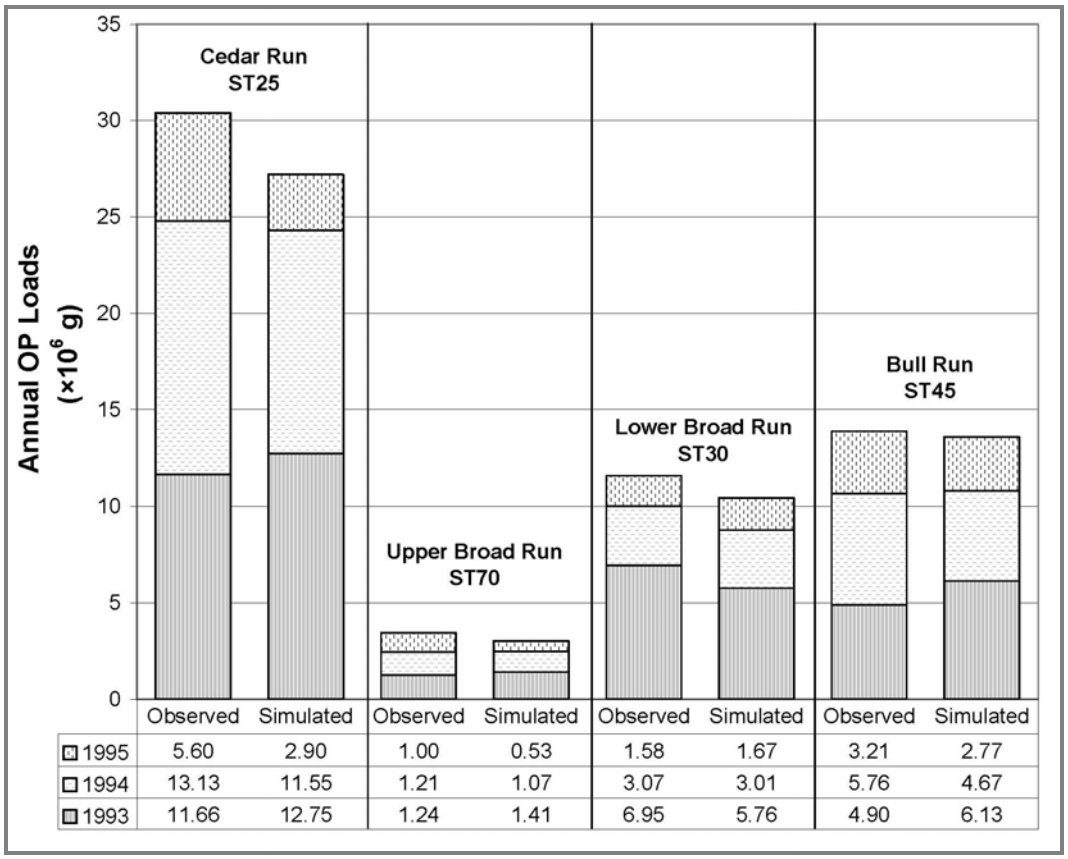

Figure 6-4: Comparison of Annual Orthophosphate Phosphorus Loads at Principal Stream Stations

Table 6-1: Comparison of the Three-Year Total, Annual, and Monthly OP Loads at the Principal Stream Stations in the Watershed

	Percentage Difference for Annual Loads (%)			Total Loads for the Three-Year Simulation Period			Monthly Loads
	1993	1994	1995	Observed ($\times 10^6$ g)	Simulated ($\times 10^6$ g)	PD (%)	R^2
ST25	+9.33	–12.01	–48.25	30.39	27.02	–10.51	0.520
ST70	+13.29	–11.04	–46.73	3.45	3.01	–12.62	0.709
ST30	–17.03	–1.99	–5.44	11.60	10.44	–9.99	0.276
ST45	+25.26	–18.94	–13.72	13.87	13.58	–2.13	0.712

The PD values based on annual OP load analysis range from –18.99% to +25.26%, except at ST25 and ST70 in 1995 (Table 6-1). This is because a few storm samples were unavailable, and the EMCs for those storms were missing. The missing loads were estimated from the method described above which, in this study, used an empirical regression relationship developed for the 1995-1999 period. This might explain the

relatively large PD values at those stations in 1995. However, because 1995 was a dry year and produced less flow volumes, the annual OP loads of 1995 are generally small compared to the other simulation years (Figure 6-4) and thus have limited impact on the three-year totals.

A closer investigation was performed for ST30, the stream station located downstream of the Lake. In terms of model application, it received the Lake outflow provided by the Lake W2 submodel. Therefore, the calibration of OP loads at ST30 not only depends on calibrating the Lower Broad Run HSPF submodel, but also the Lake W2, the Upper Broad Run, and the Middle Broad Run HSPF submodels. The results indicate that even though the OP loads were generally under-predicted, the percentage differences based on annual OP loads were in a reasonable range of –17.03% to –1.99% (Table 6-1). The low R^2 value for monthly loads at ST30 was partially due to missing storm EMCs in May and November 1993. The R^2 value would be improved to 0.602 without the contribution from these months. The good agreement between observed and simulated data at ST30 not only indicates that HSPF submodels were well-calibrated to capture the P transport in those subbasins, but also proves the validity of linking the two different types of models: the watershed model HSPF and the receiving waterbody model W2.

Unlike most HSPF applications, the calibration procedure in this model application focused not only on loads, but also on concentrations. This is because the W2 submodels, which use the output of HSPF submodels as input, perform mass balances based on concentrations. Comparisons of OP concentrations were performed for two stream stations located at the headwaters of the Reservoir, where HSPF submodels were linked to the Reservoir W2 submodel. When compared to observed values from storm samples, the computed concentrations were flow-weighted values based on the simulated values on the day before, day of, and the day after the corresponding storm events. Due to the uncertainty related to meteorological data and the model itself, the timing and duration of a simulated storm might be advanced or delayed by some hours (typically one to three hours), compared to observed data. Therefore, this method was used to diminish the effect of these timing differences.

Because less than ten grab storm samples were collected at ST10 during the three-year study period, they were not included in the analysis (as explained earlier, there was no automated station at this location during the study period).

The results in Table 6-2 indicate that the absolute differences between average simulated and observed OP concentrations were less than 6 μg/L for ST10 (baseflow) and less than 6 μg/L and 1 μg/L for ST40 (baseflow and storms respectively). As expected, both simulated and observed storm data show greater variation than baseflow data. This is because storm flow quality is affected by various factors such as precipitation duration and intensity, surface runoff and land uses. The submodels also demonstrated good performance in capturing the seasonal trends for both base flows and storm flows (Figure 6-5). At ST10, fall and winter season data show relatively large differences in terms of mean values. For ST40, the simulated concentrations, especially those from storm events, showed less spread than the observed concentrations. This is probably due to the flow-weighted calculation method that is likely to reduce the variation in storm concentrations.

Table 6-2: Comparison of OP Baseflow and Stormflow Concentrations at Stream Stations at the Headwaters of the Occoquan Reservoir (ST10 and ST40)

	ST10		ST40			
	Baseflow		Baseflow		Storm Flow	
	Mean	SD*	Mean	SD*	Mean	SD*
Observed (μg/L)	14	11	13	12	32	24
Simulated (μg/L)	20	16	19	7	31	18
Difference (μg/L)	+6	-	+6	-	–1	-

*SD: Standard Deviation

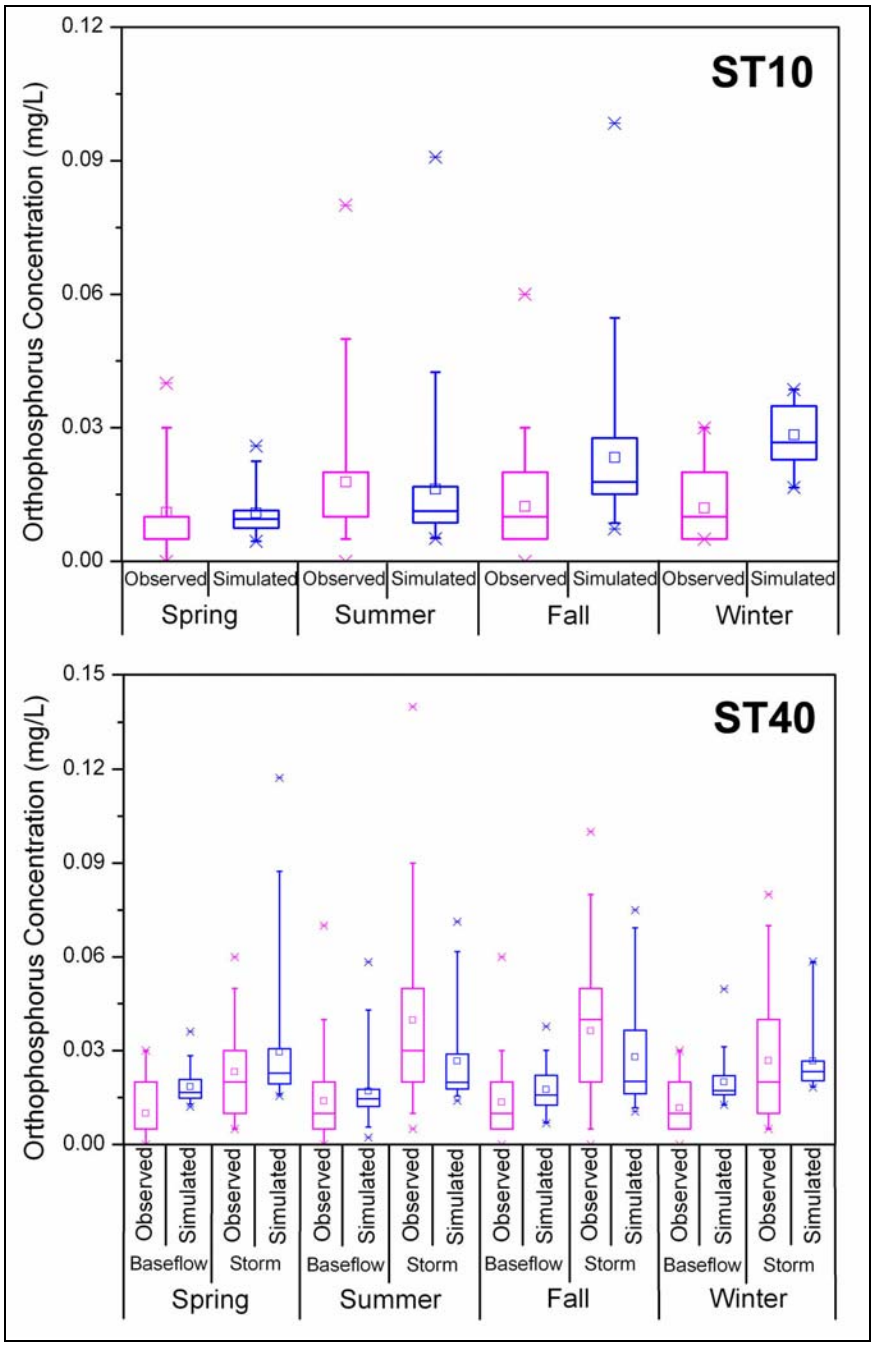

Figure 6-5: Comparison of Orthophosphate Phosphorus Concentrations in Base Flow and Storm Flow Samples at Stations ST10 and ST40

Figures 6-6 and 6-7 show the comparisons of near-surface and near-bottom OP concentrations (three-year average) as a function of distance upstream from the dams of the Lake and the Reservoir, respectively. At the Lake, the near-surface concentrations remain fairly constant along the waterbody and differences between simulated and observed values are less than 1 μg/L. Although the W2 submodel captured the increasing trend of the bottom concentrations, it tended to over-predict them except for the location near the dam. This is probably due to the bottom release under anoxic hypolimnetic conditions especially during summer months. This process is more likely to occur in the lacustrine zones than the riverine zones, but W2 allows only one sediment release rate for each waterbody. This might partially explain the differences at near-bottom layers along the waterbody.

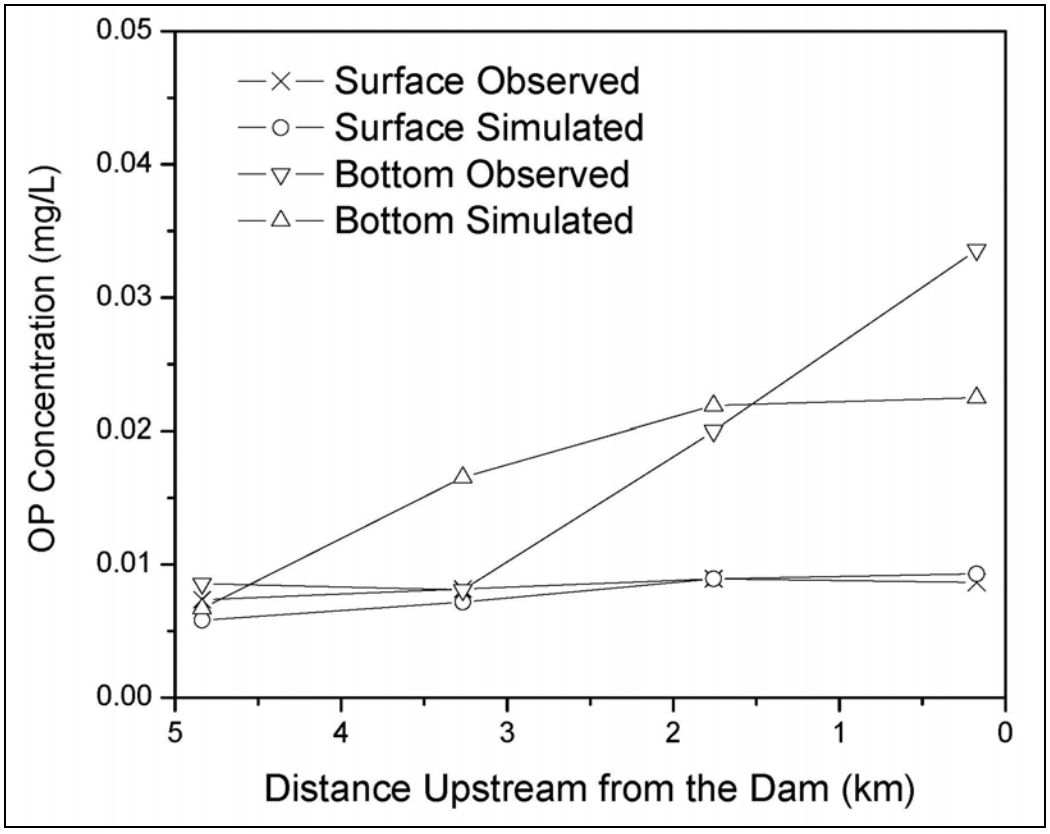

Figure 6-6: Comparison of Spatial Distributions of Orthophosphate Phosphorus along the Mainstem of Lake Manassas

The trend of surface concentrations at the Reservoir is similar to that of the Lake, although the Reservoir W2 submodel tends to over-predict the concentrations by nearly 6 μg/L. As mentioned earlier, the effluent from UOSA is nitrate rich and tends to flow along the bottom due to its cooler temperature and higher density. Therefore, the average bottom nitrate-nitrogen concentrations in the Reservoir are greater than 0.8 mg/L. The nitrate serves as an electron acceptor when oxygen is depleted and thus prevents the OP bottom release from the sediment under anoxic conditions (Randall and Grizzard 1995). However, the current version of W2 (Version 3.2) does not consider nitrate as a secondary oxygen supplement under anoxic conditions and thus will not prevent OP release from sediment even when sufficient nitrate is present. In order to simulate the oxidized sediment condition maintained by nitrate, the OP release rate is set to zero in the Reservoir W2 submodel. Although the near-bottom OP concentrations are still over-predicted in upstream sections of the Reservoir, the general bottom OP concentrations near the dam are reproduced well. The observed non-zero bottom OP concentrations might be related to the activities of benthic organisms (Wetzel 2001).

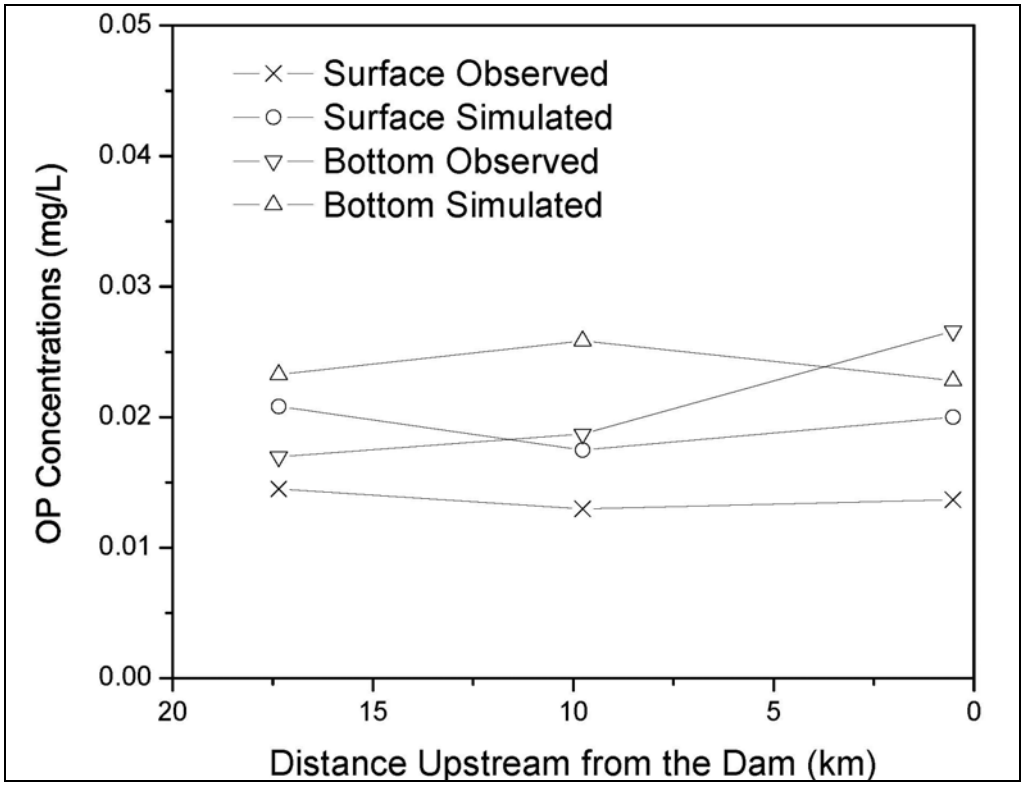

Figure 6-7: Comparison of Spatial Distributions of Orthophosphate Phosphorus along the Mainstem of Occoquan Reservoir

More detailed investigations were performed for stations near the dams (RE02 for the Reservoir and LM01 for the Lake). This is because the surface concentrations at these stations represent the water quality flowing downstream over the dams. In addition, LM01 also provides information on water quality into the water treatment plant of the City of Manassas because the plant withdraws waters primarily from the top intake at the Lake Manassas dam. The results in Table 6-3 indicate small absolute differences between simulated and observed average OP concentrations (≤3 μg/L for the Lake and ≤ 6 μg/L for the Reservoir). It also can be seen that the Reservoir, which has a drainage area ten times that of the Lake, has lower bottom OP concentrations. This confirms the reduced OP sediment release due to the oxidized zone maintained by the nitrate-rich discharge from UOSA.

Table 6-3: Comparison of OP Concentrations at In lake Stations near the Lake Manassas (LM01) and Occoquan Reservoir (RE02) Dams

	LM01			RE02		
	Observed	Simulated	Difference	Observed	Simulated	Difference
Surface (μg/L)	9	9	0	14	20	+6
Bottom (μg/L)	34	31	–3	27	23	–4

Overall, the W2 submodels capture the OP seasonal fluctuation that follows the annual cycle of phytoplankton production: the lowest surface concentrations and highest bottom concentrations found during the summer blooms (Figures 6-8 and 6-9, which includes the 1996-97 validation period). Although the Lake submodels under-predicted some relatively high OP concentrations observed at the bottom, both W2 submodels captured well the timing of bottom release and surface consumption by phytoplankton. The results from paired t-tests (Table 6-4) also indicate that simulated and observed OP concentrations have no significant differences in term of mean values (probability values greater than 0.05). The exception was at the RE02 surface where the probability value is less than 0.05. This is probably due to several extremely high simulated OP concentrations during August 1994, which is possibly related to algae simulation (Figure 6-9). In the current study, only one lumped algae species is modeled in the Reservoir W2 submodel although the observed species count data suggest three dominant algal species (blue green algae, green algae, and diatoms). The prediction of surface OP concentrations might be improved by including multiple algal species in the W2 submodels.

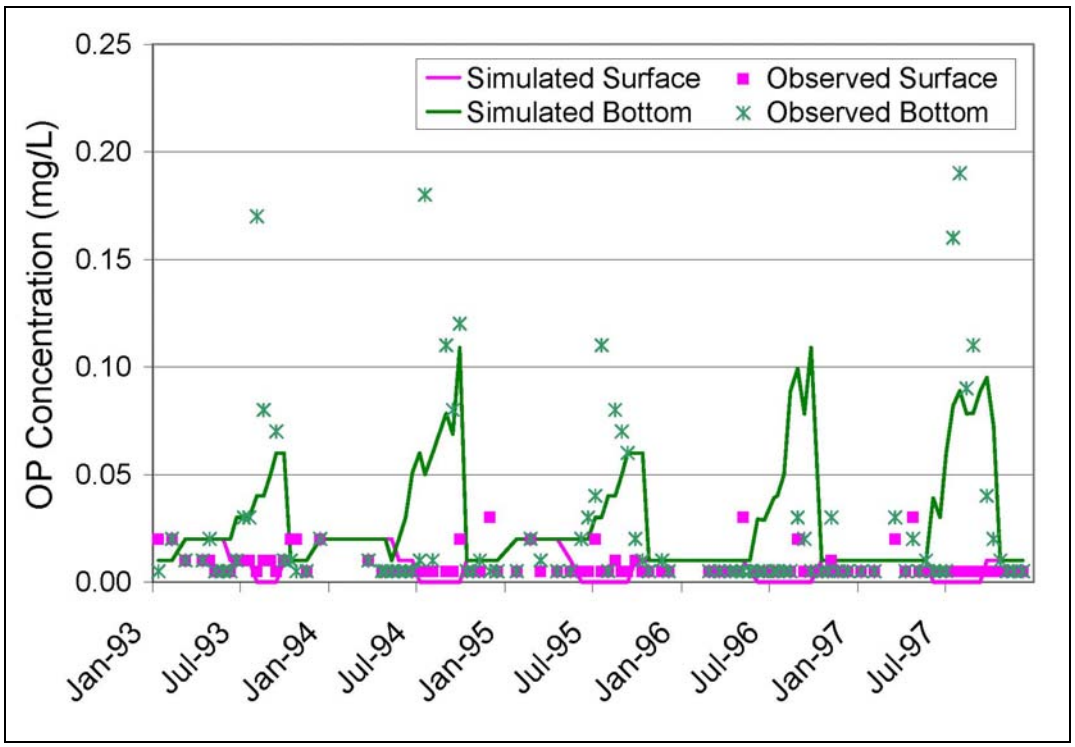

Figure 6-8: Comparison of Temporal Distributions of Orthophosphate Phosphorus at the Stations near the Dams of Lake Manassas for Model Calibration (1993-1995) and Validation (1996-1997)

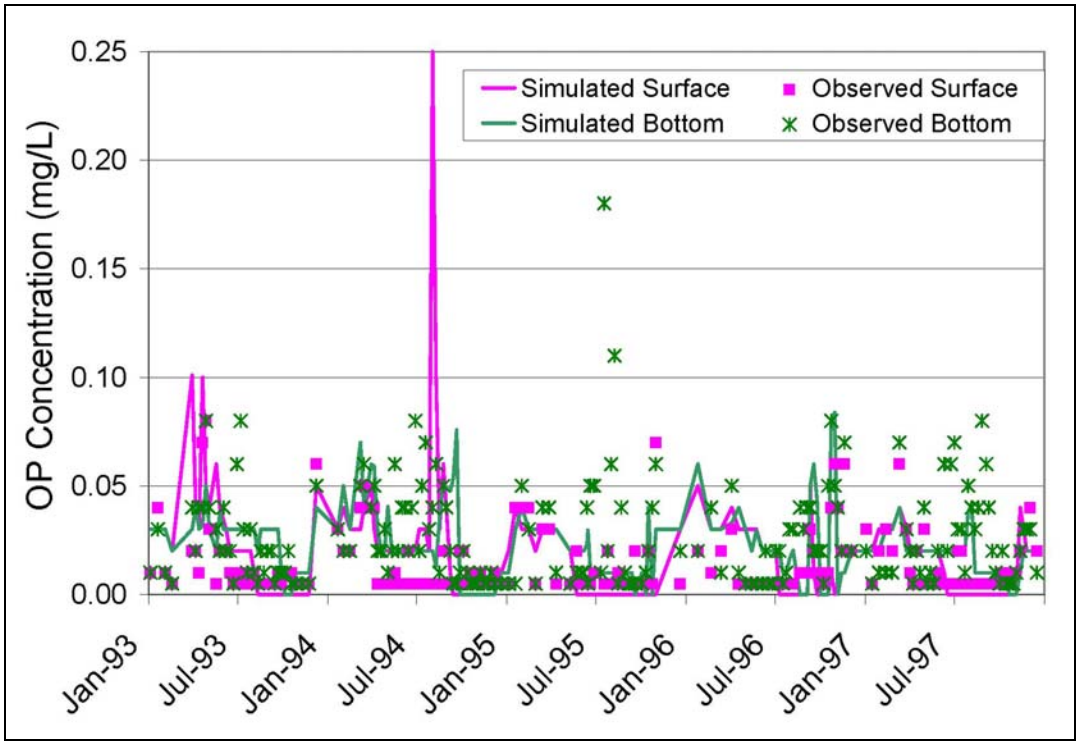

Figure 6-9: Comparison of Temporal Distributions of Orthophosphate Phosphorus at the Stations near the Dams of Occoquan Reservoir for Model Calibration (1993-1995) and Validation (1996-1997)

Table 6-4: Probability Values from t-test Analysis for In-lake Monitoring Stations near the Lake Manassas (LM01) and Occoquan Reservoir (RE02) Dams

		Surface	Bottom
LM01	Number of Samples	56	56
	Probability Value	0.62	0.52
RE02	Number of Samples	109	113
	Probability Value	0.03	0.17

6.4.1.2 Validation

Simulated and observed OP data for the years 1996 and 1997 were used for model validation. Both the calibration and validation periods were combinations of wet and dry years and are considered suitable for model calibration and validation purposes. Nutrient loads and concentrations for these two validation years were simulated using the same land use as for the calibration period (the year 1995), and the 1996 and 1997 meteorological data.

Similar to model calibration, the validation of HSPF submodels were also performed on three levels: annual production, monthly production and individual storms. The results shown here include both calibration and validation periods so that model validation can be seen in context. Figure 6-10 shows the annual OP load for the five-year simulation period, including the two-year validation period. During the validation period, major discrepancies for the nutrient load production mainly occurred in the wet year 1996, where simulated nutrients loads were greatly under-predicted partially due to the difference in hydrologic systems (Xu, et al. 2006). The validation results of the relatively dry year 1997 are better with the percentage differences in the range of –44.1% ~ –6.3% (Table 6-5), which are considered to be "poor" or "very good" simulated, according to the scale used by Donigian (2002) (See Table 3-4). The validation of the HSPF submodels captured the general trend of OP load production from the drainage areas.

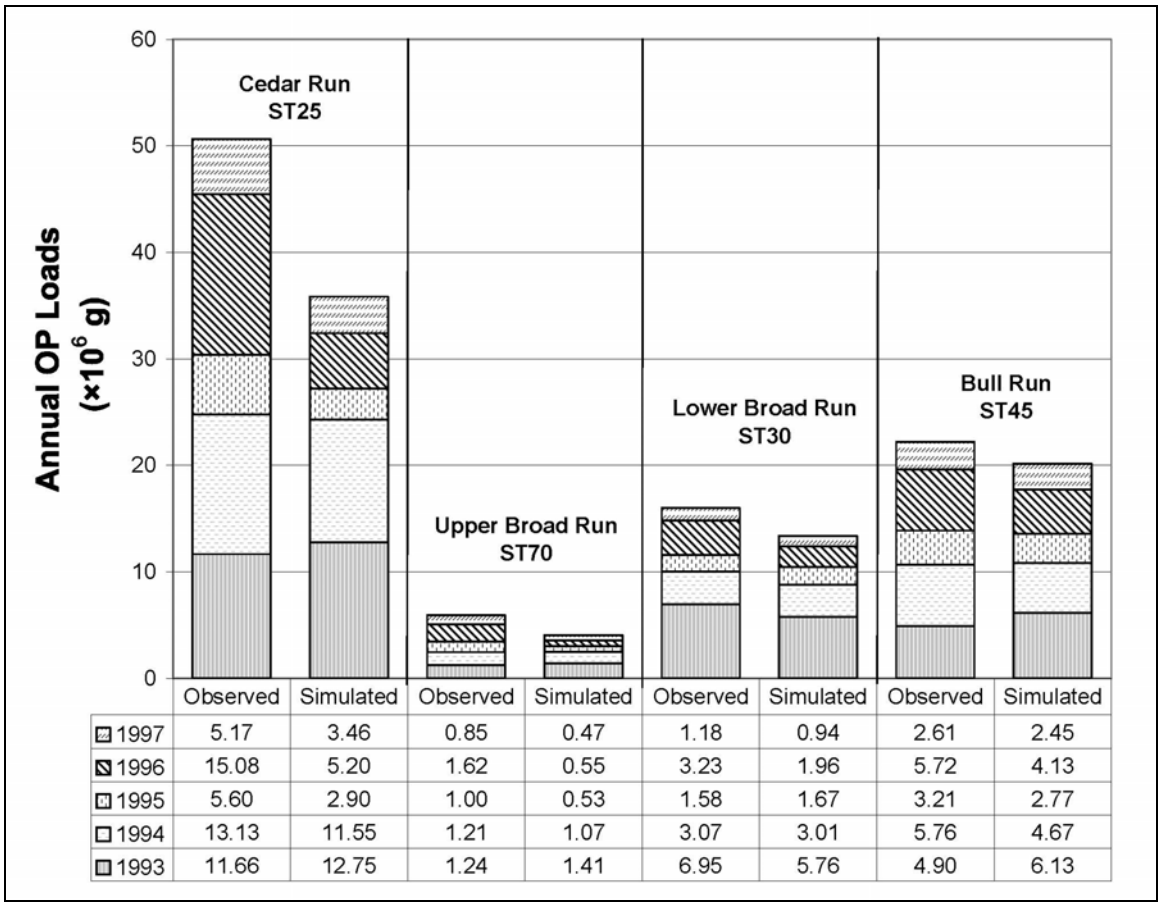

	Observed	Simulated	Observed	Simulated	Observed	Simulated	Observed	Simulated
1997	5.17	3.46	0.85	0.47	1.18	0.94	2.61	2.45
1996	15.08	5.20	1.62	0.55	3.23	1.96	5.72	4.13
1995	5.60	2.90	1.00	0.53	1.58	1.67	3.21	2.77
1994	13.13	11.55	1.21	1.07	3.07	3.01	5.76	4.67
1993	11.66	12.75	1.24	1.41	6.95	5.76	4.90	6.13

Figure 6-10: Comparison of Annual OP Loads at Principal Stream Stations for Model Calibration and Validation

Table 6-5: Comparison of Annual OP Loads at the Principal Stream Stations for Model Validation

		ST25	ST70	ST30	ST45
Calibration	1993	+9.3* Very Good*	+13.3 Very Good	−17.0 Good	+25.3 Fair
	1994	−12.0 Very Good	−11.0 Very Good	−2.0 Very Good	−18.9 Good
	1995	−48.2 Poor	−46.7 Poor	+5.4 Very Good	−13.7 Very Good
Validation	1996	−65.5 Poor	−65.9 Poor	−39.2 Poor	−27.8 Fair
	1997	−33.2 Fair	−44.1 Poor	−20.2 Good	−6.3 Very Good
Summary	1993-1995	−10.5	−12.6	−10.0	−2.1
	1993-1997	−29.2	−31.7	−16.6	−9.2

*Numbers are percent differences from observed data (%), and ratings are as based on Table 3-4.

The monthly load comparisons for the validation years at various stations are added to the calibration data and are shown in Figure 6-11. It can be seen that, although the

discrepancies for the year 1996 was the greatest, the model captured the temporal fluctuation in the validation year 1997.

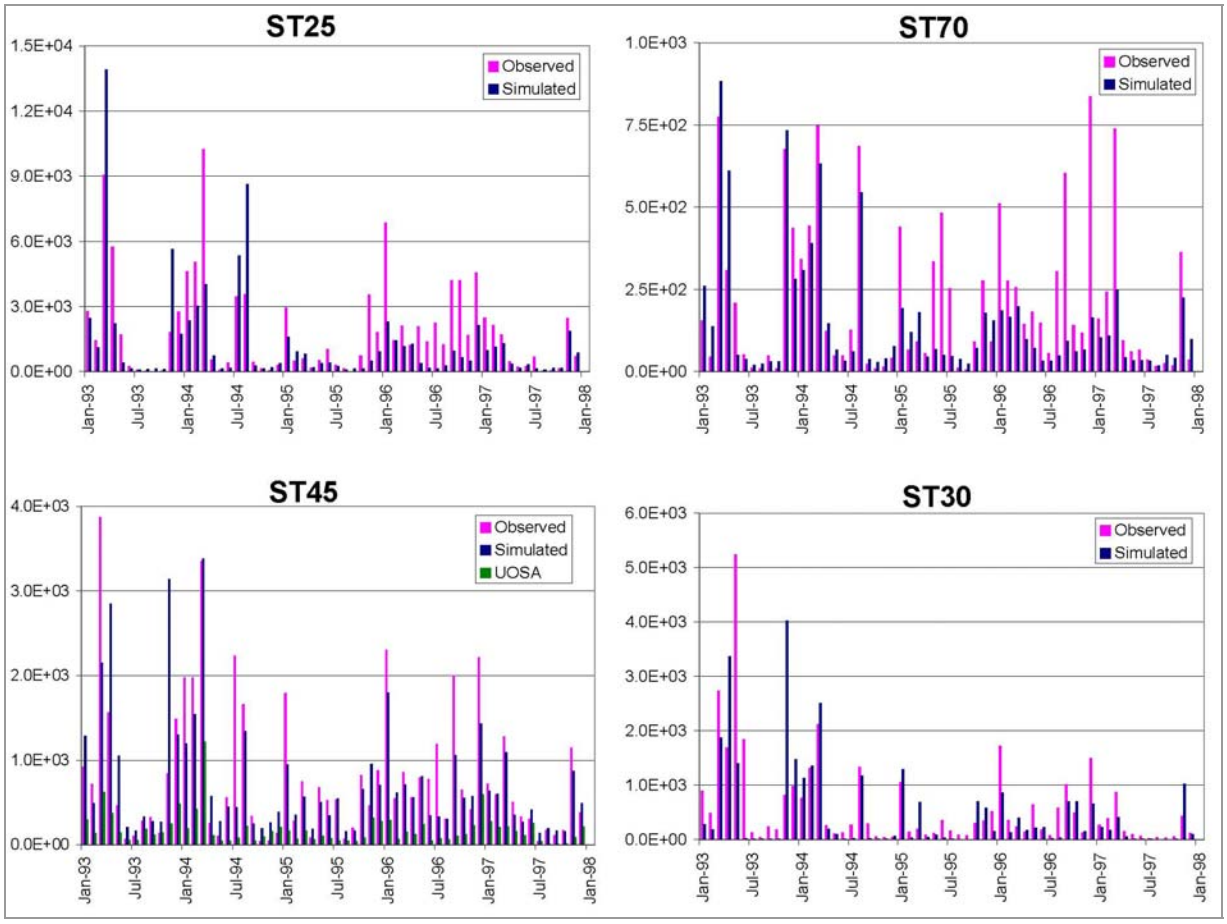

Figure 6-11: Comparisons of Monthly OP Loads (lbs) at Four Principal Stream Stations in the Occoquan Watershed for Model Calibration and Validation

The validation results for stations in the Lake and the Reservoir indicated that the simulated OP concentrations in the surface layers of the waterbodies were similar to their respective observed values (Tables 6-6 and 6-7). The differences ranged from –3 μg/L to –1 μg/L for the Lake and from –2 μg/L to +6 μg/L for the Reservoir. The differences in the bottom layers are relatively large (ranging from –2 μg/L to +8 μg/L for the Lake and from –5 μg/L to +7 μg/L for the Reservoir). The results indicate that the W2 submodels are adequately validated to capture the spatial distribution of OP concentrations.

Table 6-6: Comparison of Surface and Bottom OP Concentration at Monitoring Stations near the Lake Manassas (LM01) Dam for Model Calibration and Validation

		OP Concentrations (µg/L)									
		LM01		LM03		LM04		LM05		LM06	
		Surface	Bottom	Surface	Bottom	Surface	Bottom	Surface	Bottom	Surface	Bottom
Calibration (1993-1995)	Observed	9	34	8	9	9	21	8	8	7	9
	Simulated	9	31	8	13	9	22	7	17	6	7
	Difference	0	–3	0	+4	0	+1	–1	+9	1	–2
Validation (1996-1997)	Observed	7	29	7	8	7	28	8	10	7	8
	Simulated	6	37	5	11	5	27	5	14	6	6
	Difference	–1	+8	–2	+3	–2	–1	–3	+4	–1	–2

Table 6-7: Comparison of Surface and Bottom OP Concentration at Monitoring Stations near the Occoquan Reservoir (RE02) Dam for Model Calibration and Validation

		OP Concentrations (µg/L)							
		RE02		RE15		RE30		RE35	
		Surface	Bottom	Surface	Bottom	Surface	Bottom	Surface	Bottom
Calibration (1993-1995)	Observed	14	27	13	17	13	16	15	17
	Simulated	20	23	18	23	20	27	21	23
	Difference	+6	–4	+5	+6	+7	+11	+6	+6
Validation (1996-1997)	Observed	15	26	14	20	12	14	16	15
	Simulated	13	21	16	21	18	21	19	20
	Difference	–2	–5	+2	+1	+6	+7	+3	+5

The comparisons of surface and bottom OP concentrations at the stations near Lake Manassas and Occoquan Reservoir dams for validation periods are included in Figures 6-8 and 6-9. They indicate that the W2 submodels reproduced the seasonal patterns during the validation period and the lowest surface concentrations and highest bottom concentrations found during the summer blooms. The bottom OP concentrations in the Reservoir are generally less than those in the Lake, which confirms the oxidized sediment zone due to the nitrate-rich effluent from UOSA.

6.4.2 Alternative Land Use Development Scenario Results

Due to the total maximum daily loads (TMDL) program, the impact of land use on water quality has been intensely studied. In most research, when investigating the impact of alternative management plans, nutrient load reduction scenarios are developed by arbitrarily reducing the inflow nutrient concentrations until the TMDL goals are met (Bowen and Hieronymus 2003; Imteaz, et al. 2003). Although this approach does answer the questions on the potential impact of external nutrient load reduction on the aquatic systems, it may not provide a practical guide to implement those load reduction programs, and thus does not fully answer the management questions posed by the TMDL programs. By using the linked model approach described above, a direct cause-effect relationship is developed between upstream activities and downstream water quality. Thus, instead of using arbitrary loading reduction rates, W2 can use the boundary conditions corresponding with these land development scenarios to predict the water quality variation.

In this section, results based on two land use scenarios are presented. The watershed segments, waterbody bathymetries, and all the input parameters, except the land use data, were the same as the current case (calibration). The land use changes developed for the two management scenarios are shown in Table 6-8.

Table 6-8: Percentage of Different Land Use Categories for Various Development Scenarios

	Current			Forest			Future		
	Agriculture	Forest	Urban	Agriculture	Forest	Urban	Agriculture	Forest	Urban
Cedar Run	36.7	56.3	7.1	0.0	100.0	0.0	36.7	28.2	35.3
Broad Run	25.6	58.3	16.1	0.0	100.0	0.0	25.6	29.2	43.3
Bull Run	12.5	54.9	32.6	0.0	100.0	0.0	12.5	28.2	60.1

6.4.2.1 Forest Scenario

One scenario (Forest) was developed wherein all the lands were assumed to be covered by forests. It represents the background condition with no impact from human activities before Colonial history and can be used to evaluate the long-term impact of human activities on the water resources. The contribution of UOSA is eliminated in this scenario. With all the land areas covered by forests, natural processes such as organic matter decay and atmospheric deposition produce OP loads of $3.2\sim7.5\times10^6$ g/year on various subbasins (Table 6-9). As expected, these OP loads from the land segments are much lower than the Current condition and the model output suggests that current human activities have caused a 7.0×10^6 g/year (45.1%) increase of OP loading production compared to the pre-Colonial period.

Table 6-9: Annual OP Loads at Major Subbasins for Various Land Development Scenarios Under 1993-1995 Flow and Weather Conditions

	Annual P loads ($\times10^6$ g)		
	Forest	Current	Future
Cedar Run	7.5	10.4	27.6
Broad Run	3.2	4.0	6.2
Bull Run	5.1	8.4	10.4
Total	15.8	22.8	44.2

Figure 6-12 shows the OP load production under the three different land use scenarios. It is clear that the increase of external OP production is related to population growth and urbanization. However, different subbasins show different increase rates due to site characteristics. The Broad Run subbasin shows the lowest increase in OP yield production (26.5%) since the pre-Colonial period, because Lake Manassas probably traps this nutrient and reduces transport downstream. The Bull Run region shows the greatest increases in P production (67.1%) due to its greater urbanization.

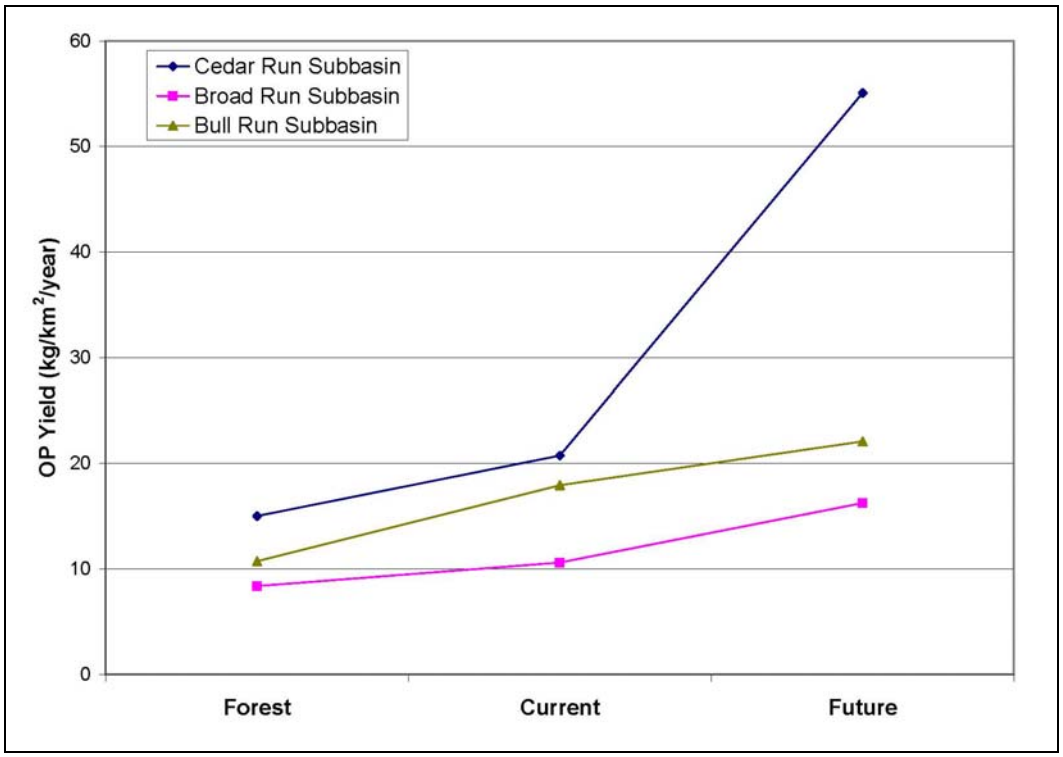

Figure 6-12: Comparison of the Impact of Different Land Development Scenarios on Orthophosphate Phosphorus Load Production

The increases of external OP loads since the pre-Colonial period lead to increases of OP concentrations delivered to the Reservoir. On the other hand, if the land use pattern is restored from the Current scenario to the Forest scenario, the reduced OP loads would reduce the OP concentrations into the Reservoir (Table 6-10). Average concentrations would be decreased by 41.7% and 25.0% for Branches 1 and 2, respectively, compared with the Current scenario.

Table 6-10: Comparison of Inflow OP Concentrations into the Occoquan Reservoir for Various Land Development Scenarios

	Branch 1		Branch 2	
	(μg/L)	PD* (%)	(μg/L)	PD* (%)
Current	24		20	
Forest	14	–41.7	15	–25.0
Future	44	+83.3	22	+10.0

* PD: Percentage Difference from the Current scenario

Although compared with the Current scenario, the external OP loads suggest significant decrease if the land use pattern is restored to the pre-Colonial period, the Reservoir W2 submodel results suggest only slight decreases of average OP concentrations near the dam (2 μg/L or 10.0% for surface and 3 μg/L or11.5% for bottom) (Table 6-11). This is

likely due to the nitrate-rich UOSA discharge that maintains an oxidized sediment zone to prevent bottom phosphorus release. The seasonal patterns of in-lake OP concentrations are shown in Figure 6-13, where spring and winter seasons show relatively greater increases in OP concentrations.

Table 6-11: Comparison of OP Concentrations at the Station near the Occoquan Reservoir Dam (RE02) for Various Land Development Scenarios

	Surface		Bottom	
	(µg/L)	PD* (%)	(µg/L)	PD*(%)
Current	20		26	
Forest	18	–10.0	23	–11.5
Future	33	+65.0	35	+34.6

* PD: Percentage Difference from the Current scenario

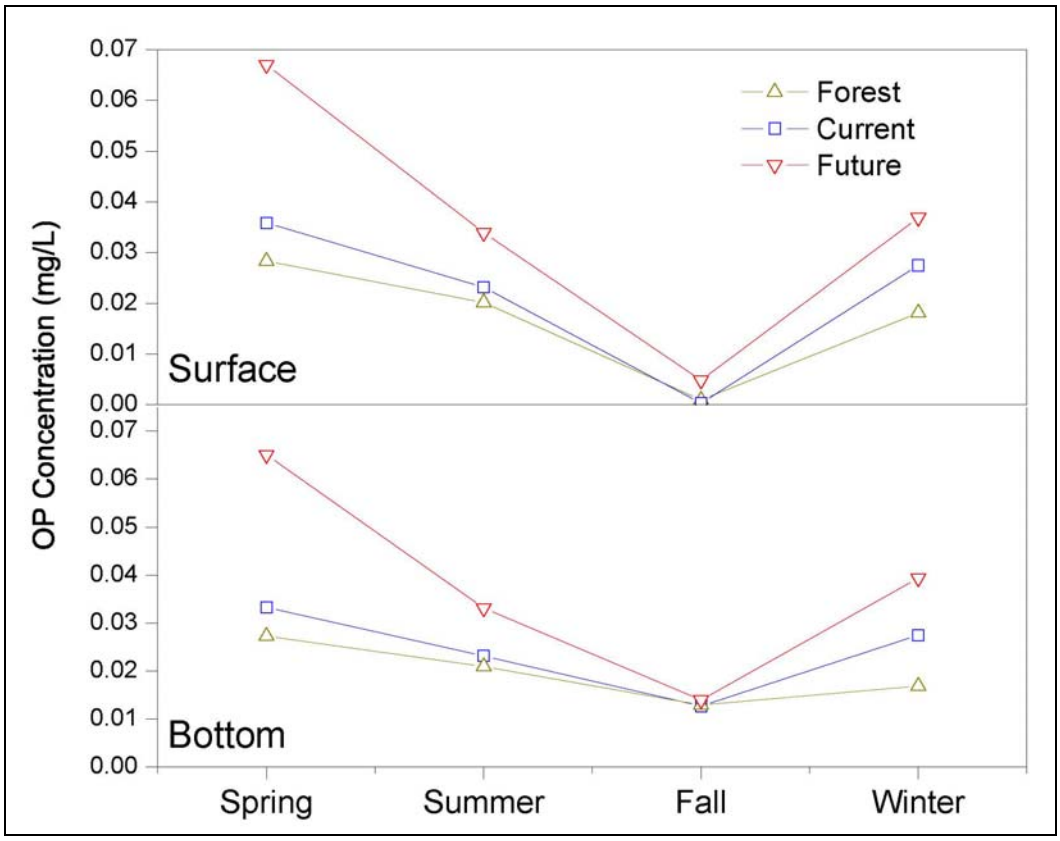

Figure 6-13: Comparison of Impact of Different Land Development Scenarios on Temporal Distributions of Orthophosphate Phosphorus at the Station near the Dam of Occoquan Reservoir

6.4.2.2 Future Scenario

The second scenario (Future) was developed by converting 50% of the existing forested areas in each segment to residential and commercial development. This is based on the rapid urbanization in northern Virginia, which is ranked as one of the fastest-growing

regions in the United States. The region has been, and will very likely continue to be, facing residential and commercial development. This scenario represents the expansion of the current urban lands by about 141.2, 129.2, and 110.4 km^2 in the Cedar Run, Broad Run, and Bull Run subbasins, respectively. Although it is highly possible that UOSA would expand as the population grows, the contribution from UOSA is assumed to be unchanged in this scenario so that the changes of water quality due to land use development would not be masked by other factors.

The results indicate that the projected land use development would double the total OP production to 44.2 $\times 10^6$ g/year, compared to the current condition (Table 6-9). The Cedar Run subbasin shows the greatest increase in OP production (165.5%) (Figure 6-12) because the dominant land use would shift from non-urban development to urban development. The urban land areas in the Cedar Run subbasin would be increased five-fold based on the projected scenario. This results in doubling the OP yield over the Current condition and tripling that over the Colonial period. This suggests that best management practices (BMPs) must be incorporated into the future land use development plans to reduce the dramatic increases of OP production.

On the other hand, the Bull Run subbasin appears to have a slower OP yield increase rate (23.1%), compared with the pre-Colonial period (Figure 6-12). The investigation of land uses in the Bull Run subbasin indicates an existing high urban development with more than 30% of the land categorized as urban. Therefore, future expansion does not result in a significant increase on the already high values of OP load production. This suggests a threshold for OP load production despite land development, and a future study of land development scenarios could provide more insight on this issue.

The dramatic change of the land use pattern in the Cedar Run subbasin due to urban expansion would increase OP concentrations delivered into the Reservoir Branch 1 (Occoquan River) by 83.3% (Table 6-10). At the same time, OP concentrations into Branch 2 (Bull Run) show a 10% increase due to the increase of external OP loads from the Bull Run subbasin. As expected, the increase of external OP loads leads to the accumulation of nutrients in the Reservoir and the model results suggest a 65.0% and

34.6% increase of surface and bottom OP concentrations in the Reservoir, respectively (Table 6-11). The comparison of seasonal patterns (Figure 6-12) indicates that increases of external OP loads have greater impacts on spring and winter OP concentrations than on those of summer and fall. The suggested high OP concentrations during winter and spring months would very likely stimulate algae growth and worsen the water quality issues such as oxygen depletion. Based on the model results, it is clear that the future land use development will play an important role in the nutrient enrichment and eutrophication of the Reservoir.

6.5 *Conclusions*

A complex linked model, using six applications of HSPF and two of CE-QUAL-W2, was applied to simulate the OP transport and fate in the Occoquan Watershed. The procedures and results of the model calibration and validation were described. In addition, two land use scenarios were developed and their impacts on the water quality of the Occoquan Reservoir were investigated.

There were several noteworthy features of this model application. One feature was the linkage of the water quality models. By linking two state-of-the-art water quality models, the modeled system behaves more as a single entity, even though this approach requires extra effort for development and application. The advantage of such an approach is to establish a direct cause-and-effect relationship between upstream activities and downstream water quality, which makes it easier for decision makers to evaluate future land use management plans and for the public to understand the decision making procedures.

The model application successfully captured the temporal and spatial distribution of OP in the watershed and the receiving waterbodies. The percentage difference values for three-year (calibration) OP loads ranged from −12.62% to −2.13%. The differences between simulated and observed OP concentrations are ≤1 μg/L at the outlet of Lake Manassas and ≤7 μg/L for that of the Occoquan Reservoir. The model was adequately validated to capture the transport and fate in the Watershed and two major waterbodies.

Two land use scenarios were developed to evaluate the impact of human activities on the water quality. This type of research has been intensely investigated, especially for TMDL programs. Many researchers focus on the changes in downstream water quality by using assumed nutrient loading reductions. This approach does not answer the question of how to achieve these reductions and thus does not provide full suggestions on regulation of upstream activities and land development. However, this problem can be addressed by linking the watershed model HSPF to the reservoir model CE-QUAL-W2. The scenarios of various levels of land use and BMP implementation could be incorporated into HSPF applications and thus, instead of using assumed loading reduction rates, W2 can use the boundary conditions corresponding with these scenarios to predict the variation in water quality.

The results verify that the increase of external OP loads into the reservoir due to human activities plays an important role in the nutrient enrichment and eutrophication of the Reservoir. The future development in the non-urban areas will greatly increase the external OP production and BMPs should be implemented to prevent potential environmental degradation. For the existing urban areas, the model results suggest a potential threshold of phosphorus loading production despite future land development. However, its impact on the receiving waterbodies might not be negligible and additional controls will probably be required.

6.6 *References*

Bicknell, B.R., Imhoff, J.C., Kittle, J.L., Jobes, T.H. and Donigian, A.S. (2001). *Hydrological Simulation Program-Fortran HSPF Version 12 User's Manual*, U.S. Environmental Protection Agency, National Exposure Research Laboratory, Athens, Georgia.

Boesch, D.F., Brinsfield, R.B. and Magnien, R.E. (2000). Chesapeake Bay Eutrophication: Scientific Understanding, Ecosystem Restoration, and Challenges for Agriculture *Journal of Environmental Quality* **30**, 303-320.

Bowen, J.D. and Hieronymus, J.W. (2003). A CE-QUAL-W2 Model of Neuse Estuary for Total Maximum Daily Load Development. *Journal of Water Resources Planning and Management*, **129**(4), 283-294.

Chen, C., Ji, R., Schwab, D.J., Beletsky, D., Fahnenstiel, G.L., Jiang, M., Johengen, T.H., Vanderploeg, H., Eadie, B., Budd, J.W., Bundy, M.H., Gardner, W., Cotner, J. and Lavrentyev, P.J. (2002). A Model Study of the Coupled Biological and Physical Dynamics in Lake Michigan. *Ecological Modelling*, **152**, 145-168.

Chen, Y.D., Carsel, R.F., McCutcheon, S.C. and Nutter, W.L. (1998). Stream Temperature Simulation of Forested Riparian Areas: I. Watershed-Scale Model Development. *Journal of Environmental Engineering*, **124**(4), 304-315.

Chun, K.C., Chang, R.W., Williams, G.P., Chang, Y.S., Tomasko, D., LaGory, K.E., Ditmars, J.D., Chun, H.D. and Lee, B.K. (2001). Water Quality Issues in the Nakdong River Basin in the Republic of Korea. *Environmental Engineering and Policy*, **2**(3), 131-143.

Cole, T. M. and Wells, S. A. (2003). *CE-QUAL-W2: A Two-Dimensional Laterally Averaged, Hydrodynamic and Water Quality Model, Version 3.2 User Manual*. U.S. Army Corps of Engineers, Washington, D.C.

Donigian, A.S. (2002). Watershed Model Calibration and Validation: The HSPF Experience. *National TMDL Science and Policy Specialty Conference 2002*, Phoenix, Arizona.

Donigian, A.S. and Crawford, N.H. (1976). *Modeling Nonpoint Pollution from the Land Surface*. U.S. Environmental Protection Agency, Environmental Research Laboratory, Athens, Georgia.

Eggink, J. (2001). *An Exploration of the Limnological Dynamics of Lake Manassas*, Master's Thesis, Virginia Polytechnic Institute and State University, Falls Church, Virginia.

Francos, A., Bidoglio, G., Galbiati, L., Bouraoui, F., Elorza, F.J., Rekolainen, S., Manni, K. and Granlund, K. (2001). Hydrological and Water Quality Modelling in a Medium-Sized Coastal Basin. *Physics and Chemistry of the Earth, Part B: Hydrology, Oceans and Atmosphere*, **21**(1), 47-52.

Garnier, J., Nemery, J., Billen, G. and Thery, S. (2005). Nutrient Dynamics and Control of Eutrophication in the Marne River System: Modelling the Role of Exchangeable Phosphorus. *Journal of Hydrology*, **304**, 397-412.

Gassman, P.W., Osei, E., Saleh, A. and Hauck, L.M. (2002). Application of an Environmental and Economic Modeling System for Watershed Assessments. *Journal of the American Water Resources Association*, **38**(2), 423-438.

Imteaz, M.A., Asaeda, T. and Lockington, D.A. (2003). Modelling the Effects of Inflow Parameters on Lake Water Quality. *Environmental Modeling and Assessment*, **8**, 63-70.

Johnston, J. (2005). Personal Communication. Manassas, Virginia.

Jordan, P., Rippey, B. and Anderson, N.J. (2001). Modeling Diffuse Phosphorus Loads from Land to Freshwater Using the Sedimentary Record. *Environmental Science and Technology*, **35**(5), 815-819.

Kao, J., Lin, W. and Tsai, C. (1998). Dynamic Spatial Modeling Approach for Estimation of Internal Phosphorus Load. *Water Research*, **32**(1), 47-56.

Longabucco, P. and Rafferty, M.R. (1998). Analysis of Material Loading to Cannonsville Reservoir: Advantage of Event-Based Sampling. *Lake and Reservoir Management* **14**(2-3), 197-212.

Mankin, K.R., Wang, S.H., Koelliker, J.K., Huggins, D.G. and deNoyelles, F. (2003). Watershed-lake Water Quality Modeling: Verification and Application. *Journal of Soil and Water Conservation*, **58**(4), 188-198.

Martin, J.L. and McCutcheon, S.T. (1999). *Hydrodynamics and Transport for Water Quality Modeling*, CRC Press. Inc., Florida.

Morgan, C. and Owens, N. (2001). Benefits of Water Quality Policies: The Chesapeake Bay. *Ecological Economics*, **39**(2), 271-284.

Mostaghimi, S., Park, S.W., Cooke, R.A. and Wang, S.Y. (1997). Assessment of Management Alternatives on a Small Agricultural Watershed. *Water Research*, **31**(8), 1867-1878.

Neitsch, S.L., Arnold, J.R., Kiniry, J.R., Williams, J.R. and King, W.K. (2002). *Soil and Water Assessment Tool Theoretical Documentation Version 2000*. Texas Water Resources Institute, College Station, Texas.

Occoquan Watershed Monitoring Laboratory. (1998). *An Updated Water Quality Assessment for the Occoquan Reservoir and Tributary Watershed: 1973-1997*. Manassas, Virginia.

Randall, C.W. and Grizzard, T.J. (1995). Management of the Occoquan River Basin: A 20-Year Case History. *Water Science and Technology*, **32**(5-6), 235-243.

U.S. Environmental Protection Agency. (1983). Methods for Chemical Analysis of Water and Wastes. U.S. Environmental Protection Agency, Cincinnati, Ohio.

Wade, A.J., Hornberger, G.M., Whitehead, P.G., Jarvie, H.P. and Flynn, N. (2001). On Modeling the Mechanisms that Control In-Stream Phosphorus, Macrophyte, and Epiphyte Dynamics: An Assessment of a New Model Using General Sensitivity Analysis. *Water Resources Research*, **37**(11), 2777-2792.

Wetzel, R.G. (2001). *Limnology: Lake and River Ecosystems*, Third Edition. Academic Press, San Diego, California.

Whittaker, G. (2005). Application of SWAT in the Evaluation of Salmon Habitat Remediation Policy. *Hydrological Processes*, **19**(3), 839 - 848.

Xu, Z., Godrej, A.N. and Grizzard, T.J. (2006). The Hydrological Calibration of a Linked Watershed-Reservoir Model for the Occoquan Watershed, Virginia. *In Preparation*.

Young, R.A., Alonso, C.V. and Summer, R.M. (1990). Modeling Linked Watershed and Lake Processes for Water Quality Management Decisions. *Journal of Environmental Quality*, **19**(3), 421-427.

Chapter 7. Modeling Algae Dynamics and the Impact of Land Use Changes on Receiving Water Quality in the Occoquan Watershed by Using a Linked Model Application

7.1 *Calibration and Validation*

Algae are important components in any water quality model due to their interaction with nutrients and DO. In the Lake and the Reservoir, the observed algae concentrations (in mg/L) were calculated by multiplying measured chlorophyll *a* concentrations (in μg/L) by a conversion factor. A value of 65 was used for this factor.

Currently, only one algae species is included in both W2 submodels. However, the algae count data indicated three dominant algae species (green algae, blue green algae, and diatoms) in the Reservoir.

In the Lake, results from the calibration and validation periods indicate that the W2 submodel tended to under-predict the algae activities with a difference in average concentrations of about –0.60 mg/L (Table 7-1). The differences are relatively large in the spring and winter seasons, which suggests possible diatom growth because diatoms grow in cooler waters than do blue green or green algae. These trends are also clearly shown by Figure 7-1.

The algae growth in the Reservoir was generally over-predicted by 0.28 mg/L for the calibration period and 0.40 mg/L for the validation period (Table 7-2). However, similar to the Lake, the model under-predicted the algae concentrations during the winter and spring seasons (Table 7-2 and Figure 7-1). It also suggests that diatoms, which grow in cooler waters, should be considered in the model application. The W2 submodels' performance will probably be improved by including multiple algae species in the simulation.

Table 7-1: Comparisons of Algae Concentrations at LM01 Station for Model Calibration and Validation

		Spring	Summer	Fall	Winter	Average
Calibration	Observed (mg/L)	0.77	0.55	0.98	2.07	0.93
	Simulated (mg/L)	0.04	0.45	0.47	0.10	0.32
	Difference (mg/L)	–0.73	–0.10	–0.51	–1.97	–0.61
Validation	Observed (mg/L)	0.96	0.67	1.01	1.08	0.90
	Simulated (mg/L)	0.06	0.41	0.45	0.12	0.30
	Difference (mg/L)	–0.90	–0.26	–0.56	–0.96	–0.60

Table 7-2: Comparisons of Algae Concentrations at RE02 Station for Model Calibration and Validation

		Spring	Summer	Fall	Winter	Average
Calibration	Observed (mg/L)	0.74	0.82	0.50	0.46	0.66
	Simulated (mg/L)	0.15	0.86	2.04	0.18	0.94
	Difference (mg/L)	–0.59	+0.04	+1.46	–0.28	+0.28
Validation	Observed (mg/L)	1.02	0.87	0.45	0.30	0.69
	Simulated (mg/L)	0.00	1.42	1.94	0.01	1.09
	Difference (mg/L)	–1.02	+0.55	+1.49	–0.29	+0.40

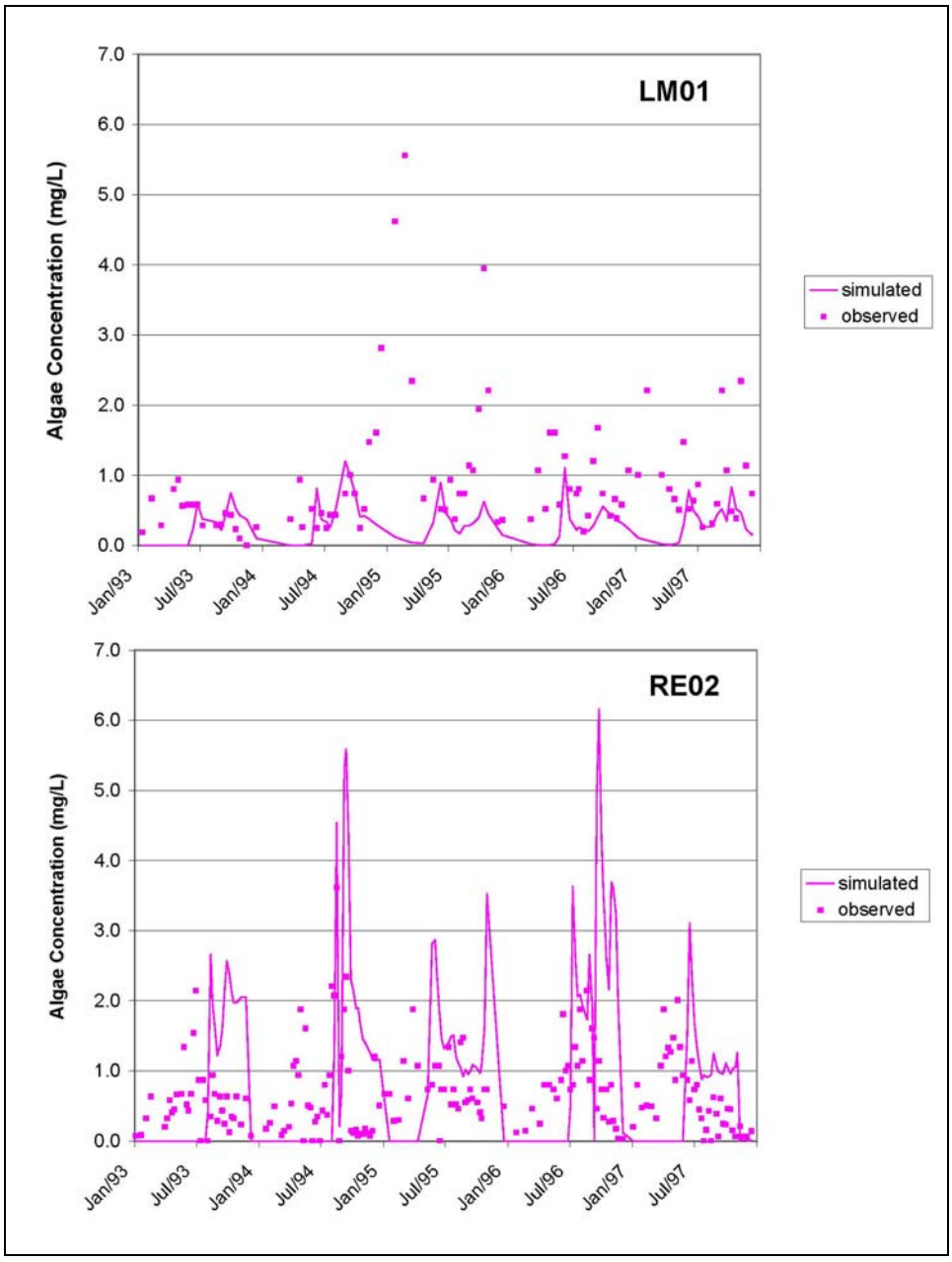

Figure 7-1: Comparison of Algae Concentrations at Stations near the Dams of Lake Manassas and Occoquan Reservoir for Model Calibration and Validation

7.2 *Algae Simulation under Different Scenarios*

An investigation was performed for algae growth under the different land scenarios. A detailed description of land development scenarios can be found in previous sections (Chapters 5 and 6).

Table 7-3 shows the comparison of average algae concentrations under the various scenarios. It indicates that the increases of external nutrient loads not only result in nutrient enrichment of the receiving waterbody, but also stimulate algae growth. Future development (represented by the Future scenario) would dramatically increase average algae concentrations by 105.3%, which is partially due to the significant increase of nutrient production in the Cedar Run subbasin. On the other hand, if the land use pattern is restored from the Current scenario to the Forest scenario, the reduced nutrient concentrations in the Reservoir would result in a 17.0% decrease in the average algae concentration.

Table 7-3: Comparison of Algae Concentrations at the Station near the Occoquan Reservoir Dam (RE02) for Various Land Development Scenarios

	Algae (mg/L)	PD (%)*
Current	0.94	
Forest	0.78	–17.0
Future	1.93	+105.3

*PD: Percentage Difference from Current scenario

Further investigation of the impact on the seasonal variation of algae growth was performed at station RE02 (Figure 7-2). The results indicate that the increases of algae concentrations due to excess external nutrient loads were not evenly distributed across the seasons. The warm seasons, especially the early fall season, show greater increases than the spring and fall seasons. The algae concentrations almost doubled for the summer and fall seasons. This suggests that future land development could worsen the water quality and result in degradation of aquatic systems. Careful management plans are needed for future land use development proposals.

In the current model application, one lumped algae species was simulated in the Reservoir even though the algae species count data suggest three dominant species (blue green, diatoms, and green). Thus the growth of diatoms, a species preferring cool temperatures, was not well captured. When multiple algae species are included in the W2 submodels, the timing and magnitude of algal growth probably will be better captured under the different scenarios.

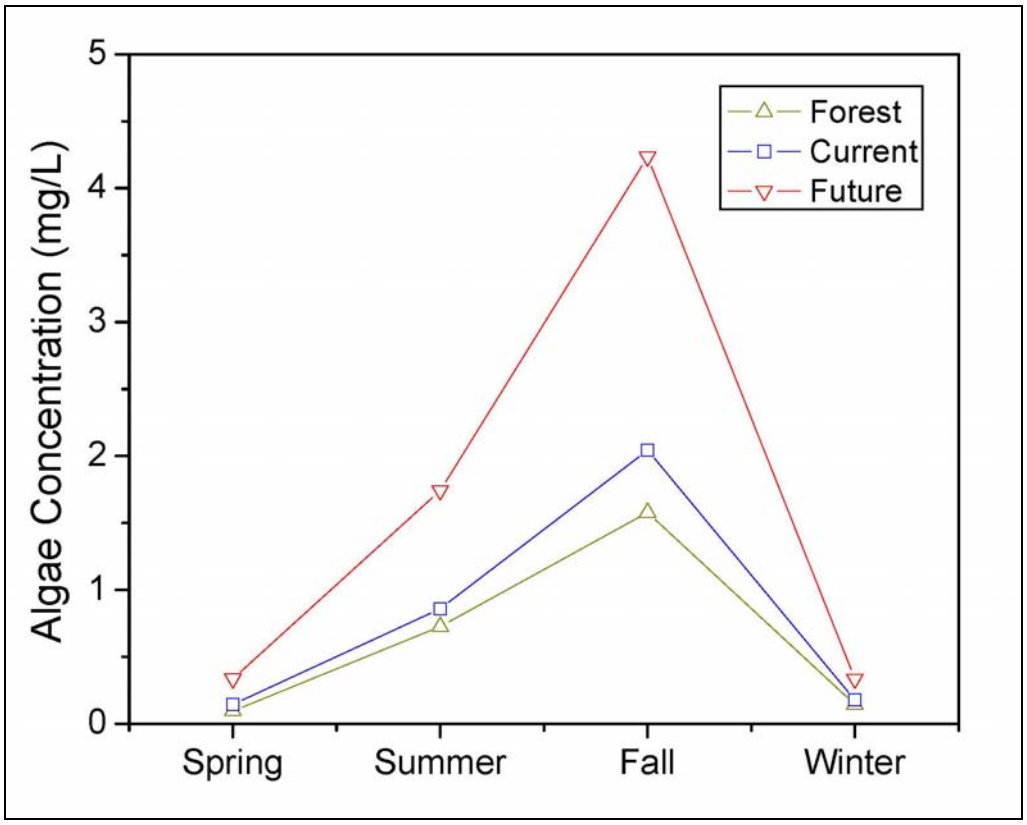

Figure 7-2: Seasonal Comparison of Impact of Different Land Development Scenarios on Algae Concentration at the Station near the Occoquan Reservoir Dam (RE02)

Chapter 8. Conclusions and Recommendations

8.1 *Summary of Objectives Attained*

This research forms a part of an ongoing study to perform continuous improvements to the Occoquan model. The principal goal of the Occoquan model project is to develop and apply the best possible model science to improve modeling of the Occoquan watershed and associated waterbodies.

The principal goals of this research were to develop, calibrate and validate a complex linked model to simulate hydrology and water quality in the Occoquan Watershed and its principal waterbodies, and to explore its application to land use scenarios. These goals were achieved by completing the following objectives:

1. To develop a complex linked hydrology and water quality model for the Occoquan Watershed, which allows better representation of the physical, chemical and biological processes in the watershed and two principal waterbodies: Occoquan Reservoir and Lake Manassas;
2. To calibrate and validate the linked model, including hydrology, nutrients (nitrogen and phosphorus), temperature, dissolved oxygen, and algae; and,
3. To investigate the potential impact of urbanization on nutrient enrichment in the Occoquan Reservoir and to identify the critical land areas in the watershed.

8.1.1 First Objective

The first objective was to develop a complex linked hydrology and water quality model for the Occoquan Watershed. This was achieved by 1) performing finer segmentation for the Watershed and two waterbodies based on high-resolution data; 2) collecting required input data, 3) building user control files and linking individual submodels into an entity.

1) The watershed delineation and segmentation was completed by using an EPA BASINS utility based on local 1:24,000 scale (7.5 minute) Digital Elevation Model data, 1:100,000-scale National Hydrography Dataset data, local land use data, etc. Some

site-specific features were included in this process: a relatively small segment was added to account for the contribution from the UOSA WRF, and additional segments were added to prepare the model to be used when future development plans are implemented. The 1,515 km^2 (584.8 square miles) watershed was divided into six subbasins with a total of 56 land (HSPF) segments, which approximately tripled those in the previous model application. The average segment size was 27.0 km^2 (10.4 square miles).

Similarly, the Occoquan Reservoir and Lake Manassas were defined by finer computational grids. Bathymetry survey data were collected by OWML using an integrated differential global positioning system and depth sounding system, which provided high-resolution bathymetry data (less than 3.0 feet for horizontal positioning and less than 0.1 feet for depth measurement). The data were then processed using SURFER to determine the size of the computational grids.

The modeled region of Lake Manassas extended from just downstream of station ST70 to the dam, a distance of 5.97 km. It was divided into four branches: the mainstem, North Fork, and two unnamed arms, and had a total of 29 active computational segments. The segment length varied from 173 m to 568 m. There were 4 to 28 computational layers, each 0.5 m thick. The average width of the top layers were 297.2 m

The Reservoir encompassed streams from approximately downstream of the Lake Jackson dam (station ST10) on the Occoquan River arm and from approximately station ST40 on the Bull Run arm. It was divided into four branches: Occoquan River (mainstem, Branch 1), Bull Run (Branch 2), Sandy Run (Branch 3) and Hooes Run (Branch 4). It had a total of 69 active computational segments. The average segment length was 583 m with a maximum of 838 m (segment 55 at the very upstream end of Bull Run) and a minimum of 74 m (Segment 32, at Ryan's Dam, a submerged feature with a narrow vertical opening). There were from 1 to 39 computational layers, each 0.5 m thick. The average width of the top layers was 149.7 m, about half of that for the Lake.

The resultant finer segmentation of the Occoquan Watershed and two waterbodies allowed more precise representation of hydrology, hydrodynamics, and associated water quality activities in the whole watershed.

2) The required data for HSPF and CE-QUAL-W2 include meteorological data, land use data, water withdrawal from the waterbodies, etc. Extensive efforts were made to collect, analyze, and infill the meteorological data because they are significant driving factors in hydrological and water quality models. These included precipitation, temperature, wind speed, cloud cover, and potential evapotranspiration. In HSPF, these time series were stored in a utility called Watershed Data Management Utility (WDMUtil). For CE-QUAL-W2, these input time series were stored in text format.

Land use data for 1995 for the HSPF submodels were obtained from the Northern Virginia Regional Commission, and were initially classified into fourteen land use categories. They were then consolidated into nine categories based on imperviousness and soil properties to reduce the complexity of the HSPF applications without significantly affecting simulation results.

Daily water withdrawals from the Reservoir, water usage for power generation and bypass flow were provided by Fairfax Water. Water withdrawal data from the Lake were provided by the water treatment plant of the City of Manassas with missing values filled in with average values.

Time-varying boundary conditions for W2 include upstream flow, tributary flow, distributed tributary flow, and water withdrawal. Water quality inputs for each of these flows, as well as for rainfall, were also required. This information was provided by the upstream HSPF submodels.

3) After the input time series were prepared, user control files were created for each submodel with most coefficients set at default values, and these were linked into the complex linked model framework.

The Upper Broad Run HSPF submodel provided direct input (including daily inflows, temperature, DO and other water quality concentrations) to the Lake W2 submodel. The ungauged distributed tributary flows along the Lake and associated water quality were estimated by the Middle Broad Run HSPF submodel. The outputs from the Lake W2 submodel served as inputs for the Lower Broad Run HSPF submodel. Similarly, the Lower Broad Run HSPF application, including the contribution from the Cedar Run subbasin, provided flows and water quality time series for the Occoquan River branch of the Reservoir. The input time series of the Bull Run branch were provided by the Bull Run HSPF submodel. The Lower Occoquan HSPF submodel provided the ungauged distributed tributary flows and associated water quality along the Reservoir. Thus, six HSPF (Cedar Run, Bull Run, Upper Broad Run, Middle Broad Run, Lower Broad Run, Lower Occoquan) and two W2 (Lake Manassas and Occoquan Reservoir) submodels were linked together to fully represent the hydrology and water quality activities in the Watershed and two waterbodies.

8.1.2 Second Objective

The second objective was to calibrate the linked model for 1) hydrology; 2) ammonium nitrogen (NH4-N) and oxidized nitrogen (Ox-N); 3) orthophosphate phosphorus (OP); 4) temperature and dissolved oxygen; and 5) algae. The second component of this objective was to 6) validate the model

Model calibration was performed for the years 1993-1995 to establish good representation of the hydrology and water quality activities in the Watershed and two waterbodies. The calibration period was a combination of wet and dry years. Model coefficients were adjusted within a meaningful range to provide the best match between simulated and observed data.

The comparison of simulated and observed data for HSPF submodels were performed primarily at ST25 (the Cedar Run subbasin), ST70 (the Upper Broad Run subbasins), ST30 (the Lower Broad Run subbasin), and ST45 (the Bull Run subbasin). In addition, data at ST10 and ST40, two stations at the headwaters of the Reservoir, were also

examined because they represented the water quality that was generated by upstream HSPF submodels and fed into the Reservoir W2 submodel. In the Lake and the Reservoir, comparisons were performed primarily at in-lake stations. In the Lake, these were LM01 (near the dam), LM04, LM05, and LM06 (headwater of the mainstem). Those in the Reservoir included RE02 (near the dam), RE15, RE30 (headwater of Branch 2), and RE35 (headwater of Branch 1). Both graphical and statistical methods were used to evaluate model performance.

1) The hydrological calibration performance of HSPF submodels was evaluated by comparing simulated and observed flow data on a daily, monthly and annual basis. The water budgets in the W2 submodels were evaluated by comparing simulated and observed daily water surface elevations. The results indicated that the overall flow balances based on the calibration period at four principal stream stations showed agreement ranging from –3.95% to +3.21%. According to the scale used by Donigian (2002), the HSPF submodels were generally calibrated "very good" based on annual flow balances, and the percentage difference values ranged from –5.84% to +21.14%. The HSPF submodels were calibrated "good" based on monthly flow balances and the R^2 values were 0.815 or greater. The water surface elevations at Lake Manassas and Occoquan Reservoir were well calibrated, and the R^2 values based on daily comparisons were 0.937 and 0.926, respectively. Missing flows estimated by a W2 utility called WaterBalance accounted for 0.2% and 0.9% of the average outflows of Lake Manassas and Occoquan Reservoir, respectively.

2) The simulated NH4-N and Ox-N loads from HSPF were compared with observed loads of individual storms, aggregated on both a monthly and an annual basis. The results indicated good model performance and the PD values of four principal stream stations based on the three-year simulation period ranged from –3.95% to +10.22% for NH4-N and from –11.89% to +6.10% for Ox-N. Based on annual load comparisons, the HSPF submodels were generally "good" to "very good" calibrated and the absolute percentage difference values were less than 25% for most sites. The R^2 values based on monthly loads were equal to or greater than 0.531 for NH4-N and 0.606 for Ox-N for most sites. The W2 submodels captured the temporal and spatial variation of the nitrogen species.

The results indicated that the differences of average simulated and observed NH4-N concentrations in flow over the dams were equal to or less than 0.01 mg/L for both Lake Manassas and Occoquan Reservoir. The differences of average Ox-N concentrations in flow over the dams were equal to or less than 0.01 mg/L for Lake Manassas and 0.07 mg/L for the Occoquan Reservoir.

3) The simulated OP loads from HSPF submodels were also compared with observed loads of individual storms, aggregated on both a monthly and an annual basis. The results indicated good model performance on OP loads and the PD values based on the three-year simulation period ranged from –12.62% to –2.13% for four principal stream stations. The annual OP loads were generally "good" to "very good" calibrated and the percentage difference values ranged from –18.99% to +25.26% for most sites. R^2 values based on monthly load comparisons were equal to or greater than 0.520 for most sites. The spatial and temporal variations in the Lake and the Reservoir were well reproduced by the W2 submodels. The absolute differences between simulated and observed average OP concentrations were equal to or less than 1 μg/L for the Lake and 7 μg/L for the Reservoir.

4) The simulated temperature and DO from HSPF submodels were compared on a daily and seasonal basis. The results indicated that R^2 values based on comparison of daily data were greater than 0.882 for temperature and 0.487 for DO. The differences of seasonal averages ranged from –1.87 ºC to +0.38 ºC for temperature and from –0.53 mg/L to +1.75 mg/L for DO. According to the scale used by Donigian (2002), these HSPF submodels were well calibrated for both temperature and DO for most sites. The longitudinal and vertical variations of temperature and DO in the Lake and Reservoir were generally well reproduced by the W2 submodels. The differences of temperatures at surface layers are less than 0.42 ºC and 1.38 ºC for the Lake and Reservoir, respectively. The differences of surface DO concentrations at various stations were less than 1.25 mg/L for the Lake and 1.42 mg/L for the Reservoir. The hydrodynamic differences between these two waterbodies were also well-captured by the W2 submodels.

5) The timing and magnitude of algae growth were generally captured reasonably well by the W2 submodels. The seasonal differences were equal to or less than 1.97 mg/L for the Lake and 1.46 mg/L for the Reservoir. In this application, only one lumped algae species was modeled in both submodels. However, the observed species count data suggest three dominant algae species (diatoms, green algae, and blue green algae) in the Reservoir. The W2 submodels' performance might be improved by including multiple algae species in the simulation.

6) Model validation was performed for the year 1996-1997 with the same parameter set to verify the reliability of model performance under difference conditions. The validation period was a combination of wet and dry years with the year 1996 being a very wet year. The validation results indicated that in the HSPF submodels, although the hydrology and nutrient production from drainage areas were not well validated for the very wet year 1996, the HSPF submodels validated generally well for the relatively dry year 1997. The W2 submodels were adequately validated to capture the temporal and spatial distribution of temperature, DO, and nutrients.

8.1.3 Third Objective

The third objective was to develop two land use scenarios to investigate the potential impact of urbanization on nutrient enrichment in the Occoquan Reservoir and to identify the critical land areas in the watershed. One scenario (Forest) was developed wherein all the lands were assumed to be covered by forests. It represented the background condition with no impact from human activities before Colonial history and can be used to evaluate the long-term impact of human activities on the water resources. The contribution from UOSA was eliminated in this scenario. The other one (Future) was developed by converting 50% of the existing forested areas in each segment to residential and commercial development. It represented the potential environmental stress from future urbanization. The contribution from UOSA was assumed to be unchanged. The changes of nutrient yields from land areas were investigated for each scenario and their potential impact on water quality in the Reservoir were demonstrated.

As expected, these nutrient loads from the land segments in the Forest scenario were much lower than the Current condition. The model output suggested 11.89×10^6 g/year (71%), 597.35 $\times10^6$ g/year (224%), and 7.11 $\times10^6$ g/year (45%) increase of annual NH4-N, Ox-N, and OP load production, respectively, over the pre-Colonial period. The significant increase of Ox-N loads was due to the nitrate-rich UOSA effluent. The increase of external nutrient loads since the pre-Colonial period suggested nutrient enrichment and enhance algae activities. On the other hand, if the land use pattern is restored to the pre-Colonial period, the average surface concentrations near the Reservoir dam would be reduced by 10.0% (2 μg/L) for OP and 66.7% (0.60 mg/L) for Ox-N. The average surface NH4-N concentrations would be increased 33.3% (0.01mg/L) probably due to reduced algae activities. The results indicated that the average algae concentration would decrease by 17.0% (0.16 mg/L).

The comparison between the Current condition and the Future condition confirmed the increasing trend of external nutrient loads due to human activities. The results indicated that the annual NH4-N and OP production based on the Future scenario would be almost doubled, compared to the current condition. The slight increase of Ox-N load production (6.7%) was due to the dominance of the UOSA contribution. Future development would cause nutrient enrichment and enhance algae activities. The results indicated that the average surface concentrations near the Reservoir dam would increase by 65.0% for OP (13 μg/L), 43.3% (0.39 mg/L) for Ox-N, 100.0% (0.03 mg/L) for NH4-N, and 105.3% (0.99 mg/L) for algae.

Investigation of the nutrient yields from each land segment indicated that the increases of external nutrient loads were not evenly distributed across the Watershed. From the Forest scenario to the Current condition, the Bull Run region showed the greatest increases in nutrient load production (87.9% for NH4-N, 33.8% for Ox-N and 67.1% for OP) due to its greater urbanization. The Broad Run subbasin showed the lowest increase in yield production (10.3% for NH4-N, 5.1% for Ox-N, and 26.5% for OP) because Lake Manassas probably trapped these nutrients and reduced transport downstream. From the Current condition to the Future condition, the Cedar Run subbasin showed the greatest increase in nutrient production (177.4% for NH4-N, 36.3% for Ox-N, and 165.5% for

OP) because the dominant land use would shift from non-urban development to urban development. The Bull Run subbasin appeared to have a slower increase rate for nutrients, compared with the pre-Colonial period. The investigation of land uses in the Bull Run subbasin indicated an already existing high urban development with more than 30% of the land categorized as urban. Therefore, future expansion might not result in a significant increase on the already high values of nutrient load production. This suggested a threshold for nutrient load production despite land development, and a future study of land development scenarios could provide more insight on this issue. Based on the comparison of nutrient changes over the three scenarios, the critical areas in the Watershed have been identified and future BMP plans should be considered in these locations in future land use development.

8.2 *Contributions*

Few studies have been performed to link two or more state-of-the-art water quality models due to the complications involved and insufficient data availability. In this research, a complex linked hydrology and water quality model has been developed to simulate the important processes in the Occoquan Watershed and two principal waterbodies (Lake Manassas and Occoquan Reservoir). The linked model has been successfully calibrated and validated, thus indicating that the linked models can be adequately calibrated with moderate additional effort.

One of the advantages of such a complex linked model application is to better represent the physical reality in the Occoquan Watershed, which consists of two principal waterbodies. The interaction between drainage areas and receiving waterbodies was represented by linking individual submodels into an entity. The results from such applications would be more easily accepted by managers and the general public because it can be more readily seen to represent a natural system that is not unlinked.

Another advantage is to develop a direct cause-effect relationship between upstream activities and downstream water quality. The scenarios of various levels of land use, BMP implementation, and point source reduction could be incorporated into HSPF

applications, and thus W2 submodels can use the boundary conditions corresponding with these scenarios to predict the variation in water quality. This makes it easier for decision-makers to evaluate alternative management plans. In addition, it also makes it easier for the public to understand and accept the decision-making processes without leaving an impression that something might be inapt in how the natural system is represented by submodels that are not linked.

The complex linked model can serve as a useful scientific tool for local parties. The possible applications of the complex linked model are, but not limited to:

- Due to the advantages of the complex linked model, it could be used in the future DO TMDL project for the Occoquan Reservoir.
- Alternative land use scenarios could be developed for local groups to investigate the impacts on water quality in neighborhood streams.
- A short-term prediction based on the projected meteorological data could be applied to forecast the hydrology and water quality activities in the watershed and the waterbodies. Such information could be used by water treatment plans on dam operation and water withdrawal.
- Alternative scenarios could be developed for UOSA to investigate the environmental responses to its future expansion.

8.3 *Future Research*

Several questions have been left uninvestigated by this research. Potential research topics derived from this work can be grouped into immediate and long-term projects.

8.3.1 Potential Immediate Projects

1. Multiple algae species should be included in the W2 submodels, especially for the Reservoir because the algae count data indicate three dominant algae species.
2. A detailed investigation of the impact of upstream land development on the water quality in Lake Manassas could be performed.

3. A modified W2 program with a special code to account for the algae kill by copper compound should be used to account for the application of copper compounds in the Lake and the Reservoir.

8.3.2 Potential Long-Term Projects

1. The complex linked model could be updated to the current years when land-use data and meteorological data have been updated.
2. In HSPF, the agri-chemical section could be considered to replace the simple method used in this study to estimate nutrient load production from drainage areas. This is because the agri-chemical section provides a process-oriented method to estimate the nutrient cycling in the soil profiles. This would be particularly helpful to simulate nutrient production from the Cedar Run subbasin, where the agricultural activities are significant.
3. A scenario with expanded UOSA capacity should be considered. In the Future scenario in this study, the contribution from UOSA was assumed to be constant. However, it is highly possible that the capacity and water chemistry from UOSA discharge will be changed with the plant expansion and possible application of new treatment techniques. Due to the significance of this point source, a scenario with expanded UOSA capacity and future land use development would provide a more realistic prediction of water quality changes due to human activities in the receiving waterbody.
4. The current version of W2 model (Version 3.2) does not consider nitrate as a secondary electron acceptor when oxygen is depleted, which is an important process in the Occoquan Reservoir due to the nitrate-rich UOSA effluent. Studies have shown its significant impact on the water quality management in the Reservoir. A specific code should be developed and incorporated in the W2 model to account for this phenomenon in the Reservoir. This would provide better simulation of nitrogen and phosphorus dynamics, especially in the bottom layers of the Reservoir.
5. In Lake Manassas, an inflatable bladder has been applied since 2000 to adjust the water surface elevation based on precipitation. Because this process would have an

impact on the water balance calculation in Lake Manassas, a code corresponding with this procedure should be developed and incorporated into the W2 submodel.

6. In the current study, Ryan's dam was represented as a relatively short and narrow segment based on the bathymetry. The submerged dam function in the W2 model could be applied to provide a better representation of the hydrodynamics and water quality activities around Ryan's dam.
7. This study suggests a threshold for nutrient load production for existing urban areas despite future land development, and a further study of land development scenarios should be performed to provide more insight on this issue.

References Cited

40.C.F.R.§130.7. Total Maximum Daily Loads (TMDL) and Individual Water Quality-Based Effluent Limitations. *Federal Register*, **40. C.F.R.**(§130.7).

Albek, M., Ögeütveren, U.B. and Albek, E. (2004). Hydrological Modeling of Seydi Suyu Watershed (Turkey) with HSPF. *Journal of Hydrology*, **285**, 260-271.

Anderson, J.D., Orlob, G.T. and King, I.P. (1997). *Linking Hydrodynamic, Water Quality, and Ecological Models to Simulate Aquatic Ecosystem Response to Stress: Case Study of Juvenile Salmon Migration in the Sacramento River and San Francisco Bay/Delta System*. Environmental and Coastal Hydraulics: Protecting the Aquatic Habitat, American Society of Civil Engineers, New York.

Anderson, M.L., Chen, Z.Q., Kavvas, M.L. and Feldman, A. (2000). Coupling HEC-HMS with Atmospheric Models for the Prediction of Watershed Runoff. *Building Partnerships - 2000 Joint Conference on Water Resource Engineering and Water Resources Planning & Management*, Virginia.

Beasley, D. B., Huggins, L.F. and Monke, E.J. (1980). ANSWERS: A Model for Watershed Planning. *Transactions of the ASAE*, **23**(4), 938-944.

Bicknell, B.R., Imhoff, J.C., Kittle, J.L., Jobes, T.H. and Donigian, A.S. (2001). *Hydrological Simulation Program-Fortran HSPF Version 12 User's Manual*, U.S. Environmental Protection Agency, National Exposure Research Laboratory, Athens, Georgia.

Black & Veatch Corporation. (2000). *Safe Yield of Lake Manassas*. Manassas, Virginia.

Boesch, D.F., Brinsfield, R.B. and Magnien, R.E. (2000). Chesapeake Bay Eutrophication: Scientific Understanding, Ecosystem Restoration, and Challenges for Agriculture *Journal of Environmental Quality* **30**, 303-320.

Borsuk, K.E., Stow, C.A. and Reckhow, K.H. (2003). Integrated Approach to Total Maximum Daily Load Development for Neuse River Estuary using Bayesian Probability Network Model (Neu-BERN). *Journal of Water Resources Planning and Management*, **129**(4), 271-282.

Bosch, D.J., Lohani, V.K., Dymond, R.L., Kibler, D.F. and Stephenson, K. (2003). Hydrological and Fiscal Impacts of Residential Development: A Virginia Case Study. *Journal of Water Resources Planning and Management*, **129**(2), 107-114.

Bouraoui, F. (1994). *Development of a Continuous, Physically-Based, Distributed Parameter, Nonpoint Source Model*, Ph.D. Dissertation, Virginia Polytechnic Institute and State University, Blacksburg. Virginia.

Bowen, J.D. and Hieronymus, J.W. (2003). A CE-QUAL-W2 Model of Neuse Estuary for Total Maximum Daily Load Development. *Journal of Water Resources Planning and Management*, **129**(4), 283-294.

Brown, L. C. and Barnwell, T. O. (1987). *The Enhanced Stream Water Quality Models QUAL2E and QUAL2E-UNCAS: Documentation and User Manual*, Environmental Resources Laboratory, Environmental Protection Agency, Athens, Georgia.

Brun, S.E. and Band, L.E. (2000). Simulating Runoff Behavior in an Urbanizing Watershed. *Computers, Environment and Urban Systems*, **24**(1), 5-22.

Burian, S.J., Streit, G.E., McPherson, T.N., Brown, M.J. and Turin, H.J. (2001). Modeling the Atmospheric Deposition and Stormwater Washoff of Nitrogen Compounds. *Environmental Modelling & Software*, **16**(5), 467-479.

Campbell, S.G., Hanna, R.B., Flug, M. and Scott, J.F. (2001). Modeling Klamath River System Operations for Quantity and Quality. *Journal of Water Resources Planning and Management*, **127**(5), 284-294.

Carey, W.P. and Simon, A. (1984). *Physical Basis and Potential Estimation Techniques for Soil Erosion Parameters in the Precipitation-Runoff Modeling System (PRMS)*, U.S. Geological Survey, Nashville, Tennessee.

Cerco, C.F., Linker, L., Sweeney, J., Shenk, G. and Butt, A.J. (2002). Nutrient and Solid Controls in Virginia's Chesapeake Bay Tributaries. *Journal of Water Resources Planning and Management*, **128**(3), 179-189.

Cerucci, M. and Conrad, J.M. (2003). The Use of Binary Optimization and Hydrologic Models to Form Riparian Buffers. *Journal of the American Water Resources Association*, **39**(5), 1167-1180.

Chen, C., Ji, R., Schwab, D.J., Beletsky, D., Fahnenstiel, G.L., Jiang, M., Johengen, T.H., Vanderploeg, H., Eadie, B., Budd, J.W., Bundy, M.H., Gardner, W., Cotner, J. and Lavrentyev, P.J. (2002). A Model Study of the Coupled Biological and Physical Dynamics in Lake Michigan. *Ecological Modelling*, **152**, 145-168.

Chen, C.W., Herr, J., Ziemelis, L., Goldstein, R.A. and Olmsted, L. (1999). Decision Support System for Total Maximum Daily Load. *Journal of Environmental Engineering*, **125**(7), 653-659.

Chen, Y.D., Carsel, R.F., McCutcheon, S.C. and Nutter, W.L. (1998a). Stream Temperature Simulation of Forested Riparian Areas: II. Model Application. *Journal of Environmental Engineering*, **124**(4), 316-328.

Chen, Y.D., Carsel, R.F., McCutcheon, S.C. and Nutter, W.L. (1998b). Stream Temperature Simulation of Forested Riparian Areas: I. Watershed-Scale Model Development. *Journal of Environmental Engineering*, **124**(4), 304-315.

Chesapeake Bay Program Office. (2000). *Geology of the Chesapeake*, Chesapeake Bay Program Office, Annapolis, Maryland.

Chow, V.T. (1951). A Practical Procedure of Flood Routing. *Civil Engineering And Public Works Review*, **46**(452), 586-588.

Chow, V.T., Maidment, D.R. and Mays, L.W. (1988). *Applied Hydrology*, McGraw-Hill Inc., New York.

Christierson, B., Dabbs, C., Soerensen, H. and Kjelds, J. (2001). An Integrated Flood Management Model for the Estero-Imperial-Cocohatchee Watershed. *Urban Drainage Modeling*, Reston, Virginia.

Chun, K.C., Chang, R.W., Williams, G.P., Chang, Y.S., Tomasko, D., LaGory, K.E., Ditmars, J.D., Chun, H.D. and Lee, B.K. (2001). Water Quality Issues in the Nakdong River Basin in the Republic of Korea. *Environmental Engineering and Policy*, **2**(3), 131-143.

Cole, T. M. and Wells, S. A. (2003). *CE-QUAL-W2: A Two-Dimensional Laterally Averaged, Hydrodynamic and Water Quality Model, Version 3.2 User Manual*. U.S. Army Corps of Engineers, Washington, D.C.

Cole, T.M. and Tillman, D.H. (2001). *Water Quality Modeling of Allatoona and West Point Reservoirs Using CE-QUAL-W2*. U.S. Army Engineer Research and Development Center, Vicksburg, Mississippi.

Conrads, P.A. and Roehl Jr., E.A. (1999). Comparing Physics-Based and Neural Network Models for Simulating Salinity, Temperature, and Dissolved Oxygen in a Complex, Tidally Affected River Basin. *Proceedings of the 1999 South Carolina Environmental Conference*, Myrtle Beach, South Carolina.

Crawford, N.H. and Linsley, R.K. (1966). *Digital Simulation in Hydrology: Stanford Watershed Model IV*. Stanford University, Palo Alto. California.

Cunge, J.A. (1969). On the Subject of a Flood Propagation method (Muskingum Method). *Journal of Hydraulics Research*, **7**(2), 205-230.

Dai, T. and Labadie, J.W. (2001). River Basin Network Model for Integrated Water Quantity/Quality Management. *Journal of Water Resources Planning and Management*, **127**(5), 295-305.

Darcy, H. (1856). *The Public Fountains of the City of Dijon (translation of les fontaines publiques de la Ville de Dijon)*, Patricia Bobeck (translator), Kendall/Hunt Publishing Company, Dubuque, Iowa (2004).

DePinto, J.V., Freedman, P.L., Dilks, D.M. and Larson, W.M. (2004). Models Quantify the Total Maximum Daily Load Process. *Journal of Environmental Engineering*, **130**(6), 703-713.

Donigian, A.S. (2002). Watershed Model Calibration and Validation: The HSPF Experience. *National TMDL Science and Policy Specialty Conference 2002*, Phoenix, Arizona.

Donigian, A.S. and Crawford, N.H. (1976). *Modeling Nonpoint Pollution from the Land Surface*. U.S. Environmental Protection Agency, Environmental Research Laboratory, Athens, Georgia.

Dymond, R.L., Regmi, B., Lohani, V.K. and Dietz, R. (2004). Interdisciplinary Web-Enabled Spatial Decision Support System for Watershed Management. *Journal of Water Resources Planning and Management*, **130**(4), 290-300.

Eggink, J. (2001). *An Exploration of the Limnological Dynamics of Lake Manassas*, Master's Thesis, Virginia Polytechnic Institute and State University, Falls Church, Virginia.

EMS-I Inc. . (2002a). *SMS8.1-Overview*. South Jordan, Utah.

EMS-I Inc. (2002b). *WMS7-Overview*. South Jordan, Utah.

Engel, V.C., Stieglitz, M.M., Williams, M. and Griffin, K.L. (2002). Forest Canopy Hydraulic Properties and Catchment Water Balance: Observations and Modeling. *Ecological Modelling*, **154**(3), 263-288.

Feigner, K.D. and Harris, H.S. (1970). *Documentation Report- FWQA Dynamic Estuary Model*, U.S. Department of Interior, Federal Water Quality Administration, Washington D.C.

Flanagan, D.C. and Nearing, M.A. (1995). *USDA Water Erosion Prediction Project Hillslope Profile and Watershed Model Documentation*, USDA-ARS National Soil Erosion Research Laboratory, West Lafayette, Indiana.

Flowers, J.D., Hauck, L.M. and Kiesling, R. (2001). *USDA: Lake Waco-Bosque River Initiative: Water Quality Modeling of Lake Waco Using CE-QUAL-W2 for Assessment of Phosphorus Control Strategies*, Texas Institute for Applied Environmental Research, Texas.

Francos, A., Bidoglio, G., Galbiati, L., Bouraoui, F., Elorza, F.J., Rekolainen, S., Manni, K. and Granlund, K. (2001). Hydrological and Water Quality Modelling in a Medium-Sized Coastal Basin. *Physics and Chemistry of the Earth, Part B: Hydrology, Oceans and Atmosphere*, **21**(1), 47-52.

Freeze, A.R. and Cherry, J.A. (1979). *Groundwater*, Prentice-Hall, Inc, New Jersey.

Frick, W.E., Roberts, P.J.W., Davis, L.R., Keyes, J., Baumgartner, D.J. and George, K.P. (2001). *Dilution Models for Effluent Discharges, 4th Edition (Visual Plumes) Draft*, U.S. Environmental Protection Agency, Athens, Georgia.

Garnier, J., Nemery, J., Billen, G. and Thery, S. (2005). Nutrient Dynamics and Control of Eutrophication in the Marne River System: Modelling the Role of Exchangeable Phosphorus. *Journal of Hydrology*, **304**, 397-412.

Gassman, P.W., Osei, E., Saleh, A. and Hauck, L.M. (2002). Application of an Environmental and Economic Modeling System for Watershed Assessments. *Journal of the American Water Resources Association*, **38**(2), 423-438.

Gatling, L.A., Kardash, A.O. and Yoon, J. (2000). Spatiotemporal Water Quality Modeling of Pipeline Water Intake Lake Gaston, Virginia. *Building Partnerships - 2000 Joint Conference on Water Resource Engineering and Water Resources Planning & Management*, Virginia.

Georgia Department of Natural Resources (2003). *Draft: Total Maximum Daily Load Evaluation for the Little River Embayment in the Coosa River Basin for Chlorophyll α.*, Georgia.

Giorgino, M.J. and Bales, J.D. (1997). *Rhodhiss Lake, North Carolina: Analysis of Ambient Conditions and Simulation of Hydrodynamics, Constituent Transport and Water-Quality Characteristics, 1993-1994*. U.S. Geological Survey, Raleigh, North Carolina.

Golden Software, Inc. (2002). *Surfer 8: Contouring and 3D Surface Mapping for Scientists and Engineers User's Guide*. Golden, Colorado.

GRASS Development Team. (2005). *Geographic Resources Analysis Support System (GRASS) Programmer's Manual*. Trento, Italy.

Green, W.H. and Ampt, G.A. (1911). Studies on Soil Physics, Part I: The Flow of Air and Water Through Soil. *Journal of Agricultural Science*, **4**(1), 1-24.

Gunduz, O., Soyupak, S. and Yurteri, C. (1998). Development of Water Quality Management Strategies for the Proposed Isikli Reservoir. *Water Science and Technology*, **37**(2), 369-376.

Hadjerioua, B., Lindquist, K.F. and Siler, V. (2001). Linking TVA's Norris and Melton Hill Reservoirs Water Quality: CE-QUAL-W2 Models. *World Water Congress 2001, Bridging the Gap: Meeting the World's Water and Environmental Resources Challenges*, Florida.

Hamon, R.W., Weiss, L.L. and Wilson, W.T. (1954). Insolation as an Empirical Function of Daily Sunshine Duration. *Monthly Weather Review*, **82**(6), 141-146.

Hamrick, J.M. (1996). *User's Manual for the Environmental Fluid Dynamics Computer Code*, Virginia Institute of Marine Science, Virginia.

Hayashi, S., Murakami, S., Watanabe, M. and Xu, B. (2001). HSPF Simulation of Runoff and Sediment Loads in the Upper Changjiang River Basin, China. *Journal of Environmental Engineering*, **137**(7), 801-815.

Hicks, B.B., DeLuisi, J.J. and Matt, D.R. (1996). The NOAA Integrated Surface Irradiance Study (ISIS)-A New Surface Radiation Monitoring Program. *Bulletin of the American Meteorological Society*, **77**(12), 2857-2864.

Horton, R. E. (1933). The Role of Infiltration in the Hydrological Cycle. *Transactions of the American Geophysical Union*, **14**, 446-460.

Horton, R. E. (1940). An Approach Toward A Physical Interpretation of Infiltration-Capacity. *Soil Science Society of America*, **5**, 399-417.

Huber, W.C., Harleman, D.R.F. and Ryan, P.J. (1972). Temperature Prediction in Stratified Reservoirs. *Proceedings of American Society of Civil Engineers, Journal of Hydraulics Division*, **98**(4), 645-666.

Huber, W.C. and Dickinson, R.E. (1988). *Storm Water Management Model User's Manual, Version 4*, U.S. Environmental Protection Agency, Athens, Georgia.

Hydrological Engineering Center. (1986). *HEC-1 Flood Hydrograph Package: User's Manual*. Davis, California.

Imteaz, M.A., Asaeda, T. and Lockington, D.A. (2003). Modelling the Effects of Inflow Parameters on Lake Water Quality. *Environmental Modeling and Assessment*, **8**, 63-70.

Hydrocomp Inc. (1978). *The Occoquan Basin Computer Model Calibration, Verification and User's Manual*. Georgia, USA.

Ishii, A.L., Charlton, T.J., Ortel, T.W. and Vonnahme, C.C. (1998). Operational Modeling System with Dynamic-Wave Routing. *Water Resources and the Urban Environment: Proceedings of the 25th Annual Conference on Water Resources Planning and Management*, Illinois.

Jacob, C.E. (1943). Correlation of Ground-Water Levels and Precipitation on Long Island New York. *Transactions, American Geophysical Union*, **25**, 564-573.

Jayakrishnan, R., Srinivasan, R., Santhi, C. and Arnold, J. G. (2005). Advances in the Application of the SWAT Model for Water Resources Management. *Hydrological Processes*, **19**(3), 749-762.

Jirka, G.H., Doneker, R. L. and Barnwell, T.O. (1991). CORMIX: An Expert System for Mixing Zone Analysis. *Water Science and Technology*, **24**(6), 267-274.

Jobson, H.E. and Harbaugh, A.W. (1999). *Modifications to the Diffusion Analogy Surface-Water Flow Model (DAFLOW) for Coupling to the Modular Finite-Difference Ground-Water Flow Model (MODFLOW)*. U.S. Geological Survey, Virginia.

Johnston, J. (2005). Personal Communication. Manassas, Virginia.

Jordan, P., Rippey, B. and Anderson, N.J. (2001). Modeling Diffuse Phosphorus Loads from Land to Freshwater Using the Sedimentary Record. *Environmental Science and Technology*, **35**(5), 815-819.

Kao, J., Lin, W. and Tsai, C. (1998). Dynamic Spatial Modeling Approach for Estimation of Internal Phosphorus Load. *Water Research*, **32**(1), 47-56.

King, L., Donnell, B.P., Letter, J.V., McAnally, W.H., Thomas, W.A. and LaHatte, C. (2001). *Users Guide to RMA2 WES Version 4.5*, U.S. Army Corps of Engineers, Vicksburg, Mississippi.

King, L., Letter, J.V. and Donnell, B.P. (2003). *Users Guide to RMA4 WES Version 4.5* U.S. Army Corps of Engineers, Vicksburg, Mississippi.

Knisel, W.G. and Davis, F.M. (1999). *GLEAMS Groundwater Loading Effects of Agricultural Management Systems, Version 3.0 User Manual*, U.S. Department of Agriculture, Tifton, Georgia.

Kohler, M.A., Nordenson, T.J. and Fox, W.E. (1955). *Evaporation from Pans and Lakes*. U.S. Weather Bureau.

Laroche, A.M., Gallichand, J., Lagace, R. and Pesant, A. (1996). Simulating Atrazine Transport with HSPF in an Agricultural Watershed. *Journal of Environmental Engineering*, **122**(7), 622-630.

Laufer, S.M. (1986). *Nutrient Dynamics in the Lake Manassas (Virginia) Watershed*, Master's Thesis, Polytechnic Institute and State University, Blacksburg, Virginia.

Leavesley, G., Restrepo, P.J., Markstrom, S.L., Dixon, M. and Stannard, L.G. (1996). *The Modular Modeling System (MMS): User's Manual*. U.S. Geological Survey, Denver, Colorado.

Leavesley, G.H., Lichty, R.W., Troutman, B.M. and Saindon, L.G. (1983). *Precipitation-Runoff Modeling System: User's Manual*, U.S. Geological Survey, Denver, Colorado.

Leung, K.S., R.L., Segar Jr. and Burr, S.A. (2001). Atrazine Transport Modeling in a Rural Missouri Watershed. *Bridging the Gap: Meeting the World's Water and Environmental Resources Challenges Proceedings of the World Water and Environmental Resources Congress*, Florida.

Lighthill, M. J. and Whitham, G.B. (1955). On Kinematic Waves, I: Flood Movement in Long Rivers. *Proceedings of the Royal Society of London*, **229**, 245-252.

Lizarraga, J. (1996). *Using QUALTX and DAFLOW/BLTM to Simulate Water Quality in Texas Rivers*. U.S. Geological Survey, Maryland.

Longabucco, P. and Rafferty, M.R. (1998). Analysis of Material Loading to Cannonsville Reservoir: Advantage of Event-Based Sampling. *Lake and Reservoir Management* **14**(2-3), 197-212.

Lunetta, R.S., Cosentino, B.L., Montgomery, D.R., Beamer, E.M. and Beechie, T.J. (2003). *Watershed-Based Evaluation of Salmon Habitat*. GIS for Water Resources and Watershed Management, Taylor & Francis Group, New York.

Mankin, K.R., Wang, S.H., Koelliker, J.K., Huggins, D.G. and deNoyelles, F. (2003). Watershed-lake Water Quality Modeling: Verification and Application. *Journal of Soil and Water Conservation*, **58**(4), 188-198.

Martin, J.L. and McCutcheon, S.T. (1999). *Hydrodynamics and Transport for Water Quality Modeling*, CRC Press. Inc., Florida.

McIsaac, G.F., David, M.B., Gertner, G.Z. and Goolsby, D.A. (2002). Relating Net Nitrogen Input in the Mississippi River Basin to Nitrate Flux in the Lower Mississippi River: A Comparison of Approaches. *Journal of Environmental Quality*, **31**, 1610-1622.

McMahon, C., Alexander, R.B. and Qian, S. (2003). Support of Total Maximum Daily Load Programs Using Spatially Referenced Regression Models. *Journal of Water Resources Planning and Management*, **129**(4), 315-329.

Mississippi Department of Environmental Quality. (2002). *Fecal Coliform TMDL for the Back Bay of Biloxi and Biloxi Bay: Coastal Streams Basin, Harrison and Jackson Counties, Mississippi.*, Mississippi.

Merrill, L., Henry, T., Golliday, G., Pollison, D., Greene, R., Mirsajadi, H., Goman, W. and Morton, M. (2002). Nutrient and Dissolved Oxygen TMDL for Christina River Basin. *Watershed 2002: WEF Specialty Conference Proceedings*, Fort Lauderdale, Florida.

Metcalf & Eddy Inc. (1970). *The Occoquan Reservoir Study*. Boston, Massachusetts.

Miller, S.N., Guertin, D.P. and Goodrich, D.C. (2003). *Deriving Stream Channel Morphology Using GIS-Based Watershed Analysis*. GIS for Water Resources and Watershed Management, Taylor & Francis Group, New York.

Mockus, V. (1972). *National Engineering Handbook: Estimation of Direct Runoff from Storm Rainfall*. Soil Conservation Service, Portland, Oregon.

Morgan, C. and Owens, N. (2001). Benefits of Water Quality Policies: The Chesapeake Bay. *Ecological Economics*, **39**(2), 271-284.

Mostaghimi, S., Park, S.W., Cooke, R.A. and Wang, S.Y. (1997). Assessment of Management Alternatives on a Small Agricultural Watershed. *Water Research*, **31**(8), 1867-1878.

Mulvaney, T.J. (1850). On the Use of Self-Registering Rain and Flood Gauges in Making Observation of the Relations of Rainfall and of Flood Discharges in a Given Catchment. *Proceedings of the Institution of Civil Engineers*, **4**, 18-31.

Neitsch, S.L., Arnold, J.R., Kiniry, J.R., Williams, J.R. and King, W.K. (2002). *Soil and Water Assessment Tool Theoretical Documentation Version 2000*. Texas Water Resources Institute, College Station, Texas.

Novotny, V. (2002). *Water Quality: Diffuse Pollution and Watershed Management*, 2nd Edition. John Wiley & Sons Inc., New Jersey.

Northern Virginia Planning District Commission. (1979). *Assessments of Water Quality Management Strategies With the Occoquan Basin Computer Model*. Annandale, Virginia.

Northern Virginia Planning District Commission. (1994). *Mission Statement for the Occoquan Basin Model Upgrade*. Annandale, Virginia.

Northern Virginia Planning District Commission. (1987). *Reverification of Occoquan Basin Computer Model: Post Audit No.2 With 1982-1984 Monitoring Data*. Virginia.

Occoquan Watershed Monitoring Laboratory. (1991). *Water Quality Assessment for Lake Manassas, Virginia*. Manassas, Virginia.

Occoquan Watershed Monitoring Laboratory. (1996). *An Updated Water Quality Assessment for Lake Manassas, Virginia*. Manassas, Virginia.

Occoquan Watershed Monitoring Laboratory. (1998). *An Updated Water Quality Assessment for the Occoquan Reservoir and Tributary Watershed: 1973-1997*. Manassas, Virginia.

Park, K., Kuo, A.Y., Shen, J. and Hamrick, J.M. (1995). *A Three-Dimensional Hydrodynamic-Eutrophication Model (HEM-3D): Description of Water Quality and Sediment Process Submodels*, Virginia Institute of Marine Science, College of William and Mary, Virginia.

Penman, H.L. (1948). Natural Evaporation from Open Water, Bare Soil and Grass. *Proceedings of the Royal Society of London*, **193**, 120-146.

Perrens, S., Druery, B., Plastrier, B., Nielsen, J., Greentree, G.S. and Fisher, I. (1991). Nepean-Hawkesbury River Water Quality Modeling. *International Hydrology & Water Resrouces Symposium*, Australia.

Philip, J.R. (1957). The Theory of Infiltration: 1. The Infiltration Equation and Its Solution. *Soil Science*, **83**(5), 345-357.

Priestley, C.H.B. and Taylor, R.J. (1972). On the Assessment of Surface Heat Flux and Evaporation Using Large-Scale Parameters. *Monthly Weather Review*, **100**, 81-92.

Rahman, M. and Salbe, I. (1995). Modelling Impacts of Diffuse and Point Source Nutrients on the Water Quality of South Creek Catchment. *Environment International*, **21**(5), 597-603.

Ramireddygari, S.R., Sophocleous, M.A. , Koelliker, J.K., Perkins, S.P. and Govindaraju, R.S. . (2000). Development and Application of a Comprehensive Simulation Model to Evaluate Impacts of Watershed Structures and Irrigation Water Use on Streamflow and Groundwater: the Case of Wet Walnut Creek Watershed, Kansas, USA. *Journal of Hydrology*, **236**(3-4), 223-246.

Randall, C.W. and Grizzard, T.J. (1995). Management of the Occoquan River Basin: A 20-Year Case History. *Water Science and Technology*, **32**(5-6), 235-243.

Ross, M., Geurink, J., Aly, A., Tara, P., Trout, K. and Jobes, T. (2004). *Integrated Hydrological Model (IHM) Volume I: Theory Manual*. Tampa Bay Water and Southwest Florida Water Management District, Florida.

Saito, L., Johnson, B.M., Bartholow, J. and Hanna, R.B. (2001). Assessing Ecosystem Effects of Reservoir Operations Using Food Web-Energy Transfer and Water Quality Models. *Ecosystem*, **4**(2), 105-125.

Schueler, T. R. (1994). The Importance of Imperviousness. *Watershed Protection Techniques*, **1**(3), 100-111.

Selvarajan, M., Bhattacharya, A.K. and Penning de Vries, F.W.T. (1995). Combined Use of Watershed, Aquifer and Crop Simulation Models to Evaluate Groundwater Recharge Through Percolation Ponds. *Agricultural Systems*, **47**(1), 1-24.

Sherman, L.K. (1932). Streamflow from Rainfall by the Unit-Graph Method. *Engineering News Review*, **108**, 501-505.

Smith, R.H., Sahoo, S.N. and Moore, L.W. (1992). A GIS Based Synthetic Watershed Sediment Routing Model. *Water Resources Planning and management: Saving a Threatened Resource, In Search of Solutions: Proceedings of the Water Resources Sessions at Water Forum NY*, New York.

Sophocleous, M.A., Koelliker, J.K., Govindaraju, R.S., Birdie, T., Ramireddygari, S.R. and Perkins, S.P. (1999). Integrated Numerical Modeling for Basin-Wide Water Management: The Case of the Rattlesnake Creek Basin in South-Central Kansas. *Journal of Hydrology*, **214**(1-4), 179-196.

Stein, S.M., Goulet, N., Kammer, T., Waye, D. and Saffarinia, K. (1998). Occoquan Water Supply Protection Tool. *International Water Resources Engineering Conference: Proceedings*, Reston, Virginia.

Streeter, H.W. and Phelps, E.R. (1925). *A Study of the Pollution and Natural Purification of the Ohio River*, United States Public Health Service, Washington D.C.

Sullivan, A.B., Jager, H.I. and Myers, R. (2003). Modeling White Sturgeon Movement in a Reservoir: The Effect of Water Quality and Sturgeon Density. *Ecological Modeling*, **167**(1), 97-114.

Swain, E.D. and Wexler, E.J. (1996). *A Coupled Surface-Water and Ground-Water Flow Model (MODBRANCH) for Simulation of Stream-Aquifer Interaction*. U.S. Geological Survey Techniques of Water-Resources Investigations, U.S. Geological Survey, Virginia.

Tennessee Valley Authority. (1972). *Heat and Mass Transfer Between a Water Surface and the Atmosphere*, Tennessee Valley Authority, Tennessee.

Theis, C.V. (1935). The Relation Between the Lowering of the Piezometric Surface and The Rate and Duration of Discharge of a Well Using Groundwater Storage. *Transaction, American Geophysical Union*, **16**, 519-524.

Thornthwaite, C.W. and Holzman, B. (1939). The Determination of Evaporation from Land and Water Surfaces. *Monthly Weather Review*, **67**(1), 4-11.

Tim, U.S., Jolly, R. and Liao, H. (1995). Impact of Landscape Feature and Feature Placement on Agricultural Non-Point-Source-Pollution Control. *Journal of Water Resources Planning and Management*, **121**(6), 463-470.

U.S. Army Corps of Engineers. (2000). *Hydrological Modeling System HEC-HMS Technical Reference Manual*. Davis, California.

U.S. Environmental Protection Agency. (1983). Methods for Chemical Analysis of Water and Wastes. U.S. Environmental Protection Agency, Cincinnati, Ohio.

Udall, S.L., Quigley, J.M., McLeman, E.L., Geismar, E.V. and Thomann, R.V. (1966). *Delaware Estuary Comprehensive Study: Preliminary Report and Findings*, U.S. Department of the Interior, Philadelphia, Pennsylvania.

U. S. Environmental Protection Agency, Office of Air Quality. (2000). *Meteorological Monitoring Guidance for Regulatory Modeling Applications*. *EPA-454/R-99-005*, Washington, D.C.

U.S. Environmental Protection Agency (2001). *One-Dimensional Hydrodynamic/Sediment Transport Model for Stream Networks*. Washington D.C.

U.S. Environmental Protection Agency. (2002). *National Water Quality Inventory 2000 Report*. *EPA-841-R-02-001*, Washington, D.C.

U.S. Environmental Protection Agency. (2004a). *TMDL Modeling Toolbox Overview*. Washington D.C.

U.S. Environmental Protection Agency. (2004b). *About BASINS 3.0-A Powerful Tool for Managing Watersheds*. Washington D.C.

Virginia Department of Environmental Quality. (2004). *Final 2004 305(b)/303(d) Water Quality Assessment Integrated Report*. Richmond, Virginia.

Virginia State Water Control Board. (1971). *A Policy for Waste Treatment and Water Quality Management in the Occoquan Watershed*. Richmond, Virginia.

Wade, A.J., Hornberger, G.M., Whitehead, P.G., Jarvie, H.P. and Flynn, N. (2001). On Modeling the Mechanisms that Control In-Stream Phosphorus, Macrophyte, and Epiphyte Dynamics: An Assessment of a New Model Using General Sensitivity Analysis. *Water Resources Research*, **37**(11), 2777-2792.

Walton, R., Wexler, E.J., Chapman, R. and Welter, D. (2000). MODNET: An Integrated Groundwater/Open-Channel Flow Model. *Building Partnerships - 2000 Joint Conference on Water Resource Engineering and Water Resources Planning & Management*, Virginia.

Water Resources Engineers, Inc. (1968). *Prediction of Thermal Energy Distribution In Streams and Reservoirs*, Water Resources Engineers, Inc.

Weber, A., Fohrer, N. and Moeller, D. (2001). Long-term Land Use Changes in a Mesoscale Watershed Due to Socio-Economic Factors — Effects on Landscape Structures And Functions. *Ecological Modelling*, **140**(1-2), 125-140.

Wells, S. (2005). Personal Communication. Portland, Oregon.

Wetzel, R.G. (2001). *Limnology: Lake and River Ecosystems*, Third Edition. Academic Press, San Diego, California.

Whittaker, G. (2005). Application of SWAT in the Evaluation of Salmon Habitat Remediation Policy. *Hydrological Processes*, **19**(3), 839 - 848.

Watermark Numerical Computing. (2004). *PEST: Model-Independent Parameter Estimation, User's Manual 5th Edition*. Brisbane, Australia.

Wool, T.A., Ambrose, R.B., Martin, J.L. and Cormer, E.A. (2003). *Water Quality Analysis Simulation program (WASP) Version 6.0 Draft: User's Manual*. U.S. Environmental Protection Agency, Atlanta, Georgia.

Xu, Z., Godrej, A.N. and Grizzard, T.J. (2006). The Hydrological Calibration of a Linked Watershed-Reservoir Model for the Occoquan Watershed, Virginia. *In Preparation*.

York, J.P., Person, M., Gutowshi, W.J. and Winter, T.C. (2002). Putting Aquifers into Atmospheric Simulation Models: An Example from the Mill Creek Watershed, Northeastern Kansas. *Advances in Water Resources*, **25**(2), 221-238.

Young, R.A., Alonso, C.V. and Summer, R.M. (1990). Modeling Linked Watershed and Lake Processes for Water Quality Management Decisions. *Journal of Environmental Quality*, **19**(3), 421-427.

Young, R.A., Onstad, C.A., Bosch, D.D. and Anderson, W.P. (1994). *AGricultural Non-Point Source Pollution Model, Version 4.03 AGNPS User's Guide*, U.S. Department of Agriculture, Washington, D.C.

Zarriello, P.J., Barlow, P.M. and Duda, P.B. (2001). Simulating the Effects of Ground-Water Withdrawals on Streamflow in a Precipitation Runoff Model. *Bridging the Gap: Meeting the World's Water and Environmental Resources Challenges*, Virginia.

Zhen, X.Y., Yu, S.L. and Lin, J.Y. (2004). Optimal Location and Sizing of Stormwater Basins at Watershed Scale. *Journal of Water Resources Planning and Management*, **130**(4), 339-347.

Appendix A. Meteorological Data Collection and Infilling Methods for the Occoquan Model

This Appendix discusses data beyond the 1993-97 period of the research reported in this dissertation because the Occoquan model project is an ongoing effort. However, only data from the 1993-97 period were used in the current study. Other data are mentioned in the appendix to provide a complete documentation of steps taken in the overall Occoquan model project.

Efforts were made to collect, analyze, and infill the meteorological data, because these are some of the most significant driving factors in hydrological and water quality models. Because the simulation periods will be extended into 2001 for coming model updates, the corresponding meteorological data need to be updated. To obtain consistency in meteorological data from different simulation periods, similar refinement methods have to be adopted. This document includes the discussion of the availability of meteorological data for extended simulation periods. To estimate some meteorological constituents that weren't measured routinely, algorithm methods based on the available meteorological data were applied. At the same time, the infilling and disaggregation methods to complete the gaps in meteorological data time series are also discussed in detail.

Required Meteorological Data

The meteorological time series that are required by HSPF (Bicknell, et al. 2001) and CE-QUAL-W2 (Cole and Wells 2003) are as following:

Table A-1: Meteorological Data Required by HSPF and CE-QUAL-W2

	HSPF Version 12	CE-QUAL-W2 Version 3.11
Air Temperature	Required	Required
Cloud Cover	Required	Required
Dew Point Temperature	Required	Required
Potential Evapotranspiration	Required	Not Required
Precipitation	Required	Required
Solar Radiation	Required	Optional
Wind Speed	Required	Required
Wind Direction	Not Required	Required

There are some differences in meteorological data formats between these two models:

Units: In HSPF, the units are user-specified. Either English or Metric unit systems could be specified for input and output time series. CE-QUAL-W2 applies the metric unit system to both input and output data. To maintain consistency with other input data, such as distributed flow, withdrawal, land use area, dry/wet atmospheric deposition, the English system was adopted in HSPF for the Occoquan Model.

Time-step: Hourly meteorological input time series are applied by HSPF in order to precisely simulate the hydrological processes and water quality. The meteorological data interval and simulation time step can vary in CE-QUAL-W2, which makes the simulation process more flexible.

Data management and storage: In order to manage and manipulate a considerable amount of meteorological data, Watershed Data Management Utility (WDMUtil), a HSPF utility developed by AQUA TERRA (Hummel et al. 2001), is used to develop and store the time series input files for HSPF. There is no such software available for CE-QUAL-W2; all the input time series are stored in text format.

Estimation Methods for Some Meteorological Constituents

Since not all the meteorological data required by the model are routinely measured at weather stations, WDMUtil provides some calculation methods that estimate various meteorological data based on the available meteorological data. The methods that were used in the Occoquan Model are discussed below:

Cloud Cover

The hourly cloud cover data are available for two weather stations: Dulles International Airport and Reagan National Airport. But the data are not available at these two stations after 1996/05/01 (yyyy/mm/dd format used) and 1998/01/01 respectively, due to termination of cloud cover data collection.

Since 1996/05/01, Dulles International Airport weather station has recorded hourly cloud cover conditions as 5 categories. They are SKC/CLR (Clear, 0/8), FEW (few, 2/8), SCT (scattered, 4/8), BKN (broken, 6-7/8), OVC (overcast, 8/8). Such records have been converted into cloud cover in tenths, based on the corresponding value ranges in eighths. However, such a conversion might give rise to some inaccuracy in the model simulation and this impact is hard to predict. The data were obtained from the State Climatology Office, University of Virginia (Stenger 2004).

Solar Radiation

Solar radiation data are required by HSPF, and are optional but desirable in CE-QUAL-W2. For missing data, both models provide some methods to calculate solar radiation from cloud cover. In WDMUtil, latitude and daily cloud cover information are required by Hamon's empirical function (Hamon, et al. 1954) to calculate the daily solar radiation (in langleys), which, in turn, are disaggregated to hourly solar radiation time series. In CE-QUAL-W2, either the user supplies measured solar radiation data or they are calculated from cloud cover and geographic information, such as latitude. Although the cloud cover data are not fully recorded due to the reasons discussed above, NOAA's Air Resources Laboratory has performed an Integrated Surface Irradiance Study (ISIS) to collect solar radiation data nationwide since August 1995. The hourly solar radiation data are available at Sterling, Virginia since 1995/08.

Correlation coefficient comparisons were performed for a nine-month period (1995/08/01 to 1996/04/31) to evaluate the temporal and spatial consistency of solar radiation based on the Hamon's calculation method (Dulles and Reagan) and those from direct observations (Sterling). The results are given in Table A-2.

Table A-2: Correlation Coefficients of Solar Radiation Data from Direst Measurement and Estimated from Hamon's Empirical Method

Correlation Coefficient (Hourly/Daily)	Sterling (Direct)	Dulles (Hamon's)	Reagan (Hamon's)
Sterling (Direct)		0.918/0.918	0.921/0.929
Dulles (Hamon's)	0.918/0.918		0.994/0.982
Reagan (Hamon's)	0.921/0.929	0.994/0.982	

From Table A-2, the spatial difference among stations seems to be negligible. Hamon's method provided by WDMUtil appears to be quite suitable to calculate the solar radiation data when the direct measurements are not available. Since the Dulles Airport station is closer to the watershed, its data were used to calculate the solar radiation data to 1995/12/31. After 1996/01/01, the direct measurements from Sterling station were applied to the whole watershed.

Evaporation and Transpiration

HSPF requires the potential ET (evapotranspiration) for the water budget. Since direct measurement data are usually not available, WDMUtil provides three empirical methods to calculate the potential ET. These are the Jensen formula, Hamon formula and Penman Pan formula (Hummel, et al. 2001). For the Penman Pan method, maximum daily air temperature, minimum daily air temperature, average daily dew point temperature, total daily wind movement and total daily solar radiation time series are needed in order to calculate the evaporation from open waterbodies. They are used to account for the water lost due to evaporation in the RCHRES modules. The Jensen formula and Hamon formula are for the potential ET calculation. The results from the two methods indicated that the potential ET based on the Hamon formula is slightly smaller than from the Jenson formula. Because both methods tend to underestimate potential ET, especially for winter months (Hummel et al. 2001), the potential ET from the Jensen method might represent the reality better, and it was used in the model applications.

In CE-QUAL-W2 Version 3, evaporation is used in the heat and water budget. Six empirical functions are provided to perform evaporation calculations based on the wind speed, and other meteorological information. The default formula is adapted from Edinger et al.(1974). In the current model application, the default formula was applied.

Simulation Periods

Four simulation periods were chosen for the Occoquan Model. They are 1982-1987, 1988-1992, 1993-1997 and 1998-2001. The criteria for selecting simulation time periods are based on the availability of data and update of land use information. The land use

data, which are updated every five years, are available for 1984, 1989, 1995, and 2000. The simulation periods were chosen to be four-to-six-year periods approximately centered on the land use update years.

Meteorological Data Sources, Coverage and Infilling Methods (except Precipitation)

Data Sources and Coverage

The meteorological data (except precipitation) were collected from several data sources. These include NOAA's National Climatic Data Center (NCDC), NOAA's Integrated Surface Irradiance Study (ISIS) and Virginia State Climatology Office (VSCO).

Table A-3: Meteorological Data (except Precipitation) Coverage for Period One (1982/01/01- 1987/12/31)

	Units	Time Step	Location	Data Source	Missing Hours/Days	Coverage (%)
Air Temperature	°F	Hourly	Reagan	NCDC	1	99.9
			Dulles	NCDC	0	100.0
Cloud Cover	Tenths	Hourly	Reagan	NCDC	0	100.0
			Dulles	NCDC	23	99.9
Dew Point Temperature	°F	Hourly	Reagan	NCDC	2	99.9
			Dulles	NCDC	27	99.9
Wind Speed/ Wind Direction	Knots/–	Hourly	Reagan	NCDC	0	100.0
			Dulles	NCDC	23	99.9
Max. Air Temperature	°F	Daily	Reagan	NCDC	0	100.0
			Dulles	NCDC	0	100.0
Min. Air Temperature	°F	Daily	Reagan	NCDC	0	100.0
			Dulles	NCDC	0	100.0
Solar Radiation[1]	Langley	Hourly				

[1] Refer to the discussion in the solar radiation section.

Table A-4: Meteorological Data (except Precipitation) Coverage for Period Two (1988/01/01- 1992/12/31)

	Units	Time Step	Location	Data Source	Missing Hours/Days	Coverage (%)
Air Temperature	°F	Hourly	Reagan	NCDC	0	100.0
			Dulles	NCDC	2	99.9
Cloud Cover	Tenths	Hourly	Reagan	NCDC	0	100.0
			Dulles	NCDC	1	99.9
Dew Point Temperature	°F	Hourly	Reagan	NCDC	0	100.0
			Dulles	NCDC	15	99.9
Wind Speed/ Wind Direction	Knots/–	Hourly	Reagan	NCDC	0	100.0
			Dulles	NCDC	4	99.9
Max. Air Temperature	°F	Daily	Reagan	NCDC	0	100.0
			Dulles	NCDC	0	100.0
Min. Air Temperature	°F	Daily	Reagan	NCDC	0	100.0
			Dulles	NCDC	0	100.0
Solar Radiation[2]	Langley	Hourly				

Table A-5: Meteorological Data (except Precipitation) Coverage for Period Three (1993/01/01- 1997/12/31)

	Units	Time Step	Location	Data Source	Missing Hours/Days	Coverage (%)
Air Temperature	°F	Hourly	Reagan	NCDC	1	99.9
			Dulles	NCDC	0	100.0
Cloud Cover	Tenths	Hourly	Reagan[2]	NCDC	5817	86.7
			Dulles[3]	NCDC	5	99.9
Dew Point Temperature	°F	Hourly	Reagan	NCDC	3	99.9
			Dulles	NCDC	62	99.8
Wind Speed/ Wind Direction	Knots/–	Hourly	Reagan	NCDC	3	99.9
			Dulles	NCDC	4	99.9
Max. Air Temperature	°F	Daily	Reagan	NCDC	7	99.5
			Dulles	NCDC	0	100.0
Min. Air Temperature	°F	Daily	Reagan	NCDC	0	100.0
			Dulles	NCDC	0	100.0
Solar Radiation	Langley	Hourly	Sterling	ISIS[4]	0	100.0

[2]Refer to the discussion in the solar radiation section.
[3] Data after 1996/05/01 are recorded as five descriptive categories. Refer to the discussion in cloud cover.
[4] Before 1996/01/01 solar radiation data are calculated from cloud cover, and after 1996/01/01 solar radiation data from Sterling are used.

Table A-6: Meteorological Data (except Precipitation) Coverage for Period Four (1998/01/01- 2001/12/31)

	Units	Time Step	Location	Data Source	Missing Hours/Days	Coverage (%)
Air Temperature	°F	Hourly	Reagan	NCDC	25	99.9
			Dulles	NCDC	53	99.8
Cloud Cover	Tenths	Hourly	Dulles	VSCO	0	100.0
Dew Point Temperature	°F	Hourly	Reagan	NCDC	60	99.8
			Dulles	NCDC	54	99.8
Wind Speed/ Wind Direction	Knots/–	Hourly	Reagan	NCDC	49	99.8
			Dulles	NCDC	54	99.8
Max. Air Temperature	°F	Daily	Reagan	NCDC	7	99.5
			Dulles	NCDC	12	99.1
Min. Air Temperature	°F	Daily	Reagan	NCDC	0	100.0
			Dulles	NCDC	7	99.5
Solar Radiation	Langley	Hourly	Sterling	ISIS	0	100.0

Infilling of Missing Data (except Precipitation)

Based on the spatial and temporal characteristics of the data, the availability of alternative data sources, and the extent of missing or invalid periods, the applied substitution procedures of the missing data are described below:

If the missing data gap was less than or equal to 6 hours, then linear interpolation was applied.

If the missing data gap was greater than 6 hours, then data for the corresponding period at the alternative weather station were used to fill the gap.

This procedure was based on the classification of the gaps in meteorological data ((Latini and Passerini 2004)). Usually, the data gaps are classified into four categories, based on the gap duration. They are: very short gaps (1-2 hours); short gaps (up to 4 hours); medium gaps (up to 8 hours) and long gaps (up to 80 hours). There are several common techniques to handle the medium gaps, including the interpolation, mean or medium imputation, nearest neighbor techniques, etc. Based on the recommendation from EPA (USEPA 2000), linear interpolation is considered to be the “best estimator” and thus was adopted to fill the medium gaps in the meteorological data.

An evaluation of the validity of the substitution by data from the neighbor weather station data was done (Table A-7). The R^2 values of one-year data (1995/01/01-1995/12/31)

from Dulles and Reagan were analyzed in order to evaluate the validity of restoring missing data in Dulles by filling the data from Reagan, or vice versa.

Table A-7: R^2 Values of Meteorological Data (except Precipitation) between Dulles and Reagan Weather Stations

Data	Unit	Time Step	R^2
Air Temperature	°F	Hourly	0.987
Cloud Cover	Tenths	Hourly	0.880
Dew Point Temperature	°F	Hourly	0.989
Wind Speed	Knots	Hourly	0.672
Max. Air Temperature	°F	Daily	0.996
Min. Air Temperature	°F	Daily	0.981

From Table A-7, it can be seen, except for the wind speed, other meteorological data in these two stations were highly correlated and thus it would be reasonable to infill the missing data of one station by using the corresponding data from the other one. For wind speed data, these two stations were considered to be weakly positively correlated. However, the data coverages for the four periods are all above 99.8% (Tables A-3–A-6), that it was still reasonable to use this substitution method for the remaining 0.2% of missing data.

Precipitation Data Sources, Coverage and the Infilling Methods

Data Sources

Precipitation is one of the most important components in hydrological processes. The quality and quantity of the precipitation data are the key factors to calibration and validation of the hydrological and water quality models. After realizing the lack of adequate precipitation information, more rain gauge stations were established in the Occoquan Watershed during calendar year 2001. Before 2001, there were nine rain gauge stations located in or close to the watershed. Of them, rain gauge stations at OWML, Lake Manassas, and Lake Jackson, Prince William County Regional Landfill and Balls Ford Road Yard Waste Facility are located within the watershed, and are operated by OWML. The Lorton station is located just outside the watershed and is operated by Fairfax Water. The rain gauge stations at Dulles International Airport, the Plains and Warrenton are operated by the National Weather Service (NWS).

In 2001, another 8 rain gauge stations were installed by OWML within the watershed. These are Airlie (operating since Jan, 2001), C. Hunter Ritchie Elementary School (Feb, 2001), Clifton Elementary School (Feb, 2001), Crockett Park (Apr, 2001), Cedar Run Wetlands (Feb, 2001), Fair Oaks Police Department (Feb, 2001), Evergreen Fire Department (Jun, 2001) and Camp Snyder Wetlands (Mar, 2001). All these stations are shown in Figure A-1. Although data are available for these new stations, they will not be used in the current model application until the period after 2002 is simulated. This decision was based on the consideration of consistency of maintaining the same Thiessen Polygons for the whole simulation period (1998-2001).

The availability of the data for the periods of interest (1982-2001) from each station is given below (Table A-8).

Table A-8: Total Precipitation Data Coverage at Various Rain Gauge Stations

Location	Hourly data	Daily data
Balls Ford Road Waste Yard Facility	1995-2001	1995-2001
Dulles International Airport	1997-2001	1982-2001
Lake Jackson	1993-2001	1993-2001
Lake Manassas	1990-2001	1985-2001
Lorton	-	1982-2001
OWML	1989-2001	1982-2001
Prince William County Regional Landfill	1995-2001	1995-2001
The Plains	1982-2001	1982-2001
Warrenton	-	1982-2001

The coverage of the precipitation data from each simulation period from each station are given below (Table A-9).

Table A-9: Precipitation Data Coverage for Four Simulation Periods

Coverage (%)	1982-1987	1988-1992	1993-1997	1998-2001
Balls Ford Road Waste Yard Facility	-	-	60.0	100
Dulles International Airport	-	-	-	>95
Lake Jackson	-	-	96.5	100
Lake Manassas	-	-	78.7	43.8
Lorton	100	100	100	100
OWML	-		90.1	96.7
Prince William County Regional Landfill	-	-	60.0	100
The Plains	91.7	91.1	96.3	87.1
Warrenton	95.1	99.6	99.7	98.5

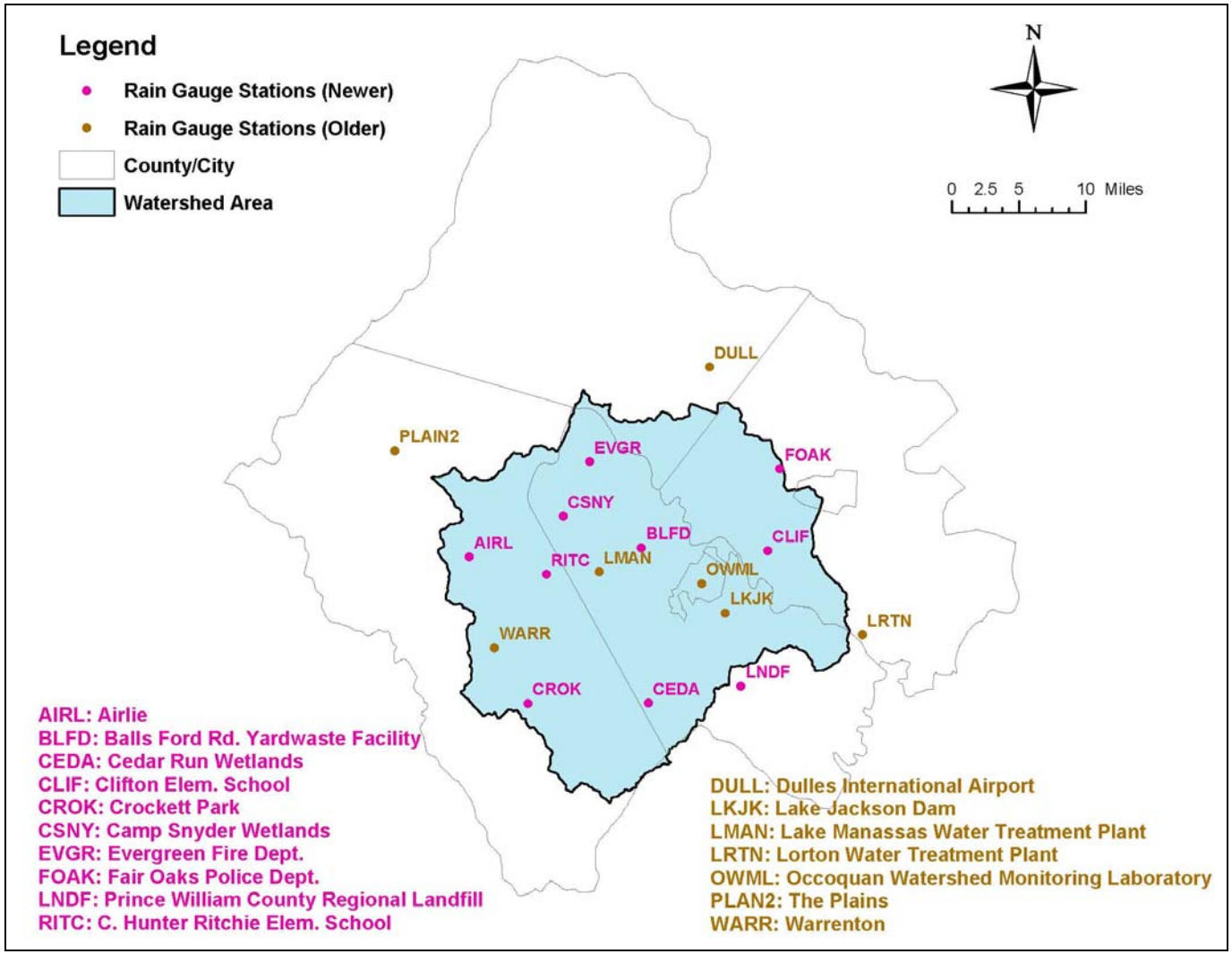

Figure A-1: Rain Gauge Station Map

Missing Data Infilling Strategy

The infilling of missing rainfall data was a challenge. Due to the complicated spatial and temporal distribution of the rainfall events, there is no uniform distribution pattern that can be applied to missing rainfall events at each individual station. Even at the same station, the distribution of the rainfall varies for discrete rainfall events.

The basic assumption behind the infilling strategy was that the hourly distribution of a rainfall event at one station is similar to that at the neighbor station. So if hourly rainfall data were missing at one station when daily rainfall records showed non-zero rainfall events, the hourly distribution data from the nearby station were adopted to fill in the missing rainfall data. This suggested that even if the daily rainfall might vary at two close stations, the distribution of the rainfall event was assumed to be similar. This assumption might be reasonable if there was no temporal difference between these two stations. But during the summer time, when thunderstorm events or other extreme events are not unusual in this region, such an assumption might be questionable.

For each of the specific stations, the strategies are discussed below.

OWML

Situation I: if there was 0.0 inch rainfall recorded in the electronic daily rainfall database (EDRD), then the missing hourly rainfall data for this specific date were filled with 0.0.

Situation II: if there was non-zero data recorded in the EDRD, then the total daily rainfall in OWML was disaggregated into hourly data before filling in the missing data. The hourly distribution pattern was based on that of the neighbor rain gauge station. In this case, it was Lake Manassas, for which data were available back to 1990.

Two full months of data (Feb. and March) were missing in 1989, when the data from Lake Manassas were also not available. The infilling method for missing data for this period hasn’t been decided yet.

Situation III: if there was no record in the EDRD, then daily rainfall summary sheets were consulted. If zero rainfall was recorded in the paper sheets, then the missing hourly rainfall data on this specific date were filled with 0.0. If a non-zero rainfall event was recorded, then the filling method would be similar to Situation II.

Situation IV: if the records were missing both in the EDRD and the daily summary sheets, then data from the nearby station (Lake Manassas) were used directly without modification.

Lake Manassas

The infilling methods were similar to those for the OWML station. For Lake Manassas, there was more than one station that could possibly be used in filling missing data. They were the OWML, Balls Ford and Robert Trent Jones Golf Course station (RTJ). Due to their distance from Lake Manassas, the priority of the alternative stations was: RTJ> Balls Ford>OWML. That meant that if the data from RTJ were available, then they would be applied to fill the missing data. If they were not, then the data from Balls Ford, if available, were used to fill the missing data at Lake Manassas.

The biggest rainfall gap at Lake Manassas was from 1997/01/01 to 1999/03/31 when no hourly data were available (the station was being relocated). For this period, the RTJ data was used to fill in this gap.

Since the hourly precipitation data from Lake Manassas were only available after 1990, how to use the uncompleted data set in the simulation of Period Two (1988-1992) hasn't been decided yet.

Lake Jackson

The infilling methods were similar to those for the OWML station. But the alternative rain data source for missing data infilling was usually OWML, because it is the closest station to Lake Jackson.

Because the hourly precipitation data from Lake Jackson were only available after 1993, it might only be used in the Model for Period Three and Period Four.

Dulles International Airport

Hourly precipitation data were only available for the period 1998-2001. For the other three simulation periods, only daily data were available. This means disaggregating of the daily data into the hourly data was done before its application to modeling.

For the simulation periods I to III, the infilling of missing data included two steps:

Step one: filling the missing data in the daily rainfall data records.

If the daily data were missing, then the data at Dulles station in the EDRD file were consulted. If there were data recorded for the specific date, then the data from the EDRD were used. Otherwise, the daily data from the closest station (OWML, in this case) were used.

Step two: disaggregating the daily data into hourly data.

The WDM utility provides the function to distribute the daily data into hourly data based on the distribution of the neighbor stations. The distribution method is similar to what was suggested above. If the daily rainfall data were recorded as zero, then all the hourly data at that day were assigned 0.0. If the daily rainfall data were non-zero, then the distribution was following that of the neighbor stations whose total daily rainfall data were closest to the daily total. If the difference of daily rainfall data between these two stations was out of a user-specified tolerance, the triangular distribution method with the center at noon was used. Because the triangular method was not accurate, a high tolerance value (95%) was used. OWML and Lake Manassas station were chosen to be the secondary stations for the Dulles station.

In order to investigate the validation of this method, desegregation for the Dulles station (Period Four) was performed. In this four-year period (1416 days), 458 days were recorded as rain days. The triangular method was used 70 times and the remaining rain

days were distributed based on the secondary station (OWML). Among these 70 rain events, 49 of them had a total daily rainfall less than 0.05 inches, 13 of them had a total daily rainfall 0.05-0.1 inches. Eight out of 70 rainfall events had daily rainfall records greater than 0.1 inches and might have some impact on the later model applications. These eight events are shown in the table below.

Table A-10: Daily Precipitation Events Distributed by the Triangular Method

Precipitation Range (inches)	Counts	Date	Precipitation (inches)
0.1~0.2	3	2001/08/17	0.16
		1999/07/06	0.16
		1999/08/27	0.17
0.2~0.3	2	1998/06/02	0.23
		1999/07/07	0.21
0.3~0.4	0	---	---
0.4~0.5	1	2000/06/25	0.49
>0.5	2	2000/01/25	0.84
		2001/06/13	0.65

The Plains

Hourly data from The Plains were available for the four simulation periods. The missing data infilling methods were similar to that for the OWML station, but the alternative stations were Lake Manassas and OWML, based on the availability of the data. Lake Manassas was preferred due to its proximity.

For the missing data before 1989, the restoration methods haven't been decided yet.

Warrenton

Only daily data were available for the four simulation periods. The missing daily data substitution approach was similar to that for Dulles, but the alternative station is The Plains.

Lorton

Only daily data were available for the four simulation periods. The missing daily data substitution approach was similar to that for Dulles, but the alternative stations are Lake Jackson and OWML.

The Resultant Hourly Precipitation Time Series

Table A-11 shows the resultant precipitation time series based on the above suggestions. The checked boxes indicate that the hourly precipitation time series in the specific location and period were ready to be used.

Table A-11: Hourly Precipitation Time Series at Various Rain Gauge Stations in the Four Simulation Periods

Hourly Precipitation Time Series	1982-1987	1988-1992	1993-1997	1998-2001
Dulles			Y	Y
Lake Jackson	N/A	N/A	Y	Y
Lake Manassas			Y	Y
Lorton			Y	Y
OWML			Y	Y
The Plains	Y	Y	Y	Y
Warrenton	Y	Y	Y	Y

For the earlier periods (1982-1987 and 1988-1992), the daily data were available at most of the locations. However, only The Plains station (1982-1987, 1988-1992) and OWML (1989-1992) had the hourly precipitation data. That implies the distribution from the daily data in other locations into the hourly data was based only on these two stations. Because The Plains is located in the Bull Run mountain region outside the watershed, its temporal distribution of rainfall events might be different from stations located on the other side of the mountain. It is questionable to apply its distribution to other stations as the only secondary station. Plus the concerns of this study are on the simulation period 1993-1997, and more efforts are focused on the latest periods. For the earlier periods, the daily data were ready. After the distribution patterns are chosen, the hourly precipitation time series will be ready with some extra work.

References

Bicknell, B.R., Imhoff, J.C., Kittle, J.L., Jobes, T.H. and Donigian, A.S. (2001). Hydrological Simulation Program-Fortran HSPF Version 12 User's Manual, U.S. Environmental Protection Agency, National Exposure Research Laboratory, Athens, Georgia.

Cole, T. M. and Wells, S. A. (2003). CE-QUAL-W2: A Two-Dimensional Laterally Averaged, Hydrodynamic and Water Quality Model, Version 3.2 User Manual. U.S. Army Corps of Engineers, Washington, D.C.

Edinger, J.E., Brady, D.K. and Geyer, J.C. (1974). Heat Exchange and Transport in the Environment. Electric Power Research Institute, Palo Alto, California.

Hamon, R.W., Weiss, L.L. and Wilson, W.T. (1954). Insolation as an Empirical Function of Daily Sunshine Duration. Monthly Weather Review, 82(6), 141-146.

Hummel, P., Kittle, J.L. and Gray, M. (2001). WDMUtil Version 2.0: A Tool for Managing Watershed Modeling Time-Series Data User's Manual, AQUA TERRA Consultants, Decatur, Georgia.

Latini, G. and Passerini, G. (2004). Handling Missing Data: Applications to Environmental Analysis, WIT Press, Southampton, United Kingdom.

Stenger, J. (2004). Personal Communication. Manassas, Virginia.

U. S. Environmental Protection Agency, Office of Air Quality. (2000). Meteorological Monitoring Guidance for Regulatory Modeling Applications. EAP-454/R-99-005, Washington, D.C.

Appendix B. Watershed Delineation and Segmentation

Watershed delineation and segmentation was the first step in HSPF model setup. This appendix provides general background information about watershed delineation and segmentation. In addition to spatial data and their sources, this appendix summarizes the results of Occoquan Watershed delineation and segmentation.

Definitions

Watershed delineation is the process to define the boundaries of a watershed.

Watershed segmentation is the process to divide a watershed into smaller sub-watersheds and generate watershed segments for model applications.

Five characteristics that play an important role in watershed segmentation are "1) rainfall or important meteorological data; 2) soil type; 3) land use conditions; 4) reach characteristics; 5) any other important physical characteristic (infiltration, overland slope, etc.)" (USEPA 2004a).

Software

USEPA BASINS package (Version 3.1), ArcView (Version 3.11) and Spatial Analyst (Version 1.1) were used in watershed delineation and segmentation. ArcGIS (Version 8.2) was also used in spatial data analysis.

Data and Their Sources

Both regional and local data were used in watershed delineation and segmentation. These are described in greater detail below.

Regional Data

A BASINS extension, Data Extraction function, was used to extract regional data from the EPA web site (http://www.epa.gov/waterscience/ftp/basins/gis_data/huc/), which was organized by the U.S. Geological Survey (USGS) eight-digit Hydrological Unit Code

(HUC). The data set for the Middle Potomac-Anacostia-Occoquan Watershed (HUC 02070010) was downloaded.

This data set includes four types of data: base cartographic data, environmental background data, environmental monitoring data and point sources/loading data. Table B-1 lists some BASINS data products that are available from the EPA web site. These data are at the regional or state level and most of them are provided by USGS, USEPA, and NOAA.

Table B-1: BASINS Data Products

Type of Data	BASINS Data Products
Base Cartographic Data	Hydrological Unit Boundary, Major Roads, State and County Boundaries, etc.
Environmental Background Data	Reach File Version 3 (RF3), National Hydrography Database (NHD), Digital Elevation Model (DEM), etc.
Environmental Monitoring Data	Water Quality Monitoring Stations and Data Summaries, Gage Sites, National Sediment Inventory (NSI) Stations and Database, etc.
Point Sources/Loading Data	Permit Compliance System (PCS) Sites and Annual Loadings, Industrial Facilities Discharge (IFD) sites, Toxic Release Inventory (TRI) Sites, etc.

These data provided necessary information for the Occoquan Model application and facilitated watershed delineation and segmentation.

Table B-2: Local Spatial Data for the Occoquan Watershed

Spatial Data	Description	Source
Digital Elevation Model (DEM)	1:24,000 Scale DEM for the Northern Virginia Region	NVRC
National Hydrography Database (NHD)	NHD Waterbody and waterbody reach themes for the Occoquan Watershed	NVRC
Road Map	Road Map for the Northern Virginia Region	NVRC
Land Use Map	1995 Land Use Map (14 Land Use Categories with forest/idle as default) for the Occoquan Watershed	NVRC
Water Quality Monitoring Station Map	Long-term Stream Water Quality Stations in the Occoquan Watershed	OWML
Point Discharge Map	UOSA Discharge Location in the Occoquan Watershed	UOSA
Weather Station Sites Map	Weather Stations in the Occoquan Watershed	OWML, NOAA
Precipitation Station Sites Map	Rainfall Gauge Stations in the Occoquan Watershed	OWML

Local Data

Local spatial data were preferred over regional or state data in watershed delineation and segmentation. This is because they provide more accurate and detailed information about the watershed. Table B-2 lists the local data and their sources that were used in this model application.

Methodology

The BASINS package provides two delineation functions: automatic and manual delineation. The manual delineation tool allows users to apply their knowledge of the watershed topography to manually disaggregate watersheds into smaller sub-watershed, while the automatic delineation tool allows users to delineate the watershed based on a DEM file. In this model application, the automatic delineation function was used because it provided fast results and reduced uncertainty during the delineation process. Then, manual delineation function was used for specific considerations (see discussion below).

Step One: Projection and Coordinate System Definition

Before ArcView and BASINS were applied for watershed delineation and segmentation, all spatial distribution maps were assigned with the same projection and coordinate system. This process is extremely important because ArcGIS will not perform geographic transformation if the coordinate systems are not defined. More importantly, spatial data will not display or overlay properly if an appropriate projection and coordinate system are not used. In addition, because the unit systems are different for each projection system, it might result in confusion in spatial analysis. For example, NAD 1983 State Plane uses the metric system and measures surface areas as square meters. However, the NAD 1927 State Plane applies the English system, and the surface areas are described as square feet. Therefore, one specific projection system has to be applied to all spatial data to avoid mistakes.

In this model application, the spatial data from NVRC were in digital map formats and the original projection and coordinate systems were lost during the transfer, and were provided by NVRC later. The maps were defined in NAD 1983 State Plane Virginia

North FIPS 4501 as the projection coordinate system and GCS North American 1983 as the geographic coordinate system.

The spatial data from OWML were created from dBASE tables with corresponding geographic information. ArcGIS was used to convert dBASE format to shape files that could be used by BASINS. The projection coordinate system for these shape files was defined as NAD 1983 State Plane Virginia North FIPS 4501 and the geographic coordinate system as GCS North American 1983.

Step Two: DEM Set Up

The basis of the automatic delineation tool is related to flow direction and accumulation based on topographic characteristics. DEM is a raster file that represents surface characteristics with regular size cells. For example, the DEM for the Northern Virginia Region is a 1:24K DEM coverage map that has a grid spacing resolution of 30 m and vertical resolution of 1 m. ArcView and Spatial Analyst used the DEM file to determine the flow direction and accumulation for each grid cell. These data helped to identify boundaries, inlets, outlets, channel lengths and slopes for each segments. The NHD file provided by NVRC was used to adjust stream locations by forcing flow directions to match observed stream sites.

Step Three: Stream Definition

In this process, the minimum size of the subbasins was defined, which helped to determine the size and the total number of the created sub-watersheds. The suggested threshold area was 1,500 hectares that was adopted in the following processes. The resultant number of sub-watersheds was 63. Compared with the current watershed model application with 20 subbasins, the updated watershed segmentation tripled the number of the subbasins and was expected to enhance the resolution of the model application.

Smaller threshold areas could be applied in the watershed segmentation. This will result in smaller segment sizes and more segment numbers. However, due to the consideration of availability of meteorological data, this is not adopted in the current model application (detailed explanation given later in this appendix).

Step Four: Outlet and Inlet Definition

After the subbasin threshold area was defined, the outlets for each subbasin were generated based on flow direction and accumulation. The accurate definition for outlets in this process is the "stream junction points" (USEPA 2004b). They include both the most downstream and upstream points of a segment.

The total number of the outlets depends on the subbasin threshold and DEM. When the suggested threshold area was applied, the resultant outlets were 30. However, some outlets were very close to each other and thus the correspondent subbasins areas would be too small to be properly simulated in HSPF. For example, there were two outlets located in the upper Bull Run region, and the drainage area between these outlets was less than 4 hectares. Because the duration of hydrologic activities in such a small area was so short, compared to available meteorological data, the change of runoff would not to be captured by HSPF. Thus, these tiny subbasins will not increase the accuracy of HSPF. Instead, they would complicate the user control files of HSPF and increase the simulation time. Due to these considerations, such outlets were deleted from future procedures. In total, three such outlets were deleted.

The process allows for adding or deleting outlets and inlets based on site-specific considerations. Several considerations contributed to this process. First were the water quality stations. Because model calibration and validation are based on the comparison between observed and simulated water quantity and quality data, it is reasonable to adjust outlet locations of sub-watersheds so that the most downstream sites match with water quality stations. Thus, the simulated stream data can be directly compared with those from water quality stations. Table B-3 lists the stream sampling stations that were defined as outlets in the Occoquan Watershed segmentation.

However, some water quality stations were very close to the outlets generated by the program. For example, there was one outlet located within 1 mile upstream of ST60, and the correspondent drainage area was less than 5 hectares. Such a small subbasin would

give rise to problems similar to those mentioned earlier. Because the water quality station would provide observed data for calibration and validation, the outlet was deleted.

Table B-3: Stream Sampling Stations Used in the Occoquan Watershed Segmentation

Station ID	Locations	Latitude	Longitude
ST01	Occoquan Reservoir near the Dam	38° 41.633´ N	77° 16.633´ W
ST10	Occoquan River near Manassas	38° 42.310´ N	77° 26.729´ W
ST25	Cedar Run near Aden	38° 36.905´ N	77° 33.223´ W
ST30	Broad Run near Bristow	38° 44.933´ N	77° 33.853´ W
ST40	Bull Run near Clifton	38° 45.983´ N	77° 24.900´ W
ST45	Bull Run near Manassas Park	38° 48.187´ N	77° 26.977´ W
ST60	Broad Run near Catharpin	38° 53.348´ N	77° 34.234´ W
ST70	Broad Run near Buckland	38° 46.822´ N	77° 40.356´ W

The second concern was point source input. The UOSA discharge enters into Bull Run and drains approximately 1.0 stream miles before passing the water quality station ST45. This provides sufficient mixing opportunity before it reaches the water quality station. From the modeling point of view, the UOSA discharge should be represented as a point discharge in a specific land segment so that the discharge will be completely mixed with upstream flows before reaching a segment outlet.

The first consideration was to assign UOSA as an inlet in the watershed. Inlets are defined as “either the outlet of draining watersheds (part of the overall watershed that is not intended to be simulated) or point sources of discharge”. The resultant inlet for UOSA was located inside a subbasin. However, a point discharge is added directly to a completely mixed stream in HSPF. The stream routing could not distinguish the location of the point discharge and it is assumed to be at the very upstream end of the stream. Thus, although UOSA was represented as a point discharge in the middle of the stream in the watershed segment, it was actually assumed to be located at the upstream end of the watershed segment in HSPF. Thus, the location of UOSA was moved a few miles upstream in HSPF. Because the relative upper stream location of UOSA would provide more detention time in the stream segment, it probably will increase the potential for physical and chemical reactions such as settling, nitrification and denitrification. The resultant water quality changes due to UOSA location adjustment are hard to predict. Previous experience indicated that UOSA has a significant influence on the water quality in the Occoquan Reservoir. Thus, the accurate description of UOSA in the model would

provide more confidence on the model application. As the result, the idea to represent UOSA as an inlet was aborted.

Because UOSA could not be represented as an inlet in the watershed segmentation, the next consideration was to describe it as an outlet. As mentioned earlier, outlets in this process are locations where streams join. They link the upper stream segments to the lower stream segments. When UOSA was defined as an outlet, a segment was generated between UOSA and ST45. In this segment, the UOSA outflow was discharged at the starting point of the stream and well mixed before reaching the outlet (ST45). Thus the location of UOSA accurately represented the physical location of UOSA. The segment area was relatively small (around 115 hectares or 0.5 square miles) and overland hydrological activities would not be accurately represented. However, this small segment is kept in the watershed segmentation. There were two reasons for this. Firstly, the major purpose of this segment was to represent UOSA as a point source discharge, and it was achieved by this segmentation. At the same time, the mixture of UOSA discharge with the stream flow would also be represented. Secondly, because the segment area was so small, the surface and subsurface flow generated in this area would be relatively small when compared with upstream inflow. Thus, its impact on overall simulation would probably be ignored.

The third concern in the outlet definition was the land use patterns. Although HSPF distinguishes physical properties associated with different land uses, there is no mechanism to specify locations for each land use at each segment. For example, if a segment has 1000 acres of forest and idle area, HSPF assumes that all of these 1000 acre forest and idle area are evenly distributed inside the segment. This could lead to some potential inaccuracies.

A tributary of Bull Run River, Flat Branch, provides a good example. Upstream of Flat Branch lies the Manassas National Battlefield Park and Bull Run Regional Park, with more than 5000 acres covered by forest vegetation. It is called “one of the region’s most unspoiled areas”, and the stream is protected from nonpoint source pollution (NPS 2004). However, before draining into Bull Run, Flat Branch passes the relatively highly

developed Cities of Manassas and Manassas Park. Such urbanized areas modify the hydrological systems by reducing pervious land surface, and thus increase the potential for nonpoint source pollution for receiving streams. Thus, these two land pieces in the Flat Branch drainage area are expected to have different impacts on water quality of neighborhood streams. However, such impacts cannot be appropriately characterized if they are represented by one big land segment in HSPF, because HSPF would assume that the vegetated parks and urban areas are evenly distributed in this land segment. Such an assumption might moderate impacts from urbanized area before Flat Branch drains into Bull Run. When individual segments are assigned for these two land pieces, even though this will be undistinguishable in term of water quality of the Occoquan Reservoir, it is expected to show differences on the neighborhood stream water quality.

Another example was segments 40 and 55 in the Cedar Run Subbasin. An outlet was manually added to separate these two segments. One reason was to break a large segment into two, so that these two segments had average sizes. Another reason was to account for their different land uses. The 1995 land use map indicated that the dominant land use categories for subbasin 40 are forest (42.4%) and high till crop (31.3%). However, forest (55.9%) was the dominant land use for subbasin 55 and the high till crop areas only accounted for 13.1% of this subbasin. Because the agricultural land uses were located more downstream on Cedar Run (segment 40), more agricultural-related pollution such as sediment and nutrients were expected in the receiving streams, especially during spring and fall. However, if these two segments were assumed to be one big segment as they originally were, HSPF would evenly distribute these agricultural land uses into the one big segment. Thus, the impact of the agricultural activities on the receiving streams probably would have been moderated. Because no other specific consideration was accounted for to add this outlet, the location was somewhat arbitrary.

Step Five: Main Watershed Outlet Selection and Definition

The most downstream outlet (close to ST01) was selected as the main watershed outlet. It defined the total drainage area of the watershed. After the main watershed outlet was selected, the program automatically performed the calculation of geomorphic parameters

for each subbasin and associated stream reach. The parameters calculated for the subbasin included the area, perimeter, length, stream length, etc. (Table B-4). These data were used to select physical coefficients for HSPF.

Table B-4: Subbasin Theme Data Generated by BASINS (Source: USEPA 2004a)

Field Name	Description	Unit
GRIDCODE	ArcView internal field	–
SUBBASIN	Subbasin number	–
AREA	Subbasin area	Hectares
LEN1	Stream reach length	Meters
SLO1	Subbasin slope	%
SLL	Field slope length	Meters
CSL	Reach (longest path) slope	%
WID1	Reach width	Meters
DEP1	Reach depth	Meters
LATITUDE	Latitude of the subbasin centroid	Decimal degrees
ELEV	Elevation of the subbasin centroid	Meters

Summary

The resultant final number of segments was 56 and this is approximately triple that in the previous model application. The average subbasin area was reduced to 2704 hectares (10.4 square miles) and the total area was 151467.8 hectares (584.8 square miles). Tables B-5 and B-6 give a detailed summary of the Occoquan Watershed segmentation. Figure B-1 gives the segmentation map.

Table B-5: Occoquan Watershed Segmentation Summary

Parameters	Average	Maximum	Minimum	Sum
Subbasin Area (hectares)	2704.8	6989.5	64.0	151467.8
Stream Reach Length (meters)	12100.6	20230.4	1547.5	677634.7
Subbasin Slope (%)	19.9	54.0	7.91	1111.4
Field slope length (meters)	19.2	61.0	0.05	1073.8
Reach (longest path) slope (%)	2.9	13.4	1.0	161.2
Reach width (meters)	8.9	16.5	1.0	495.7
Reach depth (meters)	0.5	0.7	0.1	25.7
Elevation (meters)	293.27	632	146	16423.0

Table B-6: Summary of Occoquan Watershed Subbasins

Summary of Occoquan Watershed Subbasins				
Subbasin	**Area (hectares)**	**Length (meters)**	**Slope (%)**	**Elevation (meters)**
1	3730.59	13527.50	8.38	272
2	2007.09	11550.83	14.43	311
3	2353.14	12038.59	19.66	310
4	3194.82	14521.17	18.10	228
5	4131.18	18708.21	9.36	291
6	2420.91	13468.72	16.06	316
7	6946.56	20230.44	31.91	554
8	2463.84	9649.63	36.30	632
9	2485.62	17726.96	27.26	410
10	2284.02	16708.08	20.85	354
11	1971.45	10701.79	15.00	211
12	1789.38	10087.65	16.86	217
13	1552.23	10403.88	13.72	223
14	1856.16	7723.70	11.61	218
15	442.71	4097.32	18.39	174
16	1825.2	11257.32	19.03	265
17	2407.23	10788.64	23.98	303
18	4835.88	16560.91	26.56	262
19	404.28	4644.65	14.94	352
20	1812.96	13215.61	24.09	515
21	1632.15	8365.17	13.08	327
22	1605.42	10139.07	17.73	258
23	5073.66	18787.72	31.44	225
24	2378.7	13256.45	33.47	278
25	1749.24	7012.18	10.70	229
26	2777.4	14749.88	13.18	280
27	2045.7	11793.49	28.34	294
28	5043.96	18749.87	30.57	272
29	1852.47	10169.86	29.11	465
30	5434.65	16313.77	31.17	507
31	3486.6	16431.78	11.17	209
32	924.48	8613.71	16.21	244
33	513.9	4480.53	20.84	241
34	307.08	4372.61	23.60	191
35	3173.22	12058.31	7.91	182
36	6989.49	19306.41	19.82	235
37	2414.43	13356.41	19.87	368
38	4328.73	18587.71	17.02	406
39	1624.05	8443.45	12.49	299
40	3647.34	11956.43	13.19	282
41	3981.96	17950.87	11.25	294
42	1365.93	7283.72	8.19	187
43	5088.42	15071.01	13.97	275
44	3793.32	14394.61	17.26	262
45	1839.87	12364.86	28.83	220
46	2317.32	13090.99	27.83	170
47	1740.96	11746.02	12.93	207
48	674.82	4646.28	13.62	209
49	63.99	1547.46	53.95	175
50	115.92	2195.57	17.14	146
51	6384.24	13120.70	21.66	339
52	3211.47	14250.73	36.56	386
53	1204.29	7445.89	13.50	198
54	3252.51	15164.93	17.81	375
55	4429.98	16722.25	13.22	404
56	4084.92	16082.40	16.28	366

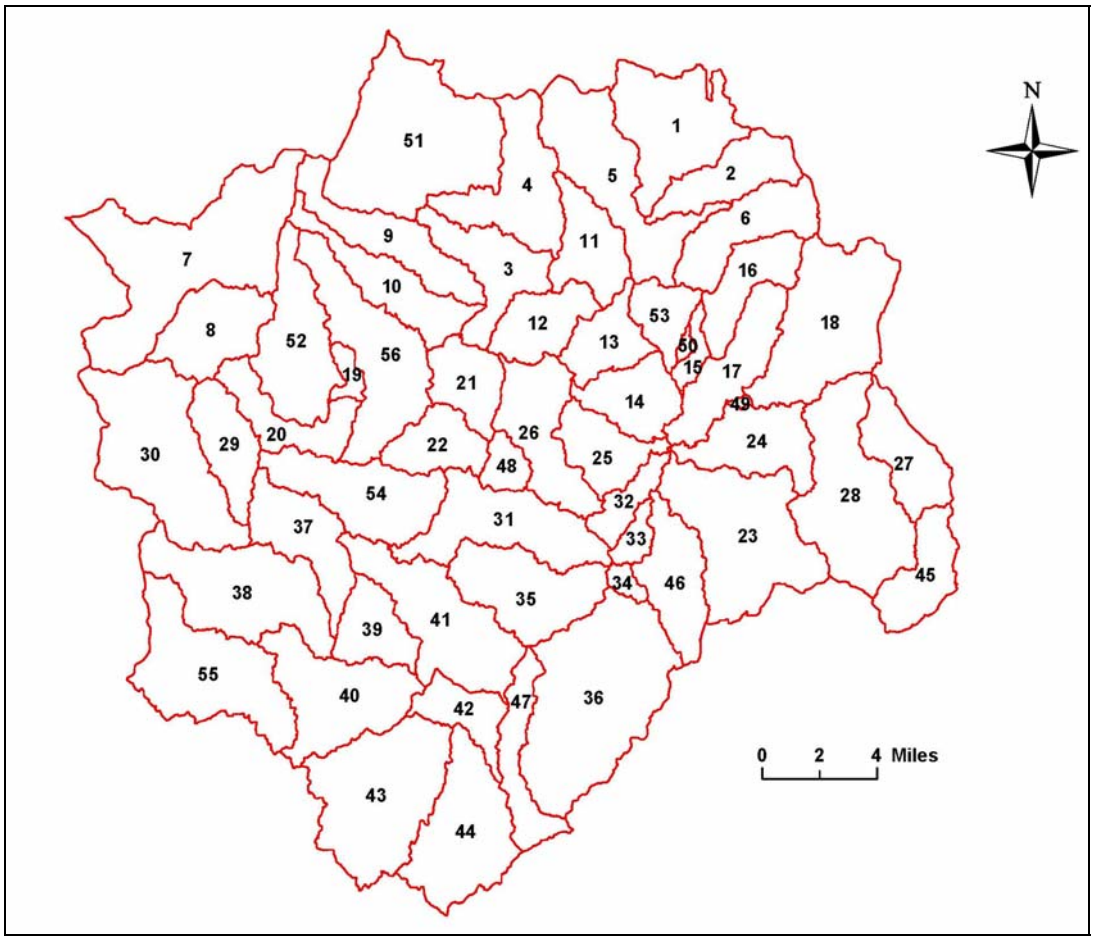

Figure B-1: Occoquan Watershed Subbasins

References

U.S. Environmental Protection Agency. (2004a). *Better Assessment Science Integrating Point and Nonpoint Sources BASINS Version 3.0 User's Manual*. *EPA 823-B-01-001*, Washington, D.C.

U.S. Environmental Protection Agency. (2004b). *BASINS/HSPF Training Handbook*. Athens, Georgia.

Appendix C. Lake Manassas and Occoquan Reservoir Bathymetry and Segmentation

Waterbody bathymetry and segmentation was the first step in CE-QUAL-W2 (Cole and Wells 2003) model setup. This appendix provides general background information about waterbody segmentation for two principal waterbodies in the Occoquan Watershed: Occoquan Reservoir and Lake Manassas. In addition to spatial data and their sources, this appendix summarizes the results of waterbody segmentation.

Definitions

Waterbody segmentation is the process to define the length, depth and width dimensions of each computational cell. This is an iterative procedure where the calculated volume-area-elevation table generated by the process is compared and adjusted with the observed one to provide a better match.

There are several factors that play important roles in this process. These are 1) areas with greatest gradients; 2) computational and memory requirement; 3) bottom slope; and 4) results. The recommended horizontal spacing ranges from 100 to 10,000 m and the vertical grid spacing ranges from 0.2 to 5.0 m.

Some restrictions in grid sizing are 1) cell widths cannot increase with depth; 2) a branch cannot enter or leave itself; 3) two branches might not connect at the same segment of another branch (Cole and Wells 2003).

Software

SURFER (Version 8.0) (Golden Software 2002) was used to calculate the average cross-sectional widths for each cell, based on projected horizontal and vertical cell dimensions. ArcGIS (Version 8.2) was also used in spatial data analysis. Several public ArcGIS utilities were used to facilitate the process.

Data and Their Sources

The waterbody boundaries and its centerlines are obtained from USGS 1:100,000 National Hydrography Dataset (NHD) provided by NVRC. The data set used is Middle Potomac-Anacostia-Occoquan catalog unit (HND 02070010).

OWML collected bathymetry survey data using an integrated differential global positioning system and depth sounding system, which provided high resolution bathymetry data (less than 3.0 feet for horizontal positioning and less than 0.1 feet for depth measurement) (OWML 2000, 2002). These data provided necessary information for the Occoquan Model application and facilitated waterbody segmentation.

Methodology

Step One: Determination of Horizontal Grid Spacing

The first step to create the bathymetric data for CE-QUAL-W2 was to determine the horizontal grid spacing. The initial horizontal spacing was set to be 1,000 ft for Lake Manassas and 2,000 ft for Occoquan Reservoir. A public ArcGIS utility called ET GeoWizard (Version 8.0) (ET SpatialTechniques, 2004) was used to split the waterbody centerlines into evenly spaced segments. The results from the previous model application indicated that Ryan's dam had a significant impact on the hydrodynamics and water quality transport in the Occoquan Reservoir. Thus, in this bathymetry update process, the potential impact of Ryan's dam was considered and a relatively short grid segment (approximately 300 ft) was manually created. The segment boundaries were defined by two slices perpendicular to the centerlines, which were performed by using the Editor function under ArcGIS (Figure C-1).

In this process, the Occoquan Reservoir is divided into four branches: Occoquan River (mainstem, Branch 1), Bull Run (Branch 2), Sandy Run (Branch 3) and Hooes Run (Branch 4). It has a total of 69 computational segments and the average segment length is 583 m with a maximum of 838 m (segment 55 at the very upstream end of Bull Run) and a minimum of 74 m (Segment 32, at Ryan's Dam, a submerged feature with a narrow vertical opening).

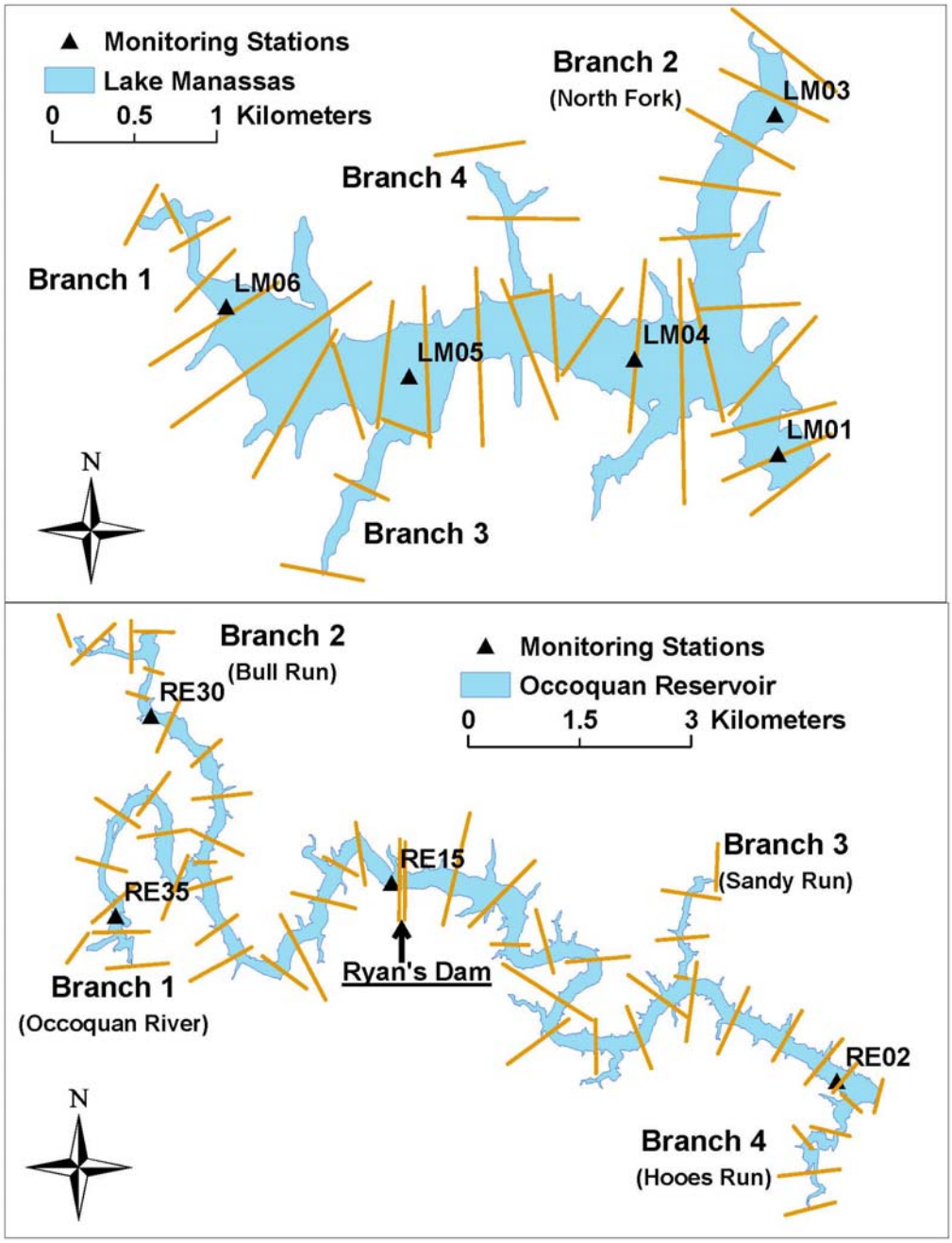

Figure C-1: Top View of Lake Manassas and Occoquan Reservoir Bathymetries

Lake Manassas is also divided into four branches: the mainstem, North Fork, and two unnamed arms, and has a total of 29 active computational segments. The horizontal grid spacing ranges from 173 m to 568 m.

Step Two: Determination of Vertical Grid Spacing

The vertical grid spacing was set to be 0.5 m for both waterbodies. Compared with the previous CE-QUAL-W2 application for the Occoquan Reservoir, the grid depth was reduced 50% to provide output with higher resolution (Figures C-2 and C-3). Lake Manassas has 4 to 28 computational layers, each 0.5 m thick. Occoquan Reservoir has 1 to 39 layers, each 0.5 m thick.

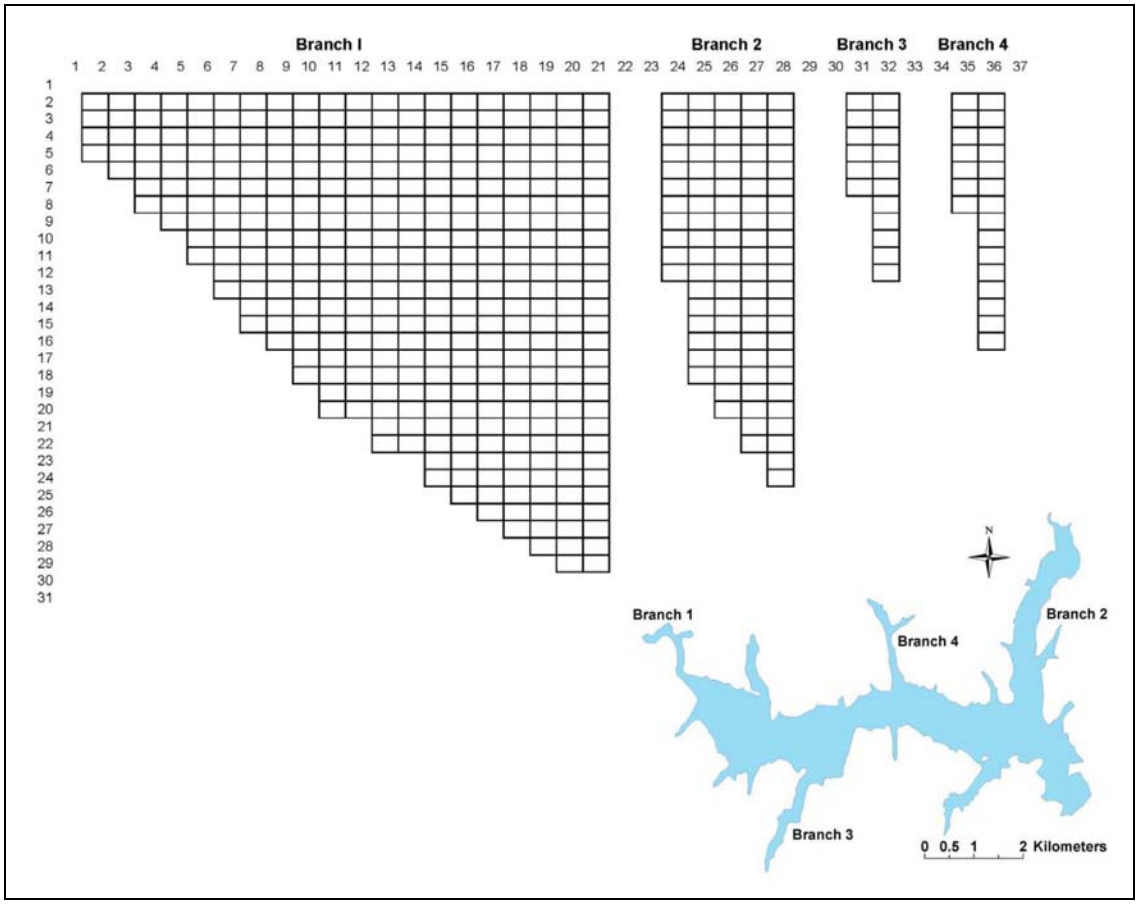

Figure C-2: Side View of Lake Manassas Bathymetry

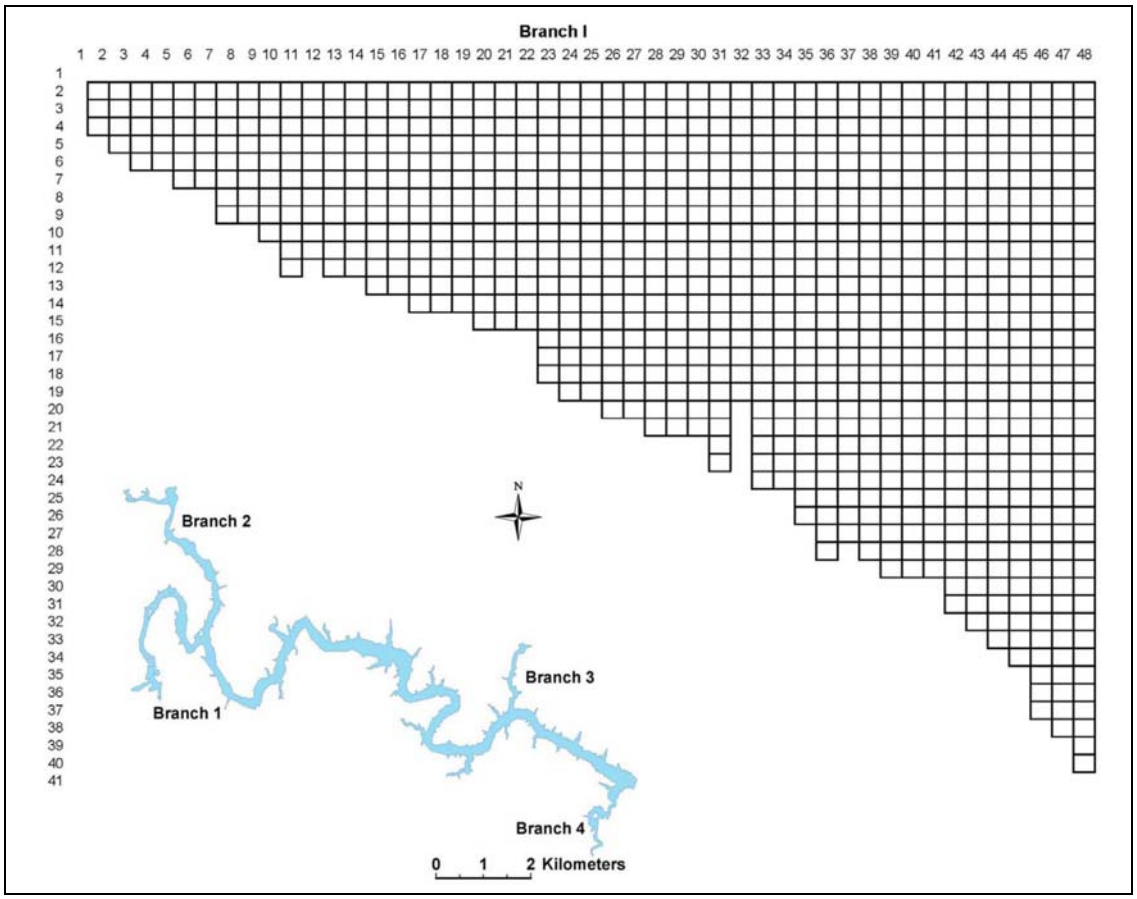

Figure C-3: Side View of Occoquan Reservoir (Mainstem) Bathymetry

Step Three: Determination of Average Cross-Section Width

This step was the most critical and time-consuming step in the waterbody segmentation process. The transects along the waterbody centerline were transferred from ArcGIS to Surfer, thanks to a public Arc script called shapes2points (Rathert, 2004). The original bathymetry was split into individual segments based on these transects. Then the Volume function under Surfer was used to determine the volumes between specified upper surface and lower surface elevations. Based on the corresponding horizontal and vertical grid spacing, the averaged cross-section widths were calculated (Figures C-4 and C-5). The average width of the top layer in Occoquan Reservoir was 149.7 m, which is approximately half of that for Lake Manassas (331.2 m).

Segment	21	20	19	18	17	16	15	14	13	12	11	10	9	8	7	6	5	4	3	2	28	27	26	25	24	32	31	36	35
Length (m)	173.7	439.8	249.9	280.7	205.7	406.9	301.8	305.7	249.0	280.4	373.4	305.7	307.8	303.9	303.6	352.7	259.1	302.4	304.2	260.9	438.0	304.2	307.2	330.4	276.1	447.1	568.8	471.5	493.8
Width (m)																													
1	258.8	166.6	292.8	634.1	360.6	677.7	417.5	266.6	323.0	352.8	336.5	534.3	369.1	347.0	595.6	724.3	203.5	75.9	77.0	50.3	306.2	232.4	209.5	261.9	178.5	119.1	95.3	76.0	74.9
2	243.9	157.6	275.1	620.4	343.1	640.5	408.3	261.5	314.6	333.4	324.2	529.8	355.4	328.5	574.2	663.2	193.5	67.4	52.3	38.9	289.7	220.9	200.2	251.1	160.6	106.9	71.8	71.3	59.8
3	227.4	149.8	257.3	606.2	328.7	590.2	397.0	256.0	305.6	316.4	309.5	520.6	342.0	310.6	549.9	597.5	181.6	41.4	18.0	20.7	273.1	210.5	190.1	237.6	140.8	91.5	41.8	65.8	40.3
4	210.9	142.7	241.1	593.2	316.2	540.6	385.2	250.6	298.1	300.9	290.8	510.6	329.1	294.6	530.7	542.2	164.9	27.2	6.7	8.0	259.0	202.5	182.3	225.4	122.2	78.9	25.2	58.5	25.2
5	198.7	136.3	225.1	580.6	304.0	511.1	373.1	245.4	290.9	287.0	270.6	500.5	316.5	280.4	515.0	499.1	133.5	18.9	3.7	2.5	248.8	195.9	175.9	215.4	105.5	69.0	16.0	50.3	15.4
6	188.2	130.4	210.2	569.2	290.7	486.9	360.9	240.3	284.1	275.3	253.0	487.7	303.6	269.5	499.5	447.3	78.8	11.6	1.9	0.6	240.6	190.2	170.0	205.8	87.2	59.5	7.8	43.3	8.2
7	179.0	124.9	196.1	558.7	279.4	465.0	350.1	234.7	277.3	265.4	238.0	468.7	291.4	259.7	483.0	364.9	28.1	4.9	0.4	0.0	233.2	185.2	164.2	196.0	70.9	48.4	1.5	36.7	4.9
8	170.3	119.7	184.6	548.6	270.7	443.3	340.5	229.4	270.1	255.7	226.0	449.7	279.4	250.2	462.5	237.2	11.0	1.8	0.0		226.4	180.4	158.7	187.1	48.6	34.3	0.0	30.7	2.3
9	162.1	114.9	174.8	538.1	263.1	423.5	331.2	224.3	262.3	246.7	216.2	427.4	265.5	240.5	427.3	78.1	2.1	0.6			219.7	175.7	153.6	178.6	33.3	24.3		25.3	0.3
10	154.6	110.7	165.5	528.6	256.2	403.4	321.7	218.6	253.9	237.9	206.0	400.7	248.5	228.8	322.9	12.7	0.1	0.0			212.7	170.6	148.2	169.4	20.8	16.0		20.9	0.0
11	148.2	106.7	156.4	519.4	249.7	383.2	311.1	211.8	245.1	228.3	194.3	365.2	225.0	194.0	134.2	1.9	0.0				205.3	166.0	142.7	157.9	10.1	7.3		17.4	0.0
12	142.1	102.9	148.3	510.7	242.7	364.5	299.5	203.3	236.2	219.0	183.1	323.5	193.3	130.0	26.1	0.0					199.0	161.7	137.0	138.3	2.1	0.5		14.3	
13	135.8	99.2	140.8	501.9	234.5	345.7	287.6	193.3	226.5	209.0	171.4	270.0	160.4	63.5	2.0						193.2	157.5	131.4	112.1	0.4	0.0		11.0	
14	129.6	94.8	133.5	492.7	225.9	324.1	274.5	180.7	215.6	198.2	159.7	221.7	113.2	10.4	0.0						187.3	153.0	125.4	88.6	0.0			7.8	
15	122.8	88.9	126.3	483.3	218.7	303.6	259.5	170.2	203.2	185.8	143.0	158.9	46.9	1.0							181.1	148.1	118.6	66.3				4.9	
16	117.4	81.5	119.5	473.5	212.4	280.7	242.2	160.7	188.7	169.9	116.4	64.4	6.6	0.0							173.8	142.5	110.1	37.2				2.4	
17	113.4	75.0	113.3	463.0	206.1	259.9	224.2	150.8	174.7	146.7	68.9	14.3	0.0								166.6	135.6	96.2	13.8				0.4	
18	109.7	69.7	107.4	451.5	199.5	242.4	203.7	139.6	153.5	93.8	22.5	3.7									158.9	126.8	73.4	1.6				0.0	
19	105.9	64.6	101.6	440.2	190.7	225.5	179.7	124.8	87.7	28.2	7.9	0.4									148.7	113.6	38.6	0.1					
20	101.9	59.5	95.9	429.0	181.3	204.1	144.7	80.0	37.5	9.6	2.1	0.0									134.1	82.9	5.1	0.0					
21	97.7	54.1	90.0	416.2	168.1	168.8	74.3	25.3	18.2	2.2	0.1										112.9	34.5	0.0						
22	93.2	48.8	83.6	398.6	127.3	81.6	27.8	4.6	4.3	0.1	0.0										75.4	4.0							
23	88.0	42.8	76.4	342.8	46.5	25.0	9.9	0.2	0.0	0.0											20.4	0.0							
24	81.1	36.0	67.7	216.9	15.6	9.7	2.6	0.0													1.8								
25	72.9	28.1	56.6	99.0	6.1	2.9	0.1														0.0								
26	51.2	22.0	38.1	32.5	2.0	0.5	0.0																						
27	22.8	16.2	14.0	3.8	0.2	0.0																							
28	9.1	10.1	4.1	0.0	0.0																								
29	2.9	3.8	1.2																										
30	0.4	0.3	0.1																										
31	0.0	0.0	0.0																										

Figure C-4: Width of Individual Grids in Lake Manassas

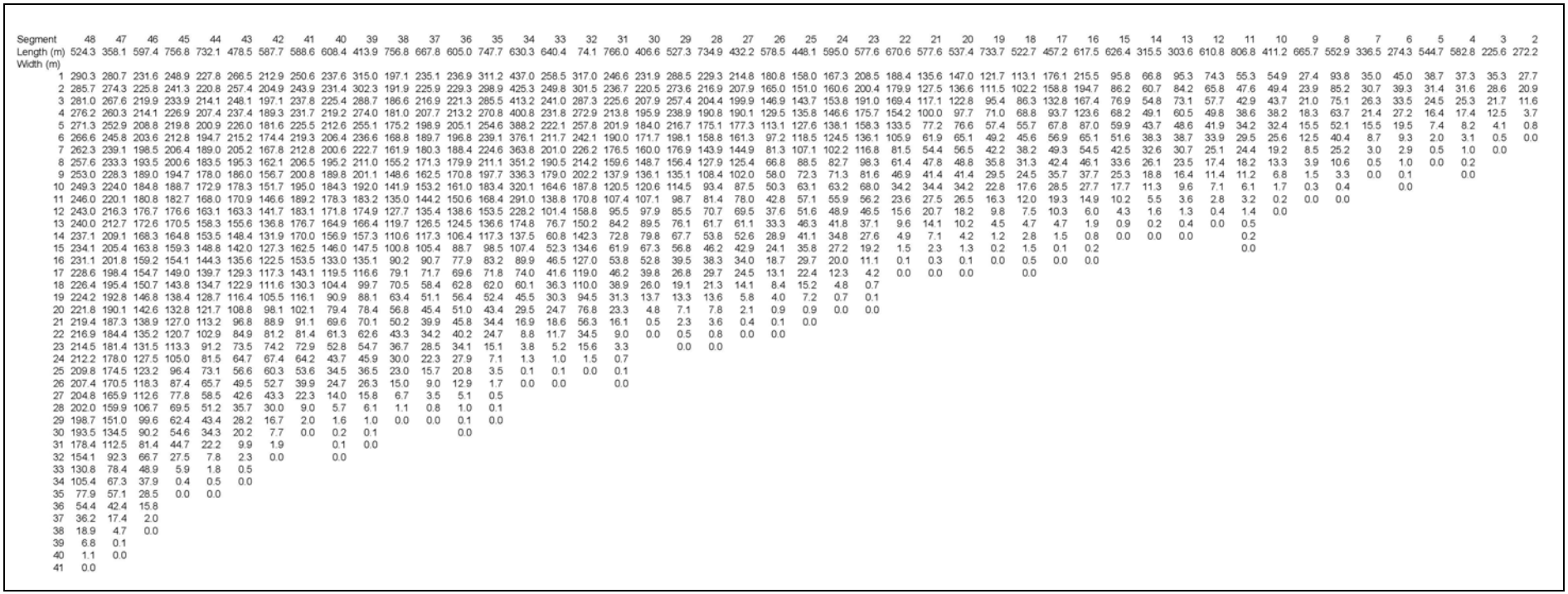

Segment	48	47	46	45	44	43	42	41	40	39	38	37	36	35	34	33	32	31	30	29	28	27	26	25	24	23	22	21	20	19	18	17	16	15	14	13	12	11	10	9	8	7	6	5	4	3	2
Length (m)	524.3	358.1	597.4	756.8	732.1	478.5	587.7	588.6	608.4	413.9	756.8	667.8	605.0	747.7	630.3	640.4	74.1	766.0	406.6	527.3	734.9	432.2	578.5	448.1	595.0	577.6	670.6	577.6	537.4	733.7	522.7	457.2	617.5	626.4	315.5	303.6	610.8	806.8	411.2	665.7	552.9	336.5	274.3	544.7	582.8	225.6	272.2
Width (m)																																														
1	290.3	280.7	231.6	248.9	227.8	266.5	212.9	250.6	237.6	315.0	197.1	235.1	236.9	311.2	437.0	258.5	317.0	246.6	231.9	288.5	229.3	214.8	180.8	158.0	167.3	208.5	188.4	135.6	147.0	121.7	113.1	176.1	215.5	95.8	66.8	95.3	74.3	55.3	54.9	27.4	93.8	35.0	45.0	38.7	37.3	35.3	27.7
2	285.7	274.3	225.8	241.3	220.8	257.4	204.9	243.9	231.4	302.3	191.9	225.9	229.3	298.9	425.3	249.8	301.5	236.7	220.5	273.6	216.9	207.9	165.0	151.0	160.6	200.4	179.9	127.5	136.6	111.5	102.2	158.8	194.7	86.2	60.7	84.2	65.8	47.6	49.4	23.9	85.2	30.7	39.3	31.4	31.6	28.6	20.9
3	281.0	267.6	219.9	233.9	214.1	248.1	197.1	237.8	225.4	288.7	186.6	216.9	221.3	285.5	413.2	241.0	287.3	225.6	207.9	257.4	204.4	199.9	146.9	143.7	153.8	191.0	169.4	117.1	122.8	95.4	86.3	132.8	167.4	76.9	54.8	73.1	57.7	42.9	43.7	21.0	75.1	26.3	33.5	24.5	25.3	21.7	11.6
4	276.2	260.3	214.1	226.9	207.4	237.4	189.3	231.7	219.2	274.0	181.0	207.7	213.2	270.8	400.8	231.8	272.9	213.8	195.9	238.9	190.8	190.1	129.5	135.8	146.6	175.7	154.2	100.0	97.7	71.0	68.8	93.7	123.6	68.2	49.1	60.5	49.8	38.6	38.2	18.3	63.7	21.4	27.2	16.4	17.4	12.5	3.7
5	271.3	252.9	208.8	219.8	200.9	226.0	181.6	225.5	212.6	255.1	175.2	198.9	205.1	254.6	388.2	222.1	257.8	201.9	184.0	216.7	175.1	177.3	113.1	127.6	138.1	158.3	133.5	77.2	76.6	57.4	55.7	67.8	87.0	59.9	43.7	48.6	41.9	34.2	32.4	15.5	52.1	15.5	19.5	7.4	8.2	4.1	0.8
6	266.6	245.8	203.6	212.8	194.7	215.2	174.4	219.3	206.4	236.6	168.8	189.7	196.8	239.1	376.1	211.7	242.1	190.0	171.7	198.1	158.8	161.3	97.2	118.5	124.5	136.1	105.9	61.9	65.1	49.2	45.6	56.9	65.1	51.6	38.3	38.7	33.9	29.5	25.6	12.5	40.4	8.7	9.3	2.0	3.1	0.5	0.0
7	262.3	239.1	198.5	206.4	189.0	205.2	167.8	212.8	200.6	222.7	161.9	180.3	188.4	224.6	363.8	201.0	226.2	176.5	160.0	176.9	143.9	144.9	81.3	107.1	102.2	116.8	81.5	54.4	56.5	42.2	38.2	49.3	54.5	42.5	32.6	30.7	25.1	24.4	19.2	8.5	25.2	3.0	2.9	0.5	1.0	0.0	
8	257.6	233.3	193.5	200.6	183.5	195.3	162.1	206.5	195.2	211.0	155.2	171.3	179.9	211.1	351.2	190.5	214.2	159.6	148.7	156.4	127.9	125.4	66.8	88.5	82.7	98.3	61.4	47.8	48.8	35.8	31.3	42.4	46.1	33.6	26.1	23.5	17.4	18.2	13.3	3.9	10.6	0.5	1.0	0.0	0.2		
9	253.0	228.3	189.0	194.7	178.0	186.0	156.7	200.8	189.8	201.1	148.6	162.5	170.8	197.7	336.3	179.0	202.2	137.9	136.1	135.1	108.4	102.0	58.0	72.3	71.3	81.6	46.9	41.4	41.4	29.5	24.5	35.7	37.7	25.3	18.8	16.4	11.4	11.2	6.8	1.5	3.3	0.0	0.1		0.0		
10	249.3	224.0	184.8	188.7	172.9	178.3	151.7	195.0	184.3	192.0	141.9	153.2	161.0	183.4	320.1	164.6	187.8	120.5	120.6	114.5	93.4	87.5	50.3	63.1	63.2	68.0	34.2	34.4	34.2	22.8	17.6	28.5	27.7	17.7	11.3	9.6	7.1	6.1	1.7	0.3	0.4		0.0				
11	246.0	220.1	180.8	182.7	168.0	170.9	146.6	189.2	178.3	183.2	135.0	144.2	150.6	168.4	291.0	138.8	170.8	107.4	107.1	98.7	81.4	78.0	42.8	57.1	55.9	56.2	23.6	27.5	26.5	16.3	12.0	19.3	14.9	10.2	5.5	3.6	2.8	3.2	0.2	0.0	0.0						
12	243.0	216.3	176.7	176.6	163.1	163.3	141.7	183.1	171.8	174.9	127.7	135.4	138.6	153.5	228.2	101.4	158.8	95.5	97.9	85.5	70.7	69.5	37.6	51.6	48.9	46.5	15.6	20.7	18.2	9.8	7.5	10.3	6.0	4.3	1.6	1.3	0.4	1.4	0.0								
13	240.0	212.7	172.6	170.5	158.3	155.6	136.8	176.7	164.9	166.4	119.7	126.5	124.5	136.6	174.8	76.7	150.2	84.2	89.5	76.1	61.7	61.1	33.3	46.3	41.8	37.1	9.6	14.1	10.2	4.5	4.7	4.7	1.9	0.9	0.2	0.4	0.0	0.5									
14	237.1	209.1	168.3	164.8	153.5	148.4	131.9	170.0	156.9	157.3	110.6	117.3	106.4	117.3	137.5	60.8	142.3	72.8	79.8	67.7	53.8	52.6	28.9	41.1	34.8	27.6	4.9	7.1	4.2	1.2	2.8	1.5	0.8	0.0	0.0	0.0		0.2									
15	234.1	205.4	163.8	159.3	148.8	142.0	127.3	162.5	146.0	147.5	100.8	105.4	88.7	98.5	107.4	52.3	134.6	61.9	67.3	56.8	46.2	42.9	24.1	35.8	27.2	19.2	1.5	2.3	1.3	0.2	1.5	0.1	0.2					0.0									
16	231.1	201.8	159.2	154.1	144.3	135.6	122.5	153.5	133.0	135.1	90.2	90.7	77.9	83.2	89.9	46.5	127.0	53.8	52.8	39.5	38.3	34.0	18.7	29.7	20.0	11.1	0.1	0.3	0.1	0.0	0.5	0.0	0.0														
17	228.6	198.4	154.7	149.0	139.7	129.3	117.3	143.1	119.5	116.6	79.1	71.7	69.6	71.8	74.0	41.6	119.0	46.2	39.8	26.8	29.7	24.5	13.1	22.4	12.3	4.2	0.0	0.0	0.0		0.0																
18	226.4	195.4	150.7	143.8	134.7	122.9	111.6	130.3	104.4	99.7	70.5	58.4	62.8	62.0	60.1	36.3	110.0	38.9	26.0	19.1	21.3	14.1	8.4	15.2	4.8	0.7																							
19	224.2	192.8	146.8	138.4	128.7	116.4	105.5	116.1	90.9	88.1	63.4	51.1	56.4	52.4	45.5	30.3	94.5	31.3	13.7	13.3	13.6	5.8	4.0	7.2	0.7	0.1																							
20	221.8	190.1	142.6	132.8	121.7	108.8	98.1	102.1	79.4	78.4	56.8	45.4	51.0	43.4	29.5	24.7	76.8	23.3	4.8	7.1	7.8	2.1	0.9	0.9	0.0	0.0																							
21	219.4	187.3	138.9	127.0	113.2	96.8	88.9	91.1	69.6	70.1	50.2	39.9	45.8	34.4	16.9	18.6	56.3	16.1	0.5	2.3	3.6	0.4	0.1	0.0																							
22	216.9	184.4	135.2	120.7	102.9	84.9	81.2	81.4	61.3	62.6	43.3	34.2	40.2	24.7	8.8	11.7	34.5	9.0	0.0	0.5	0.8	0.0	0.0																							
23	214.5	181.4	131.5	113.3	91.2	73.5	74.2	72.9	52.8	54.7	36.7	28.5	34.1	15.1	3.8	5.2	15.6	3.3		0.0	0.0																									
24	212.2	178.0	127.5	105.0	81.5	64.7	67.4	64.2	43.7	45.9	30.0	22.3	27.9	7.1	1.3	1.0	1.5	0.7																													
25	209.8	174.5	123.2	96.4	73.1	56.6	60.3	53.6	34.5	36.5	23.0	15.7	20.8	3.5	0.1	0.1	0.0	0.1																													
26	207.4	170.5	118.3	87.4	65.7	49.5	52.7	39.9	24.7	26.3	15.0	9.0	12.9	1.7	0.0	0.0		0.0																													
27	204.8	165.9	112.6	77.8	58.5	42.6	43.3	22.3	14.0	15.8	6.7	3.5	5.1	0.5																																	
28	202.0	159.9	106.7	69.5	51.2	35.7	30.0	9.0	5.7	6.1	1.1	0.8	1.0	0.1																																	
29	198.7	151.0	99.6	62.4	43.4	28.2	16.7	2.0	1.6	1.0	0.0	0.0	0.1	0.0																																	
30	193.5	134.5	90.2	54.6	34.3	20.2	7.7	0.0	0.2	0.1			0.0																																	
31	178.4	112.5	81.4	44.7	22.2	9.9	1.9		0.1	0.0																																			
32	154.1	92.3	66.7	27.5	7.8	2.3	0.0		0.0																																					
33	130.8	78.4	48.9	5.9	1.8	0.5																																							
34	105.4	67.3	37.9	0.4	0.5	0.0																																							
35	77.9	57.1	28.5	0.0	0.0																																								
36	54.4	42.4	15.8																																										
37	36.2	17.4	2.0																																										
38	18.9	4.7	0.0																																										
39	6.8	0.1																																											
40	1.1	0.0																																											
41	0.0																																												

Figure C-5: Width of Individual Grids in Occoquan Reservoir (Mainstem)

Step Four: Determination of Segment Orientation

The orientations of each segment were determined by using the Edit function under ArcGIS. Unit conversion from degrees to radians was necessary.

Summary

The resultant final numbers of grids including boundary grids were 1147 for Lake Manassas and 3157 for Occoquan Reservoir. Compared to the previous CE-QUAL-W2 application for Occoquan Reservoir, the grid numbers from the updated bathymetry were almost tripled. The comparison between observed and calculated storage capacity of both waterbodies is shown in Figure C-6. The excellent match between observed and simulated storage capacity indicated that the resultant bathymetries truly represent the physical characteristics of the waterbodies.

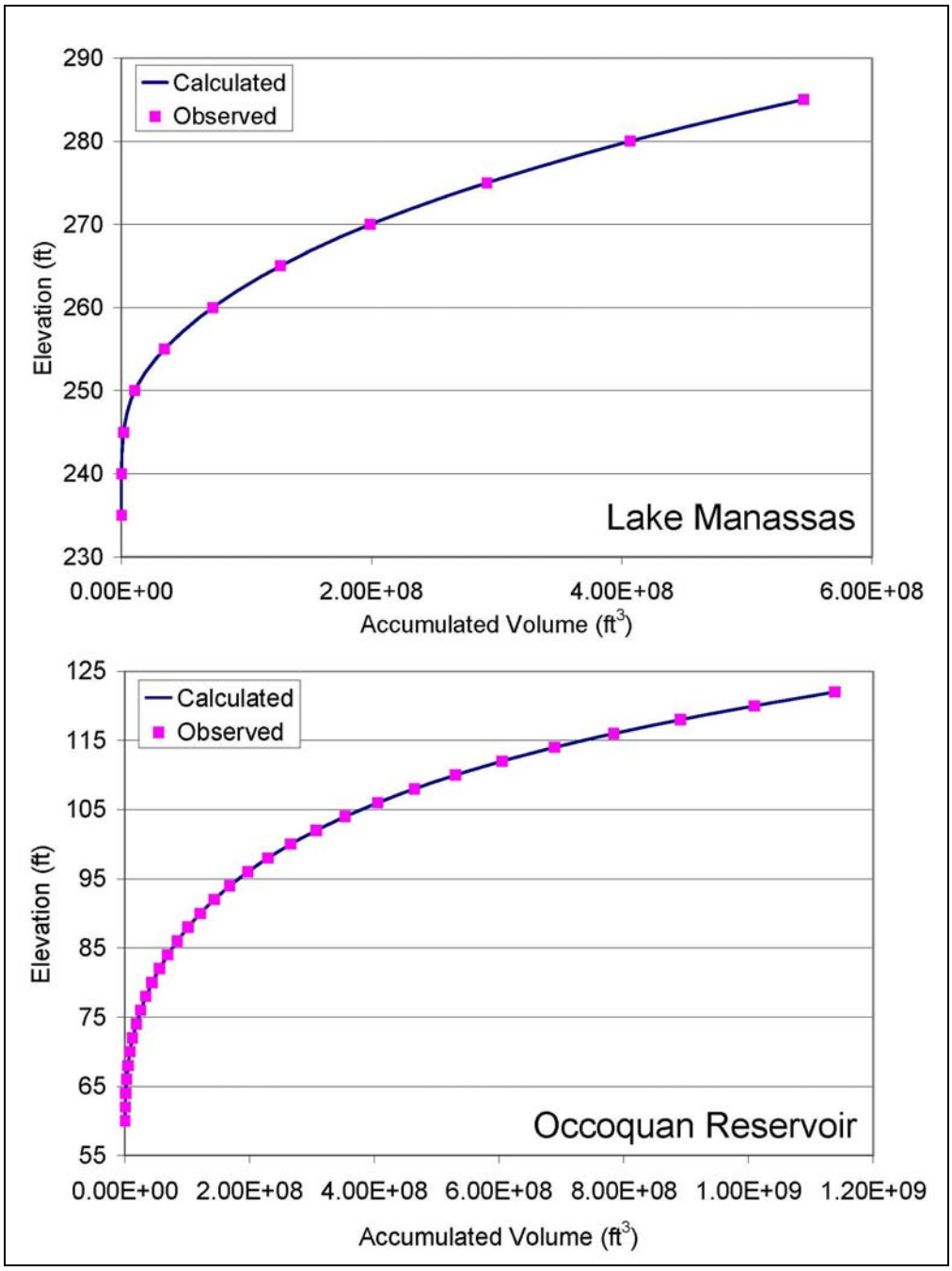

Figure C-6: Comparison of observed and calculated storage capacity of Lake Manassas and Occoquan Reservoir

References

Cole, T. M. and Wells, S. A. (2003). CE-QUAL-W2: A Two-Dimensional Laterally Averaged, Hydrodynamic and Water Quality Model, Version 3.2 User Manual. U.S. Army Corps of Engineers, Washington, DC.

Golden Software, Inc. (2002). Surfer 8: Contouring and 3D Surface Mapping for Scientists and Engineers User's Guide. Golden, Colorado.

Occoquan Watershed Monitoring Laboratory. (2000). *Occoquan Reservoir Bathymetric Survey*. Manassas, Virginia.

Occoquan Watershed Monitoring Laboratory. (2002). *Lake Manassas 2000 Hydrographic Survey*. Manassas, Virginia.

ET SpatialTechniques. (2004) *ET GeoWizards* <Available at http://www.ian-ko.com/>

Rathert, D. (2004). *ArcScript: shapes2points*. <Available at http://arcscripts.esri.com/details.asp?dbid=12666>

Appendix D. Land Use Analysis

HSPF defines two types of land segments: PERLND and IMPLND. PERLND represents comprehensive hydrological and water quality processes occurring in the pervious land areas, such as agriculture and forest. IMPLND describes a much simpler system in impervious land segments, such as paved urban areas. Each land segment is made up of different land use categories.

The land use map of 1995 was provided by NVRC. The map was generated by an aerial-photography approach. The land use has been classified into 14 land use categories and they are estate residential, low density residential, medium density residential, townhouse and garden apartment, commercial, industrial, institutional, golf courses, conventional tillage grain, mixed conventional tillage grain, conservation (minimum) tillage, mixed conservation (minimum)tillage, livestock & pasture, and forest & idle. The map had thirteen land use categories with forest/idle as default. ArcGIS software has been used to produce the 1995 land use map with all fourteen-land use categories. However, since some land uses share the similar impervious percentages and soil properties, it is appropriate to merge them into one land use category. Such process can reduce the complexity of HSPF applications without significantly affecting simulation results. Based on investigation by NVRC, the resultant land use categories that were used in model applications are shown in Table D-1 and Figure D-1.

The definition of the impervious percentages varies based on technical approaches and statistical methods involved. Dougherty (2004) compared two different methods for the Cub Run watershed: a traditional aerial-photography/land use approach and a satellite imagery/land cover approach. After comparing the results with a reference data set, he provided a list of expected range of impervious cover estimates for the Cub Run watershed, which was used as a starting point for the model applications (Table D-2).

There was another concern on impervious cover estimation. The impervious percentage used by HSPF is sometimes called “effective imperviousness”. It only accounts for the impervious land surface that directly drains into neighborhood streams. When impervious

land areas drain into adjacent pervious lands, HSPF assumes such impervious areas don't directly affect downstream water quality and would classify them into pervious land use segments. However, both estimation methods account for total impervious surfaces instead of effective ones. This will probably lead to some inaccuracies in model applications.

Table D-1: Land Use Classification

Land Use Categories in 1995 Map	Characteristics	Land Use Categories in Model Applications
Estate	Estate Single Family Housing (0.05-0.2 DU*/acre)	Low Density Residential
Low Density Residential	Large-Lot Single Family Housing (0.5-2.0 DU/acre)	
Medium Density Residential	Medium Density Single Family Housing (3.0-6DU/acre)	Medium Density Residential
Townhouse/Garden Apartment	Multi-Family Housing (>6DU/Acre)	Townhouse/Garden Apartment
Industrial		Industrial
Institutional		Institutional
Commercial		Commercial
Forest/Idle		Forest/Idle
Golf	Golf Courses	
Livestock/Pasture		Pasture
Conventional Tillage Grain		High Tillage Cropland
Mix Conventional Tillage Grain		
Min. Tillage Grain		Low Tillage Cropland
Mixed Min. Tillage		

* DU: Dwelling Units

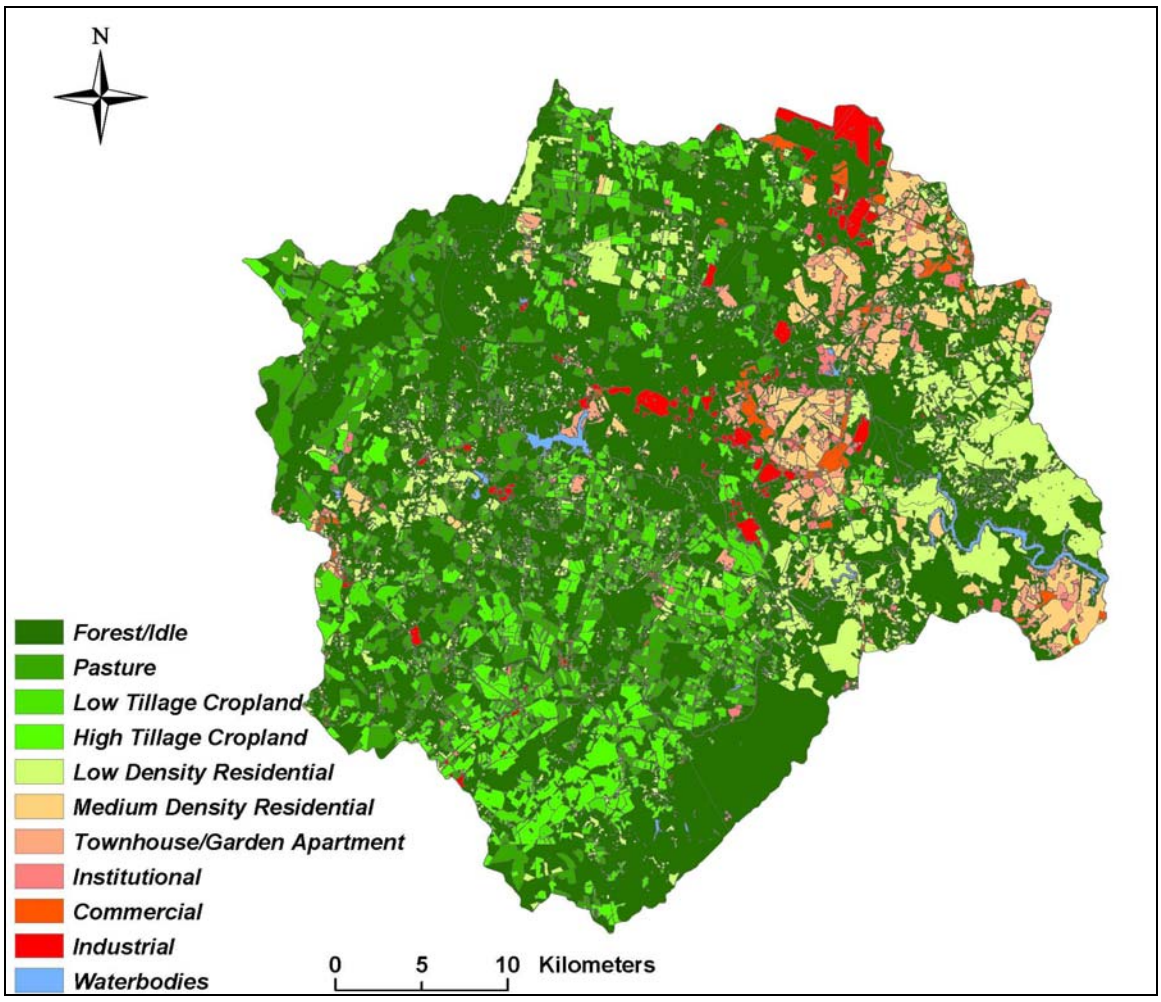

Figure D-1: 1995 Land Use Map for the Occoquan Watershed

Table D-2: Impervious Coverage Summary

Land Use Categories	Impervious Coverage*	Impervious Coverage**	Impervious Coverage***	Impervious Coverage****	Impervious Coverage in Previous Model Application (1989)	Impervious Coverage in Current Model Application (1993-97)
Low Density Residential	1.5-18%	12%	5%	5-10%	7.3-12%	5-10%
Medium Density Residential	20-35%	41%	23%	20-25%	25%	20-25%
Townhouse/Garden Apartment	35-50%	82%	41%	35-45%	40%	35-40%
Industrial	80-90%	87%	48%	35-55%	70%	50%
Institutional	50-60%	87%	48%	35-55%	35%	35%
Commercial	80-90%	87%	48%	35-55%	90%	50%
Forest/Idle	–	0%	3%	2-7%	1.1%	1.0%
Pasture	–	0%	3%	2-7%	1.1%	2.0%
High Tillage Cropland	–	0%	3%	2-7%	1.1%	3.0%
Low Tillage Cropland	–	0%	3%	2-7%	1.1%	3.0%

*(NVPDC and ESI 1992) and (NVRC 1992)
**(Dougherty 2004) Based on Aerial Photography 1979-1988 for Cub Run watershed
*** (Dougherty 2004) Based on Planimetric data 1997 for Cub Run watershed
****(Dougherty 2004) Recommended by Dougherty

The summary for each land segment is given in Table D-3 and Figure D-2. The ten land use categories were summarized into three principal land use categories (agriculture, forest and urban) for analysis purposes. It can be seen that the dominant land use category in the Occoquan Watershed is forest. However, the watershed is highly urbanized and approximately 22% of the land areas fall into the "urban" category, which includes residential, commercial, institutional and industrial areas.

Table D-3: Land Use Summary for Individual Land Segments

		Area (acres)											Percentage		
Subbasin	Segment	Forest/Idle	Pasture	High Tillage Cropland	Low Tillage Cropland	Low Density Residential	Medium Density Residential	Townhouse /Garden Apartment	Commercial	Industrial	Institutional	Total	Agriculture	Forest	Urban
Bull Run	1	5478.6	146.0	147.5	51.3	243.7	534.8	1.8	666.6	1802.0	158.6	9231.0	3.7%	59.4%	36.9%
Bull Run	2	1584.4	0.0	0.0	0.0	372.4	1454.1	698.9	141.7	578.0	140.2	4969.7	0.0%	31.9%	68.1%
Bull Run	3	3167.3	948.6	135.1	320.4	1215.1	0.0	0.0	13.0	0.0	0.0	5799.5	24.2%	54.6%	21.2%
Bull Run	4	4344.1	657.6	604.4	752.6	1267.5	0.0	43.6	3.5	158.8	26.7	7858.7	25.6%	55.3%	19.1%
Bull Run	5	6348.4	389.0	673.6	406.4	442.7	1385.7	372.8	79.2	37.8	67.9	10203.4	14.4%	62.2%	23.4%
Bull Run	6	2319.7	0.0	0.0	0.0	192.2	1497.8	1025.4	654.3	17.2	284.3	5990.9	0.0%	38.7%	61.3%
Bull Run	9	4382.0	517.8	182.9	483.5	449.9	61.3	0.0	1.4	5.3	65.0	6149.0	19.3%	71.3%	9.5%
Bull Run	10	4314.8	472.4	0.0	450.9	218.5	29.4	12.5	10.8	72.6	48.6	5630.5	16.4%	76.6%	7.0%
Bull Run	11	3456.7	691.9	0.0	246.4	110.3	16.4	179.6	60.6	79.4	8.8	4850.0	19.3%	71.3%	9.4%
Bull Run	12	3859.9	20.5	0.0	246.8	156.5	0.0	0.0	13.7	78.1	42.6	4418.0	6.0%	87.4%	6.6%
Bull Run	13	1891.8	196.9	0.0	41.9	49.5	395.5	378.4	435.9	222.6	200.8	3813.3	6.3%	49.6%	44.1%
Bull Run	14	921.0	0.0	0.0	0.0	10.3	2093.9	446.4	523.5	198.2	396.2	4589.5	0.0%	20.1%	79.9%
Bull Run	15	443.0	5.9	0.0	0.0	220.6	238.0	39.8	97.4	0.0	41.4	1086.2	0.5%	40.8%	58.7%
Bull Run	16	2141.2	0.0	0.0	0.0	362.2	1221.7	524.7	62.8	0.0	197.8	4510.5	0.0%	47.5%	52.5%
Bull Run	17	3608.4	34.2	0.0	58.7	1028.3	55.9	352.6	412.5	277.8	103.4	5931.8	1.6%	60.8%	37.6%
Bull Run	18	5388.7	217.6	0.0	0.0	4478.4	1339.2	148.8	184.2	10.9	196.2	11964.1	1.8%	45.0%	53.1%
Bull Run	49	150.8	0.0	0.0	0.0	0.5	0.0	0.0	0.0	0.0	0.1	151.5	0.0%	99.5%	0.5%
Bull Run	50	140.3	15.7	0.0	0.0	27.4	6.6	65.6	23.0	0.0	0.0	278.7	5.6%	50.3%	44.0%
Bull Run	51	7967.4	2375.9	1325.9	1717.5	1978.5	148.5	267.4	7.1	12.1	3.4	15803.8	34.3%	50.4%	15.3%
Bull Run	53	1805.3	18.7	0.0	0.0	109.6	385.1	127.1	36.7	2.8	378.9	2864.2	0.7%	63.0%	36.3%
Ceder Run	29	2530.3	498.2	467.4	83.5	969.6	1.0	0.0	5.4	21.4	10.1	4586.8	22.9%	55.2%	22.0%
Ceder Run	30	7406.3	2676.0	450.9	832.4	1086.8	529.9	55.6	173.6	15.6	271.5	13498.5	29.3%	54.9%	15.8%
Ceder Run	34	303.3	0.0	0.0	65.7	364.9	0.0	0.0	0.0	0.0	0.0	733.8	9.0%	41.3%	49.7%
Ceder Run	35	3564.0	1643.6	346.6	1764.4	400.3	0.0	0.0	13.7	0.0	124.1	7856.7	47.8%	45.4%	6.8%
Ceder Run	36	14250.2	784.9	12.6	1090.1	851.2	0.0	0.0	0.0	0.0	130.7	17119.7	11.0%	83.2%	5.7%
Ceder Run	37	2959.1	1194.3	542.1	701.3	512.6	62.8	0.0	1.8	1.0	2.3	5977.6	40.8%	49.5%	9.7%
Ceder Run	38	5004.9	1806.2	766.5	2289.5	447.6	101.3	23.1	53.7	176.4	44.8	10714.1	45.4%	46.7%	7.9%
Ceder Run	39	1336.2	1191.2	597.4	715.0	58.7	0.0	0.0	50.3	21.0	23.0	3992.8	62.7%	33.5%	3.8%
Ceder Run	40	3829.4	964.4	2822.8	1100.6	169.7	0.0	0.0	15.7	102.3	12.2	9017.1	54.2%	42.5%	3.3%
Ceder Run	41	5587.0	1936.9	1101.4	908.1	229.4	0.0	0.0	34.8	0.0	0.0	9797.6	40.3%	57.0%	2.7%
Ceder Run	42	1206.1	335.9	1430.3	305.4	86.9	0.0	0.0	7.6	0.0	3.6	3375.8	61.4%	35.7%	2.9%
Ceder Run	43	5671.6	1069.2	4580.2	918.4	347.3	0.0	0.0	0.0	0.0	11.4	12598.1	52.1%	45.0%	2.8%
Ceder Run	44	7045.4	359.3	1320.2	252.5	364.6	0.0	0.0	0.0	3.1	1.9	9347.0	20.7%	75.4%	4.0%
Ceder Run	47	2743.4	260.2	499.4	530.4	43.7	0.0	0.0	6.1	6.6	1.2	4091.0	31.5%	67.1%	1.4%
Ceder Run	55	6130.8	1654.1	1435.6	1077.4	572.8	0.0	0.0	38.8	21.0	36.7	10967.3	38.0%	55.9%	6.1%
Lower Broad Run	21	2943.2	0.0	0.0	0.0	67.1	268.1	57.9	61.8	636.1	4.1	4038.3	0.0%	72.9%	27.1%
Lower Broad Run	22	2028.5	503.6	318.2	601.6	275.8	24.2	149.3	8.8	0.0	17.5	3927.6	36.2%	51.6%	12.1%
Lower Broad Run	25	2157.3	0.0	297.1	177.1	86.3	494.3	135.7	123.1	636.2	223.3	4330.5	11.0%	49.8%	39.2%
Lower Broad Run	26	4930.8	8.8	212.7	569.5	157.2	0.0	89.0	22.3	777.4	60.0	6827.8	11.6%	72.2%	16.2%
Lower Broad Run	31	3378.1	1070.3	825.6	2282.0	765.7	0.0	202.6	45.2	0.0	5.4	8574.9	48.7%	39.4%	11.9%
Lower Broad Run	32	1071.2	27.5	73.7	261.5	300.6	341.1	115.7	33.7	3.9	37.7	2266.5	16.0%	47.3%	36.7%
Lower Broad Run	33	596.5	0.0	0.0	63.7	394.5	176.7	0.0	5.2	0.0	0.1	1236.6	5.2%	48.2%	46.6%
Lower Broad Run	46	2540.2	0.0	0.0	32.2	2862.0	49.9	0.0	27.3	4.6	76.7	5592.9	0.6%	45.4%	54.0%
Lower Broad Run	48	1283.5	128.2	9.2	88.5	129.6	0.0	0.0	3.9	0.0	11.8	1654.8	13.7%	77.6%	8.8%
Lower Broad Run	54	5106.2	1063.1	406.3	364.7	940.2	34.1	0.0	11.7	64.4	2.6	7993.4	22.9%	63.9%	13.2%
Lower Occoquan	23	7318.6	44.0	18.5	224.3	3636.0	796.7	33.2	131.3	36.6	85.0	12324.0	2.3%	59.4%	38.3%
Lower Occoquan	24	2971.9	14.3	10.3	428.6	1894.8	273.8	7.9	21.6	5.1	32.7	5661.0	8.0%	52.5%	39.5%
Lower Occoquan	27	1263.5	0.0	0.0	0.0	3722.7	0.0	0.0	7.8	0.0	25.2	5019.3	0.0%	25.2%	74.8%
Lower Occoquan	28	5548.3	81.8	0.0	10.1	4648.3	606.1	542.8	167.2	6.5	190.2	11801.2	0.8%	47.0%	52.2%
Lower Occoquan	45	1076.8	0.0	0.0	0.0	449.8	2072.9	380.9	117.2	1.8	217.1	4316.5	0.0%	24.9%	75.1%
Middle Broad Run	19	646.7	154.0	0.0	0.0	145.3	0.0	0.0	9.7	8.1	0.0	963.8	16.0%	67.1%	16.9%
Middle Broad Run	20	2243.3	956.2	0.0	49.4	1024.4	3.2	0.0	16.9	99.0	7.5	4400.0	22.9%	51.0%	26.2%
Middle Broad Run	56	6828.9	981.7	177.3	180.4	692.7	2.9	391.6	9.9	156.9	38.1	9460.4	14.2%	72.2%	13.7%
Upper Broad Run	7	8782.8	6209.2	504.1	1335.2	311.5	0.0	0.0	3.5	0.0	0.3	17146.5	46.9%	51.2%	1.8%
Upper Broad Run	8	3266.8	1783.3	295.6	557.2	197.3	0.0	0.0	0.0	0.0	0.0	6100.3	43.2%	53.6%	3.2%
Upper Broad Run	52	6052.6	767.3	0.0	396.3	590.2	0.0	0.0	24.9	50.0	34.8	7916.0	14.7%	76.5%	8.8%
Grand Total		205317.3	36876.4	22591.6	25033.6	42732.0	16703.1	6871.0	4682.4	6408.5	4104.4	371320.3	22.8%	55.3%	21.9%

The eastern part of the watershed shows rapid urbanization due to the short distance from Washington DC. The Lower Occoquan, Bull Run, and Lower Broad Run subbains have 23.7~51.4% of land areas categorized as urban usages. The Upper Broad Run and Cedar

Run subbasins have experienced great agricultural activities, and 38.0 and 36.7% of the surface areas are used for agricultural practice, respectively.

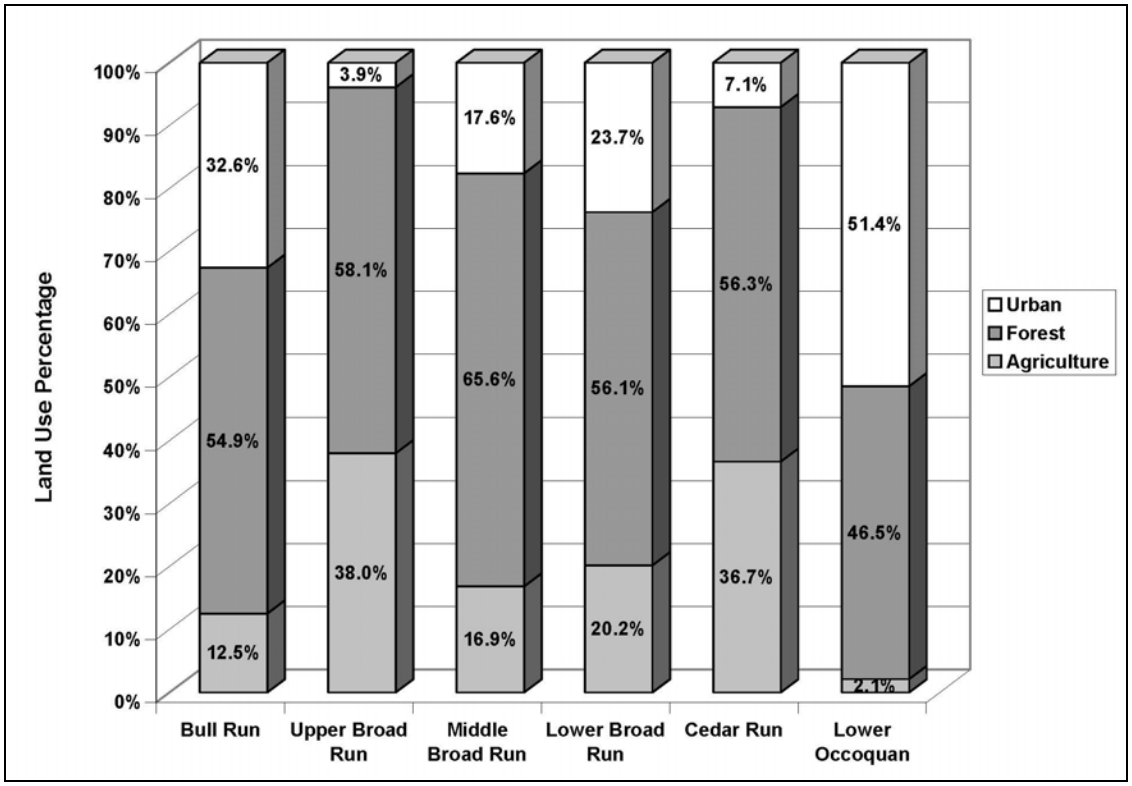

Figure D-2: Land Use Summary for Each Subbasin

References

Dougherty, M. (2004). *Quantifying Long-Term Hydrologic and NPS Pollutant Response in an Urbanizing Watershed*, Ph.D. Dissertation, Virginia Polytechnic Institute and State University, Blacksburg, Virginia.

Northern Virginia Planning District Commission (NVPDC) and Engineers And Surveyors Institute (ESI). (1992). Northern Virginia BMP Handbook: A Guide To Planning and Designing Best Management Practices in Northern Virginia. Virginia.

Northern Virginia Regional Commission. (1992). Guidebook for Screening For Urban Nonpoint Pollution Management Strategies. Annandale, Virginia.

Appendix E. Initial HSPF Calibration Performed by PEST

Introduction of PEST

Different from the previous Occoquan model calibration approach, the linked model applied PEST to perform initial hydrologic calibration for each sub-basin. PEST (WNC 2004) is an automatic Parameter ESTimation software which optimizes model parameters based on observed data. The objective goal of PEST is to minimize the weighted correlation coefficient (R^2) of simulated and observed data by using the Gauss-Marquardt-Levenberg optimization method. Because PEST adjusts model parameters only based on comparison between observed data and model-generated data, it can be applied to any kind of mathematical model as long as input and output files are in ASCII format.

Besides appropriate input and output files, PEST has to be informed of characteristics of parameters to be adjusted in order to optimize HSPF under PEST. Each parameter could follow into three categories: relative, absolute and rel_to_max. If a parameter is defined as “absolute”, its value is fixed during optimization. This function can be used to accelerate optimization speed by freezing relatively insensitive parameters. When a parameter is “relative”, the increment of the parameter is calculated as a fraction of current parameter value. For “rel_to_max” parameters, the increment is calculated as a fraction of the current highest absolute value. Different from relative parameters, the increments of “rel_to_max” vary from iteration to iteration. Because most model parameters wouldn’t have any physical meanings outside certain ranges, such value ranges have to be supplied to PEST in order to have a calibrated model with appropriate physical meaning. All this information is stored in a separate file and can be called by the PEST control file.

When HSPF is run by PEST, PEST reads these parameters and initial values and then writes them into HSPF control files. After HSPF is executed with those values, PEST calculates the weighted R^2 of simulated and observed data. Then the parameter values are adjusted based on their characteristics and new values replace corresponding values used in the previous model run. Then HSPF is run with the updated parameter values and the

R^2 is calculated and compared with the previous model run. The process is iterated until the minimum R^2 value is found. The parameter value set corresponding to the minimum R^2 value is called the optimal parameter set because it minimizes the gap between observed and simulated data. For the linked Occoquan model, PEST was used to perform the initial hydrological calibration. The parameter adjustment was to minimize the discrepancy between observed and simulated daily flow rates.

Supplementary Input Files and Corresponding UCI Files

A supplementary file, supplied to HSPF along with its normal UCI files, contains a series of lines pertaining to lines of data read from a UCI file. An "array identifier" in front of each pair of lines is used to locate the relevant lines in the UCI file (Figures E-1 and E-2). Seven principal hydrological parameters (Table E-1) were optimized in this PEST-HSPF application.

Table E-1: Calibrated HSPF Parameters

Parameters	Definition	Unit	Suggested Range
LZSN	Lower zone nominal storage (inches)	Inch	3.0-8.0
INFILT	Infiltration rate	Inch/interval	0.01-0.25
AGWRC	Groundwater recession rate	1/day	0.92-0.99
INTFW	Interflow inflow parameter	–	1.0-3.0
IRC	Interflow recession rate	1/day	0.5-0.7
MON-UZSN	Monthly upper zone nominal storage	Inch	0.1-1.0
MON-LZETPARM	Monthly Lower zone ET	–	0.2-0.7

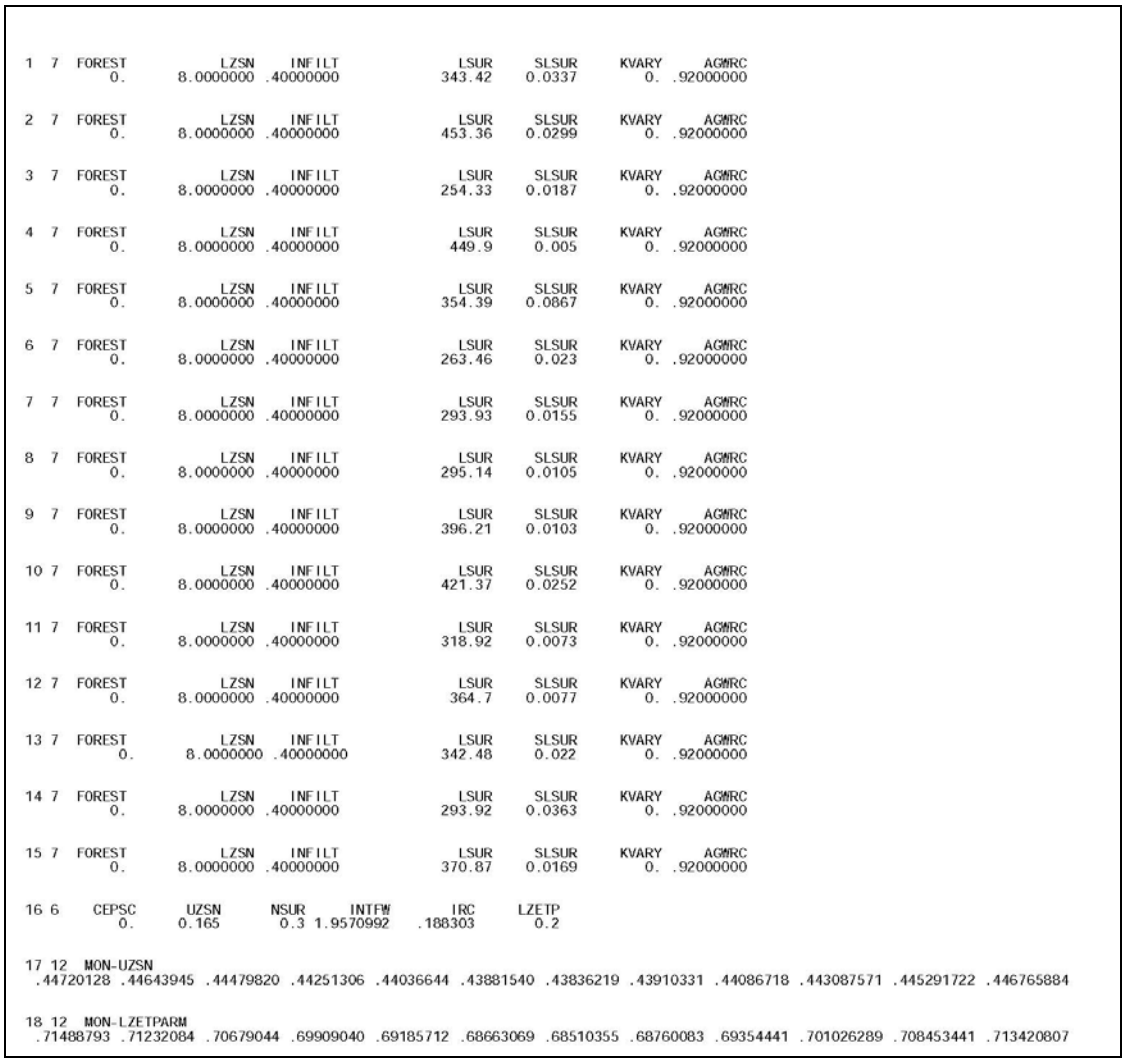

Figure E-1: An Example of a Supplementary Input File

Parameter Pre-Processing

A PEST utility called PAR2PAR is used to manipulate and adjust parameters before providing them to the model. When used with HSPF, a template file is created so that the current values of these parameters can be replaced by values generated from PAR2PAR (Figures E-3 and E-4). The initial values and parameter characteristics are provided by separate files (Figures E-5 and E-6). Four of the seven principal HSPF hydrology parameters were calibrated without transformation. The other three, IRC, MONTH USZN, and MON-LZETPARM, were not directly calibrated. Instead of IRC, PEST adjusts a parameter called IRCTRANS, which defined IRC through the following equation:

$$IRC = \frac{IRCTRAN}{1 + IRCTRAN}$$

This parameter transformation reduced nonlinearity and thus reduced the execution time.

MON-UZSN and MON-LZETPARM were calibrated through a similar approach. Instead of assigning different values to each month, it was assumed that those monthly variables were in a sinusoidal waveform dependent on time of year. So only two values (mean value and amplitude), instead of twelve values were needed to define those monthly values. This approach reduced the PEST execution time greatly.

$$MONV = MV + A \cdot \sin((J - 270) \cdot 0.1721)$$

Where MONV is Monthly value; MV is Mean Value; A is Amplitude and J is the starting Julian Day of the month.

```
  PWAT-PARM1
*** <PLS >                  Flags
*** x -  x CSNO RTOP UZFG  VCS  VUZ  VNN VIFW VIRC  VLE IFFC  HWT IRRG IFRD
  291  557    1    1    1    1    1    0    0    0    1    1    0    0    0
  END PWAT-PARM1

  PWAT-PARM2
*** < PLS>    FOREST      LZSN     INFILT      LSUR      SLSUR     KVARY      AGWRC
*** x  - x                (in)    (in/hr)      (ft)                (1/in)   (1/day)
  291  298         0.       8.0       0.08    343.42    0.0337        0.       0.92 ~1~
  301  309         0.       8.0       0.08    453.36    0.0299        0.       0.92 ~2~
  341  343         0.       8.0       0.08    254.33    0.0187        0.       0.92 ~3~
  351  357         0.       8.0       0.08     449.9     0.005        0.       0.92 ~4~
  361  366         0.       8.0       0.08    354.39    0.0867        0.       0.92 ~5~
  371  378         0.       8.0       0.08    263.46     0.023        0.       0.92 ~6~
  381  389         0.       8.0       0.08    293.93    0.0155        0.       0.92 ~7~
  391  397         0.       8.0       0.08    295.14    0.0105        0.       0.92 ~8~
  401  407         0.       8.0       0.08    396.21    0.0103        0.       0.92 ~9~
  411  417         0.       8.0       0.08    421.37    0.0252        0.       0.92 ~10~
  421  427         0.       8.0       0.08    318.92    0.0073        0.       0.92 ~11~
  431  436         0.       8.0       0.08     364.7    0.0077        0.       0.92 ~12~
  441  447         0.       8.0       0.08    342.48     0.022        0.       0.92 ~13~
  471  477         0.       8.0       0.08    293.92    0.0363        0.       0.92 ~14~
  551  557         0.       8.0       0.08    370.87    0.0169        0.       0.92 ~15~
  END PWAT-PARM2

  PWAT-PARM3
*** < PLS>     PETMAX     PETMIN     INFEXP     INFILD     DEEPFR     BASETP     AGWETP
*** x  - x    (deg F)    (deg F)
  291  557        40.        35.         2.         2.         0.         0.         0.
  END PWAT-PARM3

  PWAT-PARM4
*** <PLS >      CEPSC      UZSN      NSUR     INTFW       IRC     LZETP
*** x -  x        (in)      (in)                        (1/day)
  291  557         0.     0.165       0.3        1.       0.7       0.2 ~16~
  END PWAT-PARM4

  PWAT-STATE1
*** < PLS>  PWATER state variables (in)
*** x  - x       CEPS      SURS       UZS      IFWS       LZS      AGWS      GWVS
  291  557         0.       0.5      0.25        0.       7.0        1.      0.01
  END PWAT-STATE1

  MON-INTERCEP
*** <PLS >  Interception storage capacity at start of each month (in)
*** x -  x  JAN  FEB  MAR  APR  MAY  JUN  JUL  AUG  SEP  OCT  NOV  DEC
  291  557 0.07 0.07 0.09 0.09 0.09 0.12 0.12 0.12 0.12 0.09 0.09 0.09
  END MON-INTERCEP

  MON-UZSN
*** <PLS >  Upper zone storage at start of each month  (inches)
*** x -  x  JAN  FEB  MAR  APR  MAY  JUN  JUL  AUG  SEP  OCT  NOV  DEC
  291  557 0.40 0.40 0.66 0.66 0.70 0.70 0.80 0.80 0.70 0.66 0.60 0.40 ~17~
  END MON-UZSN

  MON-LZETPARM
*** <PLS >  Lower zone evapotransp   parm at start of each month
*** x -  x  JAN  FEB  MAR  APR  MAY  JUN  JUL  AUG  SEP  OCT  NOV  DEC
  291  557  0.2  0.2  0.4  0.5  0.6  0.7  0.7  0.7  0.7  0.4  0.4  0.2 ~18~
  END MON-LZETPARM
```

Figure E-2: An Example of Part of a Modified UCI file

```
ptf $
1  7  FOREST          LZSN     INFILT              LSUR     SLSUR     KVARY     AGWRC
          0.      $ lzsn  $ $ infilt$            343.42    0.0337       0. $  agwrc$

2  7  FOREST          LZSN     INFILT              LSUR     SLSUR     KVARY     AGWRC
          0.      $ lzsn  $ $ infilt$            453.36    0.0299       0. $  agwrc$

3  7  FOREST          LZSN     INFILT              LSUR     SLSUR     KVARY     AGWRC
          0.      $ lzsn  $ $ infilt$            254.33    0.0187       0. $  agwrc$

4  7  FOREST          LZSN     INFILT              LSUR     SLSUR     KVARY     AGWRC
          0.      $ lzsn  $ $ infilt$             449.9     0.005       0. $  agwrc$

5  7  FOREST          LZSN     INFILT              LSUR     SLSUR     KVARY     AGWRC
          0.      $ lzsn  $ $ infilt$            354.39    0.0867       0. $  agwrc$

6  7  FOREST          LZSN     INFILT              LSUR     SLSUR     KVARY     AGWRC
          0.      $ lzsn  $ $ infilt$            263.46     0.023       0. $  agwrc$

7  7  FOREST          LZSN     INFILT              LSUR     SLSUR     KVARY     AGWRC
          0.      $ lzsn  $ $ infilt$            293.93    0.0155       0. $  agwrc$

8  7  FOREST          LZSN     INFILT              LSUR     SLSUR     KVARY     AGWRC
          0.      $ lzsn  $ $ infilt$            295.14    0.0105       0. $  agwrc$

9  7  FOREST          LZSN     INFILT              LSUR     SLSUR     KVARY     AGWRC
          0.      $ lzsn  $ $ infilt$            396.21    0.0103       0. $  agwrc$

10 7  FOREST          LZSN     INFILT              LSUR     SLSUR     KVARY     AGWRC
          0.      $ lzsn  $ $ infilt$            421.37    0.0252       0. $  agwrc$

11 7  FOREST          LZSN     INFILT              LSUR     SLSUR     KVARY     AGWRC
          0.      $ lzsn  $ $ infilt$            318.92    0.0073       0. $  agwrc$

12 7  FOREST          LZSN     INFILT              LSUR     SLSUR     KVARY     AGWRC
          0.      $ lzsn  $ $ infilt$             364.7    0.0077       0. $  agwrc$

13 7  FOREST          LZSN     INFILT              LSUR     SLSUR     KVARY     AGWRC
          0.      $ lzsn  $ $ infilt$            342.48     0.022       0.  $ agwrc$
14 7  FOREST          LZSN     INFILT              LSUR     SLSUR     KVARY     AGWRC
          0.      $ lzsn  $ $ infilt$            293.92    0.0363       0. $  agwrc$

15 7  FOREST          LZSN     INFILT              LSUR     SLSUR     KVARY     AGWRC
          0.      $ lzsn  $ $ infilt$            370.87    0.0169       0. $  agwrc$

16 6    CEPSC      UZSN      NSUR     INTFW       IRC     LZETP
          0.     0.165       0.3 $ intfw $   $ irc $       0.2

17 12  MON-UZSN
 $     u1$ $     u2$ $     u3$ $     u4$ $     u5$ $     u6$ $     u7$ $     u8$ $     u9$ $     u10$ $     u11$ $     u12$

18 12  MON-LZETPARM
 $     l1$ $     l2$ $     l3$ $     l4$ $     l5$ $     l6$ $     l7$ $     l8$ $     l9$ $     l10$ $     l11$ $     l12$
```

Figure E-3: An Example of a Template for a UCI File

```
ptf $
* parameter data
lzsn    =  $ lzsn  $
infilt  =  $ infilt$
agwrc   =  $  agwrc$
intfw =  $ intfw $
irctrans=  $irctrans    $
fuvar  = $fuvar  $
uav  =  $uav    $
flvar = $flvar    $
lav=  $lav    $

uvar = fuvar*uav
lvar = flvar*lav
irc     = irctrans/(1+irctrans)

u1   = uav + uvar*sin((0  -270)*.01721)
u2   = uav + uvar*sin((31 -270)*.01721)
u3   = uav + uvar*sin((60 -270)*.01721)
u4   = uav + uvar*sin((91 -270)*.01721)
u5   = uav + uvar*sin((121-270)*.01721)
u6   = uav + uvar*sin((152-270)*.01721)
u7   = uav + uvar*sin((182-270)*.01721)
u8   = uav + uvar*sin((213-270)*.01721)
u9   = uav + uvar*sin((244-270)*.01721)
u10  = uav + uvar*sin((274-270)*.01721)
u11  = uav + uvar*sin((305-270)*.01721)
u12  = uav + uvar*sin((335-270)*.01721)
l1   = lav + lvar*sin((0  -270)*.01721)
l2   = lav + lvar*sin((31 -270)*.01721)
l3   = lav + lvar*sin((60 -270)*.01721)
l4   = lav + lvar*sin((91 -270)*.01721)
l5   = lav + lvar*sin((121-270)*.01721)
l6   = lav + lvar*sin((152-270)*.01721)
l7   = lav + lvar*sin((182-270)*.01721)
l8   = lav + lvar*sin((213-270)*.01721)
l9   = lav + lvar*sin((244-270)*.01721)
l10  = lav + lvar*sin((274-270)*.01721)
l11  = lav + lvar*sin((305-270)*.01721)
l12  = lav + lvar*sin((335-270)*.01721)
* template and model input files
cedar.tpl supplement.sup
* control data
single point
```

Figure E-4: An Example of a PAR2PAR Template File

```
 lzsn    log  factor   8.0   2.0    8.0  lzsn     1.0   0.0
 infilt  none factor   0.4  0.01    0.5  infilt   1.0   0.0
 agwrc   none factor  0.92  0.92   0.99  agwrc    1.0   0.0
 intfw   none factor   1.0   1.0    3.0  intfw    1.0   0.0
 irctrans log  factor   0.429  0.01  1000  irctrans  1.0   0.0
 uav     log  factor   1.0   0.1    1.0  uav      1.0   0.0
 fuvar   log  factor   0.2  0.01   0.99  fuvar    1.0   0.0
 lav     none factor   0.2   0.2    0.7  lav      1.0   0.0
 flvar   log  factor   0.2  0.01   0.99  flvar    1.0   0.0
```

Figure E-5: An Example of a Parameter Initial Values File

```
lzsn   relative  0.01   2e-4   switch   2   parabolic
infilt relative  0.01   1e-4   switch   2   parabolic
agwrc  relative  0.01   1e-4   switch   2   parabolic
intfw  relative  0.01   1e-4   switch   2   parabolic
irctrans  relative  0.01   1e-3   switch   2   parabolic
uav    relative  0.01   1e-4   switch   2   parabolic
fuvar  absolute  0.01      0   switch   2   parabolic
lav    relative  0.01   1e-4   switch   2   parabolic
flvar  absolute  0.01      0   switch   2   parabolic
```

Figure E-6: An Example of a Parameter Group File

Post-processing Analysis

The purpose of this PEST-HSPF application was to minimize the discrepancy between observed and simulated daily flow rates. A PEST utility called TSPROC is used to quantify the difference between observed and simulated data, including volumetric evaluation, basic statistical analysis, and exceeding time calculation. It is able to generate an optimized parameter set based on these comparisons. TSPROC receives instruction from a user-defined input file, shown as follow:

```
###########################################################################
### The settings block
###########################################################################
START SETTINGS
  DATE_FORMAT mm/dd/yyyy
#  CONTEXT model_run
  CONTEXT pest_prep
END SETTINGS
###########################################################################
##########                                        ##########
##########  The use of TSPROC as a model post-processor is       ##########
##########  programmed.                                 ##########
##########                                        ##########
###########################################################################
### Model-generated flows are extracted from the WDM file.
###########################################################################
START GET_SERIES_WDM
  CONTEXT all
  FILE cedar.wdm
  DSN 471
  NEW_SERIES_NAME nflow
END GET_SERIES_WDM
###########################################################################
### Model-generated flows are time-interpolated to the times at which
### flows were observed. Note that this is not really required in the
### present instance due to exact coincidence of the model-generated and
### observed time series. However it is included for illustrative purposes.
### First the observed flows are read from the wdm file so that the time
### base of this series is known.
###########################################################################
```

```
START GET_SERIES_WDM
  CONTEXT all
  FILE cedar.wdm
  DSN 51
  NEW_SERIES_NAME oflow
END GET_SERIES_WDM

START NEW_TIME_BASE
  CONTEXT all
  SERIES_NAME nflow
  TB_SERIES_NAME oflow
  NEW_SERIES_NAME mflow
END NEW_TIME_BASE
##########################################################################
### Monthly volumes are calculated from the modelled flows.
##########################################################################
START VOLUME_CALCULATION
  CONTEXT all
  SERIES_NAME mflow
  DATE_FILE dates.dat
  NEW_V_TABLE_NAME mvol
  FLOW_TIME_UNITS seconds
END VOLUME_CALCULATION
##########################################################################
### Exceedence times for various flows of the modelled time series are
### next calculated.
##########################################################################
START EXCEEDENCE_TIME
  CONTEXT all
  SERIES_NAME mflow
  EXCEEDENCE_TIME_UNITS days
  NEW_E_TABLE_NAME mtime
  FLOW 1.0
  FLOW 5.0
  FLOW 10.0
  FLOW 20.0
  FLOW 50.0
  FLOW 100.0
  FLOW 200.0
  FLOW 500.0

END EXCEEDENCE_TIME
##########################################################################
##########                                      ##########
##########  The next part of the TSPROC input file is for the     ##########
##########  use of TSPROC in PEST file preparation.              ##########
##########  Observed flows are processed in exactly the          ##########
##########  same way as modelled flows for comparison with       ##########
##########  the latter.                                ##########
##########                                      ##########
##########################################################################
### Monthly volumes are calculated from the observed flows.
##########################################################################
START VOLUME_CALCULATION
  CONTEXT pest_prep
```

```
  SERIES_NAME oflow
  DATE_FILE dates.dat
  NEW_V_TABLE_NAME ovol
  FLOW_TIME_UNITS seconds
END VOLUME_CALCULATION
###############################################################################
### Exceedence times for various flows of the observed time series are
### next calculated.
###############################################################################
START EXCEEDENCE_TIME
  CONTEXT pest_prep
  SERIES_NAME oflow
  EXCEEDENCE_TIME_UNITS days
  NEW_E_TABLE_NAME otime
  FLOW 1.0
  FLOW 5.0
  FLOW 10.0
  FLOW 20.0
  FLOW 50.0
  FLOW 100.0
  FLOW 200.0
  FLOW 500.0
END EXCEEDENCE_TIME
###############################################################################
##########                                    ##########
##########  The model output file is now written.             ##########
##########  This has to be done immediately preceeding the        ##########
##########  block which generates the PEST input dataset.         ##########
##########                                    ##########
###############################################################################
START LIST_OUTPUT
  CONTEXT all
  FILE tsproccedar.out
  SERIES_NAME mflow
  V_TABLE_NAME mvol
  E_TABLE_NAME mtime
  SERIES_FORMAT short
END LIST_OUTPUT
###############################################################################
##########                                    ##########
##########  The PEST input dataset is now prepared.           ##########
##########                                    ##########
###############################################################################
START WRITE_PEST_FILES

### General information is supplied.
  CONTEXT pest_prep
  NEW_PEST_CONTROL_FILE cedar.pst
  TEMPLATE_FILE par2par.tpl
  MODEL_INPUT_FILE par2par.dat
  NEW_INSTRUCTION_FILE model.ins
  PARAMETER_DATA_FILE cedar_initpar.dat
  PARAMETER_GROUP_FILE cedar_groups.dat
  MODEL_COMMAND_LINE cedar.bat
```

```
### Information pertaining to flow time series is supplied.
  OBSERVATION_SERIES_NAME oflow
  MODEL_SERIES_NAME mflow
  SERIES_WEIGHTS_EQUATION 1.0/(@_abs_value+0.001)
  SERIES_WEIGHTS_MIN_MAX 1e-5 1000

### Information pertaining to flow volumes is supplied.
  OBSERVATION_V_TABLE_NAME ovol
  MODEL_V_TABLE_NAME mvol
  V_TABLE_WEIGHTS_EQUATION 1.0e-2/sqrt(@_abs_value)

### Information pertaining to exceedence probablilities is supplied.
  OBSERVATION_E_TABLE_NAME otime
  MODEL_E_TABLE_NAME mtime
  E_TABLE_WEIGHTS_EQUATION 300.0

END WRITE_PEST_FILES
##############################################################################
```

Each block in the TSPROC input file contains commands to perform specific time series manipulation. In the SETTING block, users specify the application to be used either to optimize parameters or to generate input files for later PEST runs. Simulated and observed time series are identified in the GET_SERIES WDM block. Under the NEW_TIME_BASE block, a new time series is generated to the dates and times with corresponding observed data, so that paired observed and simulated data can be compared directly. Monthly flow volumes are accumulated in VOLUME_CALCULATION, where the date intervals are provided by the dates.dat file. The exceedence times for various flow thresholds are calculated under the EXCEEDENCE_TIME block. The output files are specified in the LIST_OUTPUT block. The WRITE_PEST_FILES block is used to generate PEST input files.

By using PEST, the hydrological calibration process was simplified. Instead of manually adjusting parameters in each HSPF run, PEST allows multiple HSPF runs with automatically-optimizing model parameters. For example, the initial PEST run for the Cedar Run subbasin included a total of 100 HSPF runs. Then, PEST was run another six times to adjust parameter ranges, initial values, and so on. The results of continuously-optimized parameters are shown in Figure E-7.

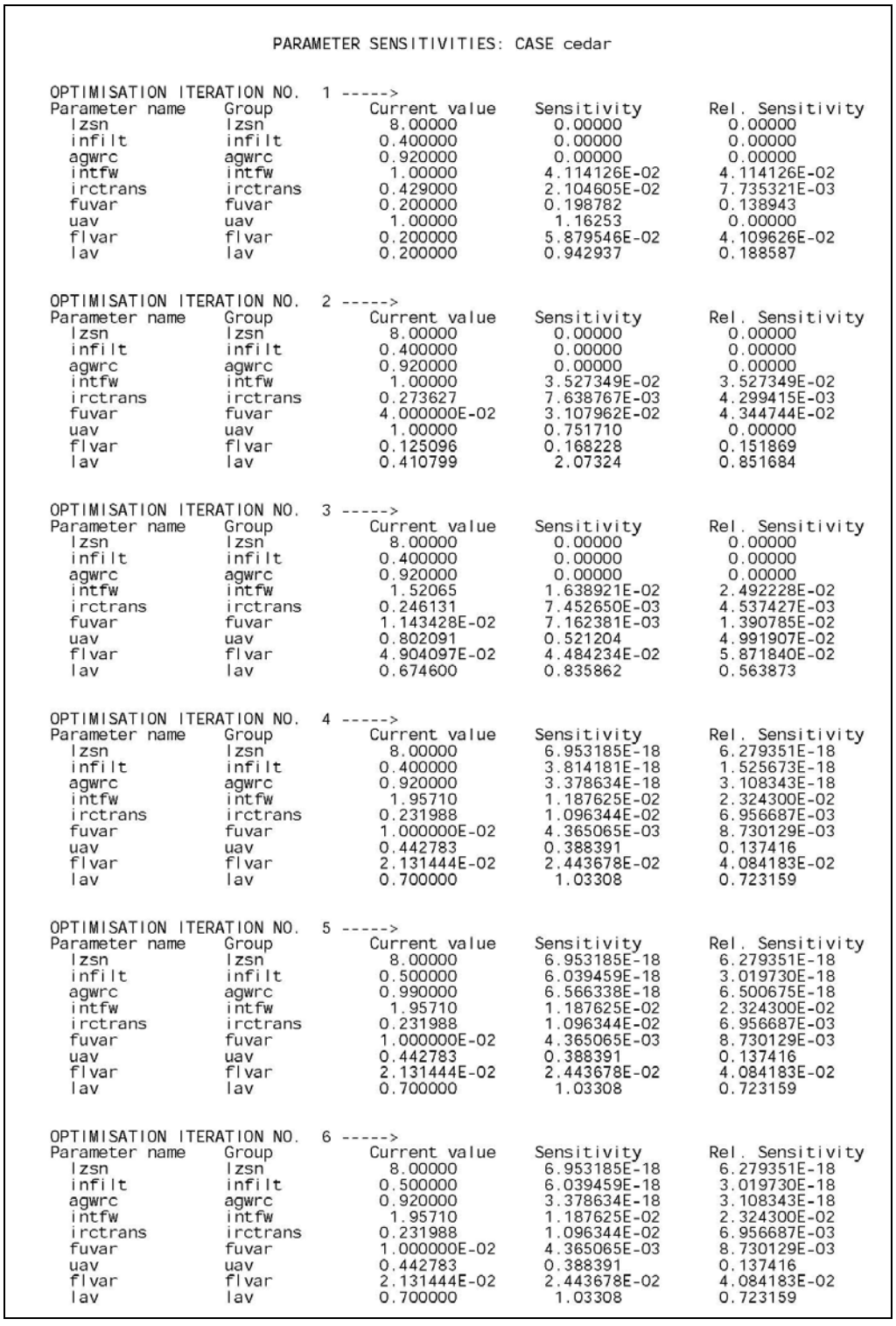

PARAMETER SENSITIVITIES: CASE cedar

OPTIMISATION ITERATION NO. 1 ----->

Parameter name	Group	Current value	Sensitivity	Rel. Sensitivity
lzsn	lzsn	8.00000	0.00000	0.00000
infilt	infilt	0.400000	0.00000	0.00000
agwrc	agwrc	0.920000	0.00000	0.00000
intfw	intfw	1.00000	4.114126E-02	4.114126E-02
irctrans	irctrans	0.429000	2.104605E-02	7.735321E-03
fuvar	fuvar	0.200000	0.198782	0.138943
uav	uav	1.00000	1.16253	0.00000
flvar	flvar	0.200000	5.879546E-02	4.109626E-02
lav	lav	0.200000	0.942937	0.188587

OPTIMISATION ITERATION NO. 2 ----->

Parameter name	Group	Current value	Sensitivity	Rel. Sensitivity
lzsn	lzsn	8.00000	0.00000	0.00000
infilt	infilt	0.400000	0.00000	0.00000
agwrc	agwrc	0.920000	0.00000	0.00000
intfw	intfw	1.00000	3.527349E-02	3.527349E-02
irctrans	irctrans	0.273627	7.638767E-03	4.299415E-03
fuvar	fuvar	4.000000E-02	3.107962E-02	4.344744E-02
uav	uav	1.00000	0.751710	0.00000
flvar	flvar	0.125096	0.168228	0.151869
lav	lav	0.410799	2.07324	0.851684

OPTIMISATION ITERATION NO. 3 ----->

Parameter name	Group	Current value	Sensitivity	Rel. Sensitivity
lzsn	lzsn	8.00000	0.00000	0.00000
infilt	infilt	0.400000	0.00000	0.00000
agwrc	agwrc	0.920000	0.00000	0.00000
intfw	intfw	1.52065	1.638921E-02	2.492228E-02
irctrans	irctrans	0.246131	7.452650E-03	4.537427E-03
fuvar	fuvar	1.143428E-02	7.162381E-03	1.390785E-02
uav	uav	0.802091	0.521204	4.991907E-02
flvar	flvar	4.904097E-02	4.484234E-02	5.871840E-02
lav	lav	0.674600	0.835862	0.563873

OPTIMISATION ITERATION NO. 4 ----->

Parameter name	Group	Current value	Sensitivity	Rel. Sensitivity
lzsn	lzsn	8.00000	6.953185E-18	6.279351E-18
infilt	infilt	0.400000	3.814181E-18	1.525673E-18
agwrc	agwrc	0.920000	3.378634E-18	3.108343E-18
intfw	intfw	1.95710	1.187625E-02	2.324300E-02
irctrans	irctrans	0.231988	1.096344E-02	6.956687E-03
fuvar	fuvar	1.000000E-02	4.365065E-03	8.730129E-03
uav	uav	0.442783	0.388391	0.137416
flvar	flvar	2.131444E-02	2.443678E-02	4.084183E-02
lav	lav	0.700000	1.03308	0.723159

OPTIMISATION ITERATION NO. 5 ----->

Parameter name	Group	Current value	Sensitivity	Rel. Sensitivity
lzsn	lzsn	8.00000	6.953185E-18	6.279351E-18
infilt	infilt	0.500000	6.039459E-18	3.019730E-18
agwrc	agwrc	0.990000	6.566338E-18	6.500675E-18
intfw	intfw	1.95710	1.187625E-02	2.324300E-02
irctrans	irctrans	0.231988	1.096344E-02	6.956687E-03
fuvar	fuvar	1.000000E-02	4.365065E-03	8.730129E-03
uav	uav	0.442783	0.388391	0.137416
flvar	flvar	2.131444E-02	2.443678E-02	4.084183E-02
lav	lav	0.700000	1.03308	0.723159

OPTIMISATION ITERATION NO. 6 ----->

Parameter name	Group	Current value	Sensitivity	Rel. Sensitivity
lzsn	lzsn	8.00000	6.953185E-18	6.279351E-18
infilt	infilt	0.500000	6.039459E-18	3.019730E-18
agwrc	agwrc	0.920000	3.378634E-18	3.108343E-18
intfw	intfw	1.95710	1.187625E-02	2.324300E-02
irctrans	irctrans	0.231988	1.096344E-02	6.956687E-03
fuvar	fuvar	1.000000E-02	4.365065E-03	8.730129E-03
uav	uav	0.442783	0.388391	0.137416
flvar	flvar	2.131444E-02	2.443678E-02	4.084183E-02
lav	lav	0.700000	1.03308	0.723159

Figure E-7: An Example of Parameter Optimization Results and Correspondent Sensitivity Analysis

Although PEST facilitated the hydrological calibration process, it was not the ultimate calibration step. One reason was that PEST tended to adopt the maximum or minimum

value of the value range as the optimized value. In order to reduce the uncertainty associated with these extreme values, HSPF was further calibrated manually. The other reason was that the physical differences among different land uses were not distinguished in the initial PEST calibration. This was to reduce the complication of PEST required input and control files. After PEST generated an optimal set of parameters, finer calibrations were performed to distinguish diverse land uses. Those calibrations not only examined the moisture distribution among surface flow, interflow, groundwater flow and ET but also distinguished the hydrological activities on different land use types. The PEST optimized parameters served as a starting point for those detailed adjustments.

References

Watermark Numerical Computing. (2004). *PEST: Model-Independent Parameter Estimation, User's Manual 5th Edition*. Brisbane, Australia.

Appendix F. The Impact of Land Use on Nutrient Load Production and Potential BMP Locations

An investigation of the water quality response to land use development has shown that increase in external nutrient loads has been a major contributor to eutrophication of the Occoquan Reservoir. In addition, nutrient load increases are not evenly distributed across the watershed due to various land use patterns, soil properties, and segment characteristics such as slopes. A closer investigation was performed to estimate the changes of nutrient loads from each land segment due to land development and human activities. This process helps to identify the critical areas in the watershed so that future BMP programs would be better implemented to reduce nutrient loads into the Occoquan Reservoir.

Nutrient loads from each segment were estimated based on three land use scenarios. The **Forest** scenario was developed wherein all the lands were assumed to be covered by forests. This scenario represents the background condition prior to the Colonial history, with no impact from human activities, and can be used to evaluate the long-term impact of human activities on water resources. The contribution of UOSA was eliminated from this scenario. The **Current** scenario represents the nutrient load distribution based on the current (1995) land use condition. The **Future** scenario was developed by converting 50% of the existing forested areas in each segment to residential and commercial development. This helps to forecast the impact of future development. The UOSA contribution was kept the same as the Current scenario in order to ensure that any increases from the Current conditions were due solely to land use changes. In reality, it is expected that UOSA will expand to serve the larger development, and it is recommended that those loads should also be increased in a modified Future scenario. Note that the inclusion, or otherwise, of UOSA does not impact anything discussed in this appendix, as discussion here is confined to loads generated from the land, rather than in-stream concentrations.

The loads produced from these three scenarios were estimated by HSPF submodels. Nutrient loads generated in individual land segments were calculated by subtracting the nutrient loads generated from immediately-upstream segments from nutrient loads up to the end of the current segment. Nutrient yield generated in individual land segments was calculated by dividing nutrient loads by the corresponding land areas. Nutrient loads computed as less-than-zero indicate that loads were reduced when delivered downstream, due to, for example, nutrient trapping in ponds.

The nutrient yield data from each land use scenario were then transferred into three separate dBASE-format databases, which were used in a GIS application to visualize and identify the critical areas in the watershed. This helps to identify future BMP locations for nutrient load reduction programs.

Table F-1 shows the average nutrient yields in three major subbasins for the three land use scenarios. Here, the Broad Run subbasin represents a greater area and includes the Upper, Middle and Lower Broad Run subbasins, and also Lake Manassas. As expected, it is clear that land use development has caused increases in nutrient yields and such increases are not evenly distributed across the whole watershed.

Table F-1: Average Nutrient Yields from Major Subbasins for Three Land Use Scenarios

		Cedar Run	Broad Run	Bull Run
NH4-N ($kg/km^2/year$)	Forest	15.8	14.8	5.6
	Current	23.6	16.4	10.5
	Future	65.4	24.6	15.0
Ox-N ($kg/km^2/year$)	Forest	176.7	152.2	304.9
	Current	229.0	159.9	408.1
	Future	312.2	240.4	437.0
OP ($kg/km^2/year$)	Forest	15.0	8.4	10.7
	Current	20.7	10.6	17.9
	Future	55.1	16.2	22.1

Figure F-1 shows the changes in NH4-N yields from the three land use scenarios. The impact of land use on nutrient yields can be clearly seen. The NH4-N yield would be dramatically increased in the Cedar Run subbasin because the dominant land use would shift from non-urban development (Forest) to urban development (Future). The nutrient yields from segment 29 and 44 have shown dramatic increases from 25.0-50.0 $kg/km^2/year$ (Forest) to more than 80 $kg/km^2/year$ (Future). Appropriate BMP

implementation in these segments would reduce nutrient generation. Based on the potential increase of NH4-N yields from land use development, the desirable BMP locations in the Cedar Run subbasin would include segments 29, 37, 42, and 47.

Although NH4-N loads from the Bull Run subbasin have increased since the pre-Colonial period (Table F-1), they have not shown as dramatic an increase as that in the Cedar Run subbasin. The desired BMP locations in the Bull Run subbasin might include segments 1, 2, 6, and 14.

In the Broad Run subbasin, segments 21 and 22 have shown high increases in NH4-N loads when compared to pre-Colonial days. Because Lake Manassas drains into segment 22, the contribution from flow over the dam was subtracted to get the nutrient yields from the land area. It is possible that the nutrient loads from the Lake Manassas overflow were not captured adequately in the simulation, and the Lake itself serves as a BMP.

Although the figures are not shown in Table F-1, an examination of Figure F-1 indicates that the other areas that might need BMPs to reduce NH4-N loads in the Lower Occoquan subbasin are segments 27 and 45.

Figure F-2 shows the changes of Ox-N yields from the three land use scenarios. Again, it is clear that the impact of land use on nutrient yields is not evenly distributed across the watershed. The Cedar Run subbasin, currently the least developed, shows a general increasing trend across the three scenarios. Segment 37 in the northern part, the southern part (segments 37, 40, 43, 42, and 44), and eastern part (segments 35 and 36) of the subbasin might be good locations for BMPs to reduce Ox-N load into the Reservoir.

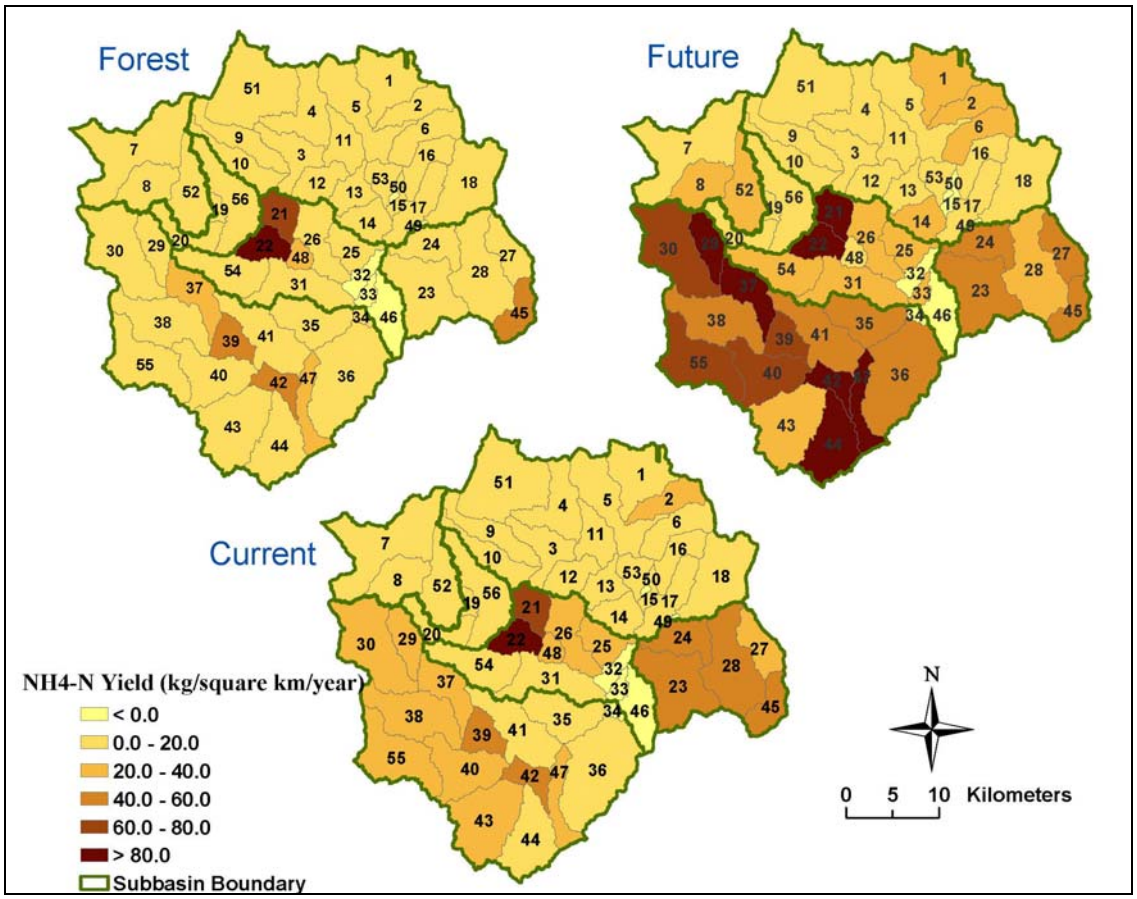

Figure F-1: NH4-N Yield Distribution in Each Land Segment Based on Three Land Use Scenarios

Even though the Ox-N yields from the Upper Broad Run subbasin show significant increases in the Future scenario, the Lower Broad Run subbasin does not show a corresponding increase in response. This is probably related to the trapping function of Lake Manassas.

The Bull Run region also shows dramatic increases due to land use development, especially on the northern and eastern parts of the subbasin. Future BMP implementation might be considered in those areas. The segments in the Lower Occoquan subbasin also show great increases in Ox-N loads. Because they directly drain into the Occoquan Reservoir, future BMPs should be included in any land development plans. A portion of segment 28 (northern shores of the Occoquan Reservoir) is currently in the downzoned area of Fairfax County, and it is unlikely that this will be developed any more intensely. However, the scenarios show the potential if development were to occur.

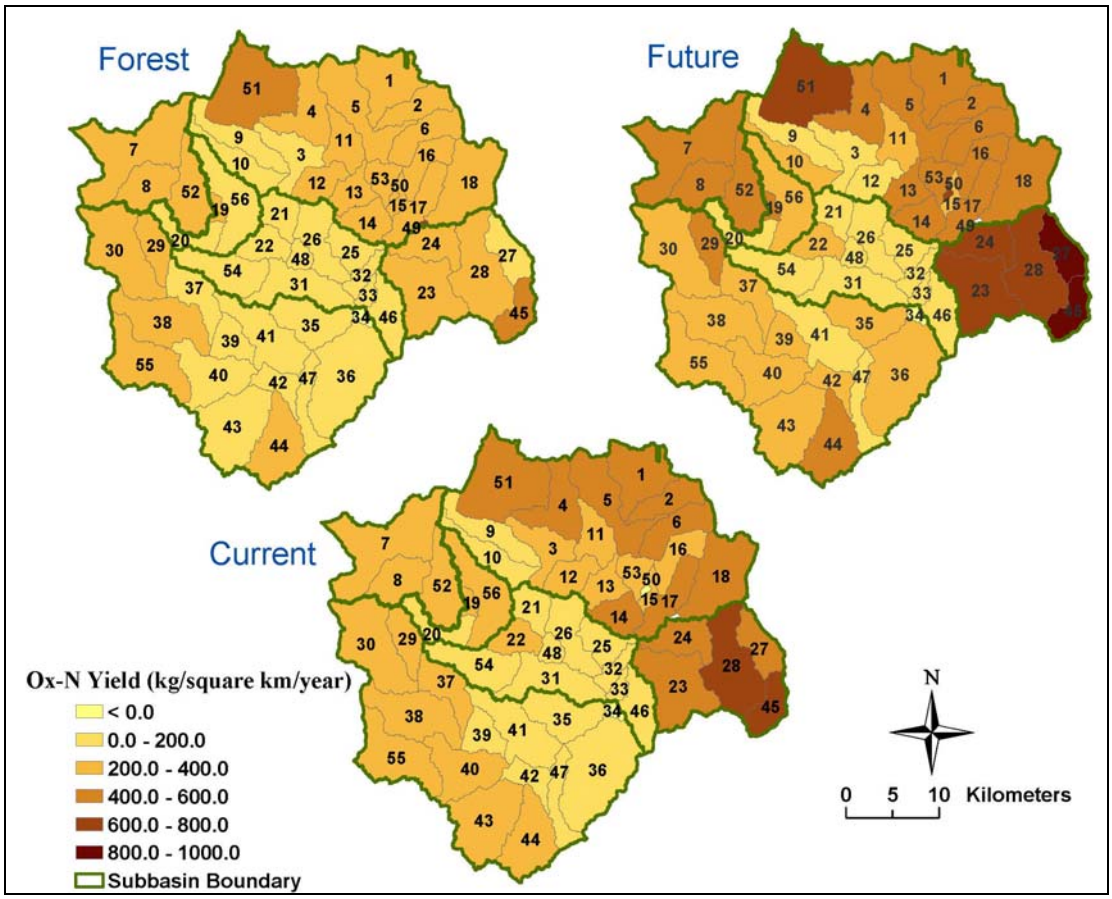

Figure F-2: Ox-N Yield Distribution in Each Land Segment Based on Three Land Use Scenarios

The OP load yield distribution across the watershed is shown in Figure F-3. As the land uses changes from the Forest to the Current and then the Future scenario, OP loads from the Cedar Run subbasin also generally increase. Segments 37 and 44 show relatively large increases and BMP plans would need to be considered in these two segments if development occurs. Segment 22 in the Lower Broad Run subbasin shows high OP production even under the pre-Colonial (Forest) scenario. As explained earlier, the loads in segment 22 were estimated by subtracting the loads up to this segment from the loads carried by Lake Manassas overflow. It is possible that the nutrient loads from Lake Manassas overflow were not simulated well enough to capture this difference with accuracy. Finally, the Bull Run subbasin also shows a generally increasing trend for OP yields due to land use development, especially in the northern part of the subbasin.

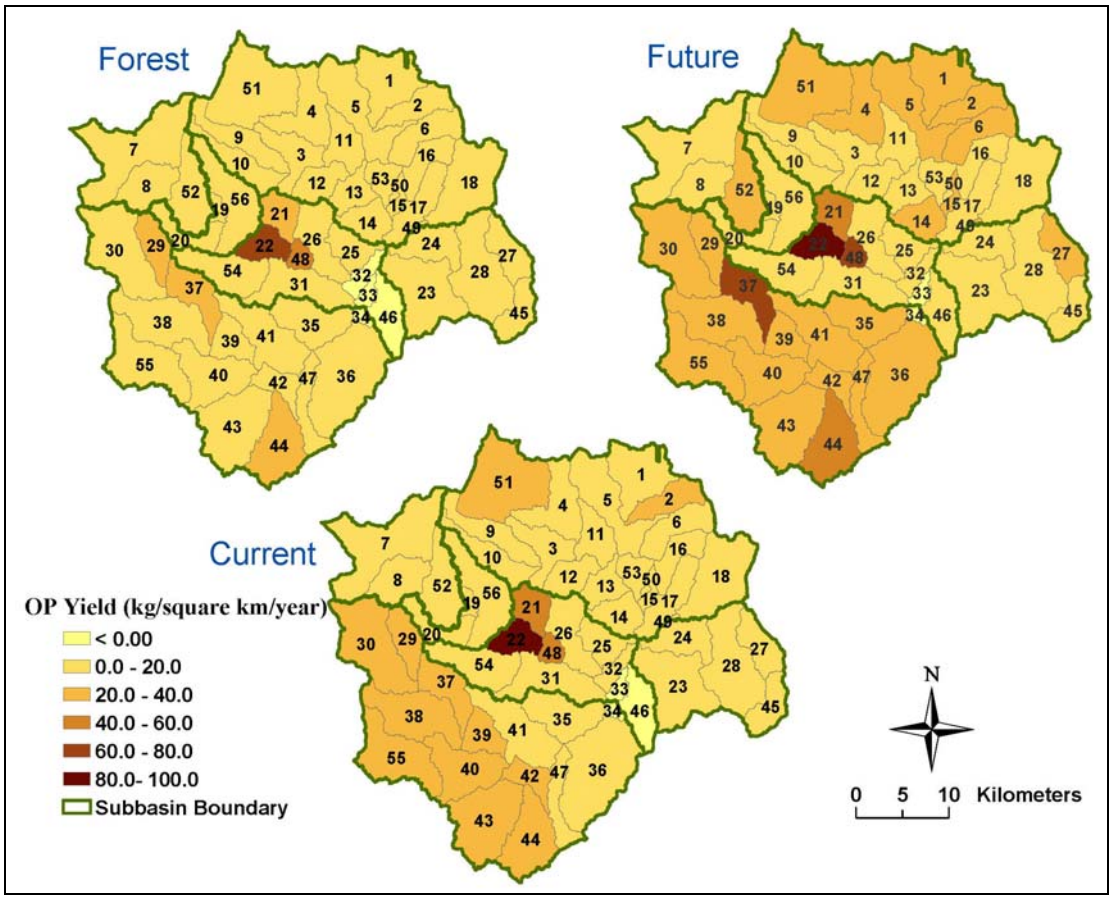

Figure F-3: OP Yield Distribution in Each Land Segment Based on Three Land Use Scenarios

It is understood that the three scenarios discussed here contain some simplifications of reality. For example, both Lake Manassas and the Occoquan Reservoir did not exist in pre-Colonial times, as they are man-made impoundments. So, their BMP functions did not really exist in pre-Colonial times. Also, it is not expected that all parts of the Cedar Run subbasin, for example, might face development in 50% of the forested areas. The southern portions of the Cedar Run subbasin are part of the Quantico Marine Base, and are not expected to be developed. Similarly, not all areas of the watershed were forested in pre-Colonial times, and there were bound to be small areas of exposed rocks, etc. Thus, the hypothetical scenarios (not including the Current one) are good approximations with some limitations. Nevertheless, the scenarios help in envisioning the changes from an undeveloped to a highly-developed state, and provide a good indication of the increased loads to be expected when development occurs.

Appendix G. The Impact of Land Use on Hydrology Activities in the Watershed

In this section, the investigation of the impact of land use development on the hydrology activities in the Occoquan watershed is described. A detailed description of land use scenarios can be found in a previous section (Appendix F).

As expected, with the increases of imperviousness from the Forest scenario, to the Current scenario, and then to the Future scenario, the flow rates at various stream stations showed an increasing trend (Table G-1). Compared with the current condition, the flow rates at ST45 showed the greatest increase (37.53%) due to the greater urbanization in the Bull Run subbasin. With the Future development, the increase of flow rates at ST45 showed a reduced rate. This is because the Bull Run subbasin in the Current condition has an existing high urban development with more than 30% of the land categorized as urban. Therefore, future expansion does not result in a significant increase in flow rates. The flow rates at ST30 also showed a reduced increase rate when the land use pattern changed from the Current condition to the Future scenario. This is probably due to the catchment function of Lake Manassas.

Table G-1: Comparison of Flow Rates at Four Principal Stations in the Occoquan Watershed under Three Land Use Scenarios

		Current	Forest	Future
ST25	m^3/s	5.06	4.99	5.46
Cedar Run	PD (%)		+1.40	+7.91
ST45	m^3/s	5.35	3.89	6.01
Bull Run	PD (%)		+37.53	+12.34
ST70	m^3/s	1.87	1.80	2.09
Upper Broad Run	PD (%)		+2.45	+2.87
ST30	m^3/s	2.80	2.45	2.87
Lower Broad Run	PD (%)		+14.29	+2.50

Figure H-1 shows the comparison of water surface elevations under different scenarios at the Occoquan Reservoir. It can be seen that the grassed areas in the Forest scenario show their water holding capability, especially during dry periods, and prevents the Reservoir from drying out. When a substantial portion of forested area is transferred into urban development, represented by the Future scenario, only 415 days out of the five-year

simulation period (1993~1997) have the water surface elevations below the dam, indicating higher runoff, compared to the Current condition (1045 days) and the Forest scenario (851 days). This indicates that appropriate dam operations or other management plans should be considered to reduce the flooding possibility downstream.

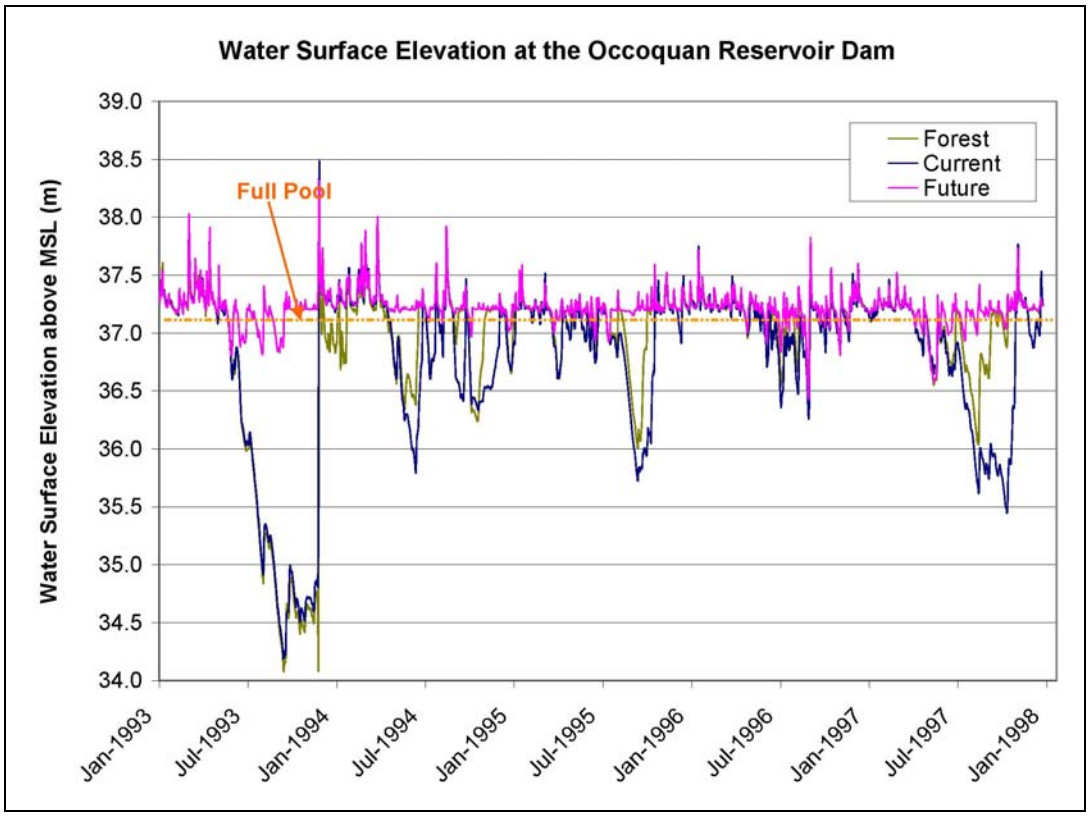

Figure G-1: Comparison of the Water Surface Elevation at the Occoquan Reservoir Dam under Various Land Use Scenarios

Vita

Zhongyan Xu was born on October 25, 1976 in Nantong, China. She received a Bachelor of Environmental Science from Nanjing University in 1998. Then she continued her study in Nanjing University and received a Master of Environmental Science in 2002.

In the summer of 2002, she was accepted by Virginia Polytechnic Institute and State University, pursuing a Degree of Philosophy degree in the Department of Civil and Environmental Engineering.